Bergvesenet rapport nr	Intern Journal nr	Internt arkiv nr	Rapport fortrolig	Gradering
5265				

Kommer fra arkiv	Ekstern rapport nr	Oversendt fra	Fortrolig pga	Fortrolig fra dato:
Grong Gruber AS		Grong Gruber a.s.		

Tittel
THE GEOLOGY OF THE JOMA SULPHIDE DEPOSIT, NORD - TRØNDELAG, NORWAY
PART II - STRATIGRAPHICAL, PETROGRAPHICAL, MINERALOGICAL AND GEOCHEMICAL STUDIES OF THE ORE AND SURROUNDINGS

Forfatter
Arne Reinsbakken

Dato: År
1986

Bedrift (oppdragsgiver og/eller oppdragstaker)
Universitetet i Trondheim

Kommune	Fylke	Bergdistrikt	1: 50 000 kartblad	1: 250 000 kartblad
Røyrvik	Nord-Trøndelag		19241	Grong

Fagområde
Geologi
Geokjemi

Dokument type

Forekomster (forekomst, gruvefelt, undersøkelsesfelt)
Grongfeltet
Joma

Råstoffgruppe
Malm/metall

Råstofftype
Cu
Zn
Kis

Sammendrag, innholdsfortegnelse eller innholdsbeskrivelse

TABLE OF CONTENTS:

INTRODUCTION
REGIONAL GEOLOGY OF THE JOMA AREA
SPILITIZATION AND SUB-SEAFLOOR CONVECTIVE HYDROTERMAL SYSTEMS
THE HOST ROCK LITHOLOGIES AT JOMA
THE JOMA ORE TYPES
SUMMARY AND CONCLUSIONS

THE GEOLOGY OF THE JOMA SULPHIDE DEPOSIT, NORD-TRØNDELAG, NORWAY

PART II

STRATIGRAPHICAL, PETROGRAPHICAL, MINERALOGICAL AND GEOCHEMICAL STUDIES OF THE ORE AND ITS SURROUNDINGS

ARNE REINSBAKKEN

1986

UNIVERSITETET I TRONDHEIM
NORGES TEKNISKE HØGSKOLE
GEOLOGISK INSTITUTT

THE GEOLOGY OF THE JOMA SULPHIDE DEPOSIT, NORD-TRØNDELAG, NORWAY

PART II

STRATIGRAPHICAL, PETROGRAPHICAL, MINERALOGICAL AND GEOCHEMICAL STUDIES OF THE ORE AND ITS SURROUNDINGS

ARNE REINSBAKKEN

1 9 8 6

UNIVERSITETET I TRONDHEIM
NORGES TEKNISKE HØGSKOLE
GEOLOGISK INSTITUTT

TABLE OF CONTENTS

		page
	SECTION 1: INTRODUCTION	1
1.1	LOCATION AND GEOLOGICAL SETTING OF THE JOMA SULPHIDE DEPOSIT	1
1.2	PREVIOUS RESEARCH AND MINING HISTORY OF THE JOMA SULPHIDE DEPOSIT	4
1.3	OUTLINE OF THE PRESENT PROJECT	7
	1.3.1 Summary of Activities	9
	1.3.2 Chemical and Mineralogical Studies	10
	SECTION 2: REGIONAL GEOLOGY OF THE JOMA AREA	12
2.1	THE REGIONAL SETTING OF THE JOMA SULPHIDE DEPOSIT	12
	2.1.1 Introduction	12
2.2	THE MIDDLE GREENSTONE	13
	2.2.1 How the Middle Greenstone was studied	13
	2.2.2 Subdivision of the Middle Greenstone	15
	2.2.3 Classification into Groups	17
	2.2.4 Group Descriptions	18
	a) Group A: Massive volcanite complex	18
	b) Group B: Pre-ore pillowed volcanite sequence	20
	c) Group C: Post-ore volcanite sequence	23
	d) Group D: Distal Greenstones	27
	2.2.5 Greenstone Lithogeochemistry	27
	2.2.6 Summary and Geotectonic Environments	29
	SECTION 3: SPILITIZATION AND SUB-SEAFLOOR CONVECTIVE HYDROTERMAL SYSTEMS	31
3.1	INTRODUCTION	31
3.2	FACTORS GOVERNING HYDROTHERMAL ALTERATION	34
3.3	SEA WATER AND BASALT REACTION EXPERIMENTS	35
3.4	RELATIVE POSITION OF THE METABASALT TYPES WITHIN THE CONVECTIVE CELL	40
3.5	SUMMARY	41
3.6	DISCUSSION ON SPILITIZATION AND HYDROTHERMAL ALTERATION	43

SECTION 4: THE HOST ROCK LITHOLOGIES AT JOMA 47

4.1. INTRODUCTION 47

4.2 SEPARATION OF HOST ROCK LITHOLOGIES 48

4.3 DESCRIPTION OF PRE-ORE, HOST ROCK LITHOLOGIES 49

4.3.1 Unit B_1 - undifferentiated Group B pillow sequence 49

4.3.2 Unit B_2 - pale, albite+sericite rich schists with po dissem. 52

4.3.3 Unit B_3 - po bearing albite+Fe-chlorite rocks 54

4.3.4 Unit B_4 - py bearing pale schist 57

4.3.5 Unit B_5 - albitite-pyrite rich rock 61

4.3.6 Unit B_6 - chlorite schists (sub units B_{6a-f} + B_H). 65

4.3.7 Distribution and Zonal Arrangements of the Host Rock Lithologies 75

4.4. CHEMISTRY OF THE HOST ROCKS 78

4.4.1 Introduction 78

4.4.2 Chemical Variations in the Host Rocks 79

4.4.3 Chemical Trends in the Host Rocks 85

4.4.4 Major Element Variation. Zonal Patterns and Hydrothermal Alteration 87

a) Introduction 87

b) CFM diagram of Host Rocks 88

4.4.5 Statistical Analysis of Whole Rock Silicate Data. 89

a) Introduction 89

b) Factor Analysis 90

c) Cluster Analysis 91

d) Summary of Statistical Analyses 93

4.5 SUMMARY OF CHARACTERISTIC FEATURES AND CHEMICAL TRENDS 94

4.5.1 Discussion 95

4.6 RELATIONSHIP OF FEEDER ZONE TO SUB-SEAFLOOR CONVECTIVE HYDROTHERMAL SYSTEMS 96

4.7 ORIGINAL VOLCANIC STRUCTURES AND IGNEOUS TEXTURES 99

SECTION 5: THE JOMA ORE TYPES 101

5.1 INTRODUCTION 101

5.2 SEPARATION OF ORE TYPES 102

5.3 DESCRIPTION OF INDIVIDUAL ORE TYPES 105

5.3.1 Type I - fine grained, massive pyritic ore 105

5.3.2 Type II - Cu-rich massive py-po-cp ore 106

5.3.3 Type III - Cu-rich cp-po breccia ore 109
5.3.4 Type IV - Zn-rich, pyritic ore, massive to semi-massive 111
5.3.5 Type V - distal exhalites 113
5.4 CHEMICAL CHARACTER OF THE ORE TYPES 113
5.5 THE USE OF Cu-Zn-Sp. GRAVITY DATA TO SEPARATE THE ORE TYPES 116
5.6 DISTRIBUTION AND ZONATION OF ORE TYPES 118

SECTION 6: SUMMARY AND CONCLUSIONS 119
6.1 SUMMARY OF THE JOMA Cu-Zn MASSIVE SULPHIDE DEPOSIT 119
6.2 GENETIC MODEL FOR JOMA ORE BODY 128
6.3 CORRELATION TO OUTSIDE AREAS 130
6.4 SUGGESTION FOR FURTHER WORK 131
6.5 'GUIDES TO ORE' - REGIONAL AND LOCAL EXPLORATION 134
6.6 SUGGESTION TO CHANGES IN RUTINE AT GRONG GRUBER 137
6.7 PRACTICAL APPLICATION OF RESULTS 138

ACKNOWLEDGEMENTS 140
REFERENCES 141
APPENDIX

Page

APPENDIX A:

A.1 CHEMICAL AND MINERALOGICAL ANALYTICAL PROCEDURES A-1

A.1.1 Introduction A-1

A.1.2 Whole Rock Silicate Analytical Techniques A-1

A.1.3 Mineralogical study, combined XRD and thin section techniques. A-2

A.1.4 Discussion A-3

A.1.5 Whole rock sulphide ore analytical techniques. A-4

A.1.6 Sampling procedures and preparation. A-5

TABLE A-1: LIST OF MINERAL ABREVIATIONS AND TERMS USED IN REPORT A-6

TABLE A-2: TERMINOLOGIES AND DEFINITIONS. A-7

APPENDIX B:

B.1 TABLES OF WHOLE ROCK SILICATE ANALYSES FOR JOMA HOST ROCK LITHOLOGIES AND DISTAL GREENSTONES B-1

B.1.1 Introduction to Tables of Whole Rock Silicate Analyses. B-1

TABLE B-1: MEAN WHOLE ROCK SILICATE ANALYSES AND MINERAL CONTENTS OF THE JOMA HOST ROCK TYPE LITHOLOGIES AND DISTAL GREENSTONES B-2

TABLE B-2: JOMA WHOLE ROCK SILICATE ANALYSES AND MINERALOGICAL CONTENTS - 1984 SERIES. B-2

TABLE B-3: JOMA WHOLE ROCK SILICATE ANALYSES - 1985 SERIES. B-2

TABLE B-4: JOMA SURFACE DDH D39 WHOLE ROCK SILICATE ANALYSES AND MINERAL CONTENTS - 1985 SERIES. B-2

TABLE B-5: JOMA WHOLE ROCK SILICATE ANALYSES AND MINERAL CONTENTS - 1986 SERIES. B-2

TABLE B-6: JOMA WHOLE ROCK SILICATE ANALYSES - 1986 SURFACE DDH SERIES. B-3

TABLE B-7: JOMA WHOLE ROCK SILICATE ANALYSES - 1977 SERIES (J. Olsen). B-3

TABLE B-8: JOMA WHOLE ROCK SILICATE ANALYSES - 1974 SERIES (G.Gale) B-3

APPENDIX C:

C.1 TABLES OF WHOLE ROCK SULPHIDE ANALYSES OF JOMA ORE TYPES C-1

TABLE C-1: JOMA ORE TYPES WHOLE ROCK SULPHIDE ANALYSES - 1985 SERIES. C-1

TABLE C-2: JOMA ORE TYPES WHOLE ROCK SULPHIDE ANALYSES - 1986 SERIES. C-1

APPENDIX D:

D.1 TABLES WITH COMPUTER PRINT-OUT FOR STATISTICAL ANALYSES PERFORMED ON WHOLE ROCK SILICATE ANALYSES DATA (355 samples) FROM 1986 SURFACE DDH SERIES (TABLE A-6). D-1

TABLE D-1: CLUSTER ANALYSIS PRINT-OUT D-1

TABLE D-2: FACTOR ANALYSIS PRINT-OUT D-1

APPENDIX E:

E.1 DETAILED LOGS OF FIFTEEN SURFACE DIAMOND DRILL HOLES (DDH). E-1

E.1.1 List of surface DDH that have been logged and sampled: D7, D10, D18, D31, D32, D36, D39, D52, D59, D61, D62, D63, D64, D65 and 2027. E-1

E.1.2 Symbols and Abbreviations used in Diamond Drill Hole (DDH) logs E-2

APPENDIX F:

F.1 TWENTY-EIGHT VERTICAL GEOLOGICAL PROFILES FROM B_1, B_2, Y AND X MINE PROFILE SERIES (SCALE 1:500). F-1

APPENDIX G:

G.1 FOUR HORIZONTAL GEOLOGICAL MAPS OF JOMA ORE BODY (SCALE 1:500). G-1

APPENDIX H:

H.1 FORTY-THREE PHOTOGRAPHS OF HOST SILICATE ROCKS, ORE TYPES AND THEIR STRUCTURAL RELATIONS TO EACH OTHER. H-1

APPENDIX I:

I.1 TWENTY-FOUR MICROPHOTOGRAPHS OF THE HOST ROCK TYPE SILICATE ROCKS. I-1

THE JOMA VOLCANOGENIC CU-ZN MASSIVE SULPHIDE DEPOSIT

SECTION 1: INTRODUCTION

1.1 LOCATION AND GEOLOGICAL SETTING OF THE JOMA SULPHIDE DEPOSIT

The Joma massive sulphide deposit is situated in the north-eastern part of the 'Grong district' of Nord-Trøndelag near the southeast end of Lake Huddingsvatnet, some 15 km east of the Røyrvik Village and c. 4 km west of the Norway-Sweden international border (Fig. 1.2). The massive sulphide deposit lies in Røyrvik Group rocks within the Leipikvatnet Nappe, which occurs at the middle Køli structural level of the larger Seve-Køli Nappe Complex in the central Scandinavian Caledonides (Fig.1.1).

Between Røyrvik and the Norway-Sweden border east of Huddingsvatnet (see Fig.1.1 and 1.2), the highly attenuated western continuation of the Stikke and Gelvenåkko Nappes are overlain by the Leipikvatnet Nappe which in turn is overlain by the Gjersvik Nappe to the west.

The inverted sequence of the Stikke nappe (Stephens & Reinsbakken 1981) comprises metagabbro-intruded calcareous phyllites (Blåsjø Phyllite or Renselvann Group of Kollung 1979) overlain by interlayered felsic and mafic metavolcanites (Stekenjokk quartz-keratophyre), and occasional lenses of quartzite conglomerate (Portfjell equivalent) and phyllite (Remdalen Group) comprise the Stikke Nappe. It is tectonically overlain by the Gelvenåkko Nappe, a complex of fine grained, often graphitic phyllites locally containing lenses of quartzite conglomerate (Ranster Formation of Kollung (1979)) and interlayered felsic and mafic metavolcanites (Fig. 1.2). These lithological units represent tectonic repetitions of the Remdalen and Stekenjokk Quartz-Keratophyre, respectively (Zachrisson 1969, Sjöstrand 1978).

Photo 1: SW view over the open pit area and the Joma ore body taken from the NW side of Orklumpen. Note the lack of rock exposure over the area (ca. 85-90 % overburden).

The volcanites belonging to the Stekenjokk Quartz-Keratophyre are overlain by a limestone mylonite (Bjurälv Limestone or Huddingsvann Limestone of Kollung 1979) and a thick sequence of mixed phyllites, layered quartz rich rock (recrystallized ribbon chert), graphitic phyllite and mafic metavolcanites (greenstone/greenschist horizons) and minor serpentinites (Røyrvik Group, Kollung 1979). All units above the Stekenjokk Quartz-Keratophyre lie in the Leipikvattnet Nappe.

This sequence is situated on the northwestern limb of a late synform (Joma Synform) whose axial surface trace trends northeastwards from Limingen to Leipikvatnet (Fig. 1.2). On this limb of the synform, the calcareous phyllites of the Brakkfjället Phyllite are absent. The Brakkfjället Phyllite outcrops to the east and south of Joma and is thought to lie in the upper part of the Leipikvatnet Nappe and to be younger than the Røyrvik Group. An erosional unconformity at the base of the Brakkfjället Phyllite, above Røyrvik Group ribbon cherts and greenstones to the south of Joma, attests to this (east Limingen-Tunnsjö Lake area).

The Røyrvik Group, lying within the Leipikvatnet Nappe, has been correlated with the Remdalen Group (Sjöstrand 1978 and Kollung 1979). The geochemistry of the mafic metavolcanites in both units, indicating a tholeiitic to alkaline character and N-MORB as well as E-MORB or WPB affinity (Olsen 1980, Stephens 1980, Stephens et al. 1985, Stephens and Reinsbakken 1986, in press) and provides support for this hypothesis. Olsen (1980) suggested a back-arc basinal environment for the sequence in the Leipikvatnet Nappe. Later Stephens and Gee (1985), on the basis of the regional geological setting and the metavolcanite geochemistry, proposed that these rocks represent the upper and probably off-axis segment of the ocean floor to a rifted arc complex. Disrupted pieces of this rifted arc and post-arc marginal basin infill occur in adjacent thrust sheets, i.e., the underlying Stikke and Gelvenåkko and overlying Gjersvik Nappes (Stephens and Gee 1985).

The Røyrvik Group rocks are of probable Lower to Middle Ordovician age and have been affected by Upper Greenschist facies regional metamorphism.

Major volcanogenic Cu-Zn massive sulphides occur both structurally above and below the Leipikvatnet Nappe. The Skorovas and Gjersvik deposits occur to the west in the higher Gjersvik Nappe. The Stekenjokk deposit occurs to east in Sweden within the lower Stikke Nappe.

Deformation.

The sequence described above occurs on the northwest limb of a late upright synform (Joma Synform, Fig. 1.2). The axial surface trace of this synform trends northeastwards from Limingen to Leipikvatnet where it merges into the post-thrusting F_3 Western Synform (Zachrisson 1969). In the thickened hinge zone of this synform southeast of Huddingsvann, three levels of mafic metavolcanites have been recognized within the Leipikvatnet Nappe (Foslie 1949 and Oftedahl 1958). The middle metavolcanite unit (Middle Greenstone or the Joma greenstone) hosts the major Cu-Zn massive sulphide deposit at Joma. Recent work (this report Section 1) suggests that these three levels represent imbricate thrust sheet repetitions of the same metavolcanite horizon and that the thrust at the base of the middle unit is a slide related to an overturned, earlier, F_2 fold. Thus, it is apparent that the Leipikvatnet Nappe is a complex of thrust sheets.

Four mesoscopic deformation phases are recognized (Section 1 this report) in agreement with the structural sequence in the underlying Køli units. D_1 and D_2 account for the early strains associated with regional schistosity development. Post thrusting D_3 structures are parasitic to the major Joma Synform and D_4 includes late folds with flat-lying axial surfaces.

1.2. PREVIOUS RESEARCH AND MINING HISTORY OF THE JOMA SULPHIDE DEPOSIT

The Joma stratiform massive sulphide deposit lies within the Røyrvik Group (Leipikvatnet Nappe) and outcrops some 2 km south-east of the mine entrance and office/concentrater complex of Grong Gruber A/S at Ornes (Fig. 1.2 and 2.1). From its surface exposure (Elvegangen) in the river which flows, via Orvatnet, into eastern end of Huddingsvatnet, the double, arc-formed, dish shaped ore body dips steeply to the SW and W, levelling off to nearly horizontal at c. 200 m depth, and has a 1200-1500 m lateral extension.

The deposit was first discovered in 1911, and explored by A/S Grong Gruber in 1912-14. Seventeen surface diamond drill holes were drilled in 1913 and nineteen in 1915-16. This material formed the basis of the first report on the Joma deposit by Chr. Münster (1915). J.H.L. Vogt briefly described the Joma deposit from a short visit in 1915. The first ore reserves were calculated by Foslie (1926) on the results of the above drilling.

Very little activity took place until the German occupational forces carried out more extensive exploration drilling (28 holes in 1943-44) and reconnaissance electromagnetic measurements in an effort to get the Joma deposit into production during World War II. New ore reserves calculations were published by Foslie (1949) on the basis of the work done during this period. An exploration adit was started in 1956 by the state owned company A/S Joma Bergverk.

Modern exploration, prior to the present operator, Grong Gruber A/S, acquiring mining rights in 1969, culminated around 1963-65. Several exploration inclines and levels were driven and mapped, some 50 surface holes were drilled and electromagnetic and gravity surveys were done. The work was carried out by NGU under the leadership of Dr. H. Bjørlykke. Grong Gruber acquired mining rights in 1969 and up until production started in 1972, carried out new detailed surface and subsurface drilling and exploration drifting, as well as driving the main 2 km long transportation tunnel south to the ore body.

When production started in 1972, the total reserves were calculated at c. 16 million metric tons of both massive and disseminated ore containing 32 % S, 1.30 % Cu, 1.70 % Zn and with only minor amounts of Pb and recoverable Ag and Au. However, since pyrite is of no economic interest at present and is not recovered, production was based on 6.8 million tons averaging 1.70 % Cu and 1.11 % Zn. The total reserves at present are calculated at c. 20 M. tons of ore. The annual production is now 400,000 metric tons/year.

By the end of the 1985 season about 38 km of mine workings and adits have been driven, extending from the surface (580 m a.s.l.) down to the 342 transport level, and c.2100 subsurface production holes and 70 surface exploration holes have been drilled, producing about 60,000 m of drill core, which, when combined with the 25,000 m of exploration drill done prior to 1972, means that approximately 85,000 m of core has been drilled on the Joma deposit to date.

Previous geological work.

Steinar Foslie mapped the area around Joma first in 1922 and was the first to recognize that the Joma deposit lies solely within a basic eruptive sequence where it has its greatest thickness in the middle of a tight arc structure. Foslie (1949) later made some geological observations on the ore thicknesses and their relationships to fold directions.

P. Fr. Trøften (1955) collected together all available data, including maps and chemical data, etc. in his degree thesis at Geologisk Institutt, Norges tekniske høgskole.

Chr. Oftedahl remapped the area around Joma in 1955-56 and combined his data with unpublished material from Foslie's mapping of 1922 and 1943 to produce a geological map in his 1958 publication plus a 1:100,000 map (Tunnsjø) published by NGU in 1958.

In the period from 1972-78, the area was again mapped in some detail on a regional scale (1:20,000) for the 'Grong Project'. A compilation of all this data was later published by Kollung (1979) and is also found as an unpublished map sheet (1:50,000 Huddingsvatn). This map sheet, and the adjoining map sheet to the west (preliminary 1:50,000 Røyrvik) compiled by O. Lutro, has formed the basis for all the regional studies done during this project.

Exploration after mining started (1972) has included the use of 'Turam' geophysical techniques, which has outlined the location of subsurface sulphide horizons (Logn and Bølviken 1974). Recent geophysical exploration using the 'differential electromagnetic potential' technique by H. Elvebakk (Dr.Ing.student, NTH) in 1984 and 1985 has added to these results.

The middle greenstone around the Joma deposit was mapped on the scale of 1:5,000 as an undergraduate project (Imperial College, London) by Romaya (1981) and the continuation of the three greenstone units to the west (into the Gåsvatn and Borvasselv area) mapped on a similar scale by R. Horbach (Clausthal University, W. Germany) during 1983 to 1985. A preliminary report on the greenstone mineralogy and geochemistry is given in Horbach and Leissmann (1985).

The mineralogy and composition of the sulphide lithologies were first described by Anger et al. (1963) and are presently under investigation by W.Leissmann (Clausthal University, W. Germany) who gives a preliminary report in Horbach and Leissmann (1985). The occurence of silver and silver bearing minerals in the sulphides has been described by Malvik et al. (1984) and Eidsmo et al. (1984). Løkjell and Malvik (XXXX) studied the sulphide mineral compositions and their flotation properties for the Joma ores.

Underground mapping of the ore body was undertaken in several periods. G. Juve mapped the main exploration level (480 level) and inclines in 1964 on a 1:200 and 1:500 scale, as well as describing the surface exploration drill holes. This work was done by NGU under contract to A/S Joma Bergverk (Juve, 1964).

A model of the Joma deposit (1:500 scale vertical profiles) was constructed by R. Kvien for the mine opening in 1972. The model was constructed from all available drill data prior to 1972.

Student mapping courses (students from Geol. Inst., NTH) have been held at Joma in two periods, 1974-76 and 1984-85. A total of 32 students participated and the project reports include maps and polished and thin section descriptions that were useful for the present project, especially those from the earlier period which were from the earlier workings (510 and 520 levels) which are inaccessible today.

During the summer of 1974 berging.stud. A. Stensrud mapped the ore boundaries along several of the upper levels (480, 520, 560) along the northern edge of the ore body, levels that are now very oxidized and partly inaccessible.

Underground mapping of the ore body was undertaken by J. Olsen from 1975-77 as part of a Dr.Ing. study at NTH. He constructed vertical sections from the upper part of the ore body (Olsen 1984). These are revised and extended to the lower parts of the ore body by Reinsbakken in the present study. Olsen (1980) described the geochemistry of the ore types and adjacent greenstones, recognizing the extensive alteration and sulphide stringer zone in the host rocks. He interprets the deposit as being of a volcanogenic, sedimentary exhalative in origin, being deposited in an ocean floor, back arc basin environment. The tectonic setting and genesis of the deposit are further discussed by Stephens and Reinsbakken (1981 and 1986 in press).

1.3. OUTLINE OF THE PRESENT PROJECT

The present project has had as its aims, an analysis of the structural setting, stratigraphy and chemistry of the Joma massive sulphide deposit and its host rocks. The project has been reported in two parts, the first (PART I), a study of the structures by N. Odling and the second (PART II), a study of the stratigraphy, petrography, mineralogy and geochemistry by A. Reinsbakken.

The project was funded jointly by NTNF and Grong Gruber A/S while Odling was in possession of a two year post doctoral fellowship from NTNF from 1st June 1984 to 1st June 1986, and Reinsbakken employed on a two year contract by Geologisk Institutt, NTH, from 1st May 1984 to 1st June 1986. Dr. B. Marshall from Sydney, Australia was involved in the project for six months in 1984. He was especially interested in ore textures and the deformational effects on the silicated and sulphide minerals and geothermometry on the remobilized silicated due to the various deformational phases.

The structural analysis by Odling involved structural mapping on the scale of 1:5,000 of the area outlined in Fig. 1.2 (See report Section 1 by N. Odling) and incorporated the measurement of minor structures and mapping of lithological types in the greenstones. Finite strain was analysed for ten specimens of pillowed greenstone containing variolites from the outer greenstone. The structure of the ore deposit was studied by underground mapping and minor structure measurement, concentrated in the newer deeper parts of the mine. A total of 12 weeks were spent on surface mapping and 12 weeks on underground mapping from June to September in 1984 and 1985.

The stratigraphical study of the ore horizon by Reinsbakken involved the construction of 4 horizontal and 28 vertical sections of the ore body extending those of Olsen (1984) to greater depth, and reclassifying the sulphides and country rock lithologies. To this end a number of levels evenly distributed throughout the mine were mapped in detail during a total of five months spent underground at Joma. Three months were devoted to detailed mapping of the open pit (1:500 scale) and regional mapping (1:5,000 scale) in the middle greenstone surrounding Joma in connection with volcanostratigraphic studies and surface drill core studies, and whole rock analyses sampling. Fifteen deep drill holes from the surface to the ore horizon and 6 underground drill holes were logged and sampled for sulphide and host rock silicate analyses. A total of 460 full silicate chemical analyses were performed on distal surface greenstone, proximal surface and underground host rock specimens and drill core samples in order to study the regional

greenstone chemical variations between the three main greenstone units (the Inner, Middle and Outer greenstones) and the hydrothermal alteration in the host rocks associated with the sulphide deposit. Statistical analysis (Cluster and Factor Analyses) was used to interpret the vast number of drill core data. In addition, 72 samples from the various sulphide ore facies were analysed for base and trace metal contents. The Cu-Zn-Sp.gravity data from the mine drill core data were used to separate the major ore types that were delineated under the detailed mine mapping.

1.3.1 Summary of Activities.

A total of four months were used on reconnaissance and detailed underground mine mapping and sampling of the host rock and ore facies lithologies. The mine mapping was divided into two categories; reconnaissance mapping on a 1:500 scale, throughout the mine, and detailed mapping (scale 1:100 and 1:250) at strategic levels in connection with the subdivision and sampling of the host rock and ore-type lithologies. These are confined for the most part to the more recent, less oxidized workings within the lower levels of the mine. The following levels have been mapped; those underlined were mapped in detail and sampled for whole rock silicate and sulphide analysis, those in brackets have also been sketched in detail and studied for structural analysis by N. Odling:
364-342 synk, (350), <u>362</u>, (<u>375</u>), (<u>387</u>), (<u>402</u>), (416), 429, <u>480</u>, (495), 500 and <u>560</u> (plus bottom of the open pit).

Four horizontal geological maps (1:500 scale) have been produced for the 375, 402, 480 and 560 levels and 28 vertical geological profiles (1:500) have been completed, evenly spaced throughout the mine along the B_2, B_1, Y and X profile series.

Two weeks were devoted to detailed surface mapping (1:500 scale) and sampling of the host rock and ore-type lithologies, within and around the open pit.

Three weeks were devoted to regional mapping (1:5000 scale) of the middle greenstone surrounding the Joma ore exposure and the rusty mineralized continuations to the NW and SSW, in connection with whole rock greenstone sampling and surface drill hole studies. Because of the general lack of good outcrop exposure in the area surrounding the mine, more time was devoted to the surface drill core descriptions, in order to maximize the information regarding the volcanostratigraphy in the area. Some time was also devoted to regional reconnaissance mapping (1:50,000 scale) of the inner, middle and outer greenstone units in collaboration with N. Odling, in connection with sampling of the greenstones distal to the Joma mine area.

Three months were devoted to detailed surface drill core descriptions (1:100 and 1:250 scale) and sampling. Fifteen surface holes, ranging in lengths from 140 to 400 m and totalling 3890 m in length were described in detail and 351, 10 m composite, samples were taken for whole rock silicate analyses in order to study the hydrothermal alteration phenomena at Joma. The following surface drill holes are described and sampled: D7, D10, D18, D31, D32, D36, D39, D52, D59, D61, D62, D63, D64, D65 and 2027. Six short (10-20 m), sub surface, mine drill holes were also logged and sampled for both host rock and ore-type whole rock analyses.

1.3.2 Chemical and Mineralogical Studies.

A total of 454 samples of distal and proximal greenstones and host rock lithologies were analysed for 36 to 20 major and trace element using whole rock silicate methods. Twenty-eight samples were analysed at the Geologisk Institutt-NTH using combined XRF, AAS and wet chemical techniques and the remaining 426 by Rautaruukki Oy, Finland, using solely XRF technique. (See Appendix A for description of analytical methods.) The whole rock silicate samples are distributed as follows:

a) 79 samples of host rock lithologies from sub surface mine workings and drill core material.
b) 25 samples from distal and proximal regional greenstones, and
c) 350 samples from the 15 surface drill holes.

Sixty-five of these whole rock silicate samples were analysed at the Geol. Inst., NTH, for their mineral contents using a combined XRD and thin section modal analyses technique.

Seventy-two samples of the ore-type sulphide facies at Joma were analysed by Bondar-Clegg, Canada, for 30 major and trace sulphide bearing elements using AAS, wet chemical and INAA (instrumental neutron activation analysis) techniques.

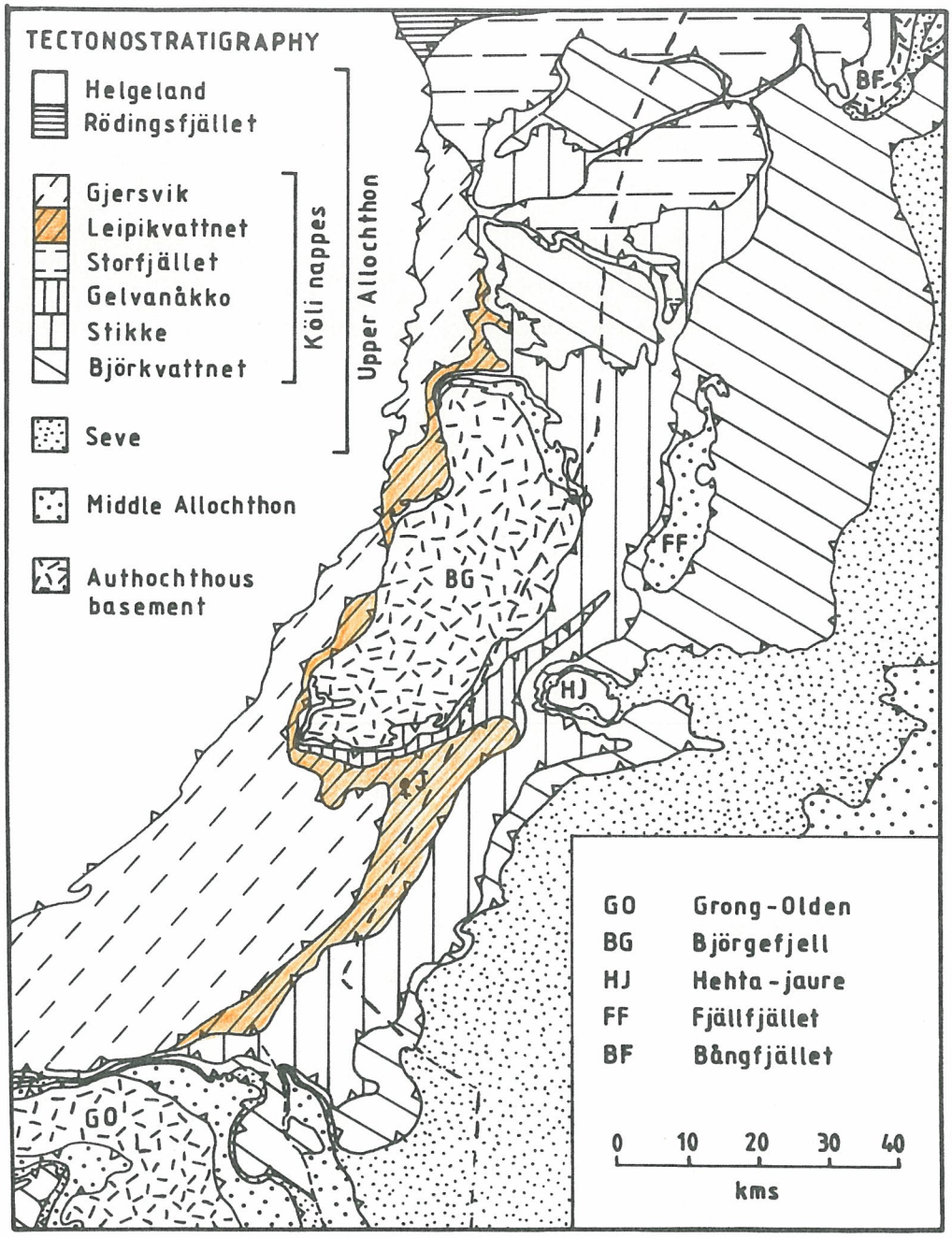

Fig. 1.1. Map of the north, central Scandinavian Caledonides after Stephens and Reinsbakken (1981), Häggbom (1978), Ramberg (1981) and Reinsbakken (unpubl. data). The Leipikvattnet nappe outcrops over a distance of 120 kms from the north side of the Grong-Olden culmination to north of the Bjørgefjell massive. The position of the Joma deposit is marked (J) (From Odling, PART I).

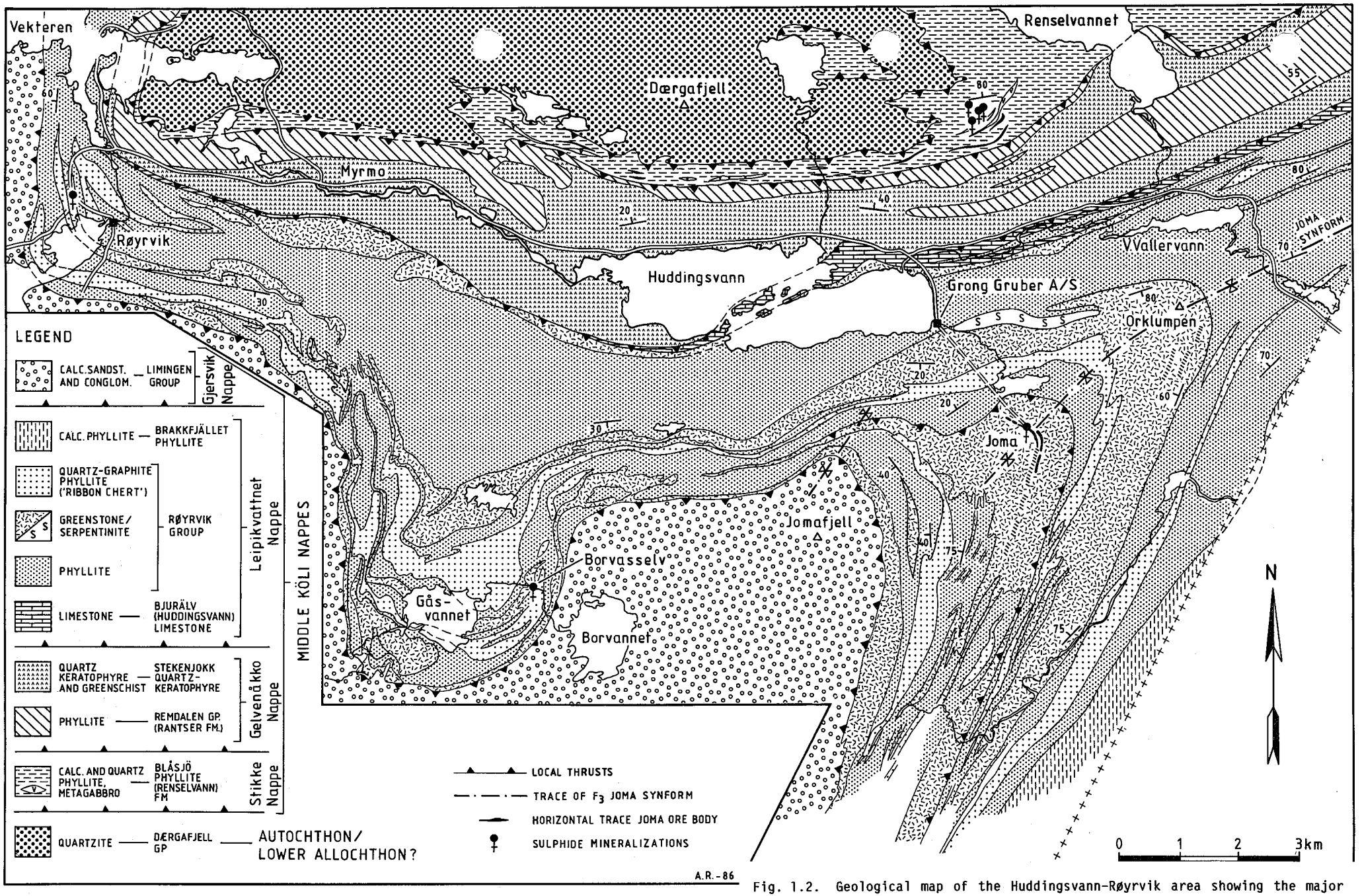

Fig. 1.2. Geological map of the Huddingsvann-Røyrvik area showing the major tectonostratigraphic units and the distribution of the major lithologies of the Røyrvik Group within the Leipikvattnet nappe. Mineralizations at the Joma stratigraphic level are designated from east to west as Joma, Borvasselv and the Røyrvik road junction. Modified after Stephens and Reinsbakken 1981, with geology based partly after Kollung (1979) and Lutro, O., and Kollung, S. (1983).

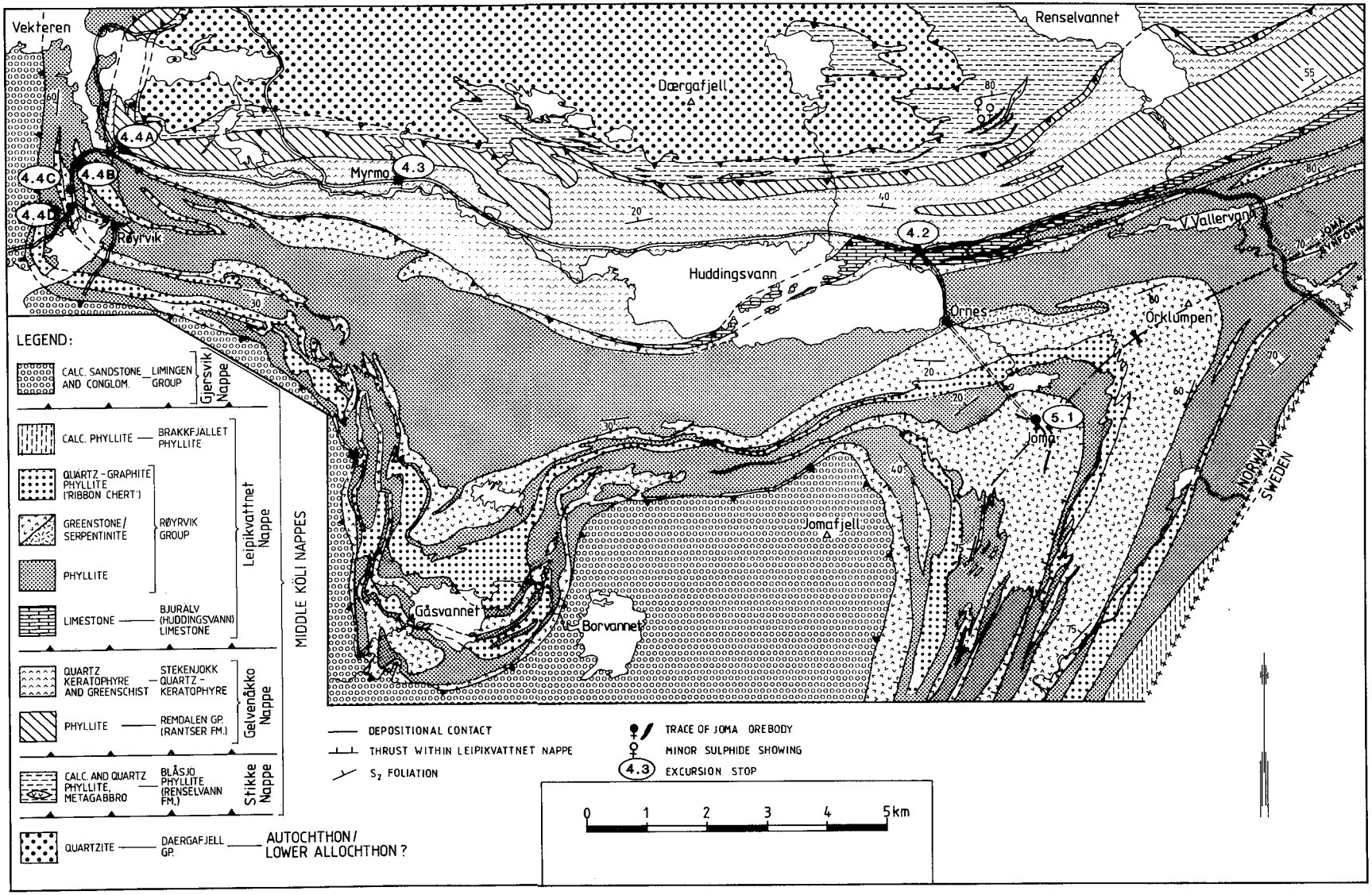
Vekteren
Renselvannet
Dærgafjell
Myrmo
4.4A
4.4B
4.4C
4.4D
4.3
4.2
Røyrvik
Huddingsvann
V.Vallervann
Ørnes
Ørklumpen
5.1
Joma
Jomafjell
NORWAY
SWEDEN
Gåsvannet
Borvannet
LEGEND:
CALC. SANDSTONE AND CONGLOM. — LIMINGEN GROUP — Gjersvik Nappe
CALC. PHYLLITE — BRAKKFJÄLLET PHYLLITE
QUARTZ-GRAPHITE PHYLLITE ('RIBBON CHERT')
GREENSTONE/ SERPENTINITE
PHYLLITE
RØYRVIK GROUP
LIMESTONE — BJURÄLV (HUDDINGSVANN) LIMESTONE
Leipikvattnet Nappe
MIDDLE KÖLI NAPPES
QUARTZ KERATOPHYRE AND GREENSCHIST — STEKENJOKK QUARTZ-KERATOPHYRE
PHYLLITE — REMDALEN GP. (RANTSER FM.)
Gelvenåkko Nappe
CALC. AND QUARTZ PHYLLITE, METAGABBRO — BLÅSJO PHYLLITE (RENSELVANN FM.)
Strikke Nappe
QUARTZITE — DAERGAFJELL GP. — AUTOCHTHON/ LOWER ALLOCHTHON ?
DEPOSITIONAL CONTACT
THRUST WITHIN LEIPIKVATTNET NAPPE
S_2 FOLIATION
TRACE OF JOMA OREBODY
MINOR SULPHIDE SHOWING
4.3 EXCURSION STOP
0 1 2 3 4 5km

SECTION 2: REGIONAL GEOLOGY OF THE JOMA AREA.

2.1 THE REGIONAL SETTING OF THE JOMA SULPHIDE DEPOSIT

2.1.1 Introduction.

The area studied in this project covers approximately 25 km^2 centred on the surface exposure of the Joma sulphide deposit (Fig. 1.2 and 2.1). The area was studied regionally on a 1:50,000 scale using Kollung's report map (1979) and unpublished 1:50,000 map-sheet Huddingsvatnet as a basis. Detailed mapping in areas of interest was carried out on a 1:5,000 scale.

The area is underlain by Røyrvik Group rocks dominated by mixed phyllites, layered quartz rich and dark phyllites (recrystallized ribbon chert), graphitic phyllites, greenstones and minor serpentinites (Fig. 2.1). The Joma deposit lies within the middle member of three distinct greenstone horizons, which have their greatest thickness within the fold-arc of the Joma Synform. The three greenstone belts are, from SW to NE, called respectively the inner, middle and outer greenstones. Remnants of volcanic structures and textures such as pillows, pillow breccias and hyaloclastites along with minor limestone beds indicate that these were deposited in a submarine environment. A detailed investigation of the three greenstone belts indicates that the middle and outer greenstones (Joma and Orklumpen respectively) are similar in their distribution of massive, pillowed lavas and volcaniclastic sequences; they are interpreted as belonging to the same volcanite complex, repeated by isoclinal folding and thrusting. The Joma ore horizon lies in the overturned limb of a major F_2 isoclinal fold structure and is probably cut out at depth by a major thrust which separates these greenstones (discussed later).

Structure.

The area has been affected by four phases of deformation. The second phase is the main event and is represented by recumbent isoclinal NNW-SSE trending folds, giving rise to a penetrative schistosity and mineral lineation throughout the area, which has almost completely overprinted a pre-existing schistosity.

The main schistosity is folded by a third phase into a large scale, partially overturned, SW-NE trending synformal structure known as the Joma Synform. The fourth phase of deformation is restricted to sporadically developed minor structures, mainly in the southern part of the area.

2.2 THE MIDDLE GREENSTONE

2.2.1 How the Middle Greenstone was studied.

An area of approximately 8 km^2 of the middle greenstone was mapped (1:5,000) by N. Odling in connection with a structural analysis and study of the regional distribution of volcanite rock types within the three greenstone belts (see PART I, p. 5) . The results of this regional mapping formed the framework for further detailed mapping of the middle greenstone in strategic areas around the surface exposures of the Joma orebody. The main aim of this study was to produce a volcanostratigraphy for the rocks hosting the Joma ore horizon, to sample these units for a detailed lithogeochemical and mineralogical investigations in order to indicate possible original magmatic differentiation trends and to outline areas of intense hydrothermal alteration within the volcanite pile and show their relationship to the Joma orebody.

Because of the general lack of good surface outcrop exposures around the Joma orebody (Photo 1, APPENDIX H), much of the detailed mapping was confined to exposures immediately surrounding the open pit, to the NW and SSW of the open pit following the rusty mineralized zones (Fig. 2.2.a), and across the most densly drilled area to the west of the orebody's surface trace.

Fresh surface specimens for lithogeochemical and mineralogical studies were gathered from recently blasted pits within the various volcanite rock types.

Fifteen surface drill holes were logged in detail to extend the volcanostratigraphy and sampled to provide material for an extensive lithogeochemical and mineralogical investigation.

These drill holes were chosen from the most densely drilled area to the west of the Joma ore exposure, from holes that penetrate the western extension of the ore horizon and its distal equivalents and into the footwall volcanites below the ore zone. The holes were evenly distributed along a NS and EW profile and the surrounding areas, in order to give the best possible coverage of the rock types in the area.

Drill hole D39 was logged and sampled first as a test case, in order to define the rock types hosting the main ore horizon at Joma. This hole is situated closest to the surface exposure of the orebody and penetrates the orebody at the 362 m level in profile X94900 (see Fig. 2.2a+b). The drill core was sampled at 10 m intervals (composed of 1 m composite samples) for whole rock silicate analyses and mineralogical investigations of the various volcanite rock types (Fig. 2.3). The test results from DDH D39 formed the basis for further drill core descriptions and a detailed sampling program on the remaining 14 surface drill holes. These were logged and sampled in the same manner to give information on the lateral distribution of the volcanite units and their relations to the Joma ore horizon. The resulting large sample population from the drill core program has provided a lithogeochemical and mineralogical data base from which the chemical variations between the volcanite units and the hydrothermal alteration processes have been studied.

Detailed surface mapping of the area surrounding the surface exposure of the Joma orebody was difficult due to the lack of outcrop exposure (10-15 % outcrop exposure, see Photo 1). Further hindrance to the interpretation of a volcanostratigraphy for the Joma area has been the high degree of deformation, especially within areas of high D_2 strain and resulting shear zones, as well as the zones of intense hydrothermal alteration found within the older volcanites near the ore horizon. Both these secondary processes destroy all hints of primary volcanic structures and igneous textures in the rocks.

2.2.2 Subdivision of the Middle Greenstone.

Earlier work (Foslie 1924, 1949) had shown that the Joma deposit lies solely within a basic metavolcanite complex, which shows pillows, pillow breccias and hyaloclastites, structures that are diagnostic of submarine volcanic sequences (Olsen 1980, 1984). Olsen also recognized that the volcanite rocks in the hangingwall of the ore zone have undergone a pervasive hydrothermal alteration manifested in sulphide veining and disseminations and zones rich in pale albitite- and dark chlorite rich rocks. Olsen's geological vertical profiles from the upper levels of the mine also showed that the altered and sulphide disseminated hangingwall rocks are different from the pale footwall greenstones. A quick inspection of these FW and HW units along, with Olsen's lithogeochemical data, showed that these two units are visibly and chemically distinct from each other. This strengthened the interpretation that the hangingwall rocks represented the pre-ore hydrothermally altered feeder zone to the orebody and the pale footwall greenstones the younger, post-ore volcanite sequence, such that the whole sequence is now lying in an inverted position.

The pre-ore, hangingwall rocks are generally darker, more chloritic and albitic, are schistose and carry abundant sulphide disseminations and veins, whereas the post-ore footwall rocks are typically paler in colour and more homogeneous, fine grained, massive and hard in nature. In addition they are richer in visible calcite, epidote and quartz. The footwall greenstones also contain layers of white limestone and lensoid bands of magnetite bearing dark grey quartzites (recrystallized chert).

Thus it was early recognized that the pre- and post-ore metavolcanites at Joma could be separated by visual inspection, using colour, texture and diagnostic mineral contents. Later thin section studies and statistical analyses of the lithogeochemical data has strengthened this separation.

Detailed mapping shows that the middle greenstone is composed of two major volcanite types, a central core comprising pillows, pillow breccias and hyaloclastites which roughly parallels the

central part of the middle greenstone arc and wedges out to the NW. This is surrounded on three sides (E, N and W) by a prominent and more laterally extensive sequence of well layered to laminated greenstones. The wedge shaped configuration of the central core to the middle greenstone at Joma is interpreted as an northward facing early D_2 fold closure. The younger layered volcanoclastics are thus folded around the central pre-ore sequence and occur both to the west of (structurally above) and to the east of (structurally below) the pre-ore volcanites and the ore horizon (see Fig. 2.1).

The Joma ore horizon lies within a pillowed and pillow breccia sequence which forms the central core to the middle greenstone, near the eastern footwall contact with the pale laminated greenstones. The orebody lies at the interface between two distinctly different pillow lava sequences. A darker, chloritic, sulphide disseminated and veined hangingwall sequence, represents the pre-ore, hydrothermally altered feeder zone to the ore zone, and a paler, calcite- and clinozoisite rich pillowed footwall sequence represents the younger, post-ore volcanites. The post-ore pillow and pillow breccia sequence grades quickly both downwards (structurally) and laterally, into a thicker sequence of layered and laminated pale greenstones interpreted as volcaniclastics and minor tuffs(?) (see Fig. 2.2a+b).

A detailed study of the distribution of volcanite units and their volcanic structures and lithogeochemical and mineralogical variations, in surface drill hole D39, shows that the greater part of the middle section of this hole consists of a thick sequence (120-130 m) of massive flows and minor high level intrusions (sills?) (see Figs. 2.3 and 2.4). This massive volcanite unit is flanked on both sides, above and below, by a thin sequence of dark, slightly altered pillowed lavas, of the pre-ore pillowed sequence. These are visibly altered especially within the bottom unit which hosts the Joma massive sulphide horizon at its lowermost contact. The pre-ore pillowed sequence near the orebody has been intensely altered, so much so that in places the original volcanite structures and igneous textures have been completely destroyed.

The altered pre-ore pillowed unit is in sharp contact, both above and below, with a post-ore, paler, pillowed volcanite unit. The uppermost unit, near the top of the drill hole, grades into a somewhat more massive, slightly layered, pale volcaniclastic sequence. Drillhole D39 terminated in pale, post-ore type pillowed metavolcanites which occurs below the ore horizon along the whole length of the mine.

Structural interpretations of the area (this report plus PART I) has shown that in this part of the middle greenstone, the thick massive flows forms the central core of a large recumbent isoclinal D_2 fold and thrust structure. The fold closure occurs up in the air above the Joma orebody. Thus the paler, pillowed sequence - occurring at the top and bottom of drill hole D39 - are interpreted as being the same post-ore unit, folded around the central pre-ore massive lava and pillow lava sequence.

2.2.3. Classification into groups.

From detailed surface mapping, drill core descriptions, litho-geochemical and mineralogical studies and structural interpretations, a probable volcanostratigraphy has been recognized and subdivided into major units, A to D. These are described from A to C in their interpreted proper stratigraphic position and are:

C_2 - laminated volcaniclastics
C_1 - post-ore pillowed sequence

B - pre-ore pillowed sequence
A - pre-ore massive volcanite sequence.

Group D comprises greenstones distal to the Joma area and not directly corresponding to the middle greenstone.

Fig. 2.4 shows the schematic volcanostratigraphy for the middle greenstone. The Joma ore horizon occurs at the interface between two locally major volcanite complexes.

The older, pre-ore volcanites, forming the structural hangingwall (HW) to the ore horizon, have been subdivided into a central part comprising massive flows and/or high level intrusives or sills (unit A) enveloped by and grading into a laterally extensive pillowed lava - pillow breccia sequence (unit B).

The younger, post-ore volcanite complex (unit C), forming the structural footwall (FW) to the ore zone, consists of a thinner pillowed lava and pillow breccia unit (sub-unit C_1). This unit contains minor, thin bands and lenses of white limestone and magnetite bearing, dark grey quartzites. It grades rapidly, both laterally and stratigraphically upwards, into a thicker sequence of layered to laminated pale greenstones which represent volcaniclastics and minor tuffs (sub-unit C_2). The laminated sequence often contains thin bands and lenses of limestone, grey phyllites and dark, graphitic phyllites and grades quickly into a thicker sequence of quartz rich graphitic phyllites and layered - quartzite-phyllites in which some minor pale green tuff horizons are still visible.

2.2.4. Group Descriptions.

The major units recognised in the proposed volcanostratigraphy will be described beginning at the bottom, Group A, and going up the stratigraphy to Group C, and ending with Group D, the distal greenstones (see Fig. 2.4).

The strongly hydrothermally altered pre-ore, host rock lithologies found within the immediate hangingwall to the orebody are subdivided into units, B_1 to B_6 and are described in section 4, p. 49-78 of this report.

a) Group A: Massive volcanite complex.

The massive greenstones are almost wholly confined to the sub surface parts west of the mine area, occurring in the central parts of diamond drillholes D39, D32 and D18, and to the south of the open pit area, south of drillholes, D64 and D65 (e.g. whole rock sample locality JD-5/84) near the bend in the river. These massive volcanites represent the central core of a massive flow- and intrusive sill complex showing a maximum thickness of c. 120-130 m in drillhole D39 (see Fig. 2.3).

The individual flows, roughly 2-3 m in thickness, are characterized by their chilled margins, both tops and bottoms, and their medium grained holocrystalline to micro-gabbro textured central parts. The flows are usually separated by layers, a few cm to 50 cm thick of dark chloritic hyaloclastitic material. Quartz and epidote filled amygdales occur generally only on one side of the individual flows. These are interpreted as marking flow tops.

The intrusive bodies (sills?) are thicker, generally greater than 3 m, and are notably coarser grained (0.5 - 1 cm) than the flows (0.03 - 1 mm). Coarse grained meta-gabbroic dykes (50 cm 1.5 m thick) have also been observed. In less deformed areas, the thicker intrusives show sharp contacts with the surrounding flows and pillowed lavas. Small (1 m or less) xenoliths of fine grained volcanites are often found along the intrusive contact area. These are often hornfelsed(?), completely metasomatized and converted to a massive mat of coarse grained, pale Mg-chlorite and coarse actinolite. Sulphides are not observed in these pale Mg-rich chlorite schists.

The massive flows are distinctly coarser grained than the surrounding pillowed lavas, and in less deformed, well preserved parts, the coarser micro-gabbroic holocrystalline parts have a speckled appearance caused by the contrast between the pale feldspars and the dark chloritized original pyroxenes. The massive units often show good primary igneous textures, ophitic to subophitic intergrowths, and the coarse grained varieties show poikilitic intergrowths between original pyroxene and ilmenite, now represented by dark chlorite and leucoxene or sphene respectively (see Microphoto 3 APPENDIX I).

The massive units are also distinctly darker coloured (10G 4/2 or 106Y 3/2 on GSA rock color chart) than the pillowed sequences, reflecting their high Fe-chlorite content. They often contain trails of large (up to 5-6 cm long) bright yellow epidote knots near the centres of the flows, as well as macroscopic epidote-quartz veins and large pyrrhotite grains which are generally found associated with the dark chlorite matrix and along later fractures.

The massive units vary somewhat in their mineral contents mainly due to zones of intense, secondary hydrothermal alteration and later mineral redistributions (mainly calcite, epidote, chlorite, quartz and pyrrhotite). These redistributions are associated with later deformational and regional metamorphic events such as D_3 shear zones and areas of strong D_3 folding and cleavage. The massive units are composed dominantly of dark Fe-chlorite, actinolite, albite or Na rich plagioclase and lesser amounts of epidote-clinozoisite, calcite, sphene and pyrrhotite, together with trace amounts of quartz and white mica, which are mostly secondary minerals associated with veins and cleavages (see Table B-1 for aveage mineral contents).

Some thicker (10 m) zones of intense hydrothermal alteration have been found cutting through the central parts of the massive volcanite complex (see surface drill holes D18 and D32 from Fig. 2.2a+b. These represent bleaching of the original rock and enrichment of both Na_2O and K_2O and of S in the form of po+py. This indicates that the hydrothermal feeder zone also penetrated the massive volcanite units.

b) Group B: Pre-ore pillowed volcanite sequence.
This also includes sub-units B_o and B_1 (units B_1 to B_6 described in section 4).

Laterally adjacent to and stratigraphically above the massive volcanite complex occurs a continuously mappable, pillowed lava and pillow breccia sequence (unit B), which forms the upper levels of the older volcanite complex and corresponds to the strongly altered rocks (units B_1, to B_6) in the immediate hangingwall zone of the Joma orebody. They form a thick continuous pillowed sequence, which can be followed throughout the mapped (subsurface drill holes) area both N-S and E-W past drill hole D61 (see Fig. 2.2a+b). Although strong isoclinal folding and shearing (D_2) have imbricated the area and complicated the details of the volcanostratigraphy, it can be seen that the pillowed sequence (unit B) shows an intimate relationship to the massive lavas (unit A).

The pillowed units are also dark in colour (moderate greenish), similar to the lower massive volcanite units. In the less deformed areas, remnants of well-preserved, close-packed pillows, pillow breccia and hyaloclastite structures can be seen during both surface mapping and drill core inspetion (see Photo 5). The pillows are characterized by their darker chloritic rims and their very fine grained microcrystalline nature. Sub ophitic textures are typical in the less deformed, less altered, massive parts (Microphoto 4 and 5). The dark pillow rims are generally 2-3 cm thick and the individual pillows vary somewhat in size , which may partly reflect the angle at which the viewing surface cuts the pillow. Individual pillows vary between 50 cm and 1 1/2 m in diameter.

Minor, small quartz filled amygdales (referred to as 'quartz eyes' in drill core descriptions) and minor epidote amygdales are also visible in some sections of pillows as 0.5 to 1.0 cm long, lensoid, glassy quartz grains concentrated near the outer rims of the pillows. Pale epidote knots are also diagnostic of the pillowed sections, the knots being mostly concentrated near the pillow centres. These knots are, however, not as large and as strongly coloured as those found in the massive volcanites below. Small epidote-quartz veinlets are recognized throughout the section, except in the sections that have undergone strong hydrothermal alteration (bleaching) up towards the ore zone. Secondary calcite veinlets are also typical of the pillowed sections - especially in areas of intense shearing and fracturing distal to the main alteration zones.

The thin, dark, chloritic pillow-rims represent original glassy chilled margins. These are enriched in both Fe and Ti and originally zoned. They have been devitrified to palagonite and then metamorphosed to Fe-rich chlorites containing characteristic zoned trails of Ti-oxides, leucoxene and sphene (see Appendix p. A-7 for reference to leucoxene). Interstitial to the pillows, in the tricuspate spacing between the individual pillows, the dark altered glassy fragments often form thicker hyaloclastite or aquagene tuff deposits. This material also constitutes the matrix to the pillow breccia units which are often an integral part of the pillowed lava pile. (See Microphoto's 8 and 9.)

The pillow breccia material occur as variably sized (in places almost whole pillows) angular to rounded, paler fragments - with remnants of quartz amygdales and internal epidote knots still visible - set in a darker hyaloclastite matrix. Within the less deformed area the hyaloclastites can be seen to be composed of small, 1 to 2 cm sized, angular fragments, often showing a zoned discolouration which under the microscope can be seen to be due to compositional variations in the Fe-Mg-chlorites and to zones of leucoxene and Fe oxides. The darker coloured zones are richer in Fe-chlorite and Ti oxides. The larger fragments are packed into a fine grained, granular matrix of hyaloclastite. The individual fragments represent glassy pillow rim fragments set in a glassy shard? tuff matrix. These hyaloclastite fragments are, as are the pillow rims, devitrified and altered to Fe-chlorites containing trails of Ti bearing silicates and oxides, generally sphene. The zoned nature and the sphene trails are characteristic for these glassy fragments.

Even in the more altered, pale, Mg enriched, chloritic parts of the hydrothermal system, the zoned nature of the original hyaloclastite remains characteristic and the trails of sphene are still visible under the microscope (see Microphoto's 21 and 22). Sphene is a refractory mineral that is stable under the whole range of greenschist facies metamorphism.

Epidote-quartz veining appears to be more prominent in pillowed lavas, while pyrrhotite disseminations occur as minute, though visible, grains. Pyrrhotite also occurs as fracture fillings along with secondary Fe-chlorite and epidote. Free calcite is often found as a matrix mineral and as zones of calcite filled veinlets and fractures and patches in areas which show strong D_2 shearing and folding and which have been fractured and cleaved during D_3. Calcite is also a prominent mineral distal to the main zones of strong hydrothermal alteration. Large patches of calcite are generally found concentrated within the hyaloclastite deposits in such areas.

Sulphide mineralizations, such as thin (max. 2 m thick) pyrrhotite bearing dark magnetiferous quartzites, representing recrystallized cherty exhalites, occur throughout the lower pillow stratigraphy. However, they do tend to be concentrated at and marking the boundaries between the massive flows and pillow sequences. Thin layers of minor massive pyrrhotite with carbonate and dark chlorite concentrations are also found generally associated within the darker hyaloclastite deposits. Some of this mineralization may be secondary in nature, deposited during both hydrothermal alteration processes or as tectonic-metamorphic redistributions.

Distal mineralization associated with the formation of the Joma ore horizon will be discussed later (section 4).

c) Group C: Post-ore volcanite sequence.
(comprises sub-units C_1 and C_2).

The younger volcanites at Joma can be subdivided into two types, a stratigraphically lower pillow and pillow breccia sequence (sub-unit C_1) and an upper and laterally dominant, layered to laminated volcaniclastic (tuff?) sequence (sub-unit C_2).

Sub unit C_1 - pillowed sequence.

The C_1 pillowed sequence does not appear to be thicker than about 40-50 m, being thicker adjacent to and to the north of the open pit, which contains the thickest part of the massive ore at Joma (see photo 4). The pillowed sequence here grades quickly into pillow breccias and then into an overlying layered volcaniclastic sequence, found structurally beneath to the east.

The C_1 pillowed lavas are distinctly paler and more fine grained to aphanitic in nature compared to the older, Group B, pillowed lavas. They show close-packed pillow structures with characteristic dark rims and very pale pillow centres (see Photo 2). Large epidote and calcite knots are generally concentrated near the centres of the individual pillows. The knots can be quite large but are generally under 30 cm in length. Minute pyrrhotite grains are also visible in these rocks.

Close to the ore horizon, the C_1 pillow laves are distinctly denser and harder, almost flinty in nature, reflecting the higher content of epidote-quartz veining and 'flooding' in the rock. There is also a marked increase of epidote (clinozoisite) and albite within the matrix of the C_1 pillows adjacent to the massive ores (see Microphoto 6). The pillowed and massive pale lavas immediately adjacent to and forming the footwall to the massive ore horizons, often have tectonic thrust boundaries, and contain a strong secondary foliation and increased albite, epidote, white mica, quartz and pyrrhotite contents. These have been subdivided as sub-unit C_{1-b} (see Microphoto 7). The anomalously high contents of ab+ep+po$\pm$qtz within the C_{1-b} unit compared to C_1 are probably due to secondary tectonic mobilizations (e.g. the pale footwall greenstones in the 385 vf.s. strosse area), (see Table B-2, APPENDIX).

The C_1 volcanites generally have a much greater content of free calcite and clinozoisite than the older volcanites (groups A+B) both within the matrix and as visible secondary veins and fracture fillings and, especially, as large knots and layers between the pillows. Some large white limestone bands and isolated lenses (often tectonic) are found within the pillowed sequences adjacent to the ore zone. These can be up to 1 1/2 - 2 m thick in places as on the 429 level (see profile X95000-X94960).

Isolated lenses and bands (1-2 m thick) of dark, magnetite bearing quartzites occur within the lower stratigraphic levels of the younger pillowed and minor massive volcanite sequence, adjacent to the main ore zone in the immediate footwall (see photo 3). These probably represent original Fe-rich cherty exhalites. Magnetite bearing grey to black quartzites within the 402 ÖL synk area (coordinates, X=94971, Y=31515, Z=362) are associated with ca. 50 cm thick bands of pale green carbonate-epidote and dark Fe-chlorite rich layers.

Both the greyish quartzite lenses and the white limestone bands have been affected by the D_{1-2} and D_3 deformations. Their lensoid, en échelon, nature and their elongations sub parallel to the main S_2 foliation are due to transportation of these units during D_2. Some of the dark magnetite-bearing quartzites

bear distinctly bleached rims along their edges and adjacent to quartz-calcite veined, D_3 piercement structures that cut them (e.g. bottom of 375 öf synk). Within the bleached parts, the magnetite has been sulphidized and converted to pyrrhotite (see APPENDIX Table C-2, no. 67+68 for chemical analyses). This demonstrates the later deformational and metamorphic effects on the country rocks.

The very pale colouration of the younger greenstones, both sub-units C_1 and C_2 reflects a marked increase in albite, white mica, calcite and clinozoisite contents and lower Fe-rich chlorite and pyrrhotite contents compared to the older (Group A and B) volcanites. Here, clinozoisite (Ca-Al silicate) dominates over epidote (Ca-Fe silicate), whereas, the older, pre-ore darker volcanite units contain mostly epidote, reflecting their higher Fe contents.

Throughout the paler greenstones in both the C_1 pillowed sequences and the C_2 laminated greenstones, large, distinct veins and tension gashes filled with quartz-calcite-clinozoisite and minor chlorite occur along S_3 cleavages axial planar to the large D_3 assymetric folds. These large veins are diagnostic for the younger footwall pale greenstones within the mine area.

Sub-unit C_2: layered - laminated pale greenstones.

Stratigraphically overlying and structurally underlying and to the east of the C_1 pillowed lava and pillow breccia sequence, occurs a thick sequence of well-layered to laminated greenstones (see C_2 unit in Fig. 2.2 and 2.4). This pale, well-layered sequence forms a thicker series of irregularly layered volcaniclastics and tuffs (?). The individual layers vary somewhat in thickness, from cm to m, but generally from cm to dm in thickness. The layers vary greatly in composition and colour; the paler, more resistant, less weathered layers are composed dominantly of albite, clinozoisite and minor white mica and quartz, whereas the darker less resistant bands are composed mostly of chlorite, actinolite and calcite, lesser sphene and disseminated pyrrhotite.

Thin layers of grey phyllite and dark graphitic phyllite are often found interlayered within the laminated greenstone, forming in parts a prominent banded greenstone-phyllite sequence. More distal to the mine area, the layered sequence thins and thicker units of both graphitic phyllites and bands of layered cherts occur. There is a complete gradation, both stratigraphically upwards and laterally between the layered greenstones with minor graphitic phyllite and layered cherts into mainly graphitic phyllites and layered quartz-phyllites with minor thin layers of pale greenstone (tuffs?).

The well-layered, pale greenstones probably represent a water lain tuff, in part volcaniclastic, sequence judging from their total lack of igneous textures and their felted, massive, character under the microscope. They were probably deposited under near surface conditions judging from their high carbonate contents, possibly above the calcium compensation depth (CCD). No coarse grained volcaniclastic deposits have been observed within the layered sequence of the Middle greenstone, suggesting the lack of major uplift and erosion or episodes of rifting during the deposition of the C_2 tuff sequence.

Distal to the mine area, the layered volcaniclastic - tuff sequence is distinctly thinner, reflecting the longer transport distance from a central volcano. Minor, thin layers of massive pyrrhotite, carbonate, chert, pale tuff and thin graphitic phyllites are found associated with white mica rich schists near the contact to the black phyllites and quartz-phyllite. At this level, distal to the Joma ore horizon, thin layers rich in quartz, minor garnets and carbonate have been observed in drill holes D61 and D59. Similar garnet rich, quartz, white mica and carbonate rich lithologies have been observed in a similar position within C_2-like stratigraphies at the road junction to Røyrvik village (see Fig. 1.2) and have also been described from the Borvasselv mineralized stratigraphy by R. Horbach (personal communication, 1985).

d) Group D: Distal Greenstones.

Regionally, the Røyrvik Group greenstones, of which the three greenstone belts at Joma are a central part, forms a laterally extensive thin belt of more or less continuous metavolcanites that stretches from south of Tunnsjø lake, where it plunges beneath the overlying Gjersvik Nappe, through Joma and the Røyrvik village, and to the north around the western edge of the Børgefjell basement window (see 1:1 M geological map of Norway, NGU 1984). Regional studies and geochemical studies (this report) from; 1) Røyrvik village, 2) Solberg - east of and between the lakes Limingen and Tunnsjø, to the south of Joma and 3) the outer greenstone (Orklumpen), show that this extensive greenstone belt is mainly part of a pillowed sequence which is intimately related to a prominent sequence of layered quartzites and phyllites (recrystallized ribbon cherts) and graphitic phyllites. The pillowed sequence appears to be stratigraphically overlain by a thin sequence of layered volcaniclastic (tuffs?) and greenschists.

These distal greenstones are homogeneous, mildly spilitized, mafic metavolcanites which are typically fine grained to aphanitic in nature and pale coloured, reflecting the dominant pale chlorite, actinolite and albite mineral contents and the minor amounts of epidote and free calcite. In less deformed areas, they show well preserved ophitic to sub ophitic microtextures and contain clusters of minute leucoxene grains(?) (microscopic intergrowths of sphene and Fe-oxides) which is a typical alteration product of the original ilmenite grains (see Microphoto's 1 and 2). The original basalt precursor was probably characterized texturally by a sub ophitic intergrowth of olivine, plagioclase and pyroxene, with small amounts of ilmenite as tiny included grains.

2.2.5. Greenstone Lithogeochemistry.

A significant number of samples of metavolcanites from the middle greenstone complex and Røyrvik Group greenstones distal to Joma have been analysed for whole rock silicate, major and trace element contents (APPENDIX Tables B-2 to B-8). These data have been used to compare these groups and define the petrochemical

character for each of them. Their trace element distribution has been used to define their tectonic environment of deposition. The 'so-called' incompatible elements (Ti, P, Zr, Y and Cr) and the major element Al are considered to be immobile during low grade hydrothermal activity (i.e. spilitization) and have therefore been used to classify the volcanic rocks at Joma.

The groups will be described from A to B, C and D going up the proposed volcanostratigraphy succession. This will outline the progressive development of the Røyrvik Group volcanic complex at Joma.

Group A.

The unaltered parts of the Group A - massive volcanite complex - show a typical highly differentiated ferro-basaltic composition, being strongly enriched in both Fe and Ti (as well as P, Zr and Y) and depleted in Mg and Cr, compared to the other groups at Joma. This is thought to represent a primary magmatic differentiation trend judging from the relationship between the incompatible elements (see Fig. 2.6 to 2.8). Well preserved igneous textures also indicate that little hydrothermal elemental redistribution or metasomatism has occurred in these rocks.

The ferro-basaltic nature of Group A is well documented on a $MgO-FeO^{tot}$ - CaO diagram (Fig. 4.10 and 4.11), when compared to the magmatic differentiation trend (Mg basalts to rhyolites) of fresh rock series from Mid-Oceanic Ridge systems (i.e. Iceland, Galapagos).

Group B.

The Group B pillowed metavolcanic series are chemically and mineralogically similar to the Group A massive volcanites. They show however, a gradation towards a hybrid facies which is transitional between the Group A and Group C series. This transitional facies contains less Ti, Zr and Y and more Cr than the more differentiated Group A ferro-basalts (see Table 4.1, Section 4) and may represent magma mixing from the different magma sources which have formed the two (Group A and Group C) volcanite series.

Group C.

The younger, post-ore, Group C metavolcanites are chemically distinct from the older, pre-ore Group A and B metavolcanites. They contain notably less Ti, P, Y and Zr and higher contents of Cr than the older volcanites. On a Ti-Zr-Y discriminant diagram (Fig.2.8) they plot well within the OFB (ocean floor basalts) field showing N-MORB affinities and probably represent a deeper more primitive mantle source than do the Group A + B series.

Trace element contents of the massive layers within the C_2 layered volcaniclastic tuff(?) sequence are similar to the C_1 pillowed sequence, suggesting a similar magma source for these two units, whether as original tuffs associated with C_1 pillow lava formation or as secondary erosional products derived from an earlier deposited pillow sequence (C_1).

Group D.

Petrographically, the distal greenstones show a homogeneous metabasaltic, mildly spilitic composition (see Fig.2.5 and TABLE 4.1). They are slightly alkaline, Mg-rich metabasalts with trace element distributions (Ti-Zr-Y and Cr) indicating that they are typically WPB (Within Plate Basalt) in character, having both high TiO_2 (>2%) and Cr (500-600 ppm) contents. The Group D series are transitional between the Group (A + B) and Group C series and may represent mixing between the magma sources for the two volcanite series.

Group A type ferro-basalts and Group C type low TiO_2, high Cr bearing metavolcanites have not been recognized distal to the Joma area.

2.2.6. Summary and Geotectonic Environments.

Group's A + B + D metavolcanites are easily distinguished from the Group C series on Ti-Cr (Fig.2.7) and Ti-Zr-Y (Fig. 2.8) discriminant diagrams and on a major element $MgO-FeO^{++}$ - CaO plot (Fig. 4.10).

Chemically, the basic metavolcanites of the Røyrvik Group have a tholeiitic to alkaline character and show both N-MORB (Group C) as well as E-MORB or WPB affinities (Group B+D). Olsen (1980) concluded that the Joma greenstones were deposited near to or at a continental margin under shallow water conditions, within a back arc basin rather than a large oceanic type basin. Recent work by Stephens and Gee (1985) and Reinsbakken (1986) concluded on the basis of the regional geological setting and the metavolcanite geochemistry that the Røyrvik Group metavolcanites and their equivalents in Sweden (Remdalen Group) represent the upper and probably off-axis segment of the ocean floor to a rifted arc complex.

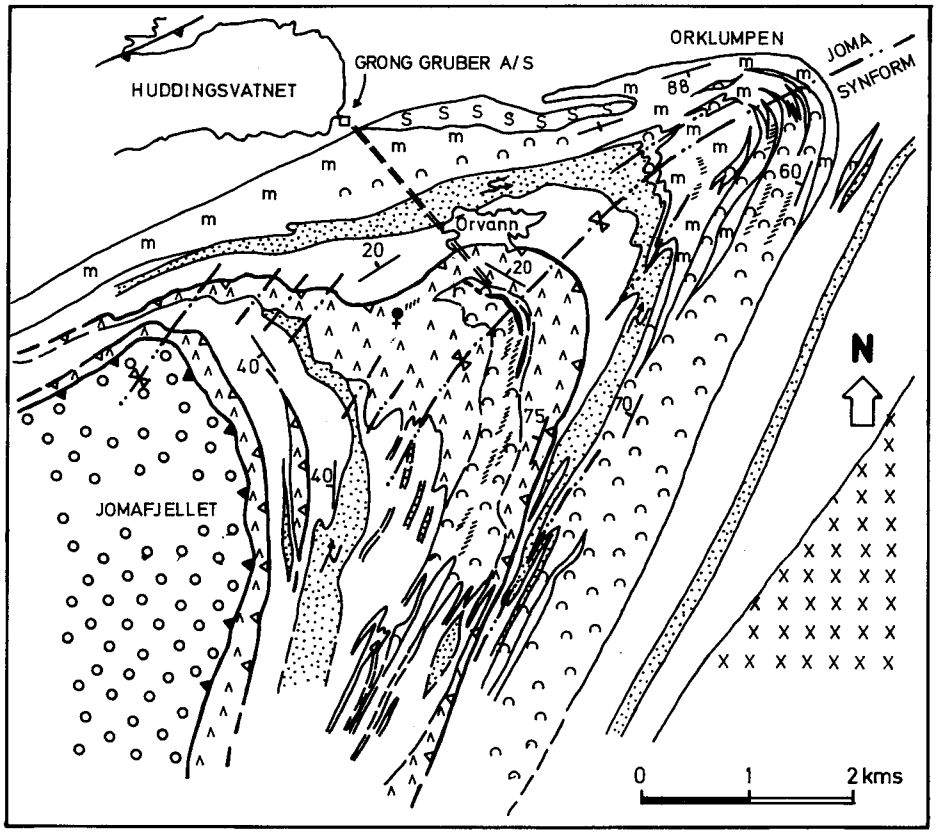

KEY

- Metasediments — Limingen Group — GJERSVIK NAPPE
- Graphitic phyllite
- Quartzitic phyllite
- Volcaniclastic greenstone
- Pillowed greenstone
- Massive greenstone
- Brakkfjell phyllite
- Röyrvik Group — LEIPIKVATNET NAPPE
- Serpentinite
- Outcrop of Joma sulphide deposit
- Rusty disseminated sulphide zones
- Sulphide showing
- Major thrust contacts to Leipikvatnet Nappe
- Minor thrusts within Leipikvatnet Nappe
- F3 fold trace
- F2 fold vergence, arrow indicates plunge
- Average dip of S2 cleavage

Fig. 2.1a. Geological map of the Joma area showing the distribution of the inner, middle and outer greenstones within the Joma synform, from SW to NE respectively. The position of the Joma ore body within the pillowed volcanites of the middle greenstone is shown. Note the traces of rusty disseminated zones to the SSW of the Joma ore body. Similar rusty zones also occur on the west side of the outer greenstone (Orklumpen). Modified after Kollung (1979) and Odling (this project, PART I).

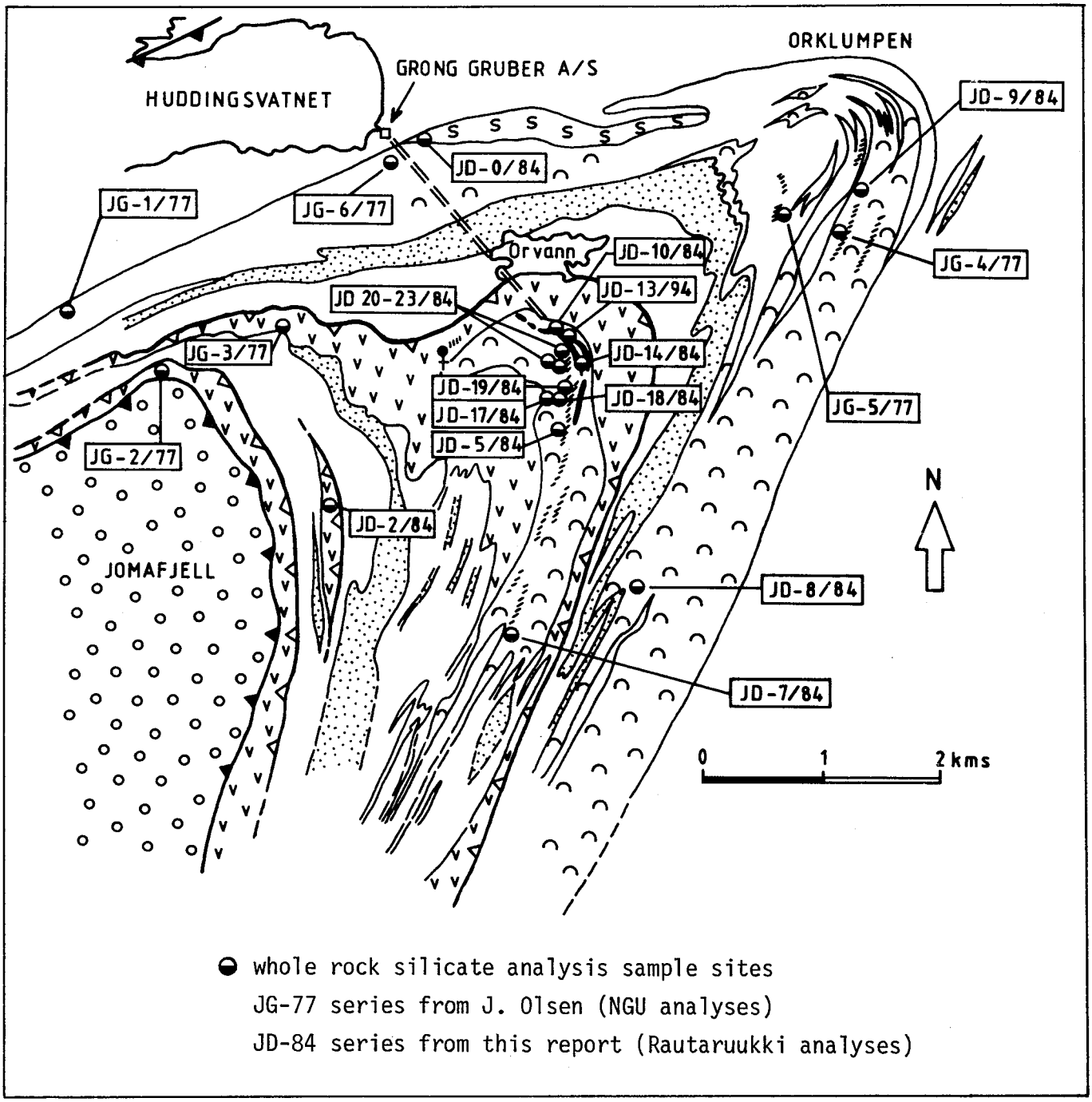

Fig.2.1b. Sample location map of the proximal and distal whole rock greenstone samples taken from the three greenstone units within the Joma synform. Geological base and legend is the same as for Fig. 2.1a.

JOMA SURFACE GEOLOGY AND DRILL HOLE VERTICAL PROFILES

LEGEND

POST-ORE VOLCANITES

Pale greenstones, epidote + calcite rich, minor pyrrhotite dissem.

Massive sulphide horizon + surface trace / thin sulphide bands, lateral extensions

PRE-ORE VOLCANITES

Undifferen., med.to dark green, chlorite + epidote rich, altered greenstones, pyrrhotite dissem. Includes massive ferrobasalts

Strongly altered pale greenstones + schists, alb+ser+Mg-chl+act rich, strong pyrite veining + dissem.

GF/QF — Porphyroblastic white mica bearing, pale schists / Dark graphitic phyllites / Layered quartz-phyllites

VOLCANIC STRUCTURES

- +++ - massive flows + intusives (ferrobasalt)
- ∩∩∩ - pillows
- △△△ - pillow-breccias + hyaloclastites
- \\//\\/ - actinolite porphyroblastic
- vvv - layered volcaniclastics
- ≡≡ - strongly schistose + layered
- //////// - rusty, sulphide dissem. zones

STRUCTURAL SYMBOLS

- major D2 thrust
- minor D2 thrusts + shear zones
- S2 schistosity
- S3 cleavage
- F2 fold axis
- F3 fold axis
- L2 lineation
- L3 lineation

SYMBOLS

- ..... - electromagnetic anomaly trace
- D39 - surface diamond drill hole location
- - whole-rock sample locality
- - bedrock outcrop pattern
- - river with flow direction
- - roads
- - buildings
- A——A' - vertical profiles

Scale: 0 100 200 300 400 m.

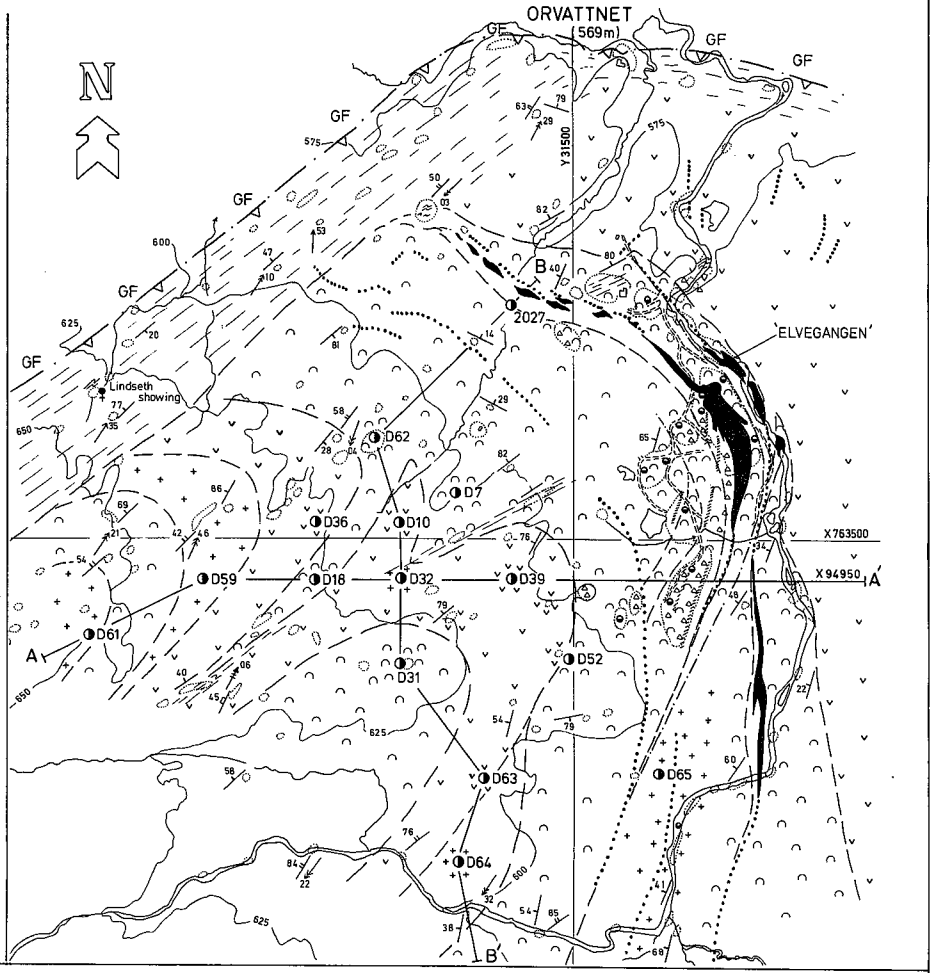

AR/86

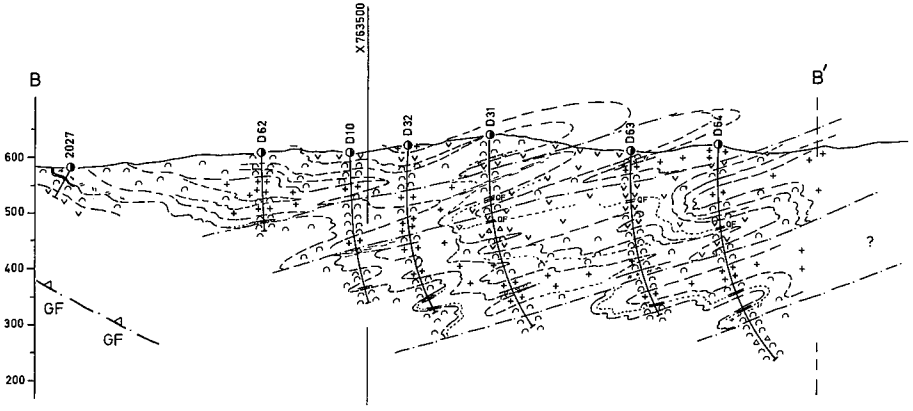

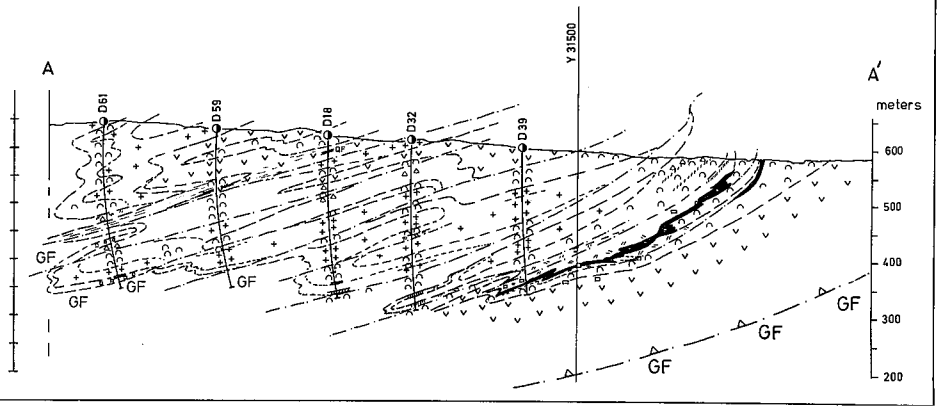

Fig. 2.2a. Geological map of the Joma mine area (1:5000 base) with horizontal trace of the massive ore lenses and the boundary of economic ore. Shows locations of the surface DDH that were logged and sampled for whole rock analyses. Vertical profiles (for Fig. 2.2b) are shown A-B and C-D.

Fig. 2.2b. Vertical profiles A-B and C-D, from Fig. 2.2a, with surface diamond drill holes and major volcano-lithological boundaries. The main ore horizon in profile A-B is a composite from profiles X94900 at bottom levels of mine, X94960 at 416, 429, 447 levels and X94980 at 480, 495 and 520 levels up to the surface.

Fig. 2.4. Proposed volcanostratigraphy for the Middle Greenstone at Joma (not to scale).

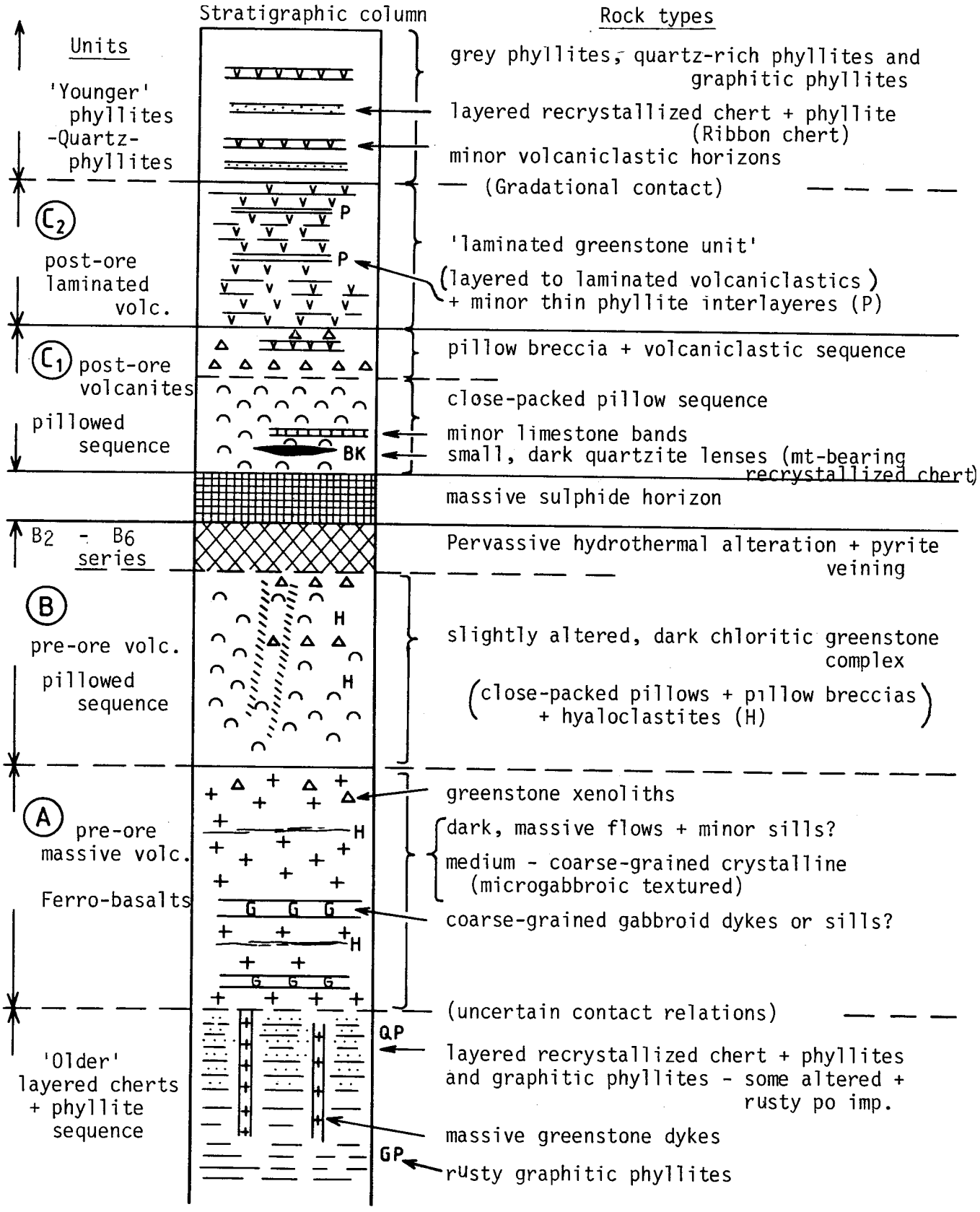

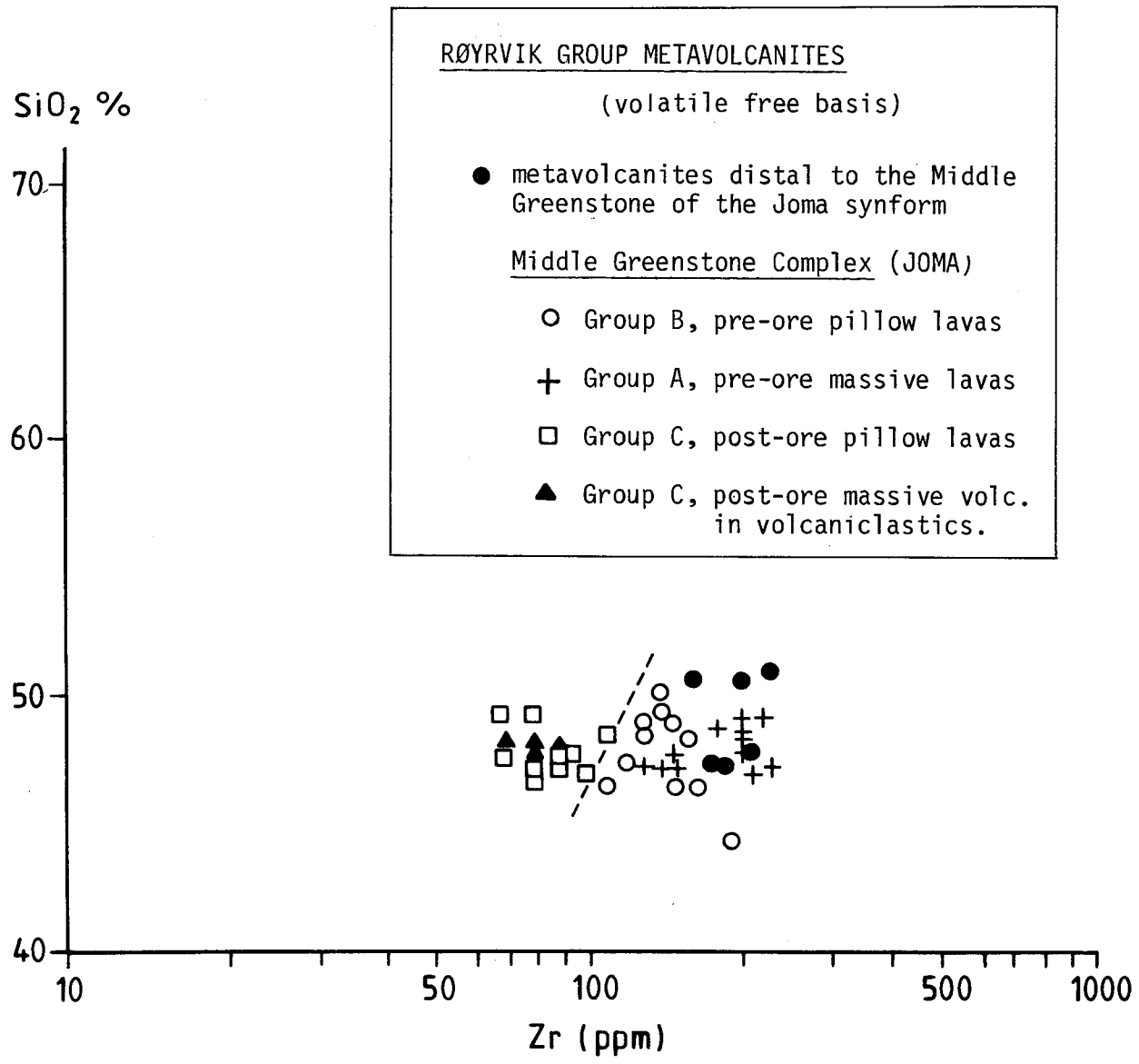

Fig. 2.5. SiO_2 vs Zr plot for the Røyrvik Group metavolcanites, both proximal and distal. Note the metabasaltic nature of greenstones and the separation between the pre- and post-ore volcanite sequences. All data for this and following plots (to Fig. 2.8) are from Appendix Tables B-2, B-3, B-4, B-5, B-7 and B-8.

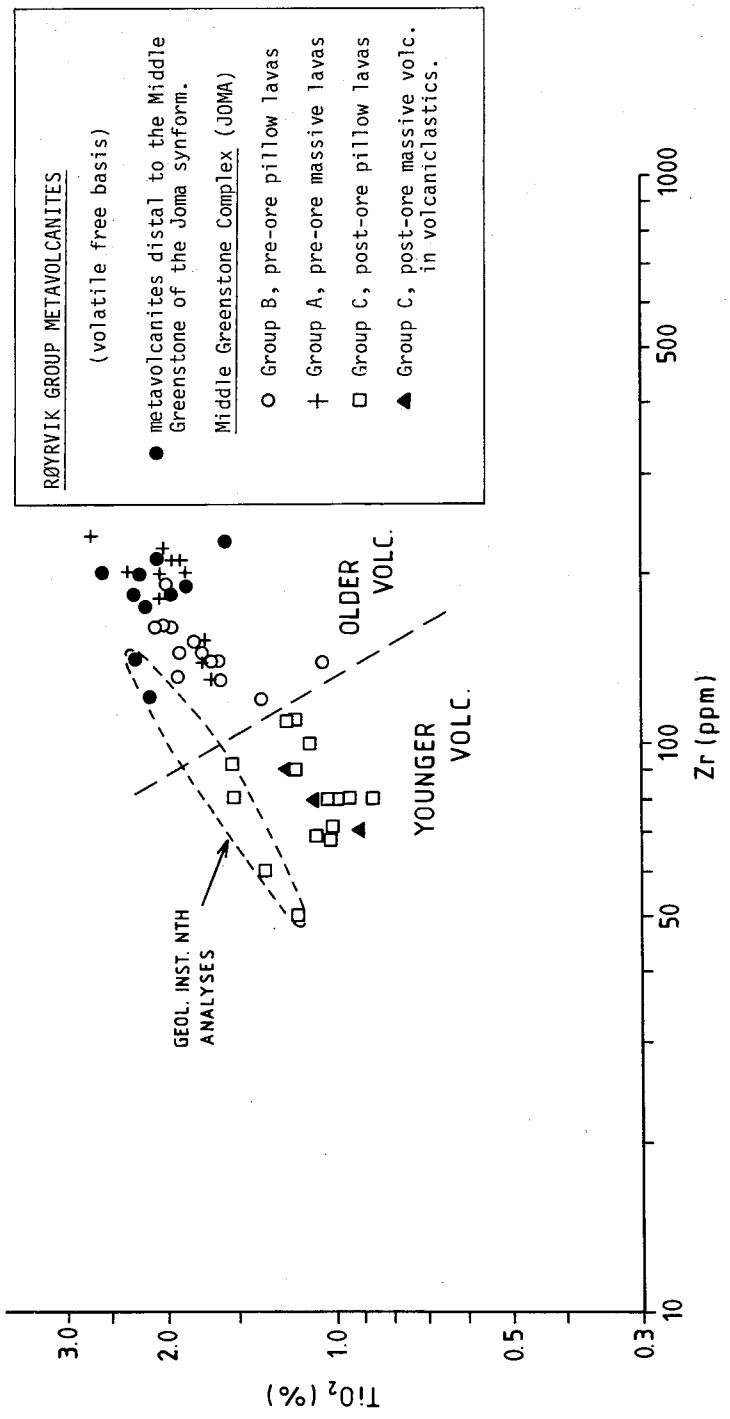

Fig.2.6. TiO_2 vs Zr plot for the Røyrvik Group metavolcanites, showing good separation between the younger (post-ore) and older (pre-ore) volcanites. Note the spread in data between the two laboratories used - The Geol. Inst., NTH analyses show a consistantly higher Ti content at constant Zr compared to the Rautaruukki analyses.

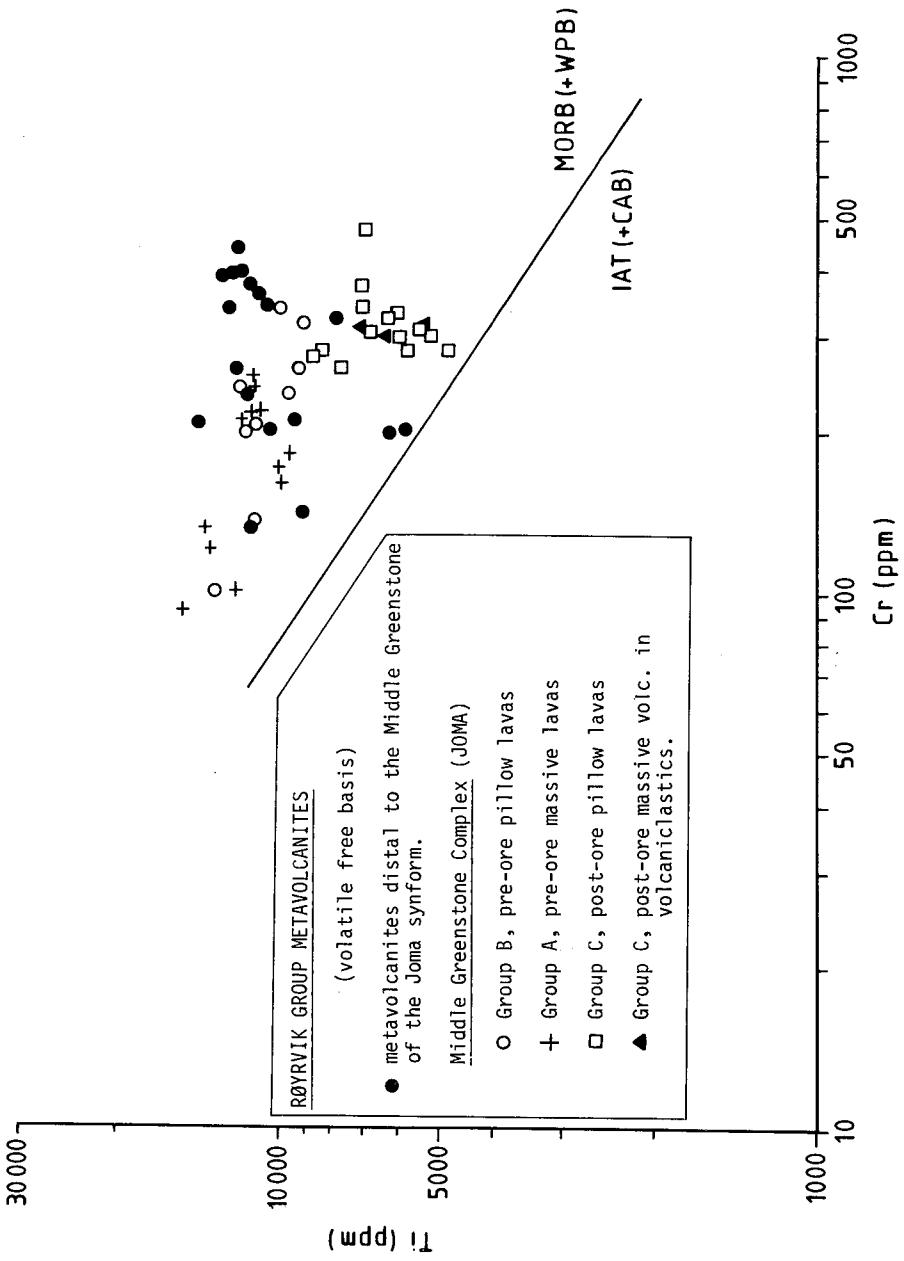

Fig. 2.7. Ti vs Cr plot for the Røyrvik Group metavolcanites showing the MORB nature of the volcanites and the separation between the pre-ore and post-ore volcanites. Note the strong differentiation trends, high Ti and low Cr in massive ferrobasalts and high Cr - low Ti in the more primitive post-ore volcanites.

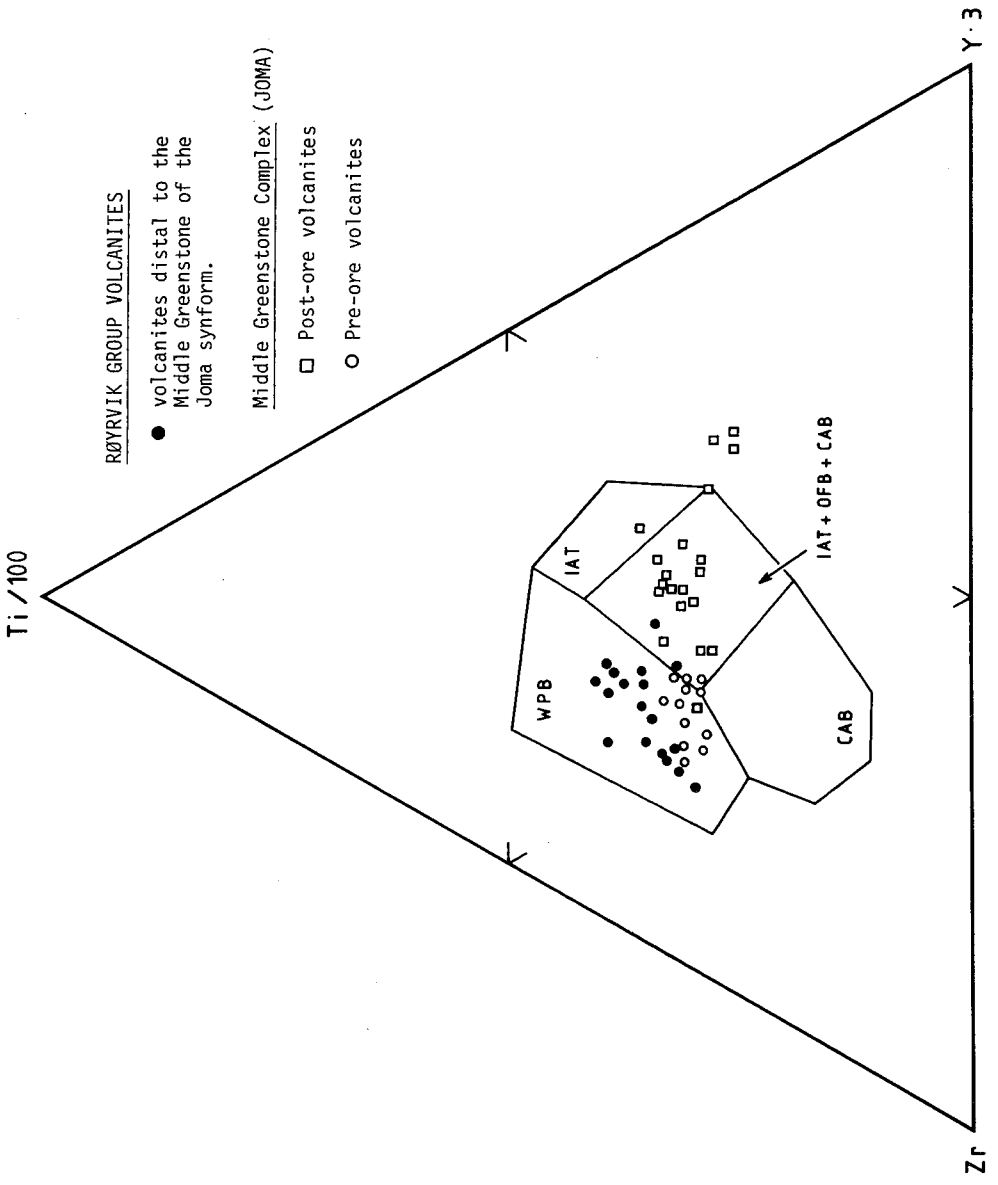

Fig. 2.8. Ti-Zr-Y discriminant diagram for the Røyrvik Group metavolcanites. The distal greenstones (D) show a good WPB affinity and the post-ore volcanites (C) show an OFB or MORB affinity. The pre-ore volcanites (B) show a slight transitional trend between the WPB and OFB fields.

SECTION 3 SPILITIZATION AND SUB-SEAFLOOR CONVECTIVE HYDROTHERMAL SYSTEMS

3.1. INTRODUCTION

Before discussing the host rock lithologies at Joma and the hydrothermal alteration facies that occur within the 'stringer feeder zone' stratigraphically beneath the massive orebody, it will be beneficial to define and summarize the most recent research done on spilitization or sub-seafloor hydrothermal alteration processes, when sea water reacts with basalt at elevated temperatures. These processes are going on today beneath the recently discovered submarine hot springs ('white and blacksmokers') on the mid-oceanic axial ridge systems. Much of the following data is taken from Humphries and Thompson (1978) and Mottl (1983) without being directly quoted as such.

"Spilitization" is defined in the Glossary of Geology as "hydrothermal albitization of a basalt to form a spilite" and "spilite" as "an altered basalt characteristically amygdaloidal or vesicular in which the feldspar has been albitized and is usually accompanied by chlorite, calcite, epidote, chalcedony, prehnite, or other low-temperature hydrous crystallization products characteristic of a greenstone. Spilite often occurs as submarine lava flows and exhibits pillow structure".

Earlier researchers such as Miyashiro (1968) and Miyashiro et al. (1971) connected spilitization to seafloor weathering and metamorphism, while Vallance et al. (1960, 1969) confined most of their studies to greenstone terrains and ophiolite suites, now on land. It was not until the great ocean drilling programs (LEG.)? on the Mid-Atlantic and Indian Ocean Ridges, that reseachers were able to study recent and presently forming spilites from the ocean floor.

In the past 10 years, an increasing amount of data has been accumulated on the chemical transfers and mineralogical transformations that occur when sea water reacts with basalts at elevated temperatures and pressures. This has been used along with geological and geophysical data to deduce the typical structure and evolutionary sequence for hydrothermal systems within the oceanic crust along the axis of the mid-ocean ridges. Direct observations have been made on springs that emanate warm, or hot water on the seafloor along the axes of the Mid-ocean ridges (e.g. Galapagos, East Pacific Rise and the Rekjanes geotherms on Iceland). The chemistry of these springs has been used to infer the alteration conditions deep within the geothermal system. These inferences were made especially in comparison with results of laboratory experiments reacting sea water with mid-ocean ridge basalt under elevated temperature and pressure (Bishoff and Dickson, 1975, Mottl and Seyfried 1980, and Mottl and Holland 1978).

Additional constraints on the structures and frequency of subseafloor hydrothermal systems were derived from modeling based on geophysical data, particularly heat-flow data (Lister, 1972) and from geological observations both from seafloor (Rona 1980, Cyamex 1981) and from ophiolite complexes (Spooner and Fyfe 1973, Coleman 1977).

Another source of information about the nature and deep structure of these systems is from hydrothermally altered rocks dredged up from the oceanic crust of the ridge systems (Mid-Atlantic Ridge and Indian ocean). These rocks show metamorphic grades ranging from zeolite to amphibolite facies but are heavily dominated by greenschist facies metabasalts. Metabasalts dredged from active oceanic ridges have the following mineralogies; albite, actinolite, chlorite, epidote, quartz, sphene, hornblende, tremolite, talc, magnetite and nontrolite.

Greenschist facies metamorphism of oceanic basalts during hydrothermal circulation at the mid-ocean ridges results in considerable mineralogical (and chemical) changes. The major mineralogical transformations during alteration of basalts are:

1) Plagioclase ⟶ albite + chlorite
Plagioclase ⟶ albite + epidote

2) plagioclase + pyroxene ⟶ chlorite + epidote

3) Olivine ⟶ chlorite (+ pyrite)

4) pyroxene ⟶ actinolite

5) glassy matrix ⟶ chlorite - actinolite intergrowths

6) ilmenite ⟶ leucoxene (sphene + Fe oxides or sulphides)

The chemical changes in metabasalts and metadiabases dredged up from the ocean floor and mid-oceanic axial ridge escarpments have been studied by Humphries and Thompson (1978). They divided these into four metamorphic categories; seafloor weathering, zeolite facies, greenschist facies and amphibolite facies, in order of increasing grade of metamorphism.

During weathering at ambient bottom water temperatures (ca. 4°C) Ca, Mg and Si are lost from the basalt, while H_2O and K increase in concentration. During zeolite facies metamorphism the only major changes in chemistry are uptake of H_2O and Na and some loss in Ca (Aumento et al. 1971, Miyashiro et al., 1971). The few chemical compositions available on amphibolites suggests that apart from H_2O, the chemical composition does not greatly change during alteration to amphibolites.

From the frequency of metamorphic rock types dredged from the ocean floor it is clear that greenschist facies metabasalts by far exceed the zeolite facies and amphibolite facies rocks.

The hydrothermally altered pillow basalts dredged from the Mid-Atlantic Ridge, and belonging to the greenschist facies have been studied by Humphries and Thompson (1978) in order to determine the mineralogical, and corresponding chemical, changes that result from basalt-sea water interactions. The mineralogical transformations are predominantly albite-actinolite-chlorite-epidote assemblages.

Quartz and pyrite and occasionally Cu-Fe-Zn sulphides are common accessory minerals found often in veins. On the bases of their mineralogy, the samples can be divided into chlorite rich (>15 % modal chlorite and <15% modal epidote) and epidote rich (>15 % modal epidote and <15 % modal chlorite) assemblages. The chlorite rich assemblages, which are the most prominent variety, show the greatest chemical changes, having gained significant MgO and lost CaO during chlorite formation. The epidote rich samples show very little changes in composition compared with their basaltic precursor, only small changes in CaO+MgO being recorded.

3.2. FACTORS GOVERNING HYDROTHERMAL ALTERATION

The main factors govering the degree of hydrothermal alteration within the oceanic crust are:

1) depth of sea water penetration
2) permeability of the rock
3) time
4) temperature and
5) pressure.

Mottl (1983) contends that there is a fair consensus that 2.5-4 km (max. 5 km) is a reasonable depth of penetration for a convective hydrothermal cell (see Fig. 3.1). The alterations require the presence of a magma chamber at a shallow crustal level to supply the neccessary heat.

The amount of rock that comes into contact with the circulating sea water depends on the permeability. This is the governing factor for the sea water/rock ratio that is central in Mottl's model (see later, pp. 39). Microfractures in the upper layers of fresh basalt extruded onto the seafloor allow pervasive circulation of sea water through the upper layers of fresh rock. Within the pillow basalt and flows, which probably have a total thickness of 1 to 2 km in typical crust, the uppermost crust at spreading centres is highly porous, estimated at 15 to 20 % to a depth of at least several hundred meters.

However, these cracks will be closed by precipitation of vein minerals or by expansion of the rock during the formation of hydrated alteration products. Hydrothermal circulation will then be controlled by the major faults and fractures in the rocks. In these situations the only rocks to be altered by reaction with sea water will be adjacent to the flow path of the fluid. In many cases only the outer few centimeters of a pillow will be altered and the interior will show very little alteration.

These phenomena are all time dependent. Mottl (1983) argues that magma chamber developments are episodic events. The periodicity of volcanism inferred for the Mid-Atlantic Ridge shows that the individual flow units probably formed in less than 100 years. Each of these periods of volcanism, which may represent times of magma chamber formation and growth of crust, was followed by a period of quiescence averaging 5,000 yr., more than ample time to cool a small to medium-sized magma chamber by convective hydrothermal circulation. Mottl also states that given the rate of Fe delivery to the seafloor via ten black-smokers, about 2,000 yr. would be required to form the largest (15×10^6 tons) massive sulphide ore deposits in the Troodos ophiolite on Cyprus if all Fe is deposited locally.

One of the principal variables affecting the degree of metamorphism is temperature, which may vary from a few hundred degrees centigrade to ambient bottom water temperatures (c. $4^{\circ}C$). For a sub-seafloor hydrothermal system, a reasonable range for the greenschist facies is about $250^{\circ}C$-$450^{\circ}C$. Allowing for adiabatic cooling, the temperature at the base of the upflow zone is probably in the range of $350^{\circ}C$ to $375^{\circ}C$ for typical axial hydrothermal systems. These temperatures fall in the middle of the range estimated for the greenschist facies.

3.3. SEA WATER AND BASALT REACTION EXPERIMENTS

Prior to the discovery of the seafloor hot springs in April 1979 (see Edmond and von Damm, 1983), numerous experiments reacting sea water with mid-ocean ridge basalts had been performed under various conditions of elevated temperatures (25-$500^{\circ}C$),

pressures (1-1000 bars), sea water/rock ratios (1-125) and time durations, in order to predict the resulting chemical and mineralogical changes during the hydrothermal alteration. These experimental results have been compared to conditions occurring within the basalt-sea water hydrothermal systems on the Galapagos Rift at 86°W, the East Pacific Rise at 21°N and the Rekjanes Penninsula on Iceland (Mottl and Holland 1978).

The experiments nearly duplicated the chemistry of high temperature solutions feeding the submarine and subaerial systems but have been less successful in reproducing the secondary mineral assemblages found in the natural systems, probably due to kinetics and elemental diffusion during metamorphic differentiations. The order of alteration of the primary mineral phases, however, generally matches those in natural samples.

The most characteristic feature of basalt-sea water interaction at elevated temperatures is the rapid removal of Mg^{2+} from sea water into secondary solids such as smectite, chlorite, tremolite-actinolite or talc in temperature ranges of 70-500°C. At 150°C and above, almost complete removel of Mg^{2+} from sea water occurs at sea water/rock ratios as great as 50; "basalt undergoing alteration has the capacity to remove all Mg^{2+} from an amount of sea water as great as 50 times its own mass" (Mottl, 1983). Mg^{2+} removal occurs rapidly at 150°C and above, leaving behind H^{+} in solution. H^{+} generation is rapid, and the pH falls dramatically. When Mg^{2+} concentrations drop to a low value, H^{+} is rapidly consumed by silicate hydrolysis reactions and pH rebounds to near neutrality. Most of the H^{+} generated by Mg uptake in the rock is consumed locally (by silicate hydrolysis) and the rock experiences both acid and near neutral conditions alternately during its alteration, with highly acid conditions ultimately prevailing as the effective sea water/rock ratio approaches a value of 50 or more. The low pH moves the solution outside the stability fields of all but the most acid resistant secondary minerals. In the sea water dominant experiments, these were mixed layer chlorite-smectite, hematite, quartz and anhydrite.

The removal of Mg^{2+} from sea water is balanced with respect to electrical change in solution by leaching of mainly Ca^{2+} from the rock on a mole for mole basis. About half of the Ca^{2+} leached at 150°C and above combines initially with sea water sulphate to form anhydrite, while the other half remains in solution. Ca in anhydrite may later be returned to solution either by dissolution at lower temperatures or by dissolution accompanying reduction of sulphate to sulphide. At sea water/rock ratios >5 sulphate reduction would play a minor role in the fate of Ca and SO_4 relative to that of anhydrite formation and dissolution.

Some Na^+ as well as Mg^{2+} is removed from sea water at sea water/rock ratios ≤ 5, into secondary albite and analcime. Na^+ removal, as is the case with Mg^{2+} removal, is largely balanced by leaching of Ca^{2+} from the basalt. At sea water/rock ratios >10 Na^+ is leached from the rock along with Ca^{2+}. The net transfer of Ca and Na between rock and solution occurs largely in response to the behavior of Mg due to charge balance constraints.

At 150°C and above, K^+ is uniformly leached from the rock. SiO_2 is generally leached from basalt during hydrothermal alteration <u>but</u>, a considerable portion of it is redistributed within the basaltic pile. The input of silica via this mechanism is controlled by the solubility of quartz or amorphous silica in the circulating fluid (Arnarasson et al., 1974, Mottl, 1976).

Experiments predict that K, Mn, Fe and SiO_2 are leached from the rocks and the Mn, Fe and SiO_2 leaching increases with increasing sea water/rock ratios (Mottl, 1983). Fe enrichments in rocks results from precipitation of pyrite from a fluid that has been leaching Fe elsewhere in the system. Extra Fe was mainly taken up with Mg into chlorite - the principal Mg-rich mineral. The excess Fe may be redistributed locally by response to chlorite formation by such a mechanism as 'metamorphic differentiation'. Al_2O_3 is assumed to be constant during alteration (Humphries and Thompson, 1978) as is the case for the 'so-called' immobile trace elements Ti, V, Cr, Y, Zr.

The continued reactions of sea water with basalts eventually produces a highly evolved hydrothermal solution (end product) rich in metals, H_2S and SiO_2.

By combining the vast amount of experimental data on basalt sea water interactions with data on naturally occurring greenschist facies metabasalt assemblages dredged from the ocean ridge systems and chemical data on the geothermal fluids entering the ocean along these ridges, Mottl (1983) has constructed a model (Fig. 3.2) which predicts the greenschist mineral assemblages in equilibrium at varying sea water/rock ratios under the reaction. Mottl's model was constructed on chemical data from experiments at 300°C and varying sea water/rock ratios; 1, 3, 10, 50, 62 and 125, combined with data on mineral assemblages and mineral compositions from naturally occurring greenstones from the oceanic ridge systems (see Mottl, 1983, for method of construction).

Mottl defined the sea water/rock ratio for a rock that has gained Mg during alteration as "the mass of unreacted sea water required to supply the added Mg, assuming the complete removal of Mg from solution, divided by the mass of fresh rock that has been altered". The ratio so defined is a minimum.

The secondary assemblages were calculated in the manner of an igneous rock, except that the minerals are from the greenschist facies. The model in Fig. 3.2 was constructed at 300°C <u>but</u> should apply approximately to the entire temperature range over which the greenschist facies assemblage is stable (250-450°C).

Mottl's model assumes that rocks that have been altered in an open system by a continuous flow-through process will resemble those altered by a batch process (from experiments) for the volume occupied by the sample;

1) all mass transport across the boundaries of the volume occurred via infiltration,
2) the effects of temperature-pressure variations in time and space were small, and

3) the exchanges of the various chemical species between rock and solution bore definite and constant relationships to each other during alteration, resulting from chemical equilibrium and/or coupled reaction rate.

Mottl's model in Fig. 3.2 predicts the following secondary mineral assemblages from increasing sea water/rock ratios:

0- 2	:	chl + ab + ep + act
2-35	:	chl + ab + ep + act + qtz
35-50	:	chl + ab + qtz
> 50	:	chl + qtz

The chl+ab+qtz assemblage is a common one dredged from the mid oceanic ridge systems.

As predicted from Mottl's model, there is an observed positive correlation between chlorite and quartz and a negative correlation between chlorite and actinolite in the altered rocks.

Two types of typical metabasalts have been recognized by Mottl (1983), chl-qtz-poor rocks that were altered at sea water/rock ratios $\leq$10 and chl-qtz-rich rocks altered at ratios of 10 to 50 and above. There are two types of chl-qtz-rich rocks recognized that occur at different locations within the hydrothermal convection cell.

The chl-qtz-poor rocks are characterized by:

- being rich in act $\pm$ ep
- small gain or loss in Mg
- small loss in Ca
- gain in Na
- loss in Fe

and having basalt or diabase as precursors. These are not directly equivalent to, but include, the epidote rich rocks found in dredge samples by Humphries and Thompson (1978). The chl-qtz-rich rocks (from high sea water/rock ratios 10-50) are characterized by showing:

- low contents of act + ep
- large gain of Mg
- large loss of Ca
- gain or loss of Na
- gain of Fe.

They also have basalts, mainly pillows, as precursors.

3.4 RELATIVE POSITION OF THE METABASALT TYPES WITHIN THE CONVECTIVE CELL

The large Mg uptake in most of these rocks, especially the chl-qtz-rich rocks indicate that they were altered by relatively unreacted sea water, that, despite having attained temperatures corresponding to those of greenschist facies metamorphism, still retained most of its Mg^{2+} when it entered the volume occupied by these rocks. This type of alteration, almost certainly occurred within the downwelling limb of a convective cell, and, because many of the chl-qtz-rich rocks are metamorphosed pillow lavas, within the upper 1 to 2 km of the crust. These rocks have <u>not</u> experienced an additional stage of alteration by an upwelling highly reacted solution (see Fig. 3.1).

The chlorites in chl-qtz-rich rocks from downwelling parts of the convective cell are rich in Mg and are formed by the alteration of basalts. The chlorites within chl-qtz-rich rocks from the upwelling parts of the convection cell are by contrast, rich in Fe and generally form as chl-qtz-rich breccias and veins or vugh infillings with most of the associated quartz and sulphides and possibly some of the chlorite precipitated directly from the hydrothermal solutions. These Fe-chlorite-quartz rocks differ from those formed by alteration of basalt under sea water dominant conditions in several respects:

1) texturally they are not primary metabasalts, although they contain fragments of such,
2) they often contain sulphide minerals,
3) their chlorites are Fe- rather than Mg-rich relative to chlorites in the typical greenstones,

4) they tend to be enriched in those species (Mn, Cu, Zn, CO_2) that are depleted in metabasalts altered to chl-qtz, and depleted in insoluable species (Mg, Ti, P, V, Y, Zr) that are abundant in the metabasalts.

Mottl (1983) contends that the sulphide bearing qtz-chl breccias, with their Fe-rich chlorites and overall metal enrichments, clearly formed within the upflow zone from a highly reacted solution rich in Fe, Mn, Cu, Zn, H_2S and SiO_2 and poor in Mg.

The chl-qtz-poor rocks, by contrast, include both metabasalts and metadiabase. They apparently were altered within zones of low permeability (low sea water/rock ratios), such as the interior of pillow or flows higher in the convective cell, early in the development of a hydrothermal system. The fact that all the metadiabases are chl-qtz-poor suggests also that alteration deeper in the system, beneath the pillowed section, is accomplished either at low sea water/rock ratios or by sea water that already has lost its Mg higher in the section (Seyfried and Mottl, 1982).

The hot-spring solutions are complementary to most of the chl-qtz-poor rocks, compatible with the conclusions that the chl-qtz-rich rocks were altered at shallow levels within the down flow zone. The chl-qtz-poor rocks on the other hand, which are the most abundant alteration products within the hydrothermal system are the typical products within the deeper levels, near the base of the upflow zone (see Fig. 3.1).

3.5 SUMMARY.

A systematic change in secondary mineral assemblages and relative abundances as a result of reaction of the rock (basalt) with increasingly larger quantities of sea water resulted from two effects illustrated by the experiments:

1. the change in bulk chemistry of the altered solids as more sea water Mg is taken up in exchange for Ca and eventually Na, and

2. the transition from rock dominated to sea water dominated conditions at a sea water/rock ratio of 50, above which the solution remains highly acid.

The low pH moves the solution outside the stability field of all but the most acid resistant secondary minerals, chlorite, quartz and anhydrite.

The chl-qtz-rich rocks suggest that, during some period in the evolution of an axial hydrothermal system, downwelling sea water experiences rapid heating to greenschist facies within shallow levels in the crust, to a depth of 200-300m in the porous crust. The fact that the bulk of Mg uptake occurs at these relatively high temperatures strongly suggests that sea water reaches these temperatures with little to no prior reaction.

As the hot sea water begins to react, it becomes enriched in soluble elements and probably ^{18}O to a degree dependent on the amount of rock with which it reacts. Ultimately, enough sea water loses its Mg within these shallow zones that they reflect reaction under fairly high sea water/rock ratios (10 to 50). The removal of Mg from sea water is coupled with Ca+Na being leached from the basalt.

These shallow levels would also be locus of deposition of nearly all sea water sulphate as anhydrite, which combines with the Ca being leached from the basalt. This begins at about 150-200°C and if much anhydrite is precipitated here it forms a permeability discontinuity below which flow of sea water will be much slower and concentrated in larger deep going fractures. If the solution, now depleted in Mg and SO_4, penetrates deeper, it would continue to leach soluble elements, and exchange oxygen isotopes, with the rock it alters. Its major element chemistry, however, would already be close to equilibrium with the alteration assemblage at this stage and so would change only slightly in response to changes in pressure and temperature. Thus, the rocks (chl-qtz-poor) altered deeper in the system as well as the solutions that finally exit as hot springs would reflect reactions at low sea water/rock ratios.

The upwelling highly reacted solutions (hydrothermal end members) would be saturated in Fe, Cu, Zn, Mn, H_2S and SiO_2 and would have a temperature of ca. 350°C. The fluids would rise quickly (adiabatically) towards the surface, where, near the sea floor, the hydrothermal end member will mix with down flowing cold ground water (sea water) within the highly permeable upper crustal zone. Here the upwelling hydrothermal fluids would cool quickly, lose pressure, probably boil, becoming very reactive, and quickly precipitate their unstable Cu-Fe-Zn sulphides, quartz and anhydrite. These precipitates would fill the pore spaces, isolating the upflowing hydrothermal fluids from further mixing with the downflowing cold sea water and force the fumarolic fluids upwards, focusing them to penetrate the ocean floor where the metals are dumped as a sulphide ore deposit. The chlorites found within the upwelling zone are Fe-rich and occur in qtz-chl-rich breccias and veins associated with sulphide precipitation.

3.6 DISCUSSION ON SPILITIZATION AND HYDROTHERMAL ALTERATION

In the chl-qtz-rich and some of the chl-qtz-poor rocks, there is generally a much higher albite content in the naturally occurring altered rocks than was predicted by experiments. The excess albite is the principal cause of the "epidote short fall" discussed by Mottl (1983). There is also a large albite content in the Joma altered rocks as will be discussed later (p. 96).

The chl-ab-qtz assemblage is a common one from dredge collections. The disappearance of actinolite before epidote with increasing sea water/rock ratios in Mottl's model is an arbitrary feature of the normative calculations. The altered rocks at Joma show that epidote dissappears before actinolite during increasing hydrothermal alteration (see Table B-1, APPENDIX).

Humphries and Thompson (1978) report that the compositions of epidote and chlorite from seafloor metabasalts fall within a narrow range, whereas actinolites vary widely even within a single rock, suggesting that they have not reached equilibrium with their surrounding environments. Mottl (1983) on the other hand, allows

both the chlorite and actinolite compositions to vary as regards Fe-Mg contents. There is also a great variation in the type of chlorites and actinolites observed at Joma (discussed later, p. 74 and 95).

Mottl's model, based on laboratory experiments, describes fairly well the chemical and mineralogical changes that occur progressively as basalt reacts with increasing quantities of sea water within the greenschist facies. The chief discrepency results from the fact that the experiments were run as a batch process and thus did not allow for localized transport of elements across the boundaries of a rock volume via diffusion rather than infiltration. The effects of temperature-pressure gradients in time and space are apparently small within the greenschist facies. Local redistribution of elements via diffusion ("metamorphic differentiation") in the natural samples is an important and probably ubiquitous process chiefly for Fe^{2+}, which diffuses into zones where chlorite is forming due to influx of sea water Mg, and for Na^{+}, which accumulates as albite in zones of less Mg influx in exchange for Ca.

Most of the chl-qtz-rich rocks are either derived from pillows or are pillow breccias with fragments on a scale of centimeters to decimeters. The altered pillows typically show progressively greater Mg uptake, and these were altered at higher sea water/rock ratios from core to rim (Humphries and Thompson, 1978) From the more thoroughly altered pillows, the distinction between chl-qtz-rich rims and chl-qtz-poor cores is identical to the distinction between hyalospilites and orthospilites drawn by Cann (1969). This relationship can explain for some samples the Fe flux (from core to rim) and the Na flux (from rim to core) and is compatible with the hypothesis that interpillow voids represent major channels for sea water flux, as discussed by Seyfried and others (1978). Likewise, the brecciated nature of some of the chl-qtz-rich rocks suggests that breccia zones also acted as conduits for large quantities of sea water.

This may well be the case at Joma, where the pillow-breccia and hyaloclastites stratigraphically beneath the orebody also

contain dark, Fe-chlorite enrichment within the hyaloclastites and pillow rims and pale, albite enrichments in pillows and pillow breccia fragments. The Fe-chlorites are associated with quartz and a high content of Fe-Cu sulphide disseminations. The Fe-rich chlorite, quartz and sulphide disseminations within the hyaloclastite and breccia matrix is compatible with the chl-qtz-rich rocks formed in the upwelling part of a convective system as described by Mottl (1983) and suggests that these rocks were used as conduits for the upflowing hydrothermal fluids that formed the massive sulphides at Joma. These rocks are probably best observed within the mine at the south end of 480 ØH level (sample No. 480 ØH-12 chlorite schist and 480 ØH-13 albite rich pillow breccia fragment) (see Photo 5, APPENDIX H).

The chlorite rich assemblages, which are the most prominent variety according to Humphries and Thompson (1978), show the greatest chemical changes, while the epidote rich samples show very little change in composition compared to their basaltic precursor. Mottl (1983) contends that the epidote rich (and equivalent chl-qtz-poor) assemblages were formed under low sea water/-rock ratios within the lowest parts of the convective cell. A similar situation may occur at Joma, as the major part of the massive flow units (Group A) occurring at a very low stratigraphical level, far below the ore horizon, are loaded with secondary epidote as matrix minerals, veins and knots. These rocks, however, show little chemical changes from their ferrobasalt precursor. By contrast, the Fe-chlorite and albite rich rocks higher up in the stratigraphy near the ore body show a much more varied chemistry.

There is a positive correlation between chlorite and quartz and the increase in quartz content with increasing sea water/rock ratio is a real feature, occurring in spite of an increasing proportion of SiO_2 leached from the rock. Because chlorite has the lowest SiO_2 content of any of these silicate minerals, the formation of chlorite frees SiO_2 to make more quartz. Excess SiO_2 is not present at low sea water/rock ratios. This observation probably explains why quartz is scarce in hydrothermally altered gabbro from the seafloor and from ophiolites (Mottl, 1983).

Variations in elemental fluxes in terms of steady state geochemistry mass balances for oceanic input and output indicates that the Ca leached from the rock during sub-seafloor hydrothermal alteration is significant and enough to form carbonates on the seafloor (Humphries and Thompson, 1978). There is a large amount of carbonate within the upper levels of the Joma ore horizon, as matrix and as individual, sometimes thick, limestone bands. There are also high contents of calcite and limestone bands within the post-ore (Group C) volcanite units which may originally have come from the dissolution of earlier formed anhydrite lower in the system, that has been redissolved by the colder fluids of the waning hydrothermal system. It is well known (Goodfellow 1974) that hydrothermal systems depositing massive sulphides on the seafloor continue to circulate hot fluids long after the orebody is capped by younger sediments or volcanites. There are often halos or zoned secondary elemental distributions within the rocks above the massive ore deposit that are formed during the cooling down of a waning hydrothermal system.

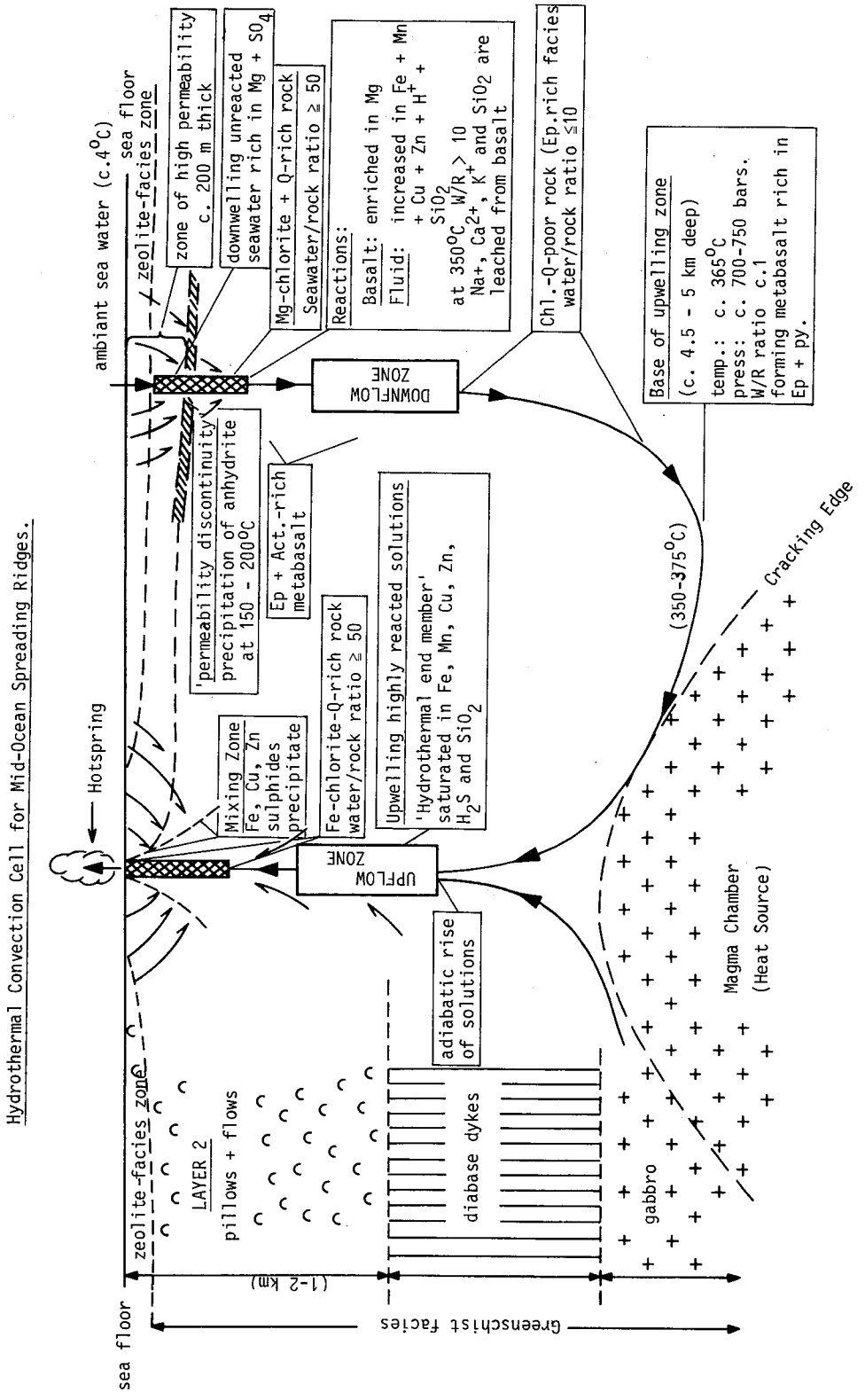

Fig.3.1. Schematic diagram showing the development of a sub-seafloor hydrothermal convective cell as along the presently forming Mid-ocean spreading ridges.

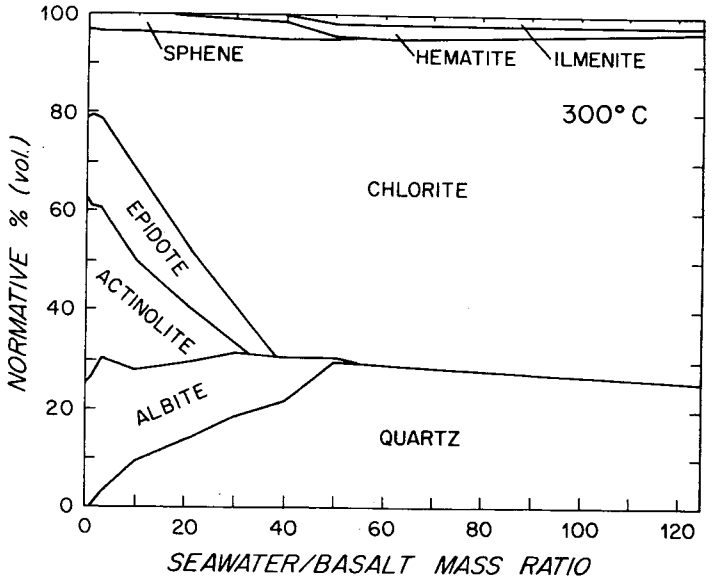

Fig. 3.2. Model predicting the mineral assemblages and proportions that are produced when basalt reacts with varying amounts of sea water within the greenschist facies. The model is based on chemical data from basalt-sea water experiments at 300°C and 500 to 600 bars (from Mottl, 1983 - see text therein for method of construction).

SECTION 4: THE HOST ROCK LITHOLOGIES AT JOMA

4.1. INTRODUCTION

The Joma sulphide horizon occurs within the Middle Greenstone, at the interface between two locally major volcanite units, the pre-ore (Group B) and post-ore (Group C) volcanites. The ore horizon lies in the overturned limb of a major isoclinal fold structure, which implies that the volcanostratigraphy is inverted, the pre-ore volcanites occurring in the hangingwall (HW) and the post-ore volcanites in the immediate footwall (FW) to the massive ore. There are, however, complications due to isoclinal D_2 folding and thrusting and D_3 overturned folding in which the stratigraphy locally is right-way up.

It was earlier recognized both by Olsen (1980 and 1984) and during the initial stages of this study that the hangingwall pre-ore volcanites have undergone extensive mineralogical and chemical changes due to intense, pervasive, hydrothermal alteration. This becomes increasingly stronger towards the main ore zone and is manifested in the 'stringer zone' or 'feeder zone' which forms the roots to the massive sulphide horizon.

The host rock lithologies at Joma, as described here, include not only the more visibly altered pre-ore rocks in the immediate hangingwall and the less altered rocks some 50-100 m to the west, but also the slightly altered post-ore (Group C_{1-b}) units which form the immediate footwall to the massive ore zone within the lower levels of the mine (i.e. below the lower ore level at 385 vf strosse, profile B_2-11).

The host rock units are separated here on the basis of detailed mine mapping and drill core descriptions, from detailed surface mapping surrounding the open pit and from surface drill core descriptions and sampling in areas distal to the Joma ore horizons.

Selected parts of the mine have been mapped in detail and sampled in order to give the best overall separation and distribution of the host rock lithologies. The following levels have been mapped more or less in detail (see Fig. 4.1); 350 ØF+VF, 362 ØF+VF, 375 VF+ØF+ØF synk, 387 ØF+VF.s.strosse, 385 vf.s.strosse, 388 VF.s.strosse, 402 whole level, 416, partly, 429 ØH, 480 ØH, 495 ØL and 560 VF+ØF to open pit, and the bottom of the open pit 560m level.

4.2. SEPARATION OF HOST ROCK LITHOLOGIES

The host rock lithologies were separated primarily on a field mapping basis, i.e. colour, textural and mineral contents, as well as their spatial relationships to each other and to the massive ores. The host rock lithologies were sampled for chemical and mineralogical investigations which further strengthened or modified the classifications. A total of 74 host rock samples were analysed for their major and trace element contents using XRF whole rock techniques. Of these, 30 were analysed for mineral contents using a combined XRD and thin section modal analysis technique, which is described in the Appendix on page A.2.

It must be emphasized here that the host rock units (Tables 4-1 and B-1) are not separated on a purely chemical statistical basis <u>but</u> from a combination of textural, mineralogical and chemical parameters.

The pre-ore (HW) host rocks form an integral part of the Group B pillow lava + pillow breccia + hyaloclastite sequence described earlier (pp. 20-23). They are classified and described in order of their apparent increasing degree of alteration. Their mineral and chemical changes are compared to a mildly spilitic distal greenstone (D) which is thought to have major and trace elemental distribution similar to the basaltic precursor (B_o) to the Group B volcanites (D = B_o). Their spatial relationship to each other and their nearness to the massive ores in also considered. As a general rule, the less altered rocks occur more distal to the main ore zone.

However, isoclinal folding and thrusting have often complicated the situation, telescoping the sequence such that two rock types originally not in contact with each other within the zoned hydrothermal alteration assemblage, now occur juxtaposed to each other. The pre-ore host rock lithologies are described here as a continuous sequence, the B_1 to B_6 series. The unit B_1 rocks are the less altered and are found deepest within the volcanic pile, furthest from the massive ore horizon, and the unit B_6 rocks are the most visibly altered, occurring directly in contact with the massive ores.

Unit C_{1-b} host rocks are described here as a slightly altered variety of the unit C_1, post-ore pillowed lava sequence, which occurs immediately beneath the minor thrust that separates them from the massive sulphide horizons within the lower levels of the mine.

4.3. DESCRIPTION OF PRE ORE, HOST ROCK LITHOLOGIES (UNITS B_1-B_6).

4.3.1. Unit B_1: Undifferentiated, slightly altered Group B Pillow and Breccia Sequence.

These rocks comprise a sequence of undifferentiated pillowed lavas and pillow breccias, that are continuous with the Group B series rocks (described on p. 20-23). They occur within the alteration zone adjacent to main massive ores west and southwest of the open pit. They are typically moderate to darker greyish-green in colour (10G 4/2 or 10GY 3/2 on GSA Rock-color chart), microcrystalline to medium grained (1 mm) and somewhat massive. They are, however, generally more schistose in nature than the B serie rocks, due to continued chlorite growth and a further breakdown of the earlier spilitic greenschist facies mineralogy (chl, act, ab, ep, cc, sp and po impregnation. See TABLE A-1, APPENDIX for abbreviations).

Hints of original sub ophitic texture is visible under the microscope (see Microphoto 4+5) but the rocks are generally more recrystallized and schistose in nature. Relicts of earlier calcic plagioclase, visible in unit B rocks, are here broken down into an intergrowth of albite and epidote, with minor to trace contents of calcite found in the matrix. Chlorite, which is the dominant mineral in this unit, occurs as large clusters of dark to moderate dark green interstitial aggregates, and comprises typically Fe-rich chlorite varieties. Actinolite is a major mineral and occurs as typical minute, pale green to colourless elongate needles, intergrown within the larger chlorite aggregates (grain size 1-2 mm). Epidote occurs as numerous small (0.3 mm) euhedral grains closely associated with larger albite aggregates and concentrations of minute sphene grains. Epidote also occurs as veins containing both quartz, calcite and in part dark chlorites. White mica (sericite) occurs only in trace quantities, generally along S_2 and S_3 cleavages. Sphene ($CaTiSiO_5$) occurs under the microscope as characteristic patchy concentrations of minute euhedral to subhedral grains (<0.1 mm) generally associated with dark, shady patches of epidote and minute dustings of opaques (pyrrhotite ?). Large anhedral grains of pyrrhotite are visible in hand specimens and show a very strong association with the dark Fe-rich chlorites and epidote-sphene concentrations.

Distinguishing features.

In hand specimens, the unit B_1 rocks are typically darker, moderate greenish in colour (due to their increase in Fe-rich chlorites) and generally more schistose in nature than the Group B rocks. They also show a slight increase in grain size and a diffuse, sub crystalline texture. Large quantities of epidote-quartz veins and minor calcite contents, as both matrix minerals and secondary veins and fracture filling are prominent features of these rocks. Disseminated pyrrhotite is ubiquitous in this rock.

Chemistry.

Unit B_1 rocks show a similar major and trace element distribution as the Group A and B volcanites (see Table B-1) except for a slight increase in Fe_2O_3 (in Fe-chlorite), CaO (in epidote) and Sr, and a slight decrease in MgO, K_2O and Ba. They show only slight increases in Cu and similar Zn contents compared to the B_o precursor and distal greenstones (D). Low K_2O contents (generally <0.10 %), and a slight increase in S contents (corresponding to the visible po disseminations) are typical for the unit B_1 host rocks.

Distribution.

The unit B_1 rocks are the most prominent and widespread of the host rock lithologies at Joma and occupy large areas of the hangingwall generally more distal to the main ore zone and deeper in the volcanite stratigraphy. To the S and SW of the open pit area, they are associated with rusty pyrrhotite dissemination zones that trend SSW at a shallow angle away from the main ore zone. Unit B_1 rocks do not occur in contact with the main ore zone, as can be seen from the vertical profiles (i.e. B_2-11 and B_1-3). There is always a thin zone of B_2-B_6 type lithologies between them and the massive ores.

The boundaries between the unit B_1 rocks and the other Group B lithologies such as B_2, B_3, B_4 are diffuse and generally completely gradational in nature. (For their distribution, see Fig. 4.2 and vertical profiles (TABLE E), horizontal maps (TABLE F)

Discussion.

Both the sphene and pyrrhotite grains show an increase in grain size and crystallinity compared to the slightly altered more distal B series rocks.

4.3.2. Unit B_2: pale, albite and white mica rich rock with disseminated pyrrhotite.

The unit B_2 rocks are typically very pale, schistose to slightly more massive, fine- to medium grained and often contain notable remnants of an original crystalline or micro gabbroic igneous texture (see Photo 9).

The pale colouration (pale, greenish-yellow, 10Y 8/2 on the GSA color-chart) corresponds to an increase in albite (c. 45 %) and white mica (2-3 %), a decrease in the chlorite content (c. 22 %, here occurring as paler Mg-rich chlorite) and lesser amounts of pale actinolite (c. 14 %). Actinolite occurs as minute pale green to colourless needles within the matrix. Calcite is also present (c. 6 %) as isolated grains within the matrix and as minor late veins. Pyrrhotite occurs as larger (2-3 mm), rounded, disseminated grains in varying amounts from 5 to 10 %. Sphene occurs in minor quantities as isolated subhedral, minute (0.3 mm) grains, but more often as clusters. Epidote and quartz are typically absent or found only in trace amounts in this rock. The rocks of this unit are somewhat coarser grained (medium grained C.1 mm) than those of unit B_1 and they show a typical metamorphic recrystallized nature although there still occurs some hint of an original crystal orientation which is pseudomorphed by the metamorphic minerals. This is especially notable in the less deformed rocks (see Microphoto 10).

The diagnostic features of the rocks in the unit is their very pale, bleached colour corresponding to an increase in albite and sericite contents, and their increased contents of pyrrhotite as large, visible, disseminated grains. Epidote and quartz veins are notably bleached or absent.

Chemistry.

The rocks of unit B_2 are enriched in Na_2O, K_2O, S, Cu

and Ba and depleted in Fe_2O_3, CaO and Sr compared to the B_o= D precursor and unit B_1 rocks. Increases in Na_2O and K_2O correspond to the increases in albite and sericite within this unit, while increases in S correspond to the visibly higher pyrrhotite content. This unit shows a marked enrichment in Cu, whereas the Zn content shows only a slight increase, (c. 300 ppm and 150 ppm respectively compared to 60 ppm Cu and 100 ppm Zn in the B_o = D precursor).

Distribution.

The unit B_2 rocks are a complete gradational series between units B_1 and B_4. They have never been seen in contact with the unit B_5 albitites (Fig. 4.8).

The unit B_2 rocks, along with the unit B_4 rocks, are probably the most laterally widespread of all the intensely altered rocks in the Joma area. They are also intimately associated with the distal exhalite mineralizations. The unit B_2 rocks are recognized at several levels within the pre-ore volcanic pile, but are for the most part confined to the immediate structural hangingwall (stratigraphic footwall) of the massive ore horizon, slightly distal to the more central, unit B_4, pyrite bearing pale schists (see Fig. 4.8). Pyrrhotite disseminated, pale albite rich pillow breccia fragments set in a dark green Fe-rich chlorite schists (altered hyaloclastites - B_{6-H}) are found at the south end of level 480 ØH (locality 10) and at surface locality (JD-26/84) just west of the open pit. These are typical for the B_2 type rocks.
Elongate zones of pale, pyrrhotite disseminated albite rich rocks also extend down within the stratigraphic deeper levels of the central 'stringer feeder zone' which forms the roots to the massive ores. The B_2 rocks are slightly enriched in Cu compared to the surrounding B_o and B_1 less altered rocks.

Pale, pyrrhotite disseminated, albite and white mica rich rocks also occur distal to the main ore horizon and central stringer zone, as thin (2 m max.), gradationally altered, bleached, zones stratigraphically beneath thin (50 cm max.) layers of massive to semi-massive pyrrhotite+carbonate+grey quartz rich

(chert) layers. These probably represent distal exhalites related to the main Joma mineralizing episode, or, most likely represent small sporadic episodes of hydrothermal activity prior to the main Joma deposition.

Discussion.

The thin distal unit B_2 zones show gradational contacts with the darker B_1 type rocks and are most strongly altered (bleached) and pyrrhotite mineralized immediately adjacent to the distal, thin layered sulphide-silicate-carbonate exhalite. The B_2 rocks here may represent an episode of 'autometamorphism' formed beneath the dense, metal laden, hot fluids that have migrated down slope from the hydrothermal vent source into local traps and basins . The hot, dense fluids causes a downward, in-situ hydrothermal alteration of the immediate stratigraphic footwall rocks, decreasing in intensity gradually downwards. These alteration zones varying from 1-3 m in thickness, and are best seen in DDH D59 and D61, distal to the main Joma ore zone.

4.3.3. Unit B_3: albite + Fe-rich chlorite + pyrrhotite disseminated rocks.

The unit B_3 rocks are typically darker in colour than units B_2 and B_4, being moderate to dark greyish-green (5G 5/2 to 10G 6/2 GSA Rock color chart). They are slightly more massive, harder and tougher in nature, although schistose zones are prominent. They are fine to medium grained showing a strong degree of metamorphic recrystallisation and foliation development (see Photo 7).

Unit B_3 rocks are rich in albite (ca. 34 %), dark (Fe-rich) chlorite (c. 41 %) and show a strong increase in larger (2-3 mm size) disseminated pyrrhotite grains (c. 10-15 %) compared to the less altered B_o-B_1 type rocks. They also show a marked decrease in actinolite (c. 6%) which occurs as minute pale needles dispersed and intergrown within the matrix chlorite and albite.

Larger (max. 8 mm long), typically elongate needles of darker orthorhombic amphiboles are found dispersed thoughout the paler rock showing random to preferred orientations paralleling the S_3 cleavage directions. White mica (sericite) is notably absent and only trace amounts of epidote and quartz have been observed - as isolated, large lensoid knots, which probably represent more resistant (less altered) remnants of unit B_1 like precursor rock. Only minor amounts of calcite are found within the matrix and occurs typically as secondary veins and fracture fillings (see Microphoto 11).

Layered varieties of this rock are found within the intensely folded and D_2 sheared (thrusted) areas close to the main ore zone (387 and 382 mine levels - see Figs. 4.3 and 4.4). The distinct, thin layers, are alternatinaly rich in albite, chlorite and moderate greenish amphibole, and probably represent metamorphic differentiation (layers paralleling S_2 foliation). The dark Fe-rich chlorites are in places altered to dark brown biotite along and surrounding S_3 cleavages and D_3 related veins that cross-cut an earlier S_2 foliation.

Chemistry.

Unit B_3 rocks are characterized by their relatively high contents of Fe_2O_3 (14.26 %), MgO (9.16 %) and Na_2O (4.07 %) and relatively low CaO (5.23 %) and K_2O (0.32 %) compared to the B_o=D precursor. The sulphur content has also increased notably (c. 3.33 %) corresponding to the increased pyrrhotite disseminations. The rock is enriched both in Cu and Zn as well as Ba (2000-3000 ppm Cu, 400-500 ppm Zn and 128 ppm Ba compared to 60 ppm Cu, 100 ppm Zn and 28 ppm Ba for the B pillows and Group A type massive volcanites). The increase in total Fe reflects not only an increase in the total disseminated sulphides (po$\pm$cp) but also an increase in the Fe-rich chlorite content.

Diagnostic features.

These rocks are characterized by their dark greyish-green colour, their more massive, hard, tough nature and their increased content of large, visible grains of disseminated pyrrhotite.

Distribution.

The unit B_3 rocks are very limited in their distribution and are restricted to the immediate vicinity of the massive ore zones at Joma. They have not been found outside the immediate mine area. The pyrrhotite bearing, darker greyish-green, unit B_3 type rocks show an intimate relationship to both the pyrite bearing pale schists (unit B_4) and the dark chlorite schists (unit B_{6a-d}) within the immediate hangingwall of the Joma ore zone, in other words, stratigraphically below the massive ores and the chlorite schists. The relationship between the unit B_3 rocks and the pale schists (unit B_4) and the dark chlorite schists (unit B_6) is best demonstrated on the 362, 375 ØF synk, and 387 ØL and 385 VF. s.strosse levels. At 387 ØL (Fig. 4.3) the three schist types are interfingered with each other within a flat lying D_2 fold and thrust structure. At 385 VF.s.strosse (Fig. 4.4 and Profile B_2-11) the more massive, po bearing unit B_3 type rock occurs as an isolated slice or layer thrust into and folded (D_2) within the massive sulphide ores.

Thin (20 cm to max. 2 m), isolated lenses and layers of unit B_3 type rocks are found within and along the basal thrust zone that separates the lower levels of the Joma massive ore zone from the younger footwall greenstone (Group C_1 and C_{1-b}). These are best seen at 375 ØF synk (Fig. 4.6) and 385 vf.s.strosse (Profile B_2-11) and Fig. 4.4. Similar rocks are seen structurally below the massive ore zone at the 402 level (see Profile B_2-9).

Numerous thin bands of dark chlorite schist are found intercalated within this highly deformed (sheared) schistose unit, very reminiscent of strongly deformed pillows and dark pillow rims and interlayered hyaloclastite beds. Minor, very elongate pillow-like structures have been observed.

The minor isolated epidote lenses that have been observed in this unit are reminiscent of deformed and transposed epidote knots found within the pillow centres of the less hydrothermally altered and deformed B_o-B_1 group pillow lavas.

Unit B_3 type rocks show gradational contacts to the unit B_2 type, bearing po, paler schist. The unit B_3 rocks form a thin gradational zone between the unit B_2 type rocks, which form the more central parts of the feeder zone, and the dark chlorite schists (B_6) and pale albitites (B_5) adjacent to the massive ores. They are laterally gradational into the less altered unit B_1 type rocks (see Fig. 4.8).

4.3.4. Unit B_4, very pale, pyrite bearing, albite+white mica+ chlorite+actinolite schists.

The B_4 unit comprises a variety of schists that are characterized by their very pale colour, their pyrite content and their visible, elongate actinolite needles. The rocks of this unit range greatly in colour from pale yellowish green (10Y 8/2) through pale green (5G 7/2) to very pale, green (10G 8/2) or pale 'apple-green', depending greatly on their variable Mg-rich chlorite, white mica, actinolite and carbonate contents. The rocks are generally coarse grained and very schistose and show a completely metamorphic recrystallized texture.

The unit B_4 type rocks vary greatly in their mineral contents (see the large range in standard deviation in Table 4.1) but are generally dominated by albite (34 %) and pale, Mg-rich chlorite (36%) and contain minor quartz (8 %), white mica (3 %), calcite (7 %), pale actinolite (2 %) and sphene (3 %). Pyrite (c. 5-10 %) as fine disseminations, concentrations and interconnected veins associated with quartz and calcite and with trace amounts of sphalerite, is characteristic for this unit. (See Photo 10 and Microphoto 13+14). Elongate, macroscopic, pale, porphyroblastic actinolite needles (0.3 - 1.0 cm long) are also diagnostic for this unit along with the general absence of epidote and pyrrhotite.

The general increase in albite, white mica, Mg-rich chlorites and calcite contents is reflected in the very pale colouration of this rock. The moderate greenish varieties are richer in Fe+Mg-rich chlorites and actinolite.

A prominent facies of this B_4 rock series is characterized by its network of pyrite and quartz rich veins and zoned fine disseminations of pyrite ('dusting') surrounding the pyrite veins. This rock is generally more massive and extremely fine grained and has a typical pale 'apple-green' colour (i.e. sample no. 2 - 402 ØL) (see Photo 8 and Microphoto 12).

Chemistry.

Unit B_4 rocks show a great variation in their mineral contents and chemical compositions as can be seen from the standard deviations (Table 4.1). This is especially noticeable for elements such as Al, Fe, Mg, Ca, K and S.

Unit B_4 rocks are notably enriched in Al_2O_3, K_2O, MgO, S, Zn, Pb and Ba compared to the mildly spilitic basaltic precursor (B_o). There is only a very slight variation noticeable in the total Fe ($Fe_2O_3^{tot}$) which generally reflects the amounts of pyrite in the rock.

The unit B_4 rocks are generally decreased in CaO and Na_2O compared to the adjacent unit B_2 and B_3 rocks. The Cu contents in the B_4 rocks are roughly similar (x=205 ppm) to the B_2 type rocks but lower than the B_3 rocks. The Zn content, however, shows a 10 fold increase (1000-2000 ppm) and the Pb and Ba contents also show a substantial increases when compared to values in the unit B_2 and B_3 type rocks.

Distribution.

The unit B_4 rocks occupy a large volume of the intensely altered rocks stratigraphically beneath and distal to the massive ore zone within the upper levels of the 'feeder stringer zone' at Joma (Fig. 4.8). These rocks now occupy a major part of the immediate structural hangingwall to the ore body at Joma (see vertical profiles, e.g. B_1-5+8).

B_4 type, pyrite veined and disseminated rocks are also conspicuous away from the main massive ore zone at Joma. The pyrite disseminated zone trending SSW and south from the main ore zone are typical for B_4 type rocks (i.e. DDH D65 120-126 m). West of the main ore zone, in surface drill holes D32 + D18, similar pyrite disseminated and veined schists are found hosting thin massive to semi-massive Zn-rich pyritic distal members of the main Joma ore horizon.

Discussion.

Judging from their great variations in major elements, especially the increases in Al_2O_3, MgO and K_2O, these rocks probably represent some of the most intensely hydrothermally altered rocks at Joma.

It should be noted here that sheared varieties of these unit B_4 type pyrite bearing, albite+white mica+chlorite rich pale schists showing layering and slight metamorphic differentiation have previously been mistaken for layered felsic tuffs or keratophyres. The high TiO_2 and low Zr and Y contents however, show that these rocks were originally basaltic in composition.

Sub-unit B_{4-b}: pale sericite + chlorite schists; pyrite bearing.

Stratigraphically beneath the massive ore-zone and distal to the central parts of the main 'stringer-feeder zone' occurs a thinner, very pale unit, rich in white mica and Mg-rich chlorite that carries less albite and actinolite than the typical unit B_4 rocks. These have been separated out as sub-unit B_{4-b}. They are typically more schistose and contain irregular concentrations of pyrite and carbonate, and thin (5-50 cm thick) greyish quartz rich bands (recrystallized chert) bearing pyrite and minor sphalerite. Pyrite in these cherty bands show framboidal structures.

Chemistry.

The B_{4-b} rocks have a much higher Al_2O_3, K_2O, S, Zn, Pb and Ba and correspondingly lower CaO and Na_2O contents than the normal unit B_4 rocks.

Distribution.

B_{4-b} rocks are found within the immediate contact zone to the massive pyritic ore at the southwest end of the open pit (e.g. locality JD-32/84, Fig. 4.2a+b). They have been interpreted as Fe, Al- and K-rich chemical sediments formed distal to the main fumarolic vent.

Sub unit B_{4-c}.

A pyrrhotite bearing variety of the pale, chlorite + white mica rich schists has also been found within the lower levels of the mine forming the footwall stratigraphy in what appears to be the distal parts of the main massive ore zone (along the footwall thrust boundary beneath the lower ore limb at Joma, see profile B_2-11.) The pyrrhotite bearing pale schist occurs immediately above the dark, Cu-rich chlorite schists and carries pyrrhotite as fine disseminations and isolated lenses and bands ($\leq$ 50 cm thick). There appears to be a sharp boundary within these pale schists separating the pyrite bearing, carbonate rich varieties (B_{4-b}) from the pyrrhotite bearing, quartz rich varieties (B_{4-c}). The B_{4-c} type pyrrhotite bearing schists can best be seen at two localities; 1) at the far end of the old 362 VF adit, between the massive ore and the younger, pale footwall greenstones (C_{1-b}), and 2) similarly at 388 VF.s.strosse (locality no. 1) between the dark chlorite schists and the pale footwall greenstones (C_1). The boundary between the po-bearing, pale schists and the pale footwall greenstone marks the thrust at the base of the ore zone at Joma.

Within DDH D61 and D59, to the west of the open pit and distal to the main Joma orebody, a thin unit of characteristic, white mica porphyroblastic, coarse grained, pale schist occurs between the pre-ore B_1 type pillowed lava sequence and the older graphitic phyllites. The pale schists are rich in white mica, Mg-rich chlorite and calcite. Minor pyrrhotite dissemination is typical along with thin quartz rich recrystallized chert bands carrying minor pink garnets (spessartine ?). These schists may be distal equivalents to the B_{4-c} rocks at Joma.

Similar chert and garnet bearing pale schists with porphyroblastic white mica and disseminated pyrrhotite have been observed at the main road junction to the Røyrvik village, associated with C_2 type, laminated pale greenschists, sandwiched between pillowed lava greenstones (Group D) and dark graphitic phyllites. Similar rocks have also been described by R. Horbach (pers. comm. 1985) within the immediate wallrocks to the Borvasselv ore zone.

Within DDH D61, which lies farthest west from the main Joma ore horizon, the B_{4-c} type schists occur at several levels and appears to be repeated in D_2 tight isoclinal and thrust structures, D61-180+207+285 m (see vertical profile Fig. 2.2).

4.3.5. Unit B_5: pale albite- and pyrite rich rocks.

This unit consists of a variety of pale, albite- and pyrite rich rocks. They vary in colour from pale creamish-white (N8) to medium light grey (N6, GSA Rock color chart) and are generally very massive, dense, hard, almost flinty in nature. They vary greatly in texture from being coarse grained, fragmental (2-3 cm max. size) to layered and moderately schistose, to thinly laminated with alternating laminae of albite, quartz and pyrite.

The unit B_5 rocks vary greatly in their mineral contents and chemical compositions. They are, however, generally totally dominated by albite and pyrite having only minor contents of chlorite, white mica (both sericite and phengite or Na-rich white mica) and sphene and trace amounts of quartz, biotite and sphalerite. Actinolite, epidote and calcite are typically absent. Sphene occurs as characteristic trails of minute euhedral grains.

Chemistry.

The albite-pyrite rich rocks show great variations in their major elements with notable increases in Fe_2O_3, Na_2O, S and decreases in MgO, CaO contents compared to the B_0 type mildly

spilitized precursor and B_1 type altered rocks. The unit B_5 type albite-pyrite rich rocks all show moderate Cu and relatively high Zn, Pb and Ba contents, similar to unit B_4 type pyrite bearing pale schists and contrasting with the B_3 rocks and B_{6a-d} dark chlorite schists.

Subdivisions.

Texturally and structurally, these B_5 rocks have been subdivided into 3 to 4 main varieties depending on their spatial distributions with respect to the main ore zone and the central parts of the hydrothermal alteration "stringer zone". The albite rocks are almost exclusively found at the contact between the massive ore and the structural hangingwall schist and are intimately interlayered with or lying stratigraphically below the dark chlorite schists. They generally occur more distal to the main pyrite veined part of the central "stringer zone", characterised by the B_4 type rocks (see Fig.4.8).

a) Sub-unit B_{5-a} type, pyrite- and quartz veined, more massive, greyish albitites are an exception (see Photo 13 a+b). They occur within and form an integral part of the B_4 type, pyrite bearing, pale schists and probably represent the central, more highly altered and veined part of the stringer zone. They grade laterally into the B_4 type pale schists. A typical example of B_{5-a} type pyrite-quartz veined albitites occurs ca. 20 m west of the massive ore at the southwest edge of the open pit (locality JD 30a/84, Fig. 4.2a+b). Here, B_{4-b} type pale schists lie between the pyrite-quartz veined massive albitite and the massive ore.

b) Sub-unit B_{5-b} type rocks are characteristically fragmental in nature as well as carrying thicker interconnected coarse grained pyrite veins and layers. They occur between the dark chlorite schists and layered albitite units, and B_4 type pale schists. Typical unit B_{5-6} albitites consist of varying sized (3 cm max.) sub angular to sub rounded, zoned, pale albitite fragments which contain pale centres and darker zoned rims consisting of very finely disseminated pyrite grains. The individual fragments are surrounded by interconnected veins or layers of coarse grained

pyrite; the darker zones of finely disseminated pyrite appearing to be related to this veining (see Photo 14).

B_{5-b} type fragmental albitites are best seen within the "Mills ort" (an inclined adit between the 510 and 520 levels).

c) Sub-unit B_{5-c} type albitites are typically thin to finely laminated, pale albite-quartz and darker pyrite rich layers (50 cm max. thickness) generally found interlayered within darker chlorite schists and in contact with some thinner massive to semi-massive pyritic ore. A good example of B_{5-c} laminated albitites occurs within DDH 2027 at 18.50-19.00 m.

Similar thin albitite bands and layers with associated thin pyrite mineralizations occurs interlayered within thicker dark chlorite schists within the western parts of the mine (e.g. 388 vf.s. strosse, see Fig. 4.5 and Photo 15). Some small lensoid, magnetite bearing, dark, recrystallized cherts have also been observed here. The thin, finely layered albitite-quartz-pyrite rich units within thicker layered, dark, chlorite schists probably represent some form of chemical sediments, judging from their thin primary laminations.

d) Sub-unit B_{5-d} occurs as thicker (75 cm max.), well layered, pale albite and pyrite rich massive rocks with notable minor contents of biotite. These biotite bearing, albite-pyrite-rich layered rocks are almost always found in contact with, or within, darker chlorite schists. The chlorite schists also bear minor contents of biotite (see Photo's 11+12 and Microphoto 15).

A variety of this pale albite-pyrite rock, bearing much calcite and visible pale green actinolite porphyroblastic needles, has been found adjacent to the chlorite schists within the massive sulphide ores along the 362 new VF. level.

These strongly contrasting pale and dark green layered rocks (pale, coarse grained pyrite-bearing albitite and darker, pyrrhotite-chalcopyrite disseminated Cu-rich chlorite schists) are typically found interlayered within or adjacent to the Cu-rich massive

pyrite-pyrrhotite ores. Isolated layers and deformed lenses of the albitite and chlorite schist within massive sulphide ore is best seen along the western walls of the 385 VF.s. strosse (see profile B_2-11). The individual albitite-chlorite schist layers occur within the massive ore as isolated F_2 or F_3 fold hinge remnants that were thrust into the massive ores during an early D_1-thrusting deformations. The biotite content which is typical for these units is secondary and metamorphic in nature (associated with D_3 deformation?).

Discussion.

Rocks of this unit are strongly deformed by intense D_2 isoclinal folding and thrusting and by later D_3 crenulation folding and renewed movements along earlier S_2 foliation, roughly parallel to the major lithological boundaries. However, the fine, continuous layering and laminations found in parts of the rocks suggest a primary sedimentary origin for some of this layering. The fine laminations are often interlayered with thin pyritic bands and minor magnetite-cherty horizons have also been noted. This suggests that some of these rocks, at least, are of chemical sedimentary origin, and that the alternating layers (albite-pyrite and pyrrhotite-chalcopyrite rich dark chlorite schists) probably represent some form of alternating Na-Fe-Zn-S enriched and Fe-Mg-Cu enriched and S deficient fluids pulsating from the main fumarolic vent. The thin alternating laminations represent some form of chemical sedimentary layering produced from alternating Na and Fe-rich density currents deposited in bottom depressions down stope and distal to the main fumarolic vents.

The B_{5-b} type fragmental albitites appear to be some form of fractured, pyrite veined, and hydrothermally altered rock. The darker, finely disseminated, zoned pyrite dustings occur along the rim of the fragments, adjacent to the pyrite veins and the fragment centres remain paler, less pyritized, reminiscent of a zoned alteration phenomena. In some places, finer grained varieties of this fragmental albitite have been found interlayered within the darker chlorite schists which may represent slumping of highly altered fumarolic vent material, transported down slope further

into the depositional basin. They occur slightly distal to the B_{5-a} type pyrite-veined, more massive albitites within the B_4 type pale schists which probably represent the more intensely altered central parts of the hydrothermal alteration - "stringer zone". The B_{5-c} type finely laminated albitites would be deposited even more distal to the main fumarolic vent; i.e. the DDH, 2027 18.5-19.0 m locality is further NW from the B_4 rocks surrounding the main ore zone at Joma than the fragmental albitites (B_{5-b}) in the 'Mills ort' 510-520 incline.

These albitites, at first glance, show a strong resemblance to quartz-keratophyres (i.e. mildly spilitized acid volcanites). However, texturally, the albitites at Joma are completely metamorphically recrystallized, showing no hints of primary igneous or pyroclastic textures, and their trace element geochemistry (Ti, P, V, Zr, Y) indicates that they were originally of basaltic composition.

The albite rich rocks are thus similar to the alteration rocks described from the Skorovas (Reinsbakken, 1980) and the Løkken-Høydal (Grenne, 1981) deposits.

4.3.6. Unit B_6 - chlorite schists;- both Fe- and Mg-rich varieties.

This group consists of a variety of chlorite rich rocks, ranging from dark, Fe-rich, to pale, Mg-rich, chlorite schists that occupy the immediate structural hangingwall or stratigraphic footwall to the Joma ore zone at various positions along the main and distal ore horizon.

Subdivisions.

Seven varieties have been subdivided (B_{6a-f}+B_H) based on their textural, structural and compositional variations. They vary greatly in their colour, thicknesses and their spatial distributions to each other and to the main ore horizon. They range from very dark to pale greyish-green in colour, from coarse to fine grained and from somewhat massive to strongly schistose in

nature. They vary in thickness from thin layers to thicker units up to 12-15 m max. thickness (see profile B_1-8) near the main Cu-rich ore zones. They also vary greatly in their spatial distribution from the thicker Cu bearing, dark chlorite schists beneath and within the main Cu-rich massive sulphide ore zone, to thin dark chloritic horizons within the stratigraphic upper levels of the Zn-rich massive ore zone to thin, moderate greenish chloritic layers associated with the more distal thin, massive to semi-massive pyritic parts of the Joma ore horizon.

They also vary considerably in their sulphide mineral contents, the dark Fe-rich chloritic schists being mostly pyrrhotite- and chalcopyrite bearing, while the paler, Mg-rich varieties bear pyrite and minor sphalerite.

However, common to all these rocks is the almost complete dominance of chlorite and lack of other greenschist facies minerals, except sphene and minor amounts of albite, quartz, biotite and stilpnomelane(?). Epidote and calcite are conspicuously absent and actinolite and calcite occur only in trace amounts in a few varieties.

a) Sub-unit B_{6-a} - Quartz-albite-biotite bearing chlorite schists.

The B_{6-a} rocks are pale coloured, coarse grained, massive and hard to slightly schistose rocks, rich in chlorite, albite, quartz and sphene. They are commonly veined by quartz and flooded with disseminations of chalcopyrite and pyrrhotite (see Photo 16).

These rocks are very limited in their spatial distribution occurring as small patchy zones associated with the thicker, dark chlorite schists (unit B_{6-d}) at the basal stratigraphic levels associated with the main Cu-rich massive ore zone along the western edges of the Joma ore body; i.e. at the bottom of 375 ØF. synk (Fig. 4.6) and 388 vf.s.strosse (Fig. 4.5).

Discussion.

Some pyrrhotite disseminated, fragment-like patches of pale albitite have been found within the dark chlorite schists at this level and probably represent intensively hydrothermally altered pillow breccia fragments, set in a dark Fe-chloritized hyaloclastic matrix.

b) Sub-unit B_{6-b} - layered, dark green chlorite schists and pale albitites.

These rocks are typified by their 'zebra like' striping of thin to thicker bands of coarse grained dark chlorite schists and paler albitites. The chlorite schist layers are rich in disseminations and thin layers of chalcopyrite-pyrrhotite while the albitites carry disseminations and bands of pyrite±sphalerite. Thin, minor magnetite rich lenses of dark recrystallized cherts have been found associated with some of the pyrite rich bands within the darker chlorite schists. The chlorite schists generally carry a strong content of biotite (secondary?) and lesser amounts of quartz and albite than sub-unit B_{6-a}. The B_{6-b} type rocks are generally much more widespread throughout the stratigraphic footwall in the western parts of the main Cu-rich ore zone than the unit B_{6-a} rocks. Here, they constitute a major part of the chlorite schist stratigraphy along with the fine grained chlorite schists. B_{6-b} type, biotite bearing layered albitite-chlorite schists are best seen on the SW (left hand) wall going up into the 388 vf.s.strosse (Fig. 4.5) and along the western side of 500 level adits and above the fragmental albitites within the 'Mills ort' or 510-520 inclined adit (see Photo's 6+15 and Microphoto 16).

c) Sub-unit B_{6-c} - coarse grained, dark chlorite schists.

Rocks of this sub-unit are characterised by their dark to almost black colour (greenish-black 5GY 2/1, GSA-color code), their coarse grained nature (3-4 cm max. grain size) their high biotite content and their limited distribution (see Photo 11).

The rocks consist of a coarse grained, randomly oriented interweaving mesh of dark Fe-chlorite flakes with coarser porphyroblastic books of biotite. Biotite can, in part, be a major component. Chalcopyrite and pyrrhotite disseminations are ubiquitous. Sphene occurs as microscopic trails of minute euhedral grains.

The B_{6-c} coarse grained, chlorite-biotite schists occur only locally within the main Joma ore zone, usually in immediate contact with the massive sulphide ores, or as isolated lenses and fragments within the massive ore, generally along minor D_2 thrust planes.

Such coarse grained chloritic rocks at massive ore contacts are best seen at the 375 ØF, 480 ØH (sample 3) and 560 ØF (sample 3) levels.

Discussion.

The biotite seems to be of a metamorphic nature, generally cross-cutting the main S_2 foliation of the chlorites. Some visible pale green zones are found within the dark chlorite schists, which are rich in pale, Mg-rich chlorites. These occur as zones surrounding a predominant S_3 cleavage and spread out along the main S_2 foliation. The Mg-chlorites are of a secondary, metamorphic alteration, origin related to late (?) D_3 events.

s) Sub-unit B_{6-d} - fine grained, dark green chlorite schists.

The B_{6-d} type rocks are fine grained, dark green generally homogeneous chlorite schists which vary greatly from massive to schistose in nature. Their colour ranges from dusky green (5G 3/2) to greenish black (5GY 2/1) on the GSA rock color chart.

These rocks are dominated by dark green, Fe-rich chlorites which occur as fine grained (<0.1 mm) randomly oriented to schistose intergrowths. Albite also occurs as a minor constituent in the rock, either as a fine grained matrix mineral or, often, as diagnostic, small, elongate, euhedral, porphyroblastic

white albite laths, 1 mm max. length ('speckled chlorite schists') (see Microphoto's 17+18+19). These generally show crosscutting relationships to the main S_2 foliation, but are often rotated into the main S_2 foliation in the most schistose rocks. Some of the albite porphyroblasts are crenulated and cleaved during D_3. They are therefore thought to be of syn- to post D_2 metamorphic origin.

Sphene is a diagnostic microscopic mineral in these fine grained chlorite schists and usually occurs as trails or zoned trails of minute (0.01-0.05 mm) euhedral to subhedral grains. They generally lie within the main compositional layering of the rock and are often transposed into the main S_2 foliation plane in the more schistose varieties, suggesting an early, pre-S_{1-2}, syn-depositional origin.

Quartz occurs as a minor constituent, locally within the matrix, but often as fracture fillings associated with secondary mobilizations of chalcopyrite and pyrrhotite.

The B_{6-d} type chlorite schists contain a ubiquitous but variable amount of chalcopyrite and pyrrhotite, as disseminations and minor banding and as remobilized veins and fracture fillings.

Distribution.

The B_{6-d} type rocks constitute a major part (c. 50 %) of all the chlorite schists within the main ore zone at Joma. They are for the most part confined to the immediate structural hangingwall of the Cu-rich massive ore horizon within the western parts of the Joma ore body. They are often associated with the B_2 pyrrhotite bearing albite+sericite rich schists and B_3 pyrrhotite bearing ab+chl-rich dark schistose rocks and show gradational contacts to the B_4 pyrite bearing pale schist.

Discussion.

The speckled albite porphyroblasts, are almost totally restricted to the massive to schistose, dark Fe-rich chlorite

schists that are intimately associated with the finely laminated to thicker interlayers of pale albitite and pyrite. These have earlier (p. 64) been described as some form metal rich bottom mud or chemical sediment.

Sphene concentrations that occur in zoned trails resemble larger fragmental textures within the chlorite schists. These are by contrast, very similar to textures seen in the Fe-rich chloritic pillow rims and hyaloclastite fragments. Some of the dark chlorite schists in part at least, are probably intensely altered original hyaloclastite deposits. Especially those, that also contain some pale, albitized pillow breccia like fragments.

e) Sub-unit B_{6-e} - pyrite bearing, moderate green chlorite schists.

The rocks of this sub facies are more moderate greyish-green (5G 5/2) in colour and are massive to schistose and quite homogeneous in nature. They are typically soapy or talc like to the touch and consist almost wholly of a fine grained, felted mass to schistose layering of moderate to pale green chlorite. The chlorites show the pale birefingerence colours typical of mixed Mg-Fe type chlorites.

The rock contains small amounts of sphene, pyrite and calcite and trace amounts of sphalerite. The sphene occurs as typical trails of minute euhedral grains and zoned fine disseminations (dustings). Pyrite is diagnostic for this unit and occurs as fine disseminations and as individual thin, massive to semi-massive, layers associated with minor carbonate (see Microphoto 20).

Distribution.

The pyrite bearing, moderate greenish chlorite schists are less voluminous but more widespread than the B_{6-a} to B_{6-d} type chlorite schists. They are, for the most part, found stratigraphically and gradationally above (structurally below) the Cu-rich dark Fe-chlorites in DDH 2027, where they are associated

with the thin pyritic ore bands. These pyrite bearing chlorite schists occur for the most part lateral to the main 'stringer-feeder' zone, above and within the stratigraphic upper levels of the main ore zone and in direct contact with the thin massive to semi-massive pyritic, distal parts of the Joma ore horizon, i.e. as far west as the base of DDH D18.

Discussion.

There is almost a complete gradation between the pyrite disseminated and layered, moderate greenish chloritic rocks within the upper parts of the chlorite schist stratigraphy, and the thin chlorite, calcite and minor actinolite bearing bands that occur interlayered within the Zn-rich, semi-massive, layered pyritic ore found stratigraphically above the Cu-rich dark chlorite schists and Cu-rich massive pyrite-pyrrhotite ores along the western edges of the Joma ore body (e.g. at the bottom of 375 ØF synk (Fig. 4.6) and along the newer workings of the 362 level).

Individual layers of dark chlorite schists and associated calcite-marble layers are found within the stratigraphic upper levels of the main massive pyritic ore horizon at Joma. These are compositionally very similar to the B_{6-e} type chlorite schists, except that some very dark, massive units rich in hornblende, chlorite and stilpnomelane are also present (see profile B_2-9).

f) Sub-unit B_{6-f}: actinolite bearing, pale, Mg-rich chlorite schists.

This unit is typically pale to moderate greyish-green in colour (10G 6/2 to 10GY 5/2 on the GSA rock color chart), massive to schistose in nature and carries diagnostic minor patches and zones of large, radiating pale actinolite needles. These chlorite schists are also talc like and soapy to the touch and are typically devoid of visible sulphides.

The B_{6-f} type chlorite schists are composed dominantly of pale, Mg-rich chlorites with varying minor contents of actinolite, white mica and sphene and trace amounts of calcite. The sphene

occurs as minute (microscopic) subhedral grains in patches and zones paralleling the original igneous textures (see Microphoto's 21+22).

Distribution.

The B_{6-f} type chlorite schists are not found within the immediate mine area but occur more distal to the main hydrothermal alteration system occupying the immediate stratigraphic footwall to the main ore zone. Numerous small to large patches (max. size 1.5 m) of B_{6-f} type actinolite bearing chlorite schists have been found in the surface drill holes, within the Group A type massive lavas near the contact with, and within, the Group B type older pillowed lava sequence (see DDH D31+D32). In some of the less deformed sections, the actinolite bearing, pale chlorite schists resemble xenoliths or blocks of earlier, fine grained volcanite material that has been hornfelsed(?) and then strongly metasomatized within the massive lavas. The intrusive contacts to the coarser grained massive lavas are well preserved here.

g) Sub-unit B_H - altered hyaloclastites.

Within the pre-ore pillowed sequence (Group B) deeper in the original lava pile, below the main ore zone, and laterally distal to the main hydrothermal alteration zone, recognizable fragmental, dark, chloritic, hyaloclastite like material is found lying interstitial to the individual pillows and as a dark matrix to the zones of pillow breccias. Here, the recognizable dark, zoned hyaloclastite fragments have been visibly altered, their boundaries becoming rather diffuse and they have taken on an increased content of calcite and pyrrhotite disseminations.

The hyaloclastite fragments are composed of predominantly chlorites which are a mixture of a dark, Fe-rich and a moderately green Mg-rich chlorite. Minor fine grained albite is found intergrown within the chlorites. Sphene also occurs as typical microscopic trails or zones of minute grains which parallel the original boundary to the individual hyaloclastite fragments. Calcite is a common and sometimes major component within the matrix and

occurs commonly as patchy concentrations typically associated with larger concentrations of disseminated pyrrhotite. Sericite occurs only in minor quantities.

Discussion.

As previously mentioned, these paler coloured, slightly altered hyaloclastites occur distal to the main hydrothermal alteration zone and deeper within the volcanic pile, stratigraphically below the Joma ore zone. Their distal position within the hydrothermal zone is reflected by their increasing contents of calcite, white mica and Mg-rich chlorites and their minor pyrrhotite and Zn contents compared to the strong Fe- and Cu enrichment within the central 'feeder zone' beneath the ore zone.

The zoned, angular nature of the sphene trails which parallel the original fragmental boundaries is typical for hyaloclastites and pillow rim structures and reflects an original zoned crystallization differentiation that forms by a quick and progressive chilling within the outer skin during pillow formations.

Chemistry of the chlorite schists.

The chlorite schists, as a whole, show great variation in their major element contents. Their SiO_2 contents are generally very low (between 29 to 42 %) and their Al_2O_3 contents show greatest variations in all the host rocks at Joma, ranging from 11 to 18 %.

The dark, Fe-rich chlorite schists, units B_{6-a} through to B_{6-d}, are all largely enriched in Fe_2O_3 and show only minor degrees of MgO, K_2O and Na_2O enrichments depending largely on their albite and biotite contents. They are generally very depleted in CaO, reflecting their complete lack of epidote, calcite and actinolite. They are notably enriched in Cu and S, reflecting their ubiquitous high content of disseminated chalcopyrite-pyrrhotite. They are also enriched in Ba and their Zn contents are moderately higher (400-500 ppm) than the basalt precursor (B_0) and slightly altered metabasalts (B_1) which carry approximately 95 ppm Zn.

The pyrite bearing, moderate green chlorite schists (unit B_{6-e}) are enriched in Al_2O_3 and MgO and depleted in CaO, Na_2O and K_2O. They are also notably enriched in both Zn ($\pm$Pb?) and Ba, but depleted in Cu compared to the dark, Fe-rich chlorite schists (units B_{6a-d}).

The actinolite bearing, pale chlorite schists (unit B_{6-f})are also enriched in MgO and show only slight increases in CaO and notable depletions in Fe_2O_3, Na_2O, K_2O and trace element S, Cu and Ba. The Zn contents are slightly higher (355 ppm) than those of the mildly spilitized basaltic precursor (B_o=D type rocks ca. 130 ppm Zn).

The slightly altered distal hyaloclastites (unit B_H) show slight increases in both Fe_2O_3 and MgO and are notably enriched in CaO compared to the darker, Fe-rich chloritic hyaloclastites which occur proximal to the main ore body and the hydrothermal alteration zone. They show lower concentrations of Na_2O and K_2O and are typically enriched in Zn and depleted in Cu and show only slight enrichments in Ba.

Discussion.

The chlorite schists at Joma were probably formed under several different modes of deposition:

1) The dark Fe-rich chlorite schists found hosting pale albititic fragments probably represent strongly altered hyaloclastite material associated pillow breccia deposits. The zoned sphene trails paralelling the fragmental contacts give evidence of remnants of glassy pillow rim fragments.

2) Larger patches of greyish-green chlorite schists within the massive greenstones (Group A), distal and stratigraphically below the main stringer root zone, probably represent xenoliths of fine grained volcanites or phyllitic material metasomatized to Mg enriched chlorite schists.

3) Some of the dark Fe-chlorite schists (unit B_{6b}) adjacent to the Cu-rich parts of the main ore zone occur as thin interlayers with pale albitite+quartz+pyrite rich layers, sometimes

containing thin dark, magnetite bearing cherty units. These probably represent alternating interlayers of Na-(albite) and Fe-rich (chlorite) chemical sediments that were deposited down slope and probably slightly distal to the main hydrothermal feeder vent.

Stilpnomelane and biotite are common secondary metamorphic minerals found within the chlorite schists near the massive ore zone. These two minerals are generally confined to areas affected by D_3 deformation, occurring along S_3 cleavages and often penetrating out along the S_2 foliation away from the cross-cutting S_3 cleavage

4.3.7 Distribution and Zonal Arrangements of the Host Rock Lithologies.

The relative distribution of the various host rock lithologies has been discussed during the descriptions of the individual lithological units. The present geogrphical distribution of the pre-ore host rock units within the structural hangingwall of the Joma ore body can be seen in the vertical geological profiles, TABLE-E, Appendix (i.e., see profiles B_2-11, B_1-8, X95200, X95000) and Fig. 2.2a+b.

The distribution and relative amounts of the various host rocks in their original stratigraphic position beneath the main ore zone is shown in Fig. 4.8. This presentation can only be considered as schematic as the post depositional intense deformations (D_2 isoclinal folding and thrusting and D_3 folding) causes great problems in interpreting the original configuration of the feeder zone which forms the root zone to the overlying main ore zone.

As can be seen from the schematic model for the distribution of the host rock lithologies at Joma (Fig. 4.8), the lithological units have distinct relations to each other and the ore types in the massive ore horizon. The host rocks show zonal arrangement patterns within the stratigraphic footwall position of the main ore zone. This is interpreted as reflecting the varying degrees

of intense hydrothermal alteration within the feeder zone during the formation of the massive ore horizon at Joma. The most intensly altered rocks from the central core within the upper levels of the feeder zone and the less altered rocks show a zonal trend or halo configuration away from the central parts of the feeder zone.

Although the true configuration of the host rock lithologies is still rather speculative, their relative positions to each other and the main ore zone and their abandancies have been interpreted as in Fig. 4.8 and described as follows.

Distribution.

The dark, Fe-rich chlorite schists (units B_{6a-d}) and pale albite-pyrite rich rocks (units B_{5a+b}) occur as inconsistant thin layers at the immediate stratigraphic footwall position to the massive sulphide horizon, slightly distal or down slope from the main feeder zone. They show a very strong association to the Cu-rich, cp+po and minor mt bearing pyritic ore facies. Some of the dark chlorite schists (units B_{6a+b}) contain quartz and albite concentrations along with quartz veining and flooding and biotite concentrations accompanying a strong Cu enrichment in the form of chalcopyrite disseminations and veins. These are very remeniscent of the veined upper parts of the stringer zone (feeder zone).

The chlorite schists at the base of and within the thinner more distal parts of the massive ore horizon (units B_{6e}) are more moderate greenish in colour, Mg+Fe-rich and pyrite bearing and often containing carbonate concentrations plus minor actinolite and Zn mineralizations.

Strongly sulphide disseminated, pale albite+sericite+chlorite and minor actinolite rich schists form the central parts to the top of the feeder zone, directly beneath and slightly lateral to the dark chlorite schists and pale albitite units. The pale schists have been divided into two major units. The po disseminated, pale schist, unit B_2, appear to be more limited in

their distribution occurring near the top, but beneath unit B_4 in the central part of the feeder zone. This unit grades laterally and upwards towards the main ore zone into a quartz and pyrite veined, actinolite porphyroblastic, pale schist, unit B_4, which is thicker and has a more widespread distribution beneath the thicker parts of the main ore zone. Unit B_{4-b} type rocks occur as thin horizons directly beneath the thicker parts of the massive pyritic parts of the Joma ore horizon.

The true position of the units B_2 and B_4 pale schists is debatable. Both the B_2 and B_4 pale schists grade into slightly daker grey-green, more massive, po disseminated ab+Fe-chl schists, unit B_3. These carry minor remnants of ep knots and calcite. The B_3 type rocks are rather limited in their distribution, confined to lateral and upper parts of the feeder zone. They grade into the B_4 type pale schists and lie directly beneath the B_{6a-d} type dark chlorite schists and the Cu-rich parts of the main ore zone. Thin zones of po disseminated pale, ab+Fe-chlorite units also penetrate down into the deeper parts of the feeder zone, unit B_1. These are represented by the thin rusty zones that project SSW from the open pit. These thin zones of po disseminated, ab-rich pale schists are thought to represent the central parts of the feeder zone that penetrate down into a wider defuse zone of darker green pillowed volcanites characterized by Fe-chlorites, ep knots, ep+qtz veins and po disseminations. These are typical of the unit B_1 type rocks.

Some >50 meters below the main ore zone, the dark Fe-chloritic, unit B_1, rocks appear as thin zones of central ab+po-rich rocks surrounded by dark, Fe-chlorite schistose zones. These are thought to mark the paths of the upwelling hot, metal rich hydrothermal fluids. The depth to which these thin, dark, Fe-chloritic (B_1) zone penetrate down into the volcanostratigraphy is uncertain, but they must exceed several hundred meters below the main ore zone, down into the massive volcanite level (Group A) (see Figs. 2.1, 2.2 and 2.4). Some alteration has been seen in the layered cherts and graphite phyllites below the massive volcanites.

Similar rocks have been described within the central parts of the feeder zone below the Løkken deposit (T. Grenne, pers. comm. 1985). The Løkken deposit and its host rocks are relatively undeformed and the lower parts of the feeder zone there occurs as a ca. 50 m wide zone composed almost totally of dark Fe-rich chlorite schists with minor quartz and po disseminations. The feeder zone at Løkken is interpreted as having formed along a major deep penetrating fault structure.

The relatively undeformed B_o type volcanites occur lateral to the deep penetrating thin zones of dark chloritic rich rocks (unit B_1) and occupies the major part of the pre-ore volcanostratigraphy beneath the Joma ore horizon. The B_o type pillowed metavolcanites are characteristically paler green in colour and rich in epidote+calcite veinlets and minor pyrrhotite disseminations. Chemically, from a hydrothermal alteration point of view, they (B_o) are considered equivalent to the mildly spilitic distal greenstones (D).

The pale chlorite and actinolite bearing schists (units B_{6f} and B_H) are typical for more lateral positions to the main feeder zone and are often found deeper within the volcanostratigraphy beneath the main ore zone. The B_{6f} rocks occur as small intensely altered and recrystallized patches within the massive volcanites complex (Group A) and probably represents metasomatized xenolithic remnants of fine grained pillowed volcanites (Group B?) or earlier phyllites ?

4.4. CHEMISTRY OF THE HOST ROCK

4.4.1. Introduction.

The major mineral and chemical features of the various host rock lithologies have been discussed in connection with the descriptions of the individual units.

This section will be devoted to the chemical variations and trends within the host rocks and the elemental zonation trends and their

relationship to the hydrothermal alteration patterns which are typical for the feeder zones of volcanogenic submarine exhalative-sedimentary deposits such as Joma.

The chemical variation in the host rock lithologies is compared to the mildly spilitic distal greenstones (Group D) and the less altered pillowed sequence (Unit B_o) of the pre-ore middle greenstone pillowed volcanites (Group B) which occurs lateral to the more intensely altered host rock series, units B_1 to B_6, that form the central feeder zone at Joma. The group D and B_o type volcanites are considered as precursors to the host rock lithologies, and against which the enrichment and depletion trends within the feeder zone have been compared.

The host rock lithologies and mildly spilitic distal greenstones, Group D and B_o rocks, have been plotted on a $CaO-FeO^{tot}-MgO$ (CFM)) diagram to show the major enrichment and depletion trends produced by increased hydrothermal alteration within the feeder zone. The major and trace element silicate analytical data for the host rock lithologies and the major volcanite groups at Joma have been subjected to a statistical analysis, both Factor and Cluster analysis. The Cluster groups are compared on a CFM diagram to the host rock lithological units that have been separated out for this report.

4.4.2. Chemical variations in the host rocks.

The major and trace element variations within the individual host rock lithologies have been studied and compared to the mildly spilitic distal greenstones (Group D) and the slightly altered middle greenstone units - massive volcanites (Group A) and pillowed volcanites (Group B).

Fig. 4.9a and b, shows the mildly spilitic precursor groups D, A and B_o on the left hand side, with the increasingly altered, pre-ore, host rock series (from B_1 to B_6) occurring across the diagram towards the right hand side. The more distal host rock units occur at the extreme right.

The mean values (circles) and standard deviations (bars) are given for each rock type to show the spread in the chemical data.

Individual elemental variations.

SiO_2: Silica shows very little variation between the host rock types compared to the mildly spilitic distal greenstones (D). There is, however, a slight increase within the more intensely altered and sulphide mineralized rocks, which probably reflects the increased quartz veining and flooding in these rocks, such as units B_2, B_5 and B_{6d}. The paler chlorite schists (B_{6-e}) associated with the distal ore horizons are low in SiO_2, being notably rich in pyrite and carbonate compared to the more proximal, dark, Fe-rich chlorite schists (B_{6d}).

TiO_2: Titanium shows a very flat pattern across the host rock lithologies, with only slight depletion in the pale schists (B_4 and B_{4-b}) and chlorite schists (B_{6a-f}) and a slight peak in the more massive, albite rich units, B_3 and B_5.

Al_2O_3: Aluminium shows a very slight decrease in the massive ferrobasalts (A) compared to the distal greenstones (D). This is most likely a magmatic trend. Otherwise, Al shows no regular trend except for the notable peaks in the proximal white schists (B_{4b}) at the top of the feeder zone and the more distal pale chlorite schists (B_{6e}). These Al peaks may be due to chlorite contents. Several of the Mg-rich chlorites are rich in Al compared to other chlorite varieties (D. Janeky, pers. comm. 1986). These two rock types are thought to be more distal from the main hydrothermally altered feeder zone and are notably enriched in white mica, some of which may represent the influx of clay minerals from a detrital source.

$Fe_2O_3^{tot}$: Total Fe, as Fe_2O_3, shows a marked increase in the Group A massive ferrobasalts compared to the distal greenstones (D) and the slightly altered lower pillowed

volcanite (unit B_1). This is a magmatic differentiation trend. Fe shows a slight depletion or a flat trend within the lower feeder zone rocks (units $B_1 + B_2 + B_4$) but is visibly enriched in the albitites ($B_5 + B_4$) and especially in the dark, Fe-rich chloritic rocks (units B_{6a-e}) that occur at the top of the feeder zone. This enrichment in Fe reflects the greater amounts of sulphides (py, po and cp) and Fe-rich chlorites and amphiboles that occur in these rocks.

MnO: Manganese shows a slight increase within the massive ferrobasalts (Group A) compared to the distal greenstones (Group D). This is also probably a magmatic trend. Mn shows an overall weak depletion within the feeder zone rocks compared to the distal greenstones (D) and chlorite schists away from the feeder zone units B_{6f} and B_H. The lowest Mn values are found within the albitites (B_5) and increase markedly within the chlorite schists (units B_{6a-f}) at the top of and distal to the main feeder zone.

MgO: Mg shows a slight decrease in the massive ferrobasalts (A) compared to the distal greenstones (D). This is considered a magmatic differentiation trend. Mg shows a very flat trend throughout the host rocks within the lower feeder zone and a marked depletion in the albitites (unit B_5) and enrichment in the chlorite schists and rocks that are distal to the main feeder zone (units B_{6e} and B_{6f}).

CaO: Calcium shows a very flat pattern within the mildly spilitic distal greenstones (D), and the stratigraphicly lower massive ferrobasalts (A) and the slightly altered lower pillowed volcanites (B_o), even though these rocks show a zonal mineralogical pattern from calcite to epidote enrichments increasing in towards the main hydrothermal feeder vent. Ca does, however, show a marked depletion with increasing hydrothermal alteration within the feeder zone. Ca increases away from the main feeder zone (i.e., see the distal chlorite schists B_{6f} and B_H).

Na_2O: Sodium shows an enrichment trend within the feeder zone culminating with the albitites (B_5) which occurs at the top of and slightly lateral to the central feeder zone, associated with the Fe-rich chlorite schists. The pyrite bearing, pale schists, units B_4 and B_{4b}, show a marked depletion in Na_2O, reflecting a decrease in albite in this, what is interpreted as the very top of the feeder zone, immediately underlying the main ore zone.

K_2O: Potassium shows an almost reverse pattern to Na_2O, being markedly depleted in the slightly altered rocks around Joma, Groups A and B_1, compared to the mildly spilitic distal greenstones (D). K increases within the upper parts of the feeder zone, units B_2, B_4 and B_{4b}, which reflects the sericite content inthe pale schists. The albitites and dark chlorite schists, lateral to the top of the central feeder zone and distal beneath the massive ores are depleted in K_2O. The pale chloritic and actinolitic rocks (units B_{6f} and B_H) which occur lower within the volcanostratigraphy lateral to the main feeder zone, show the same K_2O values as the mildly spilitic distal greenstones (D).

P_2O_5: A distinct enrichment in P_2O_5 within the distal greenstones D, compared to the lower pre-ore volcanites at Joma, Groups A and B, corresponds to similar increases in the incompatible elements, Ti, Zr and Y. (See previous discussions, section 1 pp. 28-29). This most likely represents a purely magmatic differentiation trend. The irregular pattern for P_2O_5 across the altered host rocks, with peaks in the po bearing, pale schists (B_2) and py bearing, albitites (B_5), and decreased values in the py bearing pale schists (B_4 and B_{4b}) are fluctuations that are presently unexplained.

Individual trace elements.

S: Sulphur contents are very low (0.05-0.50 %) within the distal greenstones (D) and the mildly hydrothermally

altered host rocks (Groups $A+B_0$). The sulphur content increases with increasing hydrothermal alteration and accompanied sulphide dissemination and veining within the feeder zone. This increases markedly upwards towards the main ore zone, culminating in the albitites (B_5 = ca. 8-10 % S), pyrite bearing pale schists (B_4 + B_{4b}) and the chalcopyrite-pyrrhotite bearing dark chlorite schists (B_3 and B_{6a-d}), immediately beneath the massive ore horizon.

Cu: Copper has a background values of 30 ppm within distal greenstones (D). Cu has a similar trend to S, showing a gradual enrichment with increasing hydrothermal alteration and nearness to the main ore zone. Cu, however, shows a very strong correlation with the dark Fe-rich chlorite schists (B_3 and B_{6a-d}) which contains on an average up to 4000 ppm Cu. The dark chlorite schists show a strong spacial association with the Cu-rich massive ores. The paler, Fe+Mg-rich distal chlorite schists (units B_{6e+f} and B_H) contain very low Cu values (50-100 ppm Cu).

Zn: Zinc shows a similar enrichment trend with increasing alteration and nearness to the main ore zone as does S and Cu. The Zn content shows a gradual increase from the distal greenstones (background value D=80 ppm). The high Zn content correspondsto the pyrite bearing and pyrite veined, pale schists (units B_4 and B_{4b}, 3000 ppm), the pyrite bearing albitites (B_5) and the pyrite and carbonate bearing distal chlorite schists (B_{6e}). The Zn enrichment pattern is also very similar to that of K_2O.

Ba: Barium has a background value of 130 ppm within the distal greenstones (D). Ba shows the same general trend as K_2O and partly as Zn, decreasing first within the distal and deeper parts of the feeder zone (B_1= 21 ppm) and then a increasing gradually with increasing hydrothermal alteration, culminating in the pyrite bearing, pale schists, units B_4 and B_{4b}, at the top of the feeder zone (unit B_{4b} = 197 ppm).

Sr: Strontium has a background value of ca. 230 ppm within the distal greenstones (D). Sr shows a very similar trend to CaO with an overall gradual depletion with increasing hydrothermal alteration within the central feeder zone and with closeness to the massive ore horizon. The pyrite bearing pale schists (B_{4b}) and distal, pyrite bearing, pale chlorite schists (B_{6e}) contain the lowest Sr values, ca. 20 ppm.

Ni: Nickel has a background value of ca. 160 ppm within the distal greenstones (D). Ni shows a flat trend within the host rock lithologies, being slightly lower (75-100 ppm) than the distal greenstones (D) and the post-ore volcanites (Group C_1 = 163 ppm). This probably represents a magmatic differentiation trend, the Ni content being originally lower in the pre-ore volcanites (Groups A + B) compared to the distal (D) and post-ore volcanite series (C_1).

Cr: Chronium has a background value of ca. 380 ppm within the distal greenstones (D). Cr, like Ni, also shows a lower background content within the pre-ore host rocks compared to the distal (D) and post-ore (C_1) volcanites. This is a primary magmatic differantiation trend. Cr shows, however, slightly more variation than Ni and has a pattern very similar to MgO. Cr shows slight enrichments in the pyrite bearing, pale schists (B_4 and B_{4b}) within the upper parts of the feeder zone, and a marked depletion within the albitites (B_5) and the dark Fe-rich chlorite schists (units B_3 and B_{6a-d}).

V: Vanadium has a background value of ca. 340 ppm within the distal greenstones (D). V shows a relatively flat pattern across the host rock lithologies, with only a slight increase occurring in the pyrite bearing, pale schists (B_{4b}).

Y: Yttrium has a background value of ca. 30 ppm within the distal greenstones (D). Y shows a rather flat pattern

across the host rocks, with only a slight depletion in the pyrite bearing, pale schists (B_4 and B_{4b}) and the dark chlorite schists (B_{6a-d}), and an enrichment in the albitites (B_5 = 60 ppm). Y has a similar trend as TiO_2.

Zr: Zirconium has a background values of ca. 100 ppm within the distal greenstones (D). Zr shows an identical trend to both TiO_2 and Y, having only a slight decreases with increasing hydrothermal alteration within the feeder zone and a marked increase within the albitites (B_5).

4.4.3 Chemical Trends in the Host Rocks.

Several major and trace element variation trends have been noted for the pre-ore, host rock lithologies - feeder zone alteration series, within the stratigraphic footwall of the main ore horizon at Joma. The following elemental trends have been noted (see Fig. 4.9a+b):

1) The incompatible elements Ti, P, Zr and Y are elements that show characteristic magmatic differentiation trends within different global tectonic environments. The metavolcanites at Joma are rather homogeneous in composition consisting almost solely of metabasalts. Intermediate and felsic volcanites are absent at Joma (see Fig.2.5). These elements, Ti, P, Zr and Y, and also Al, are considered to be immobile during spilitization to moderate degrees of hydrothermal alteration. These elements show very little variations (see standard deviations = bars in Fig. 4.9) from their mean values for all the host rocks at Joma. They all show a relatively flat pattern in the host rocks compared to the mildly spilitic distal greenstones. The host rocks retain their relatively high Ti, P, Zr and Y contents even in the most altered host rocks (albitites B_5). These 'so called' immobile elements do, however, show a slight depletion with inreased alteration within the feeder zone. This apparent depletion in trace elements probably reflects a volume increase within the rocks, with increased sulphide disseminations, quartz veining and generation of

hydrous minerals such as chlorite, amphibole and micas. The albitites (unit B_5) contain very little hydrous minerals.

2) Mg +Cr $\pm$ Ni are also compatible elements that vary with magmatic differentiation. A slightly lower content for these elements has been noted in the pre-ore volcanite series (Groups A + B) when compared to the distal greenstones (D). Mg and Cr both show gradual depletion with increased hydrothermal alteration within the stratigraphic lower parts of and lateral to the main feeder zone. Mg and Cr are, however, enriched within the pyrite bearing, sericite, chloritic and actinolite bearing pale schists (B_4 + B_{4b}) near the top of and slightly lateral to the feeder zone, compared to the albitites (B_5) and Fe-rich chlorite schists (B_{6a-d}) which occur slightly distal to the central feeder zone beneath the main ore zone. Mg and Cr are notably enriched within the paler chlorite schists, units B_{6e} and B_{6f} which occur immediately lateral to the feeder zone.

3) There is an overall general enrichment of Fe+Na+S+Cu+Zn with increasing alteration within the feeder zone up towards the massive ore zone. Fe enrichment corresponds to increases in sulphide mineralization and Fe-chlorite formation. The Fe-has its greatest concentrations within the dark chlorite schists at the top of the feeder zone.

An increase in Na corresponds to the general increase of albite with increasing alteration within the feeder zone, culminating in the albitites (B_5) which also carry large quantities of pyrite. Fe and Na have a clearly antipathetic trend within the albitite and Fe-rich chlorite schists at the top of the feeder zone.

Sulphur (S) shows a clear enrichment trend with increasing alteration, corresponding to the general increase in sulphide mineralization, first as po + cp disseminations deeper within the feeder zone and culminating in the albitites at the top of the feeder zone which contain great quantities of pyrite.

Cu and Zn show an overall general enrichment in towards the ore zone. They show, however, a clearly antipathetic relationship to each other, Cu having a strong positive

correlation with the po bearing, Fe-rich chlorite schists and Zn, a positive correlation with the pyrite bearing, pale schists, albitites and the more distal, pyrite and carbonate bearing, paler chlorite schists.

4) Both CaO and Sr show a marked depletion with increasing hydrothermal alteration within the upper parts of the feeder zone, beneath the main ore zone. This corresponds to the disappearance of both epidote and carbonate there. CaO and Sr depletion with increased hydrothermal alteration forms a marked zonal depression across the upper parts of the feeder zone. The higher background values within the mildly spilitized and hydrothermally altered lateral greeenstones form a marked halo covering a larger area surrounding the feeder zone. The large amounts of epidote stable within the lower parts of the feeder zone retain the CaO contents there.

5) K_2O and Ba also show a clear zonal pattern within the host rocks surrounding the Joma ore body. The mildly spilitic greenstone surrounding the Joma ore body all show moderate levels of K_2O and Ba. These are depleted rapidly in towards the highly altered rocks of the feeder zone and increase markedly within the pale schists within the upper parts of the feeder zone. This enrichment corresponds to the sericite found there. Zn shows a similar trend to K_2O and Ba within the mineralized upper parts of the feeder zone at Joma.

4.4.4. Major Element Variations, Zonal Patterns and Hydrothermal Alteration.

a) <u>Introduction.</u>

In Section 3 dealing with spilitization and sub seafloor convective hydrothermal systems it was noted that specific elements were very mobile, being depleted and enriched within the rocks with varying intensities of hydrothermal alteration. This occurs at various positions within the convective hydrothermal system, depending greatly on the amounts of rock being reacted by sea water, temperature and evolution of the reacted hot hydrothermal

fluid. Mg, Na, K, Ca, Fe and Si, all show strong zonal patterns within the hydrothermal system depending on their position within the downflow and upflow parts of the convective cell. The hydrothermal alteration within the feeder zone at Joma represents the upflow parts of a major metal transporting hydrothermal convective cell. In order to depict the major alteration trends within the host rock lithologies of the Joma feeder zone, the variations in the major elements Ca, Fe and Mg were studied and plotted onto a CFM diagram. Similar CFM plots were made for a fresh ocean floor volcanite series, basalts to rhyolites, in order to show the natural magmatic differantiation trends for such rocks.

b) CFM Diagrams of Host Rocks.

The host rock lithologies that were originally separated out on a purely textural and mineralogical basis were compared chemically on a $CaO-FeO^{tot}-MgO$ (CFM) diagram. These elements are relatively mobile under spilitization and sub seafloor hydrothermal alteration and show therefore strong zonal patterns within the hydrothermal convective cell (see section III on spilitization).

Data from fresh ocean floor volcanite series (Basalts to Rhyolites) from Iceland, Mid Atlantic Ridge (MAR) and Galapagos were plotted on a CFM diagram to show the primary magmatic differentiation trends of unaltered rocks from the oceanic crust (Fig. 4.10). The magmatic differentiation trend is presented on the CFM diagrams for the host rock lithologies as a comparison to the alteration trends in the host rocks.

The trends for the mildly spilitic, post-ore series (Group C_1) and relatively mildly altered pre-ore volcanite series, the massive volcanites (Group A) and the pillowed volcanites (Group B_o) are shown in Fig. 4.11. The massive volcanites all plot within the field of ferrobasalts of the MORB differentiation series.

The various host rock lithologies (chemical data from Appendix TABLES B-2, B-3, B-4, B-5) all plot clearly into groups on a CFM diagram (Fig. 4.13 and 4.14) and demonstrate two gradational trends. Fe and Mg enrichment trends, within the host rocks, all

projecting out from the slightly altered pre-ore type (B_0) and the slightly altered lower unit within the feeder zone (Group B_1):

1) An 'Fe' enrichment trend which extends from Group B_1 through B_2+B_3 to B_{6a-d} (dark chlorite schists) and finally B_5 (pyrite rich albitites).
2) A 'Mg' enrichment trend extending from B_1 through B_2 to the B_4 and B_{4b} pale schists.

These are real Fe and Mg enrichments within the host rocks and represent trends produced during increased hydrothermal alteration within the feeder zone, when moving upwards towards the root zone to the massive ore horizon at Joma (see Fig. 4.14).

The Mg enrichment occurs within the pyrite and actinolite bearing, pale schists (B_4) which forms the main pyrite veined stringer zone at the top lateral parts of the feeder zone, immediately beneath the main ore zone, and slightly lateral to the main quartz-pyrite veining in the pale quartz-sericite rich rocks.

The Fe enrichment corresponds to the dark Fe-rich chlorite schists and interlayered pyrite rich albitite that occurs immediately beneath the Cu-rich massive ore zone, slightly distal to the main feeder stringer zone.

4.4.5. Statistical Analysis of Whole Rock Silicate Analytical Data.

a) Introduction.

SINTEF Forsker M. Martinsen, at the Geological Institute-NTH, was engaged to carry out statistical analysis on the whole rock analytical data that was produced during this project.

After overcoming some major problems in converting the data from a floppy disc onto a magnetic tape so that the data can be read by the computer at NTH, it was found that only the data from the surface drill core 1986 sample series (TABLE B-6) could be used for the statistical program. The earlier whole rock

analytical data was not available on either discs or magnetic tapes.

The analytical data from the surface drill hole - 1986 series, 355 samples analysed for 19 elements, was converted and set up in the same table format as the earlier analytical series (see TABLE B-6). The 355 samples include 327 samples from the surface drill core, 22 samples of host rock lithologies adjacent to the ore body and 6 samples of distal greenstones and greenschists.

The 355 samples with 19 variables (elements) each were subjected to both Factor and Cluster Analyses. The complete printout of these analyses are found within the Appendix, TABLE D-1 FACTOR ANALYSES, and TABLE D-2 CLUSTER ANALYSES.

b) Factor Analysis.

The data matrix for the 355 samples and 19 variables (elements) was subjected to Factor Analysis. Approximately 80 % of the total variance can be explained by the first 5 factors (see Fig. 4.15).

The correlation matrix (Fig. 4.16) shows correlations between the following variables (elements):

1) TiO_2 shows good positive correlation with P_2O_5, V and Zr and negative correlation with Cr and Ni.
2) K_2O, positive correlation with Ba.
3) P_2O_5, good positive correlation with V and Zr.
4) V, positive correlation with Zr.
5) Cr, positive correlation with Ni and weak negative correlation with Zr.
6) MgO, weak negative correlation with Na_2O.
7) CaO, weak positive correlation with Sr, negative correlation with S and weak positive correlation with Zn.
8) S has weak positive correlation with Zn.

The rotated factor loading (Fig. 4.17) shows that the five factors can be explained as follows:

1) Factor 1 (explains 33.3 % of variance in data) is controlled by positive Ti, P, V and Zr and negative Cr and Ni. This is interpreted as a purely magmatic differentiation factor and corresponds to the major separation between the older (pre-ore), Group A+B and younger (post-ore), Groups C_1 + C_2 volcanite series at Joma.
2) Factor 2 (explains 20 % of variance) is controlled by positive values of S, Cu and Zn and negative Ca and Sr and is interpreted as a purely alteration-mineralization trend as seen in the stringer-feeder zone.
3) Factor 3 (explains 12 % of variance) is controlled by positive values of Al, Cr and Ni and is interpreted as a differentiation trend.
4) Factor 4 (explains 11 % of variance) is controlled by positive values of Si and Na and minor Fe and negative Mg and may be a combined magmatic differentiation and alteration-mineralization trends. The relatively unaltered ferrobasalts are noticably enriched in Si, Na and Fe and depleted in Mg compared to the more normal metabasalts. Si, Na and Fe are also increased in typical quartz-pyrite veined areas.
5) Factor 5 (explains 5 % of variance) is controlled by positive Mn, K and Ba and is interpreted as an alteration trend, and show good zonation patterns proximal and distal to the main hydrothermal feeder zone (see Fig. 4.9a+b).

c) Cluster Analysis

The same data base, TABLE B-6, was also subjected to a Cluster Analysis (K means clustering of cases) in which the 355 cases (samples) each with their 19 variables (elements) were forced into 5 groups. The reallocation was completed after 15 iterations for the 5 clusters.

The 5 clusters have been termed G_1 to G_5 (Groups 1-5) in order to avoid any confusion with the C_1 and C_2 group volcanites described in section 1.

The raw data (total plots Fig.4.18) and the 5 cluster groups (Fig.4.14) have been plotted onto a $CaO-FeO^{tot}-MgO$ (CFM) triangular diagram in order to compare the cluster groups with the host rock lithologies groups that have been separated out for this report on a textural and mineralogical basis (Section 4.2).

Fig.4.18 shows the spread of the total data (355 cases) on a CFM diagram. The total plot groups well into 2 major groups near the centre of the diagram and comprises the major part of the total data. The cluster groups G_1 to G_5 have also been plotted on a CFM diagram (Fig. 4.19 and 4.20) for comparison with the host rock lithologies groups (Fig.4.13+4.14) and to show Ca-Fe-Mg zonation patterns in the data.

It must be emphasized that the cluster analyses takes into account the variations in all the 19 variables when grouping the data, whereas the grouping on a CFM diagram only considers the variations in the three variables Ca-Fe-Mg. Some of the Cluster groups will not correspond to the host rock lithologies CFM groups as some of the other elements may be dominant in these groups.

The five Cluster groups have the following characteristics and have been interpreted as correlating with the following host rock lithology groups (see Fig. 4.19 and 4.20):

1) <u>Cluster 1</u> (G_1) is the largest group containing 183 cases and corresponds well with the pre-ore Group A massive volcanites, Group B pillowed volcanites and the distal greenstones (Group D). These rocks are mildly spilitic and show magmatic differentiation trends that are characterized by relatively higher values in Fe, Ti, P, Zr and lower Mg, Cr and Ni compared to the post-ore volcanites (Group C_1).
   Cluster G_1 corresponds to host rock groups B_o+B_1+A+D.

2) <u>Cluster 2</u> (G_2) is a small group containing only 5 cases and correlates well with the Group B_{6a-d}, dark Fe-rich chlorite schists. These rocks are characterized by being strongly enriched in Fe, Cu and S and depleted in Mg, Ca, Na and Zn.

3) Cluster 3 (G_3) contains 144 cases and corresponds well with the younger (post-ore) Group C, pillowed and Group C_2 volcaniclastic associated massive units. These volcanites are relatively mildly spilitic to slightly hydrothermally altered and are characterized by having magmatic trends that shows slightly lower Fe, Ti, P, Zr and higher Ca, Mg and Cr and Ni than the older, pre-ore volcanite. The G_3 cluster is therefore separated from G_1.

4) Cluster 4 (G_4) contains 15 cases and appears to correspond to the host rock lithologies B_4 and to a minor degree B_2 and B_6. These rocks are strongly enriched in both Mg + Fe and depleted in Ca, corresponding to the strongly hydrothermally altered host rock lithologies series.

5) Cluster 5 (G_5) contains 8 cases and corresponds to the Mg enriched hydrothermally altered host rock series Groups B_3, B_4 and the chlorite schists B_{6f} and B_{4-b}. These units are devoid of Cu and have little Zn and very little sulphur.

d) Summary of Statistical Analysis.

A comparison of the Cluster Analysis groupings with the host rock lithologies groupings can be summarized as follows:

Cluster Groups	Host Rock Lithologies
G_1	$A + B_o + B_1 + D$ (pre-ore volc.)
G_2	B_{6a-d} (Fe-rich chl. schist)
G_3	$C_1 + C_2$ (post-ore volc.)
G_4	B_4 + minor $G_2 + G_6$ (pale schists)
G_5	$B_3(?) + B_4 + B_{6f} + B_{4b}$ (Mg-enriched, pale schists)

Seven of the nine major host rock lithology groups separated out in the at Joma, Groups D, A, B_1, B_2, B_3, B_4, B_5, B_6 and C, can be explained by the 5 Cluster Analyses groupings. The two units, B_3 (massive to schistose albite + Fe-chlorite rich rocks) and unit B_5 (albitite + pyrite rocks) are not included in the analytical series on which the statistical analysis

is based. These two units are very limited in their lateral distribution within the hanging wall mine series and are confined to the immediate structural hanging wall in direct contact with the Cu-rich massive sulphide ores. They are not represented in the more distal parts of the hydrothermal altered series.

4.5. SUMMARY OF CHARACTERISTIC FEATURES AND CHEMICAL TRENDS

The mineralogy, chemistry and characteristic features of the various host rock lithologies and their relative distributions within the proposed feeder zone beneath the Joma ore body has been given in sections 4.1 to 4.4. These features are summarized in Fig. 4.7 and 4.8. The diagram is set up to show the relative geometric position of the host rocks to each other within the sub ore volcanostratigraphy. The features of the individual host rocks are compared to a mildly spilitic metabasaltic precursor (B_o=D) which is thought to chemically represent the original B series volcanites prior to the intense hydrothermal alteration. Fig. 4.8 shows the relative position of the main host rock lithologies within the footwall position to the main ore body.

The following elemental trends and zonal patterns are present in the chemical data for the host rocks at Joma:

1) There is a marked enrichment of S + Cu + Zn + Fe + Na with increasing alteration and nearness to the main ore zone.
2) There is a positive correlation between Cu and the quartz+pyrrhotite bearing Fe-chlorite schists at the top of the feeder zone in immediate contact with the massive sulphide ore body.
3) There is a positive correlation between Zn and the pyrite veined and disseminated pale schists and the pyrite and carbonate rich chlorite schists at the top of the feeder zone and laterally beneath the distal thinned parts of the Joma ore zone.
4) Ca and Sr show a marked depletion trend with increasing alteration in towards the feeder zone and upwards towards the ore zone.

5) K and Ba show a depletion trend with increasing alteration in towards the central feeder zone and a marked enrichment at the top of the feeder zone within the quartz-sericite rich, pale schists. Both K and Ba show a relative wide zone of depletion surrounding the main feeder zone.

4.5.1. Discussion.

According to Wynne and Strong (1984), several authors (Shirozu 1974, Riverin and Hodson 1980, Henley and Thornley, 1981) have noted a zonation in the magnesium content of chlorite with proximity to the feeder or stockwork zone or pipe of volcanogenic massive sulphide deposits, which are generally thought to result from Mg metasomatism by sea water derived hydrothermal fluids.

This study has shown that the chlorites at Joma vary greatly in texture, colour and probable chemical composition. Several chlorite types have been recognized:

1) Fe-rich chlorites (chamosites?, probably pennite) are dark green in thin section, show strong pleochroism and have violet to purple interference colours under x-nicols. They have $MgO/FeO^{tot} << 1$.
2) A fine grained variety found within the groundmass of most of the mildly spilitic metabasalts, appears olivine-green to brownish in thin section and gives anomalous blue interference colours. These may be 'repidolitic' in composition having MgO/FeO^{tot} about 1.
3) Mg-rich chlorites appear pale green to transparent in thin section and show pale grey-green interference colours and pleochroism. These are most probably 'prochlorites' having $MgO/FeO^{tot} >> 1$.

Electron microprobe analyses of chlorites related to other massive sulphide deposits such as the Strickland Prospect from S.W. Newfoundland (Wynne and Strong, 1984) have shown that the colour changes in chlorites from Berlin blue to grey-green (under X-nicols) are accompanied by a progressive increase in Mg/(Mg+Fe) ratios from 0.27 to 0.94. For comparison, the chlorites at Joma

also show similar trends (only whole rock analyses of relatively pure chlorite schists are available for the rocks at Joma). The Fe-rich chlorite schists (unit B_{6d}) show Mg /(Mg+Fe) ratios of approximately 0.27 and the Mg+Fe-rich chlorite schists (unit B_{6f}) show 0.55.

The zonal patterns of Mg enrichments in the chlorites related to hydrothermal alteration and sulphide mineralization has often been used as an exploration tool, as a guide to ore, i.e. the more Fe enriched chlorites being central within the most intensely hydrothermally altered feeder zone and the Mg enriched chlorites being distal to the stringer zone associated with the less altered rocks.

At Joma, the Fe-rich chlorites are found within the immediate stratigraphic footwall to the Cu-rich massive ores, units B_3 and B_{6a-d}, at the top of the feeder zone and at deeper levels within the feeder zone in the unit B_1 rocks. The Mg enriched chlorites occur adjacent to the feeder zone, beneath the main massive ore zone in units B_4 and B_{4b}, and lateral, immediately beneath the thinned distal parts of the Joma ore horizon (unit B_{6e}) and deeper within the volcanic pile beneath the ore zone (unit B_{6f}) (see Fig. 4.8).

Thus, it has been demonstrated that the chlorites at Joma do show evidence of Fe and Mg enrichment zonations and that there is a positive correlation between the dark, Fe-rich chlorites and Cu mineralizations, (both the massive and disseminated cp-po-rich ores) and the Mg-rich chlorites and the more Zn$\pm$Pb-rich pyritic ores, which occurs as a halo around the upper parts of the stringer zone beneath the massive ores. These observations can be used as an exploration tool at Joma.

4.6. RELATIONSHIP OF FEEDER ZONE TO SUB-SEAFLOOR CONVECTIVE HYDROTHERMAL SYSTEMS

From earlier discussions on spilitization and sub seafloor convective hydrothermal systems (see section 3.6), it was noted

that most of the chl-qtz-rich rocks are either derived from pillows or are pillow breccias with fragments on a scale of centimeters to decimeters. The altered pillows typically show progressively greater Mg uptake (or Fe in the case of upwelling highly reacted hydrothermal fluids), and these were altered at higher sea water/rock ratios from core to rim (Humphries and Thompson, 1978).

From the more thoroughly altered pillows, the distinction between chl-qtz-rich rims and chl-qtz-poor cores is identical to the distinction between hyalospilites and orthospilites drawn by Cann (1969). This relationship can explain for some samples the Fe flux from core to rim and the Na flux from rim to core and is compatible with the hypothesis that interpillow voids represent major channels for sea water flux,as discussed by Seyfried and others (1978). Likewise, the brecciated nature of some of the chl-qtz-rich rocks suggest that breccia zones also acted as conduits for large quantities of sea water.

This may well be the case at Joma, where the pillow breccias and hyaloclastites that occur stratigraphically beneath the orebody also contain dark, Fe-rich chlorite enrichments within the hyaloclastites and pillow rims and pale, albite enrichments within the pillows and pillow breccia fragments (see Photo 5). The Fe-rich chlorites are associated with quartz and a high content of Fe-Cu sulphide disseminations. The Fe-rich chlorite, quartz and sulphide mineralizations within the hyaloclastites and breccia matrix is compatible with the Fe-chl-qtz-rich rocks formed within the upwelling part of a convective system as described by Mottl (1983) and suggests that these rocks were used as conduits for the upflowing hydrothermal fluids that formed the massive sulphides at Joma. These rocks are probably best observed within the mine at the south end of the 480 ØH level (sample no.480 ØH-12 chlorite schist and 480 ØH-13 albite rich pillow breccia fragments) and to the west of the open pit on the surface (sample locations JD-18 + 23/85, see Fig.4.2a+b).

The chlorite rich assemblages, which are the most prominent variety according to Humphries and Thompson (1978), show the greatest chemical changes, while the epidote rich samples show

very little change in composition compared to their basaltic precursor. Mottl (1983) contends that the epidote rich (and equivalent chl-qtz-poor) assemblages were formed under low sea water/-rock ratios within the lower parts of the convective cell or lateral to the main zones of hydrothermal fluid transport. A similar situation occurs at Joma, as the major part of the massive flow units (Group A), which is interpreted as occurring at a very low stratigraphic level, far below the ore horizon, are rich in secondary epidote as matrix minerals, veins and knots. These rocks show, however, little chemical changes from their ferrobasalt precursor. Similarly, the pillow lavas (Group B) adjacent to the main feeder zone at a deeper stratigraphic level below the ore zone, show similar epidote concentrations and very little chemical changes compared to their pillowed basaltic precursor (B_o = D). By contrast, the Fe-rich chlorite and albite rich rocks higher within the volcanostratigraphy, near the ore body show a much more varied chemistry.

A zone of prominant Mg enrichment beneath the Joma ore horizon, lateral to the upper parts of the central feeder zone, probably represents a zone of mixing, in which cold Mg-rich sea water was drawn in towards the feeder zone and mixed with the upflowing, hot, metalliferous, highly evolved hydrothermal fluids. Mixing caused an immediate heating of the groundwater and massive deposition of Mg-rich phases such as anydrite? talc? and Mg-chlorites, accompanied by a cooling of the upwelling hot fluids which caused immediate deposition of the unstable sulphide phases (as pyrite $\pm$ sphalerite veins and disseminations) and minor quartz and carbonate as matrix.

Ca leaching from the rock during sub seafloor hydrothermal alteration is significant and enough to form carbonates on the seafloor (Humphries and Thompson, 1978). There is a large amount of carbonate within the upper levels of the Joma ore horizon, as matrix and as individual, sometimes thick, limestone bands. There are also large quantities of free calcite and limestone bands within the post-ore (Group C) volcanites which may originally have come from the dissolution of earlier formed anhydrite and carbonate lower within the system, that has been redissolved by the colder fluids in a waning hydrothermal system.

It is well known (Goodfellow 1974) that hydrothermal systems depositing massive sulphides on the seafloor continue to circulate hot fluids long after the orebody is capped by younger sediments or volcanites. There are often halos or zoned secondary mineral and elemental distributions within the rocks above the massive ore deposit that are formed during the cooling down or waning stages of a hydrothermal system. The C_{1b} rocks, rich in po disseminations, epidote, albite and actinolite and bearing lesser chlorite and calcite, may well represent such secondary hydrothermal zonations or halos within the overlying younger volcanite sequence.

There are several major difference noted between the hydrothermal alteration mineralogy at Joma compared to that described from the present sub seafloor hydrothermal convective systems. There appears to be a greater amount of albite developed within the Joma hydrothermal system. Pyrrhotite is the major Fe-sulphide facies, occurring as disseminations at all levels within the Joma hydrothermal system compared to pyrite that occurs with epidote in the lower parts of and within the downflowing parts of the presently forming sub-seafloor hydrothermal convective system. These mineralogical variations probably reflect some fundamental difference in the physiochemical conditions during the formation of the hydrothermal alteration at Joma.

4.7. ORIGINAL VOLCANIC STRUCTURES AND IGNEOUS TEXTURES

Original volcanic structures such as pillows, pillow breccia, hyaloclastites, amygdales, flow contacts and dykes, and igneous textures such as sub ophitic to ophitic textures are found within the mildly spilitic volcanites distal to the Joma ore zone. These are partially to completely destroyed with increasing hydrothermal alteration, being notably missing in the most intensely altered parts of the feeder zone at Joma.

The following structural and textural changes are characteristic at Joma with increasing hydrothermal alteration:

1) the complete destruction of all volcanic structures and igneous textures,

2) increase in grain size with increasing alteration (0.1 mm to C.3 mm), some porphyroblastic textures are visible near the ore zone,
3) a simplification of mineral contents and decrease in mineral variations, i.e. ab+chl+act+ep+cc+leuc bearing distal spilite goes to Fe-chl+qtz+po disseminated rocks near the ore zone,
4) very fine grained, diffuse, patchy disseminated concentrations of leucoxene goes to microscopically coarser, euhedral grains of sphene,
5) increased sulphide mineralization (disseminations and veining of po and py) on nearing the main ore zone.

TABLE 4.1: MEAN WHOLE ROCK SILICATE ANALYSES AND MINERAL CONTENTS OF THE JOMA HOST ROCK TYPE LITHOLOGIES AND DISTAL GREENSTONES.

	D		A		C_1		C_{1-b}		B_1		B_3	
	Pale gst. metabasalt mild.spilit pillows		dark metaferro basalt, pre-ore massive volc. deep strat.		pale gst. Cc+ep-rich spilitic post-ore pillows		v.pale gst. ab+po-rich post-ore strong alt. pillows		mod.-dark undiff.gst. pre-ore slight alt. pillows deep strat.		mod.dark ab+chl+po mass-schist pre-ore strong alt. pillows ?	
	Distal gst. (n=9)		HW (n=10)		FW (n=14)		FW ore contact (n=6)		HW (n=10)		HW near ore (n=5)	
	$\bar{X}$	SD	$\bar{X}$	SD	$\bar{X}$	SD	$\bar{X}$	SD	$\bar{X}$	SD	$\bar{X}$	SD
%												
SiO_2	44.88	1.55	47.15	1.19	46.37	1.21	47.62	1.56	46.33	1.75	44.82	3.63
TiO_2	2.04	0.12	1.90	0.25	1.04	0.12	1.23	0.16	1.71	0.29	1.84	0.42
Al_2O_3	14.99	0.43	14.47	0.75	15.73	0.71	15.03	1.38	15.03	1.17	13.99	2.17
$Fe_2O_3^{tot}$	10.87	0.47	13.10	1.01	9.44	0.99	10.76	0.57	11.96	1.46	14.26	0.54
MnO	0.16	0.01	0.18	0.01	0.13	0.02	0.13	0.03	0.15	0.04	0.10	0.03
MgO	8.07	1.31	6.83	0.93	8.64	1.18	8.21	0.91	6.36	0.84	9.16	2.84
CaO	9.46	1.63	10.04	1.38	10.99	1.69	9.57	2.25	10.25	0.79	5.23	2.03
Na_2O	3.05	0.32	3.37	0.43	2.50	0.57	2.97	0.76	3.56	0.63	4.07	0.82
K_2O	0.70	0.40	0.13	0.10	0.63	0.52	0.33	0.50	0.12	0.19	0.32	0.36
P_2O_5	0.32	0.11	0.21	0.03	0.09	0.02	0.10	0.01	0.22	0.05	0.21	0.08
LOI	4.52	1.84	2.48	0.36	2.98	1.25	2.23	0.90	2.22	0.74	3.57	1.54
% S	0.08	0.07	0.40	0.28	0.23	0.29	0.90	0.52	0.34	0.19	3.33	3.23
ppm Cu	32	24	61	25	92	29	165	76	77	24	2366	4771
Zn	78	6	98	12	69	13	133	59	95	8	485	203
Ba	129	87	28	15	69	63	102	98	21	19	128	100
V	343	30	351	37	226	23	303	64	337	31	343	62
Cr	381	62	167	46	342	70	296	96	203	52	159	93
Ni	158	23	88	15	163	48	130	70	88	23	74	51
Sr	232	63	177	50	155	42	185	64	186	37	54	45
Y	27	7	40		21	10	33	21	28	4	45	21
Zr	178	29	187	31	79	20	80	21	163	31	157	55
%	(N=2)		(N=8)		(n=8)		(n=2)		(n=5)			
act.	11	0	19	3	15	4	15	2	18	5	6	3
chl.	44	0.7	32	5	25	7	19	3	30	6	41	8
stilp.	0		0		0		0		0		0	
ab.	28	5	24	5	28	5	33	13	22	4	34	15
qtz	0		tr		0.5	0.8	tr		0		tr	
Bio.	0		0		0		0		0		0	
W.mica	2	0	0		4	5	5	5	0.5	0.9	0	0
Cc	6	3	4	3	7	7	2	2	2	3	3	5
ep.	3	3	16	4	15	6	17	13	21	6	tr	
sp.	5	0	5	0.8	3	1	3	1	5	0	5	1
po	tr		1	0.5	1	1	3	2	1	1	11	8
cp	0		0		0		0		0		tr	
py	0		0		0		0		0		0	
sl	0		0		0		0		0		0	
mt	0		0		0		0		0		0	

	B_2		B_4		B_{4-b}		B_5		B_{6-a}		B_{6-b}	
	pale,massive ab+ser+po schists pre-ore strong alt. pillows		pale, ab+ser +chl schists + py pre-ore strong alt. 'stringer z.'		pale schists ser+chl+py pre-ore strong alt. distal 'stringer z.'		pale albitite + py pre-ore strong alt. + syn-ore chem.sed.		Mod.dark Q+ab+Bio Chl.schist +cp+po pre-ore strong alt.		layered Chl-ab schist +cp+po+py syn-ore chem.sed.?	
	HW near ore altered (n=3)		HW near ore (n=19)		HW ore contact (n=3)		HW ore contact (n=3)		HW ore z. (n=4)		HW ore zone (n=2)	
	$\bar{X}$	SD	$\bar{X}$	SD	$\bar{X}$	SD	$\bar{X}$	SD	$\bar{X}$	SD	$\bar{X}$	SD
%												
SiO_2	50.00	1.44	46.18	3.39	48.10	4.00	47.35	6.00	53.86	15.88	37.12	2.11
TiO_2	1.37	0.49	1.16	0.40	1.63	0.46	2.14	0.40	1.72	0.86	1.89	0.24
Al_2O_3	14.72	0.23	17.50	1.78	19.70	0.69	14.70	1.22	11.34	3.20	15.69	1.75
$Fe_2O_3^{tot}$	9.84	0.58	11.59	2.78	11.04	1.14	14.91	7.07	16.58	6.00	24.04	0.40
MnO	0.10	0.02	0.15	0.07	0.08	0.06	0.05	0.01	0.08	0.03	0.11	0.02
MgO	7.17	1.44	8.98	2.56	7.37	4.78	1.71	1.40	6.54	3.00	8.78	2.67
CaO	6.58	1.91	3.59	2.46	2.46	0.56	3.39	2.63	1.64	0.70	1.51	0.19
Na_2O	5.10	1.14	3.04	1.21	1.48	0.38	6.65	1.35	2.70	0.69	2.91	1.16
K_2O	0.41	0.34	1.73	1.14	4.72	0.87	0.56	0.06	0.94	1.39	2.30	0.28
P_2O_5	0.42	0.50	0.11	0.04	0.18	0.08	0.36	0.40	0.05	0.03	0.16	0.06
L.O.I.	2.53	0.67	5.70	1.95	7.65	1.35	7.84	0.55	3.79	2.05	4.41	0.05
% S	1.26	0.75	2.69	2.20	4.14	2.04	8.97	4.00	3.33	1.99	3.76	1.99
ppm Cu	254	260	205	159	360	231	397	257	4096	2039	2243	1630
Zn	142	107	1111	1205	3000	3394	1264	779	138	45	202	139
Ba	80	78	115	59	197	50	150	113	148	79	185	49
V	279	37	272	57	417	49	312	166	313	116	466	8
Cr	219	68	316	51	307	21	116	92	137	60	144	9
Ni	102	39	115	43	70	10	64	56	45	40	59	27
Sr	102	76	53	48	17	6	51	18	25	19	20	0
Y	40		19	9	27	6	60	5	21	8	30	14
Zr	98	38	83	33	123	38	217	194	105	19	118	46
%	(n=1)		(n=3)				(n=2)		(n=2)		(n=1)	
act.	14		2	2			0		1	1	0	
chl.	22		36	8			13	6	38	9	16	
stilp.	0		0				0		0		0	
ab	45		34	12			57	2	24	4	23	
qtz	0		8	9			tr		9	4	0	
Bio.	0		0				tr		tr		30	
W.mica	2		3	1			tr		tr		0	
cc	6		7	7			0		0		0	
ep	0		tr				0		0		0	
sp	2		3	1			6		6	1	5	
po	6		tr				0		12	7	19	
cp	tr		0				0		6	4	4	
py	0		7	7			21	3	0		tr	
sl	0		tr				tr		0		0	
mt	0		0						0		0	

blank values =not analysed

	B_{6-c}		B_{6-d}		B_{6-e}		B_{6-f}		B_H	
	Coarse gr. dark Chl.sch. +Bio+po+cp strong alt.		Fine-gr. dark Chl.schist +po+cp pre-ore strong alt. +chem.sed.		Mod. green Chl.+act.sch. + py		Pale (Mg)-chl. +act. schist pre-ore altered		Hyaloclastite altered ch+ab+sp sch. pre-ore altered	
	HW ore con. + within ore (n=3)		HW ore contact (n=5)		ore zone distal (n=3)		distal HW deep strat. (n=2)		distal HW deep strat. (n=4)	
	$\bar{X}$	SD	$\bar{X}$	SD	$\bar{X}$	SD	$\bar{X}$	SD	$\bar{X}$	SD
%										
SiO_2	29.13	4.58	37.40	9.00	30.99	2.75	37.62	0.16	42.72	6.52
TiO_2	1.16		1.54	0.44	1.61	0.57	1.35	0.22	1.44	0.32
Al_2O_3	16.96		15.60	2.06	18.47	0.93	15.59	3.06	17.35	3.46
$Fe_2O_3^{tot}$	30.79	4.02	25.97	4.74	20.56	3.00	14.82	0.08	12.81	1.25
MnO	0.19		0.16	0.04	0.18	0.05	0.15	0.03	0.18	0.02
MgO	10.58	0.82	9.82	2.09	17.47	6.73	18.12	1.57	10.43	2.58
CaO	1.22	0.58	2.07	1.07	1.50	0.67	4.34	1.92	6.80	3.06
Na_2O	0.46	0.01	1.59	0.48	0.82	0.93	0.35	0.45	1.97	1.52
K_2O	2.90	3.95	0.02	0.03	0.52	0.77	0.35	0.11	0.93	1.48
P_2O_5	0.07		0.14	0.08	0.13	0.10	0.16	0.01	0.14	0.06
L.O.I.	5.89	2.49	6.00	0.93	8.51	1.64	6.35	0.42	4.45	2.30
% S	2.46	2.22	2.92	1.60	1.01	0.95	0.05	0.07	1.06	1.12
ppm Cu	2208	1524	3538	2744	130	199	70	99	72	44
Zn	506	264	428	213	945	543	355	346	709	1110
Ba	193	136	24	9	140	87	40	14	83	88
V	241	135	382	82	402	158	280	14	321	42
Cr	181	151	224	87	336	92	290	71	408	240
Ni	69	39	42	40	84	31	115	35	150	141
Sr	40	47	48	63	14	5	25	21	122	60
Y	45	35	17	6	35	7	20	0	25	6
Zr	57	45	128	50	110	7	120	14	108	29
	(n=2)		(n=1)		(n=1)		(n=1)		(n=1)	
act.	0		0		0		5		4	
chl.	40	40	76		93		89		45	
stilp.	0		0		0		0		0	
ab	0		13		0		0		26	
qtz	0		2		0		0		tr	
Bio.	49	54	0		0		0		0	
W.mica	0		0		0		2		4	
cc	0		0		tr		tr		15	
ep	0		0		0		0		0	
sp	8	6	4		4		4		3	
po	6	5	6		0		0		1	
cp	tr		tr		0		0		0	
py	0		0		3		0		0	
sl	0		0		tr		0		0	
mt	0		0		0		0		0	

TABLE 4.1: MEAN WHOLE ROCK SILICATE ANALYSES AND MINERAL CONTENTS OF THE JOMA HOST ROCK TYPE LITHOLOGIES AND DISTAL GREENSTONES.

	D		A		C_1		C_{1-b}		B_1		B_3	
	Pale gst. metabasalt mild.spilit. pillows		dark metaferro basalt, pre-ore massive volc. deep strat.		pale gst. Cc+ep-rich spilitic post-ore pillows		v.pale gst. ab+po-rich post-ore strong alt. pillows		mod.-dark undiff.gst. pre-ore slight alt. pillows deep strat.		mod.dark ab+chl+po mass-schist pre-ore strong alt. pillows ?	
	Distal gst. (n=9)		HW (n=10)		FW (n=14)		FW ore contact (n=6)		HW (n=10)		HW near ore (n=5)	
	$\bar{X}$	SD	$\bar{X}$	SD	$\bar{X}$	SD	$\bar{X}$	SD	$\bar{X}$	SD	$\bar{X}$	SD
%												
SiO_2	44.88	1.55	47.15	1.19	46.37	1.21	47.62	1.56	46.33	1.75	44.82	3.63
TiO_2	2.04	0.12	1.90	0.25	1.04	0.12	1.23	0.16	1.71	0.29	1.84	0.42
Al_2O_3	14.99	0.43	14.47	0.75	15.73	0.71	15.03	1.38	15.03	1.17	13.99	2.17
$Fe_2O_3^{tot}$	10.87	0.47	13.10	1.01	9.44	0.99	10.76	0.57	11.96	1.46	14.26	0.54
MnO	0.16	0.01	0.18	0.01	0.13	0.02	0.13	0.03	0.15	0.04	0.10	0.03
MgO	8.07	1.31	6.83	0.93	8.64	1.18	8.21	0.91	6.36	0.84	9.16	2.84
CaO	9.46	1.63	10.04	1.38	10.99	1.69	9.57	2.25	10.25	0.79	5.23	2.03
Na_2O	3.05	0.32	3.37	0.43	2.50	0.57	2.97	0.76	3.56	0.63	4.07	0.82
K_2O	0.70	0.40	0.13	0.10	0.63	0.52	0.33	0.50	0.12	0.19	0.32	0.36
P_2O_5	0.32	0.11	0.21	0.03	0.09	0.02	0.10	0.01	0.22	0.05	0.21	0.08
LOI	4.52	1.84	2.48	0.36	2.98	1.25	2.23	0.90	2.22	0.74	3.57	1.54
% S	0.08	0.07	0.40	0.28	0.23	0.29	0.90	0.52	0.34	0.19	3.33	3.23
ppm Cu	32	24	61	25	92	29	165	76	77	24	2366	4771
Zn	78	6	98	12	69	13	133	59	95	8	485	203
Ba	129	87	28	15	69	63	102	98	21	19	128	100
V	343	30	351	37	226	23	303	64	337	31	343	62
Cr	381	62	167	46	342	70	296	96	203	52	159	93
Ni	158	23	88	15	163	48	130	70	88	23	74	51
Sr	232	63	177	50	155	42	185	64	186	37	54	45
Y	27	7	40		21	10	33	21	28	4	45	21
Zr	178	29	187	31	79	20	80	21	163	31	157	55
	(N=2)		(N=8)		(n=8)		(n=2)		(n=5)			
%												
act.	11	0	19	3	15	4	15	2	18	5	6	3
chl.	44	0.7	32	5	25	7	19	3	30	6	41	8
stilp.	0		0		0		0		0		0	
ab.	28	5	24	5	28	5	33	13	22	4	34	15
qtz	0		tr		0.5	0.8	tr		0		tr	
Bio.	0		0		0		0		0		0	
W.mica	2	0	0		4	5	5	5	0.5	0.9	0	0
Cc	6	3	4	3	7	7	2	2	2	3	3	5
ep.	3	3	16	4	15	6	17	13	21	6	tr	
sp.	5	0	5	0.8	3	1	3	1	5	0	5	1
po	tr		1	0.5	1	1	3	2	1	1	11	8
cp	0		0		0		0		0		tr	
py	0		0		0		0		0		0	
sl	0		0		0		0		0		0	
mt	0		0		0		0		0		0	

	B_2 pale,massive ab+ser+po schists pre-ore strong alt. pillows		B_4 pale, ab+ser +chl schists + py pre-ore strong alt. 'stringer z.'		B_{4-b} pale schists ser+chl+py pre-ore strong alt. distal 'stringer z.'		B_5 pale albitite + py pre-ore strong alt. + syn-ore chem.sed.		B_{6-a} Mod.dark Q+ab+Bio Chl.schist +cp+po pre-ore strong alt.		B_{6-b} layered Chl-ab schist +cp+po+py syn-ore chem.sed.?	
	HW near ore altered (n=3)		HW near ore (n=19)		HW ore contact (n=3)		HW ore contact (n=3)		HW ore z. (n=4)		HW ore zone (n=2)	
	$\bar{X}$	SD	$\bar{X}$	SD	$\bar{X}$	SD	$\bar{X}$	SD	$\bar{X}$	SD	$\bar{X}$	SD
%												
SiO_2	50.00	1.44	46.18	3.39	48.10	4.00	47.35	6.00	53.86	15.88	37.12	2.11
TiO_2	1.37	0.49	1.16	0.40	1.63	0.46	2.14	0.40	1.72	0.86	1.89	0.24
Al_2O_3	14.72	0.23	17.50	1.78	19.70	0.69	14.70	1.22	11.34	3.20	15.69	1.75
$Fe_2O_3^{tot}$	9.84	0.58	11.59	2.78	11.04	1.14	14.91	7.07	16.58	6.00	24.04	0.40
MnO	0.10	0.02	0.15	0.07	0.08	0.06	0.05	0.01	0.08	0.03	0.11	0.02
MgO	7.17	1.44	8.98	2.56	7.37	4.78	1.71	1.40	6.54	3.00	8.78	2.67
CaO	6.58	1.91	3.59	2.46	2.46	0.56	3.39	2.63	1.64	0.70	1.51	0.19
Na_2O	5.10	1.14	3.04	1.21	1.48	0.38	6.65	1.35	2.70	0.69	2.91	1.16
K_2O	0.41	0.34	1.73	1.14	4.72	0.87	0.56	0.06	0.94	1.39	2.30	0.28
P_2O_5	0.42	0.50	0.11	0.04	0.18	0.08	0.36	0.40	0.05	0.03	0.16	0.06
L.O.I.	2.53	0.67	5.70	1.95	7.65	1.35	7.84	0.55	3.79	2.05	4.41	0.05
% S	1.26	0.75	2.69	2.20	4.14	2.04	8.97	4.00	3.33	1.99	3.76	1.99
ppm Cu	254	260	205	159	360	231	397	257	4096	2039	2243	1630
Zn	142	107	1111	1205	3000	3394	1264	779	138	45	202	139
Ba	80	78	115	59	197	50	150	113	148	79	185	49
V	279	37	272	57	417	49	312	166	313	116	466	8
Cr	219	68	316	51	307	21	116	92	137	60	144	9
Ni	102	39	115	43	70	10	64	56	45	40	59	27
Sr	102	76	53	48	17	6	51	18	25	19	20	0
Y	40		19	9	27	6	60	5	21	8	30	14
Zr	98	38	83	33	123	38	217	194	105	19	118	46
	(n=1)		(n=3)				(n=2)		(n=2)		(n=1)	
%												
act.	14		2	2			0		1	1	0	
chl.	22		36	8			13	6	38	9	16	
stilp.	0		0				0		0		0	
ab	45		34	12			57	2	24	4	23	
qtz	0		8	9			tr		9	4	0	
Bio.	0		0				tr		tr		30	
W.mica	2		3	1			tr		tr		0	
cc	6		7	7			0		0		0	
ep	0		tr				0		0		0	
sp	2		3	1			6		6	1	5	
po	6		tr				0		12	7	19	
cp	tr		0				0		6	4	4	
py	0		7	7			21	3	0		tr	
sl	0		tr				tr		0		0	
mt	0		0						0		0	

blank values =not analysed

	B_{6-c} Coarse gr. dark Chl.sch. +Bio+po+cp strong alt.		B_{6-d} Fine-gr. dark Chl.schist +po+cp pre-ore strong alt. +chem.sed.		B_{6-e} Mod. green Chl.+act.sch. + py		B_{6-f} Pale (Mg)-chl. +act. schist pre-ore altered		B_{H} Hyaloclastite altered ch+ab+sp sch. pre-ore altered	
	HW ore con. + within ore (n=3)		HW ore contact (n=5)		ore zone distal (n=3)		distal HW deep strat. (n=2)		distal HW deep strat. (n=4)	
	$\bar{X}$	SD	$\bar{X}$	SD	$\bar{X}$	SD	$\bar{X}$	SD	$\bar{X}$	SD
%										
SiO_2	29.13	4.58	37.40	9.00	30.99	2.75	37.62	0.16	42.72	6.52
TiO_2	1.16		1.54	0.44	1.61	0.57	1.35	0.22	1.44	0.32
Al_2O_3	16.96		15.60	2.06	18.47	0.93	15.59	3.06	17.35	3.46
$Fe_2O_3^{tot}$	30.79	4.02	25.97	4.74	20.56	3.00	14.82	0.08	12.81	1.25
MnO	0.19		0.16	0.04	0.18	0.05	0.15	0.03	0.18	0.02
MgO	10.58	0.82	9.82	2.09	17.47	6.73	18.12	1.57	10.43	2.58
CaO	1.22	0.58	2.07	1.07	1.50	0.67	4.34	1.92	6.80	3.06
Na_2O	0.46	0.01	1.59	0.48	0.82	0.93	0.35	0.45	1.97	1.52
K_2O	2.90	3.95	0.02	0.03	0.52	0.77	0.35	0.11	0.93	1.48
P_2O_5	0.07		0.14	0.08	0.13	0.10	0.16	0.01	0.14	0.06
L.O.I.	5.89	2.49	6.00	0.93	8.51	1.64	6.35	0.42	4.45	2.30
% S	2.46	2.22	2.92	1.60	1.01	0.95	0.05	0.07	1.06	1.12
ppm Cu	2208	1524	3538	2744	130	199	70	99	72	44
Zn	506	264	428	213	945	543	355	346	709	1110
Ba	193	136	24	9	140	87	40	14	83	88
V	241	135	382	82	402	158	280	14	321	42
Cr	181	151	224	87	336	92	290	71	408	240
Ni	69	39	42	40	84	31	115	35	150	141
Sr	40	47	48	63	14	5	25	21	122	60
Y	45	35	17	6	35	7	20	0	25	6
Zr	57	45	128	50	110	7	120	14	108	29
	(n=2)		(n=1)		(n=1)		(n=1)		(n=1)	
act.	0		0		0		5		4	
chl.	40	40	76		93		89		45	
stilp.	0		0		0		0		0	
ab	0		13		0		0		26	
qtz	0		2		0		0		tr	
Bio.	49	54	0		0		0		0	
W.mica	0		0		0		2		4	
cc	0		0		tr		tr		15	
ep	0		0		0		0		0	
sp	8	6	4		4		4		3	
po	6	5	6		0		0		1	
cp	tr		tr		0		0		0	
py	0		0		3		0		0	
sl	0		0		tr		0		0	
mt	0		0		0		0		0	

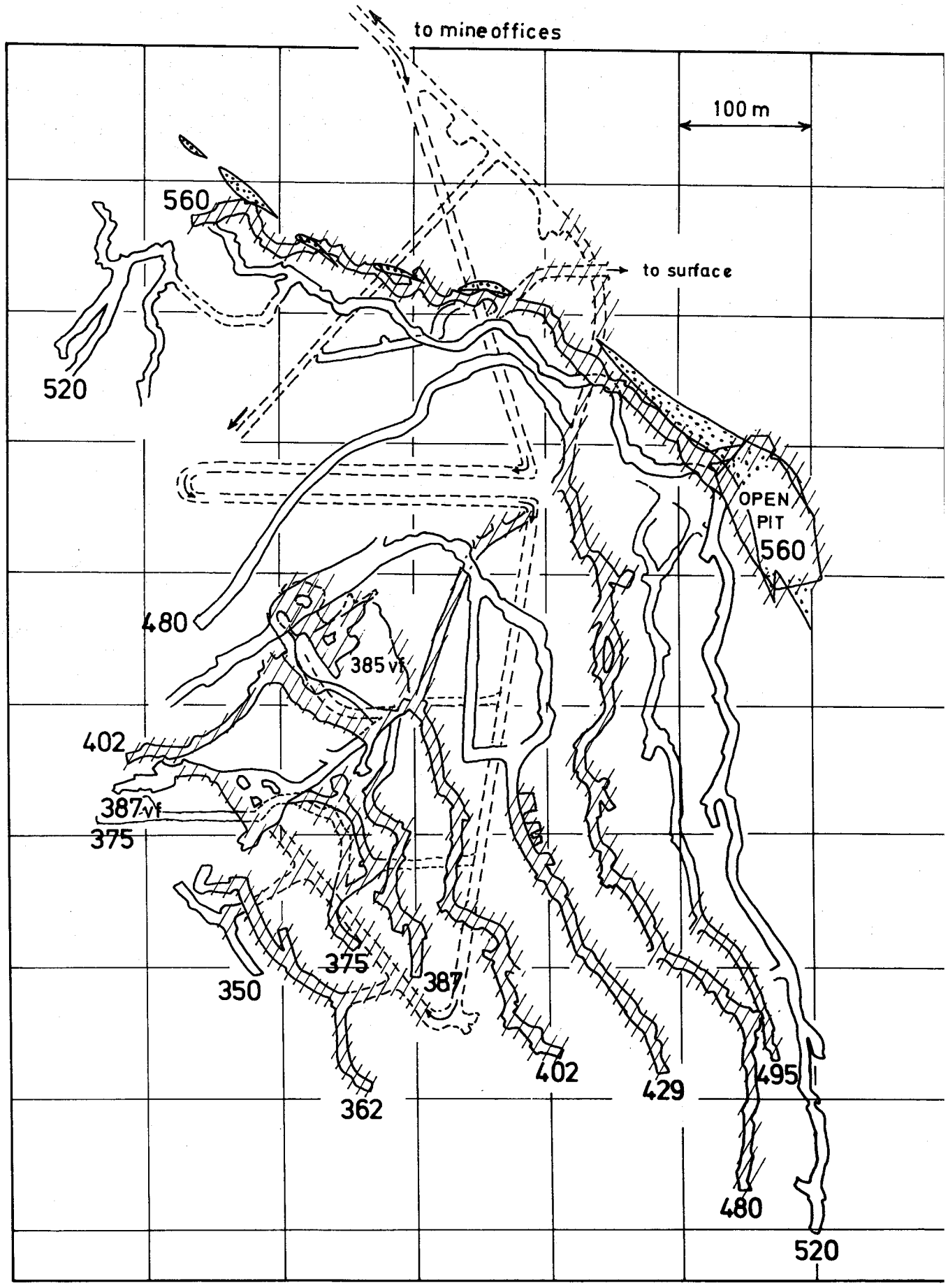

Fig. 4.1a Mine levels that have been mapped in detail in connection with this report (PART II).

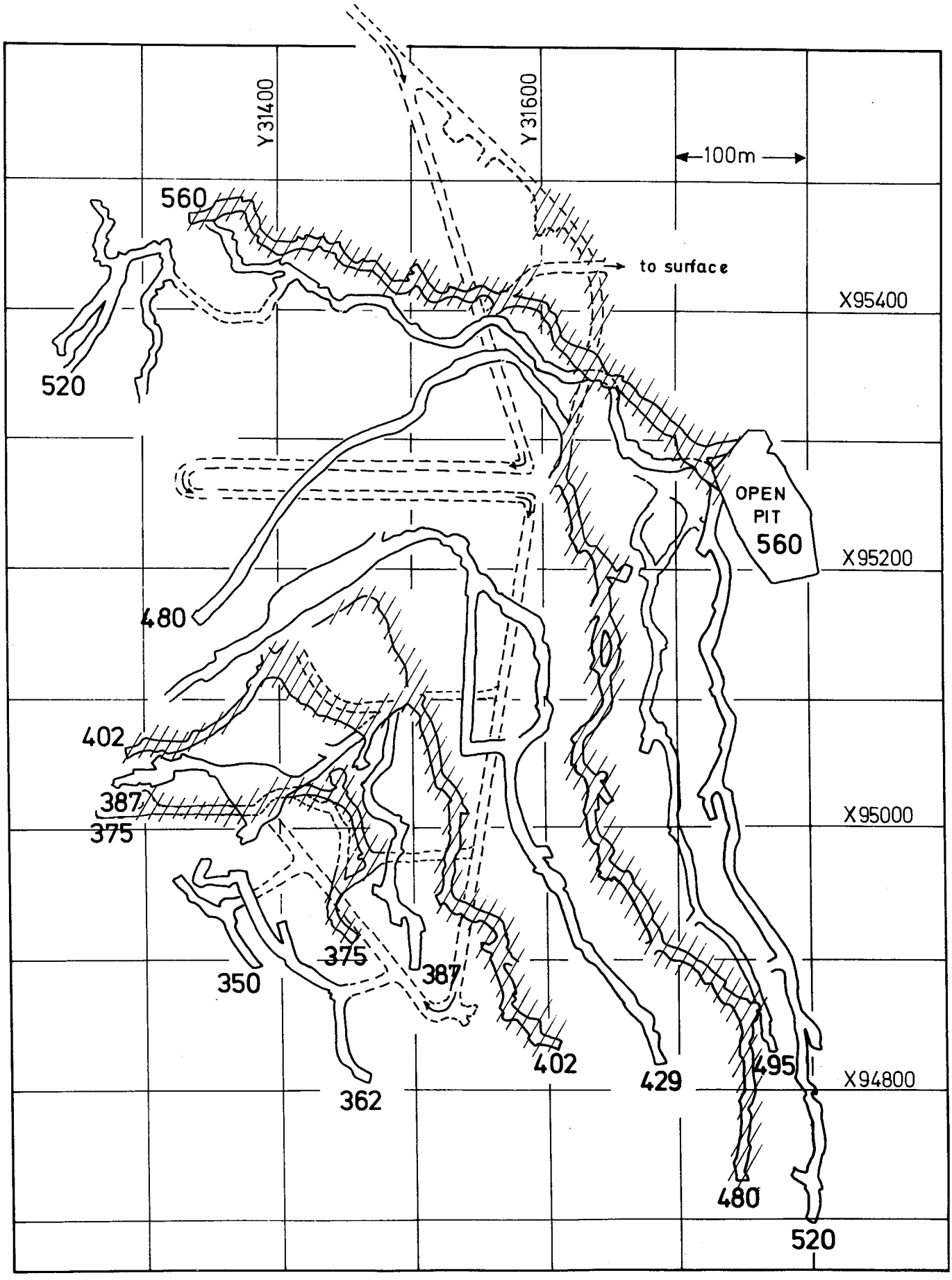

Fig. 4.1b Diagram showing the main mine levels at Joma which horizontal maps (scale 1:500) have been produced for this report (see Appendix 6).

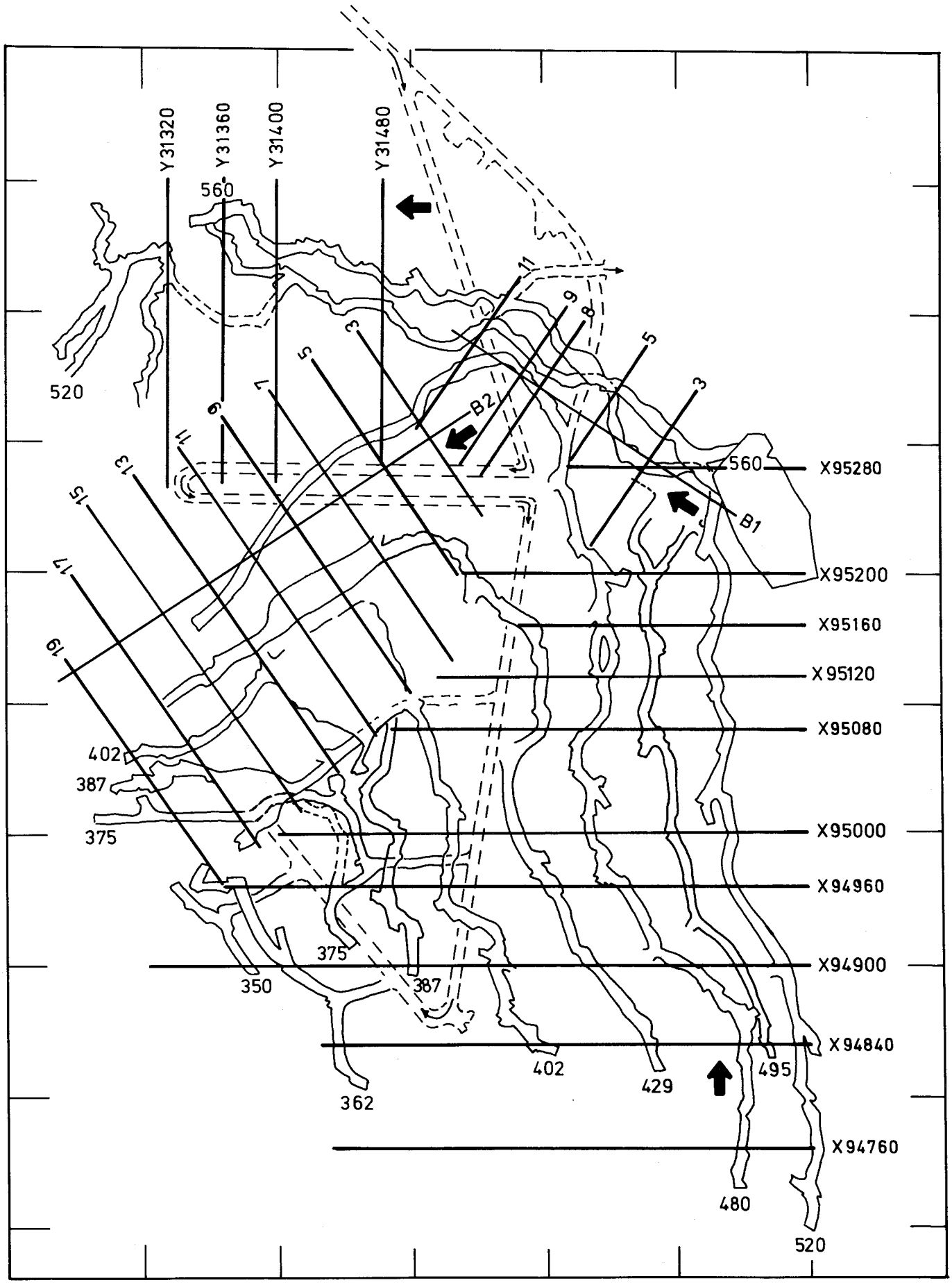

Fig. 4.1c Diagram of the main mine levels at Joma showing the distribution of 28 vertical profiles (scale 1:500) produced for this report (see Appendix F). Arrows show profile series viewing directions.

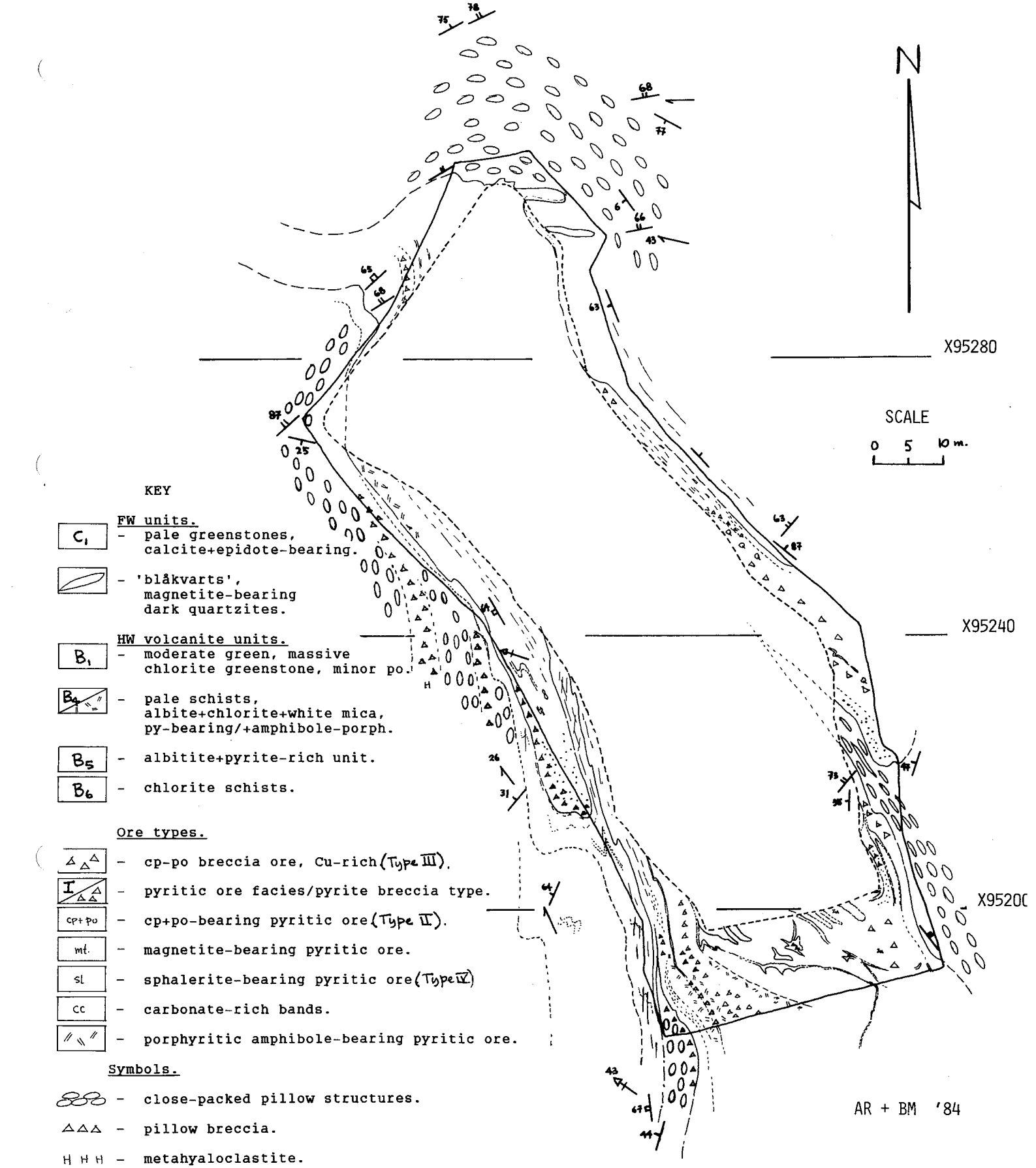

Fig. 4.2a. Geological map of the open pit and surrounding surface area (1:500 base).

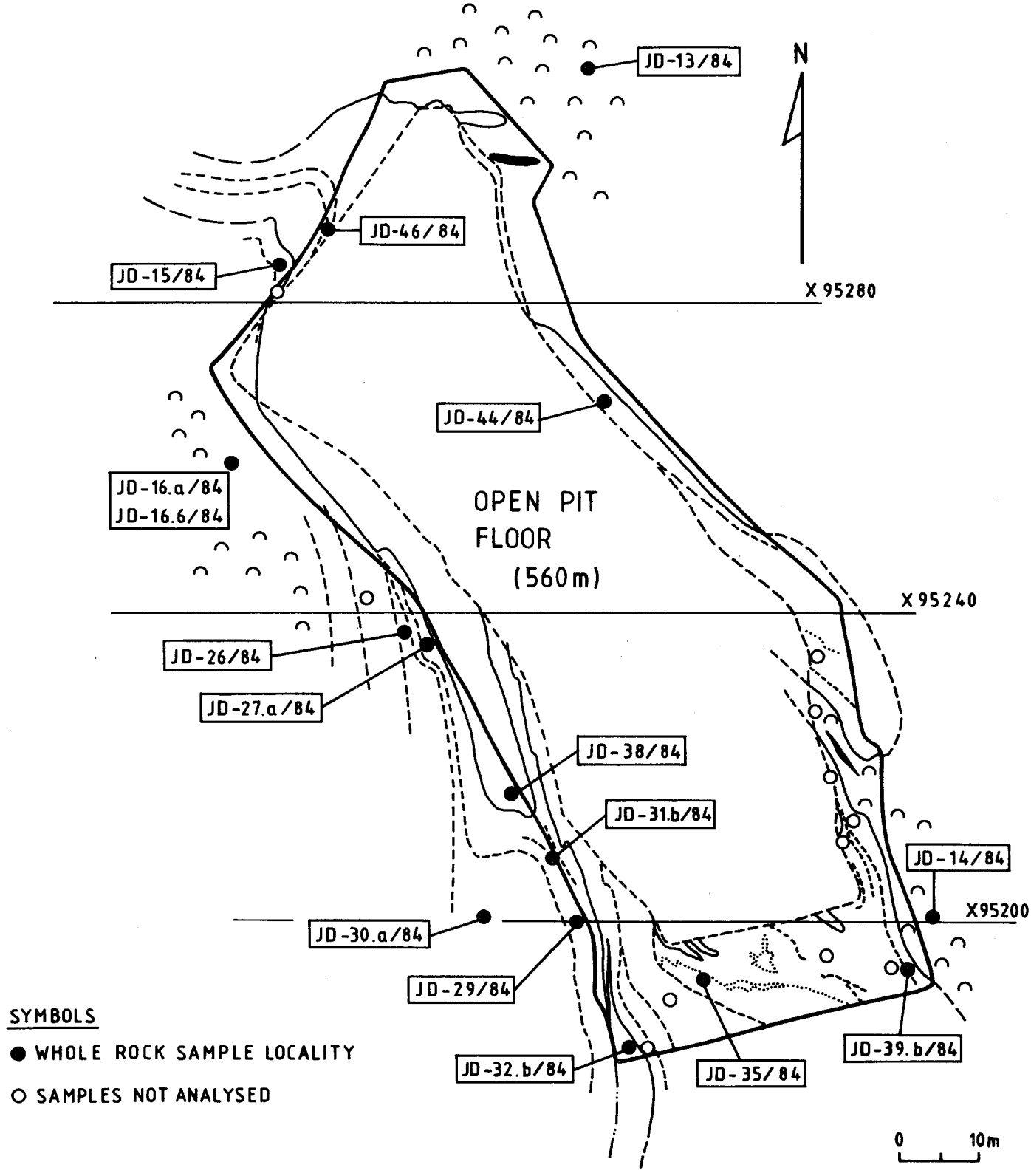

Fig. 4.2b. Map of the open pit separating the massive ore from host rock silicates and showing sample location sites for whole rock silicate and sulphide ore analyses.

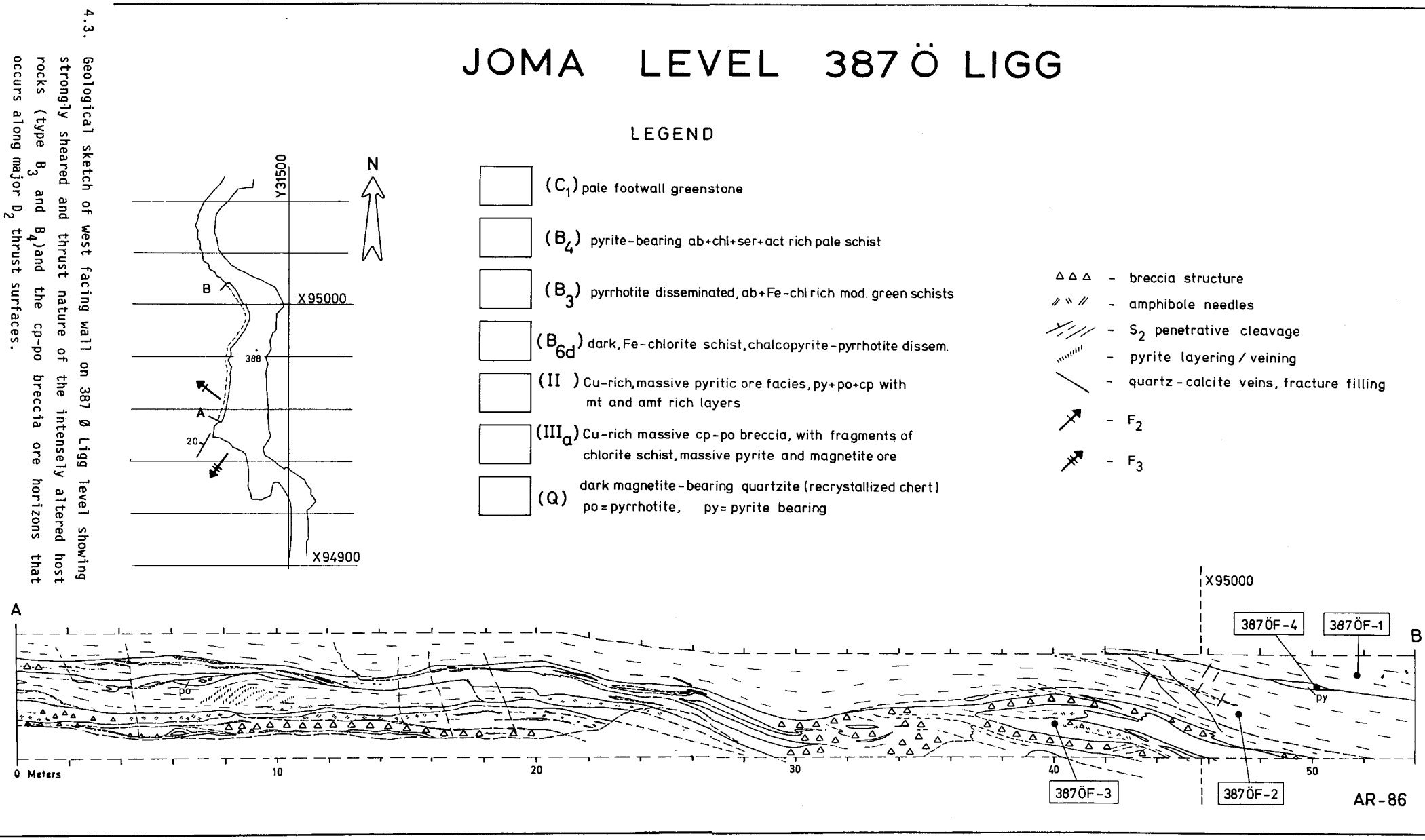

Fig. 4.3. Geological sketch of west facing wall on 387 Ø Ligg level showing strongly sheared and thrust nature of the intensely altered host rocks (type B_3 and B_4) and the cp-po breccia ore horizons that occurs along major D_2 thrust surfaces.

JOMA LEVEL 385 vf S. Strosse

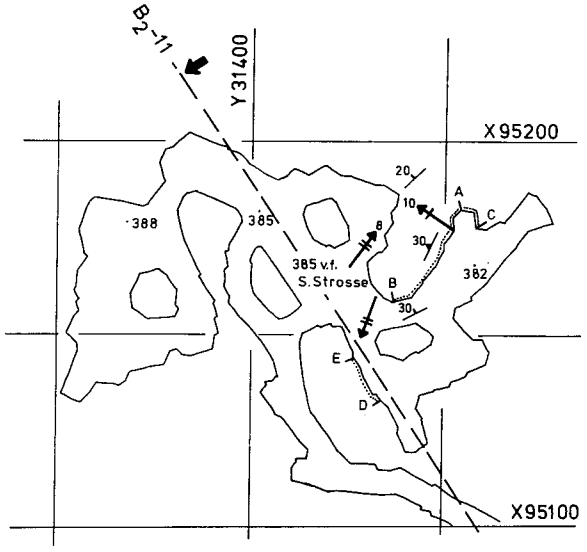

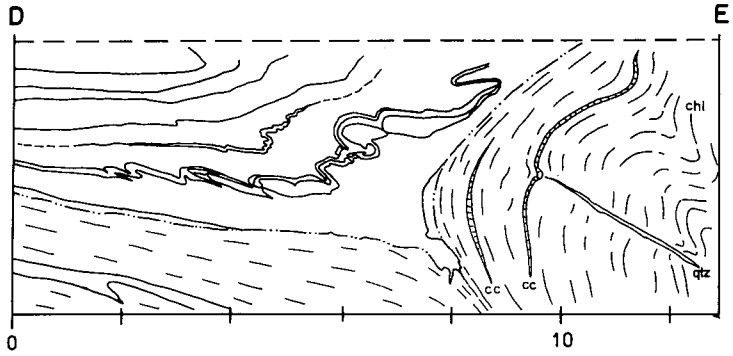

Host Rocks

- (C_{1b}) pale footwall greenstone, epidote + calcite rich
- (B_3) moderate green, albite + Fe-chlorite rich greenstone, actinolite, epidote, pyrrhotite - bearing
- (B_{6d}) dark chlorite schists, pyrrhotite + chalcopyrite rich disseminations
- (B_{5b}) pale, layered albitite, pyrite ± sphalerite rich
- white limestone - marble layer
- (Q_{mt}) dark, magnetite-rich quartzite (recrystallized chert) + chlorite + stilpnomelane ± pyrrhotite

Ore Types

- (IV_{a+b}) Zn-rich, med. grained mass. pyrite, calc.-rich, minor amphibole needles
- (II_c) Cu-rich, fine grained, mass. py-po-cp ore facies, layered, remob. cp+po, minor amphibole
- (II_e) Cu-rich, mass. pyrite-pyrrhotite ore facies, with layers of chl, amf, mt and chert lenses
- (III Cu-rich, mass. chalcopyrite - pyrrhotite breccia ore, fragments of chl, mt+py ore

- △△△ – breccia structure
- – amphibole needles
- – layering and S_2 schistosity
- – S cleavage + fractures filled with qtz+calc+ep
- – F_2
- – F_3
- – major D_2 thrust plane

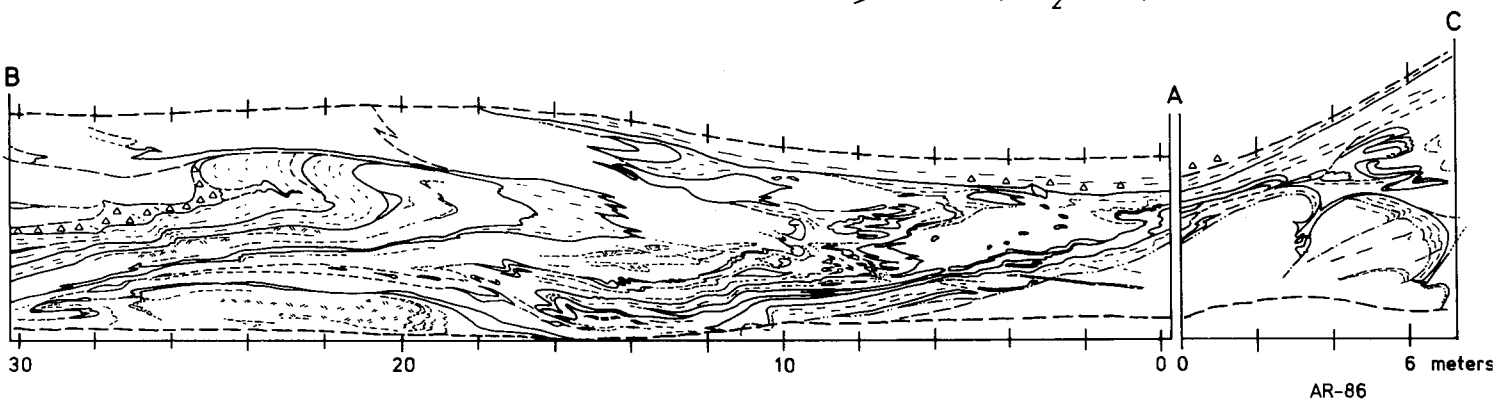

Fig. 4.4a Geological sketch of NW facing wall on 385 vf.s. strosse level. Note the various ore types and the interfolding of sulphides and silicate layers in a large recumbent, F_2 isoclinal fold structure. The bottom of the main sulphide layer is marked by a D_2 thrust plane.

JOMA LEVEL 385 vf S. Strosse

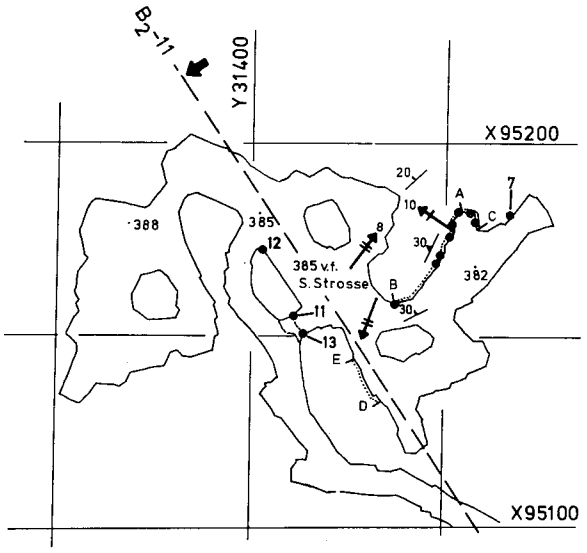

Host Rocks

- (C_{1b}) pale footwall greenstone, epidote + calcite rich
- (B_3) moderate green, albite + Fe-chlorite rich greenstone, actinolite, epidote, pyrrhotite - bearing
- (B_{6d}) dark chlorite schists, pyrrhotite + chalcopyrite rich disseminations
- (B_{5b}) pale, layered albitite, pyrite ± sphalerite rich
- white limestone - marble layer
- (Q_{mt}) dark, magnetite-rich quartzite (recrystallized chert) + chlorite + stilpnomelane ± pyrrhotite

Ore Types

- (IV_{a+b}) Zn-rich, med. grained mass. pyrite, calc.-rich, minor amphibole needles
- (II_c) Cu-rich, fine grained, mass. py-po-cp ore facies, layered, remob. cp+po, minor amphibole
- (II_e) Cu-rich, mass. pyrite-pyrrhotite ore facies, with layers of chl, amf, mt and chert lenses
- (III Cu-rich, mass. chalcopyrite - pyrrhotite breccia ore, fragments of chl, mt+py ore

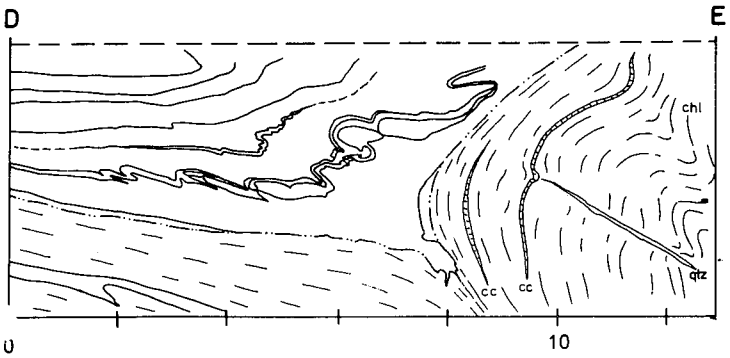

- $\triangle\triangle\triangle$ – breccia structure
- /// – amphibole needles
- – layering and S_2 schistosity
- – S cleavage + fractures filled with qtz + calc + ep
- – F_2
- – F_3
- – major D_2 thrust plane

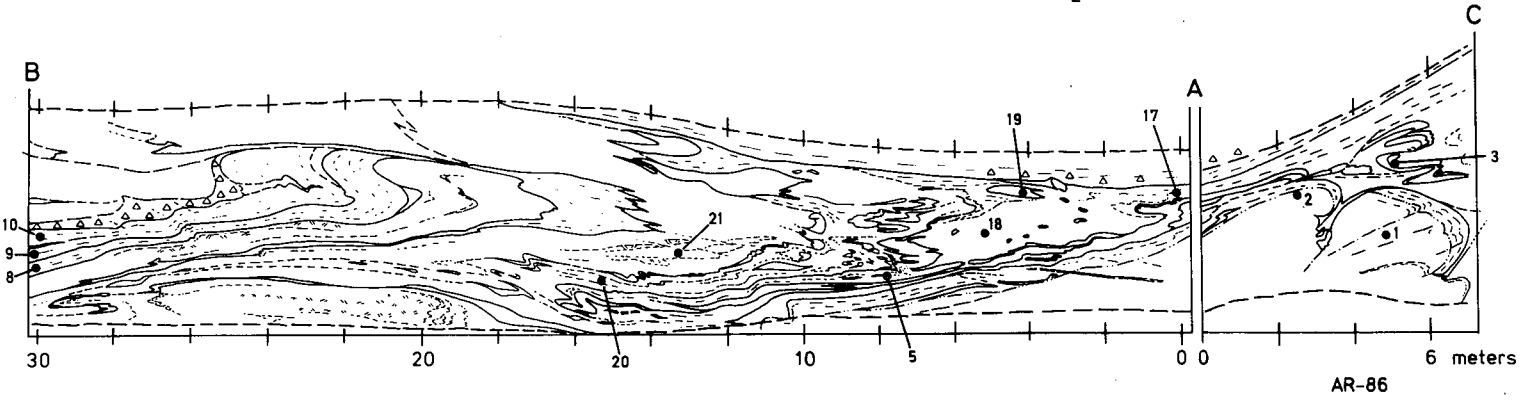

Fig.4.4b As figure 4.4a - showing locations of sample sites (no.) for whole rock silicate and sulphide ore type analyses.

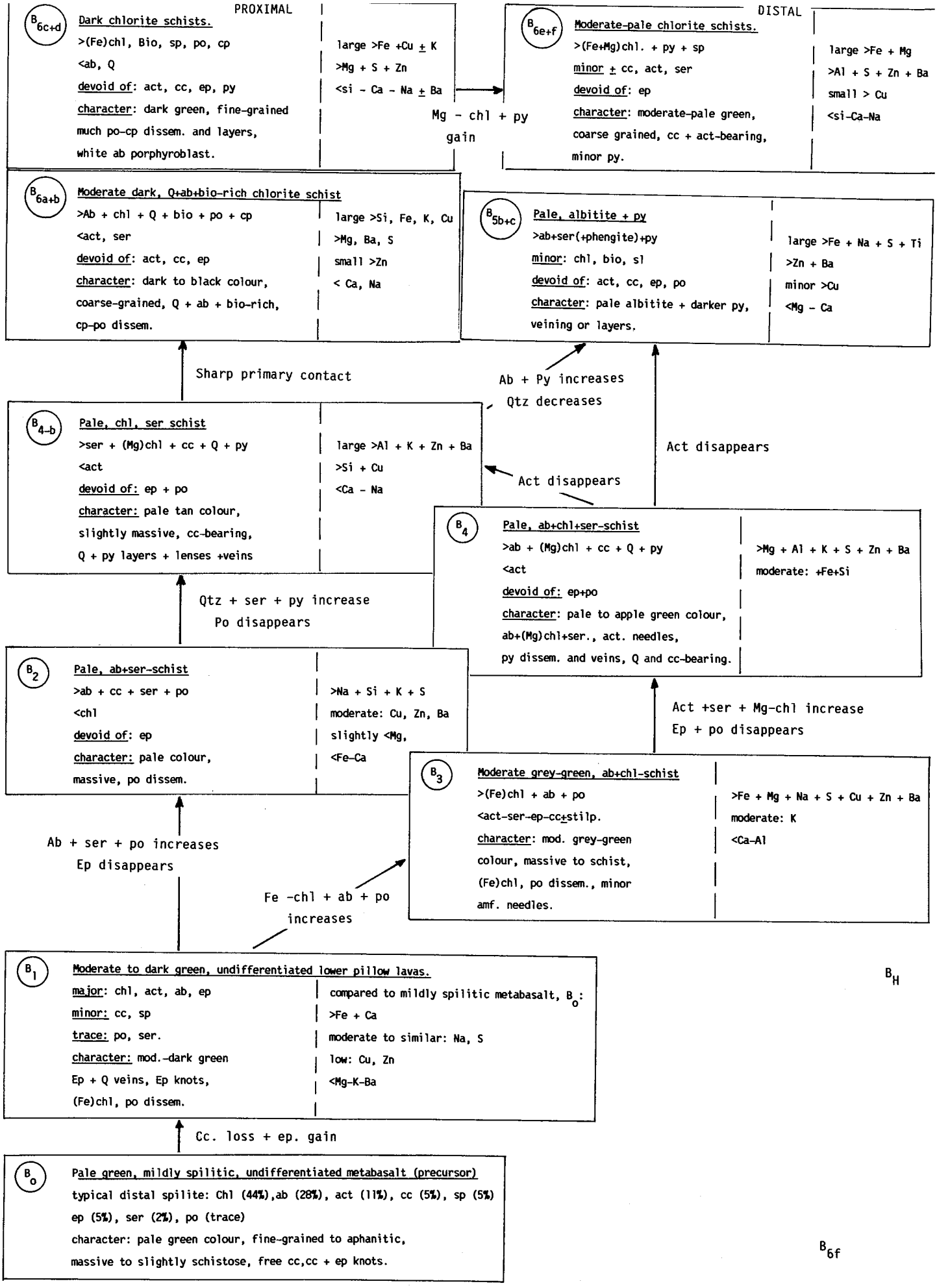

Fig. 4.7. Flow sheet diagram showing the relative positions of the pre-ore, hydrothermally altered host rock lithologies and their characteristic mineral and chemical variations for each group. The Groups show increasing alteration from B_1 to B_6.

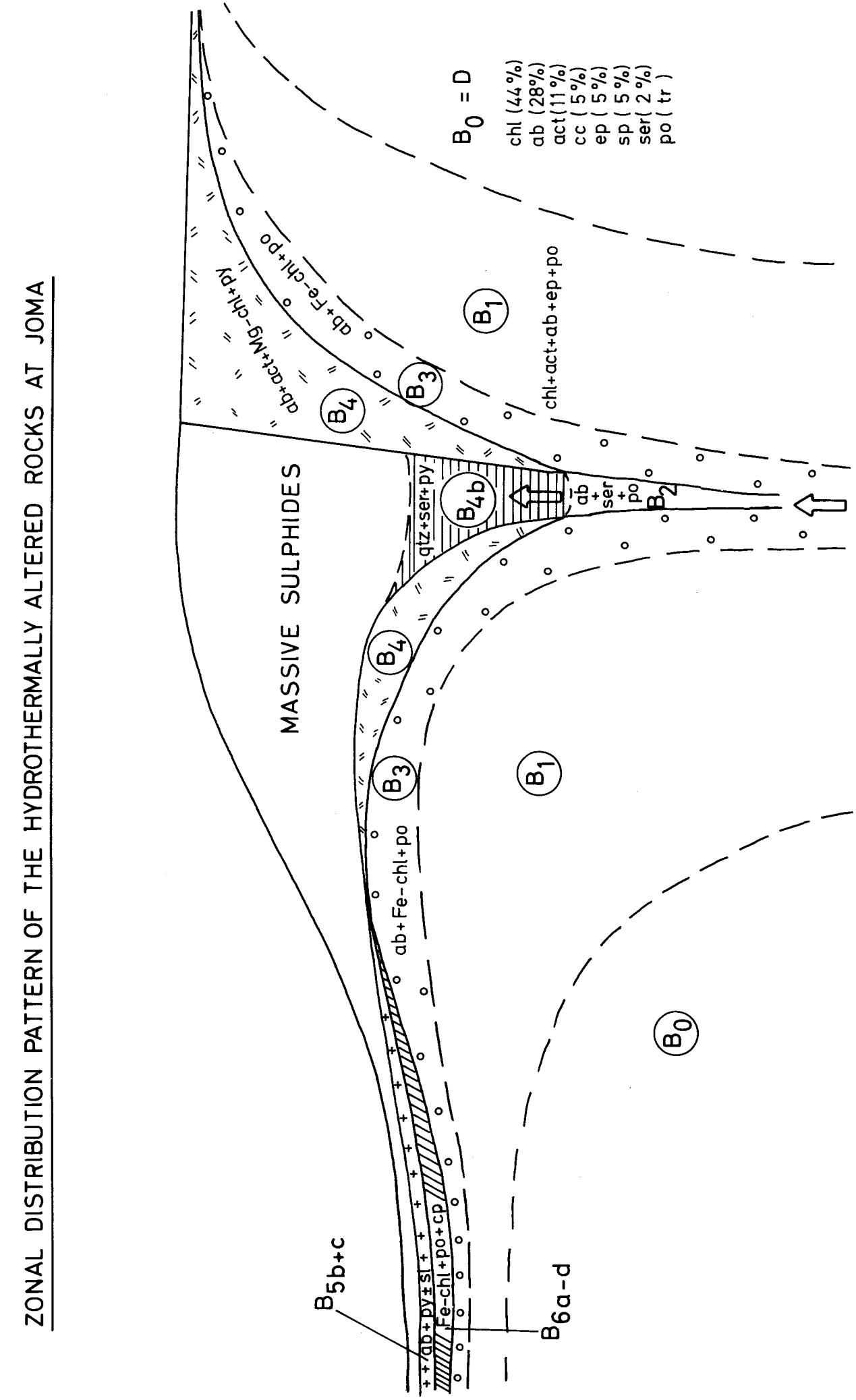

Fig. 4.8. Schematic diagram showing the relative positions of the host rock lithologies within their pre deformational feeder zone position beneath the main Joma ore horizon (not to scale).

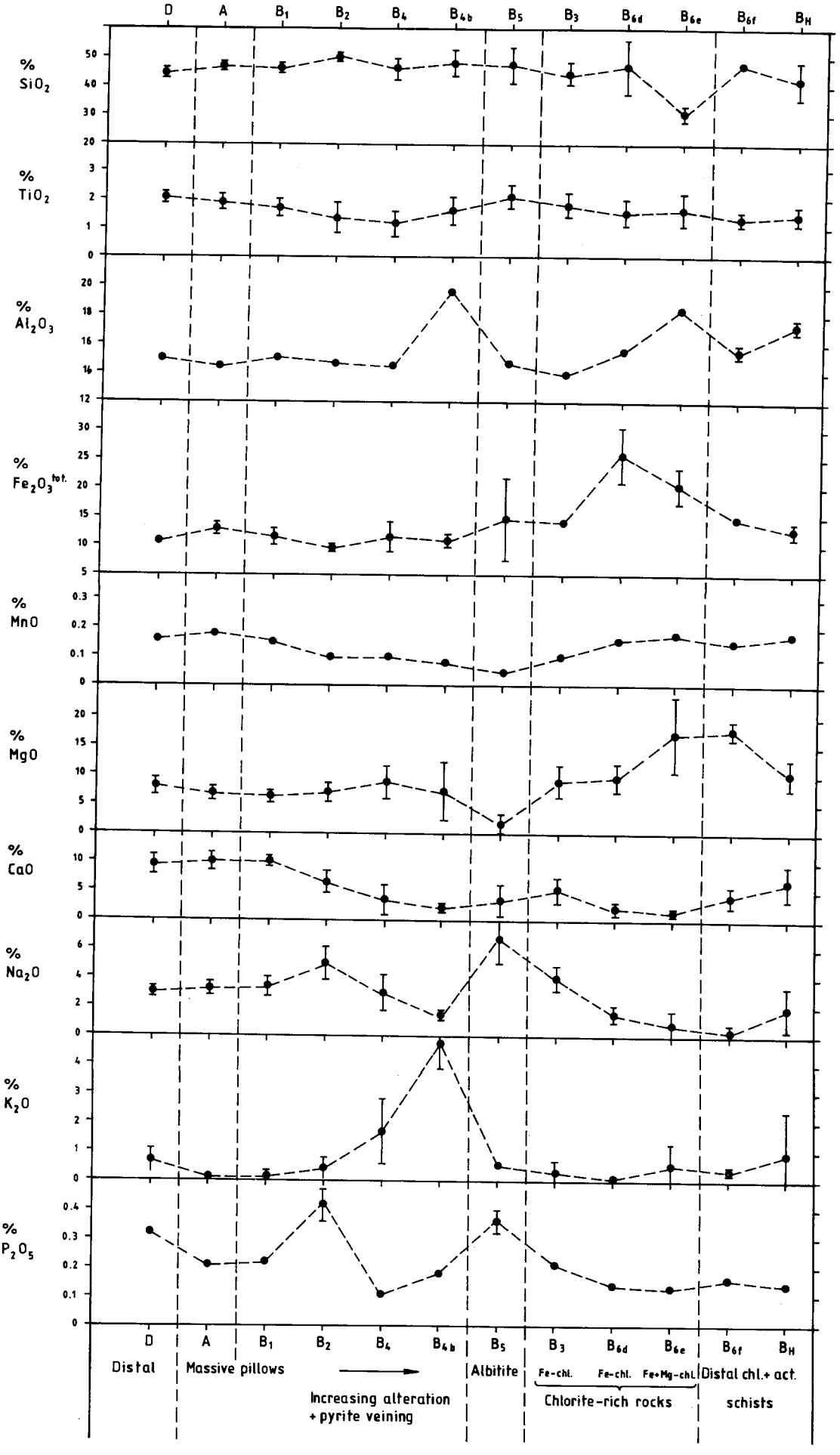

Fig.4.9a+b Diagram showing major (a) and trace (b) elemental trends within the various altered pre-ore host rock types at Joma. Mildly spilitized distal greenstones (Group D) on left hand side and increasingly altered rocks, Group B_5 and B_6 towards the right.

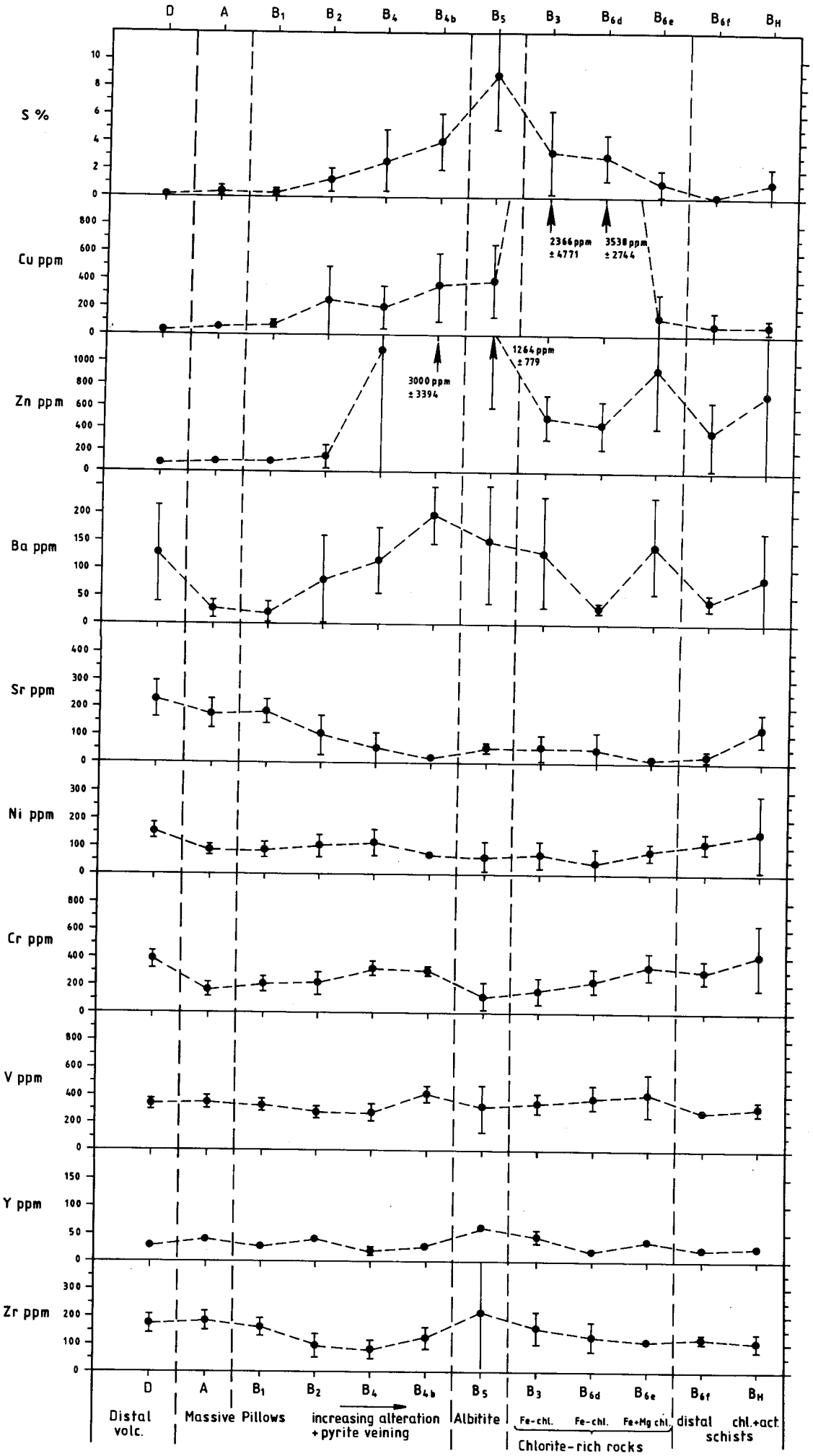

Fig.4.9a+b Diagram showing major (a) and trace (b) elemental trends within the various altered pre-ore host rock types at Joma. Mildly spilitized distal greenstones (Group D) on left hand side and increasingly altered rocks, Group B_5 and B_6 towards the right.

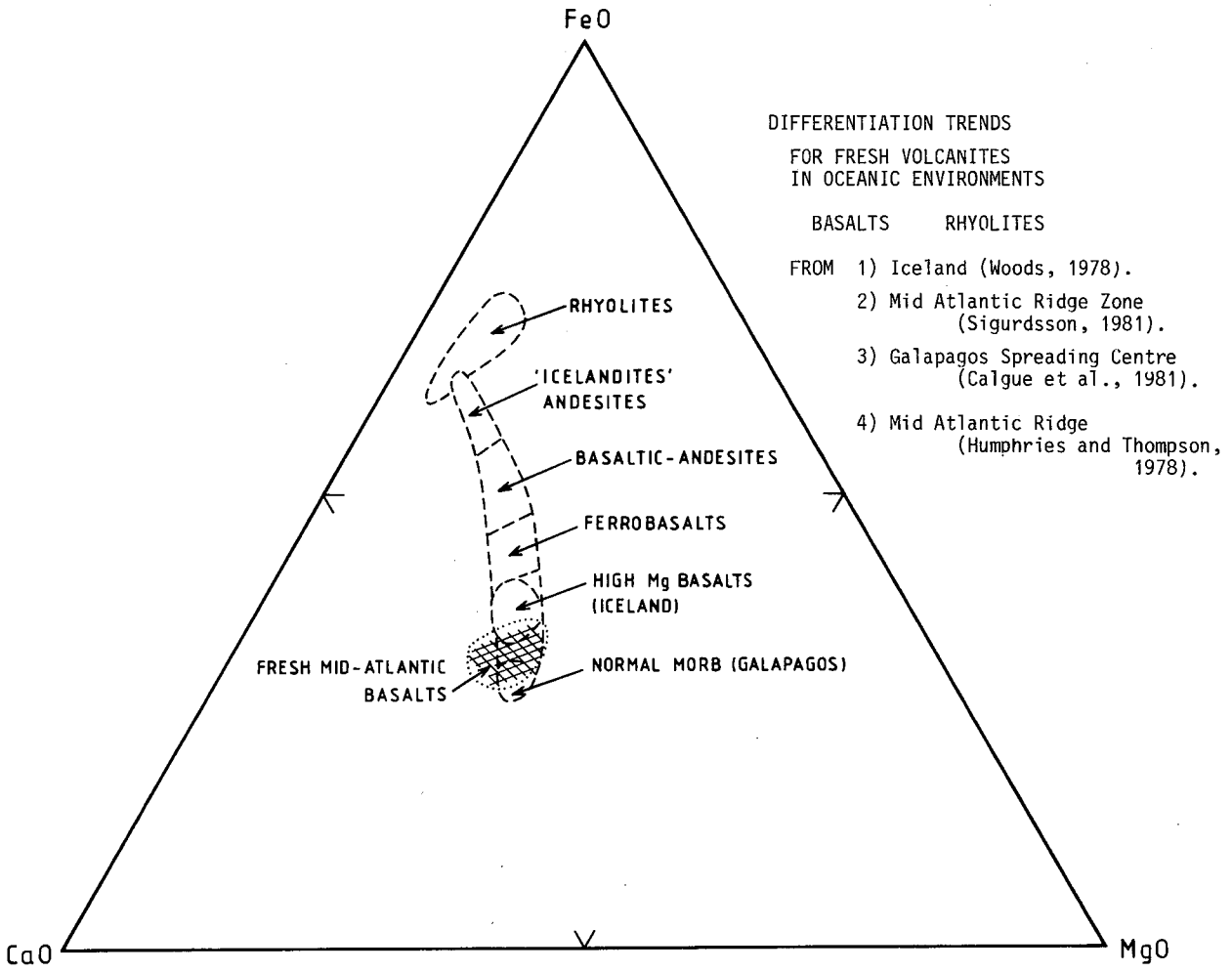

Fig. 4.10. CFM plot of fresh volcanites in Mid Ocean Ridge environments. Shows magmatic differentiation trend from normal Mid Ocean Ridge Basalt (MORB) and high Mg basalts through to rhyolites.

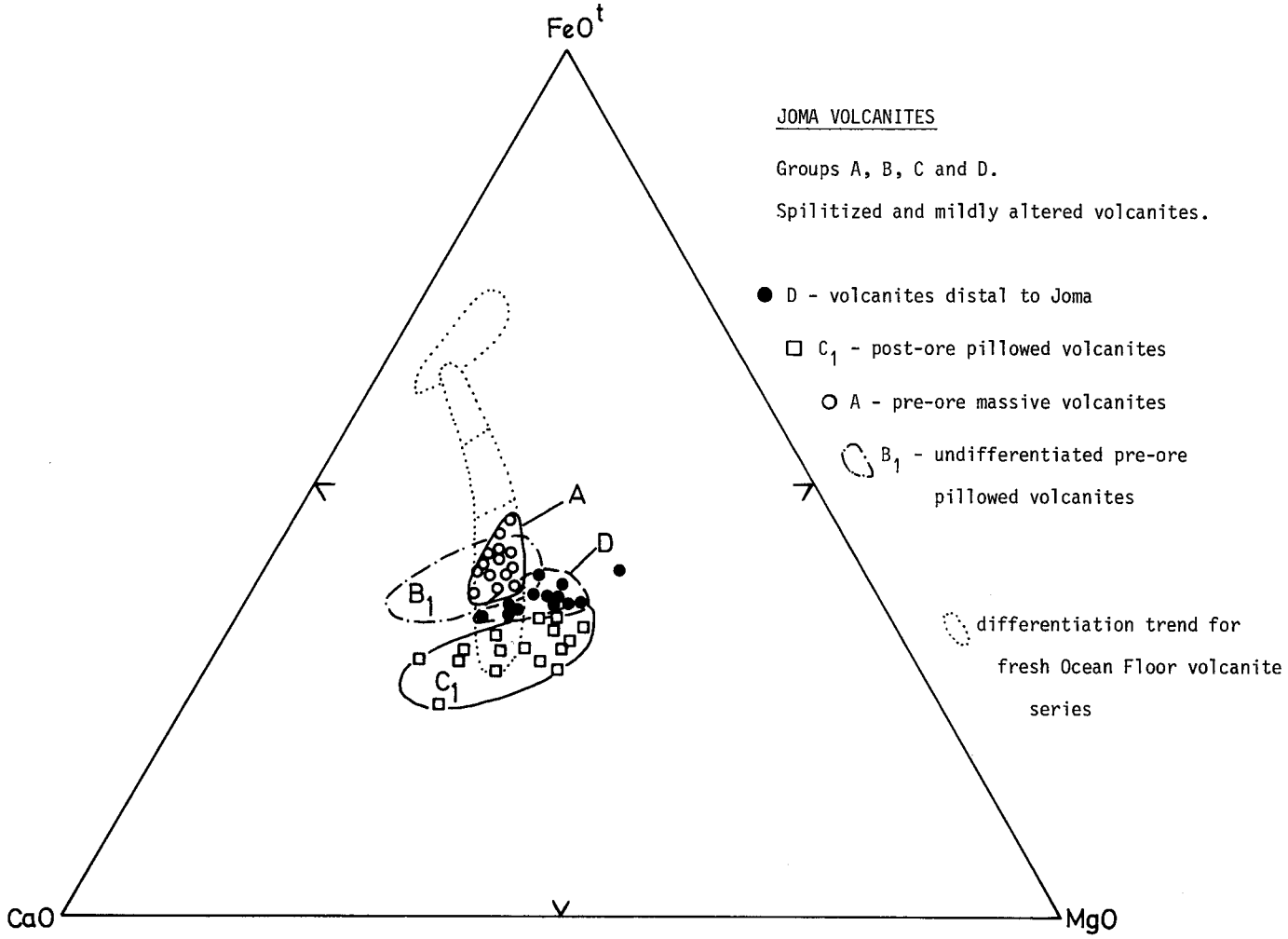

Fig. 4.11. CFM plot of the mildly altered, pre-ore massive (Group A) and pillowed (Group B) volcanites, the post-ore (Group C) and the mildly spilitized distal greenstones (Group D) of the Røyrvik Group volcanites. Note the differentiation trend for fresh MOR volcanites for comparison.

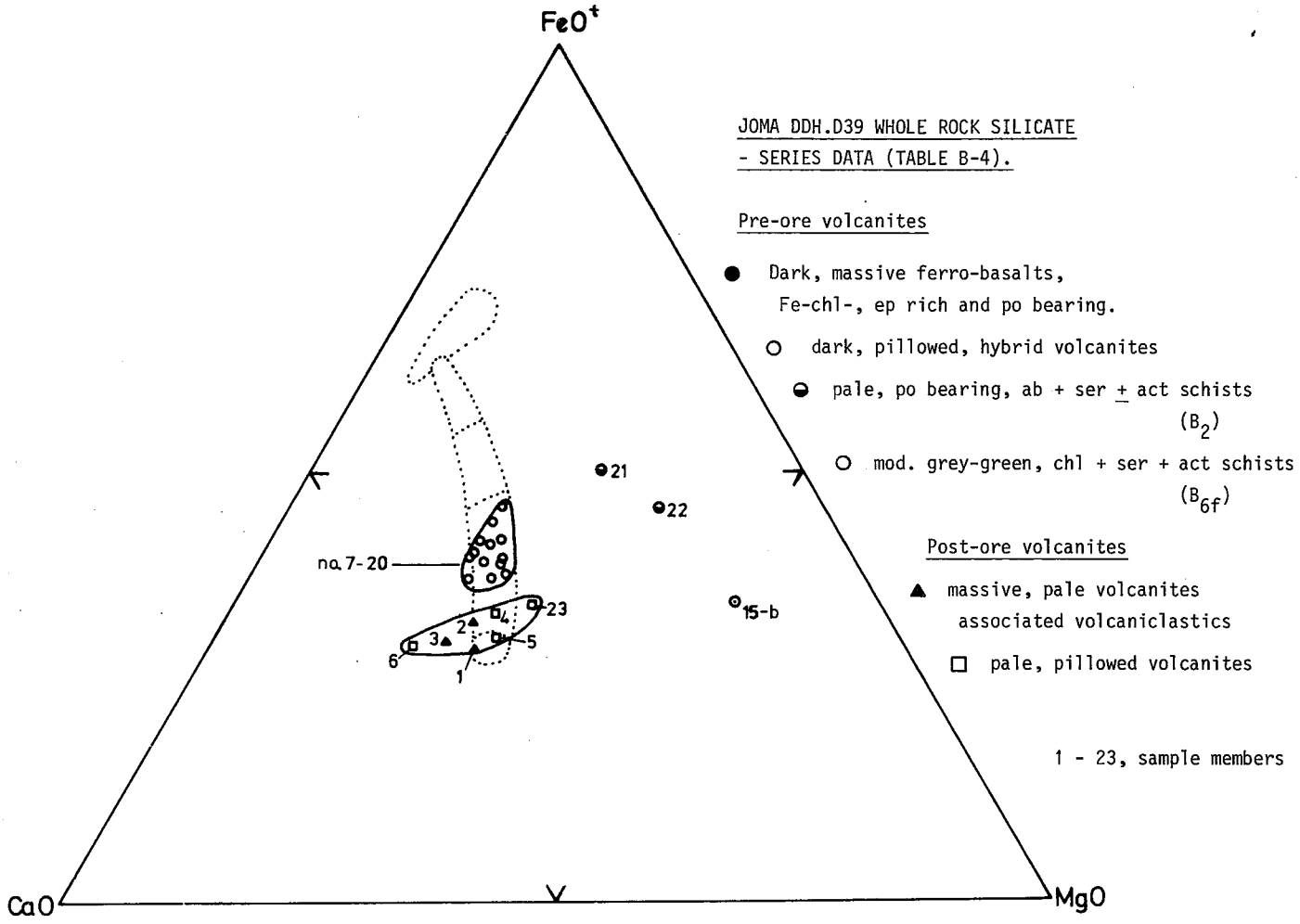

Fig. 4.12. CFM plot of 23 samples from surface DDH D39-1986 series (test case) showing separation of the post-ore volcanites from the pre-ore ferrobasalts (sample no. 7-20) and the intense hydrothermally altered host rocks, no. 21, 22 and 15-b. Note the closeness of fit of the massive volcanites to the field of fresh ferrobasalts in Fig. 4.10.

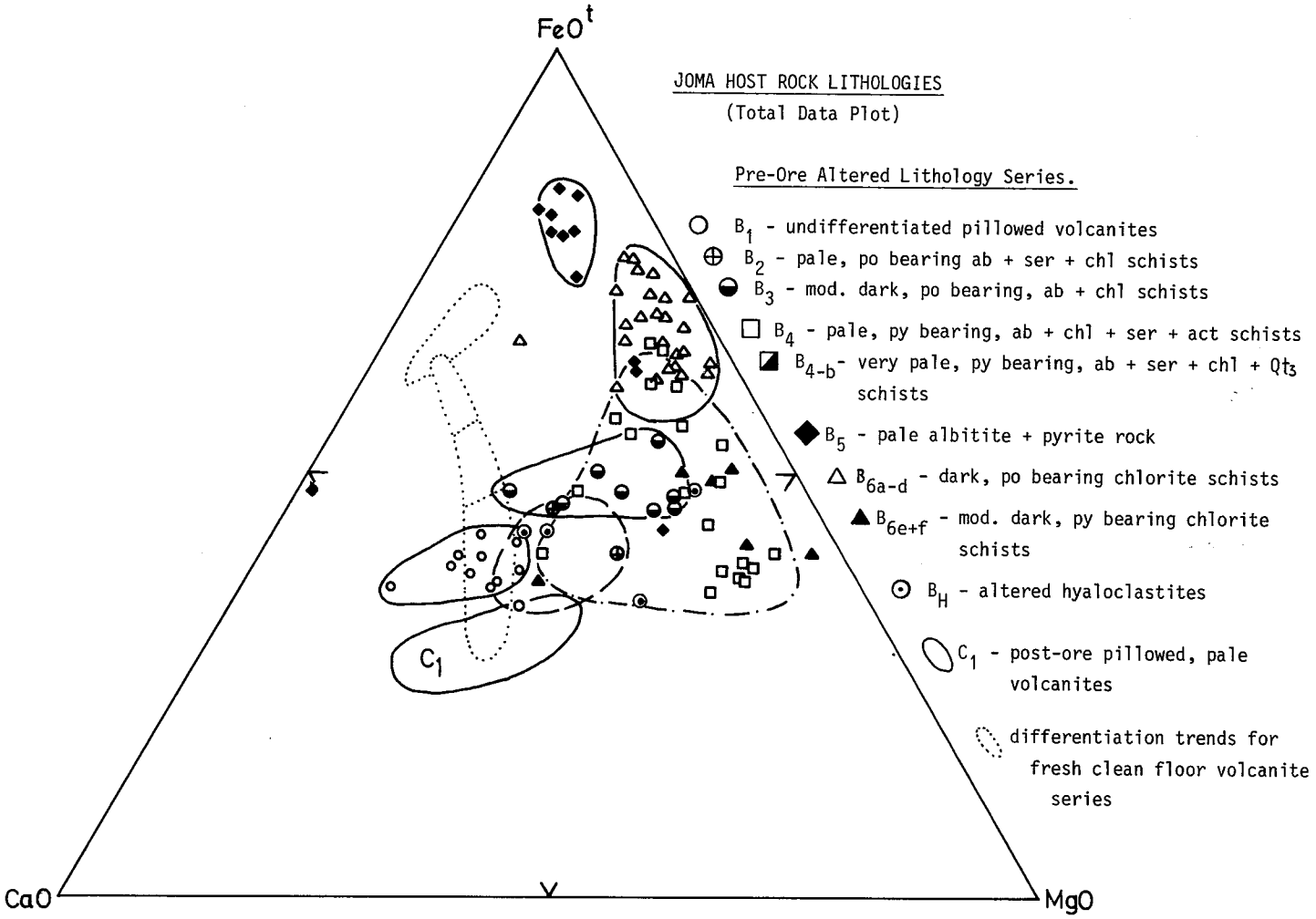

Fig. 4.13. CFM plot of total data of the altered pre-ore host rock series at Joma. Shows spread of data and grouping of the various host rock lithologies. The magmatic differentiation trend for fresh MORB volcanites and the boundary for the post-ore volcanite series (C_1) is shown for comparison.

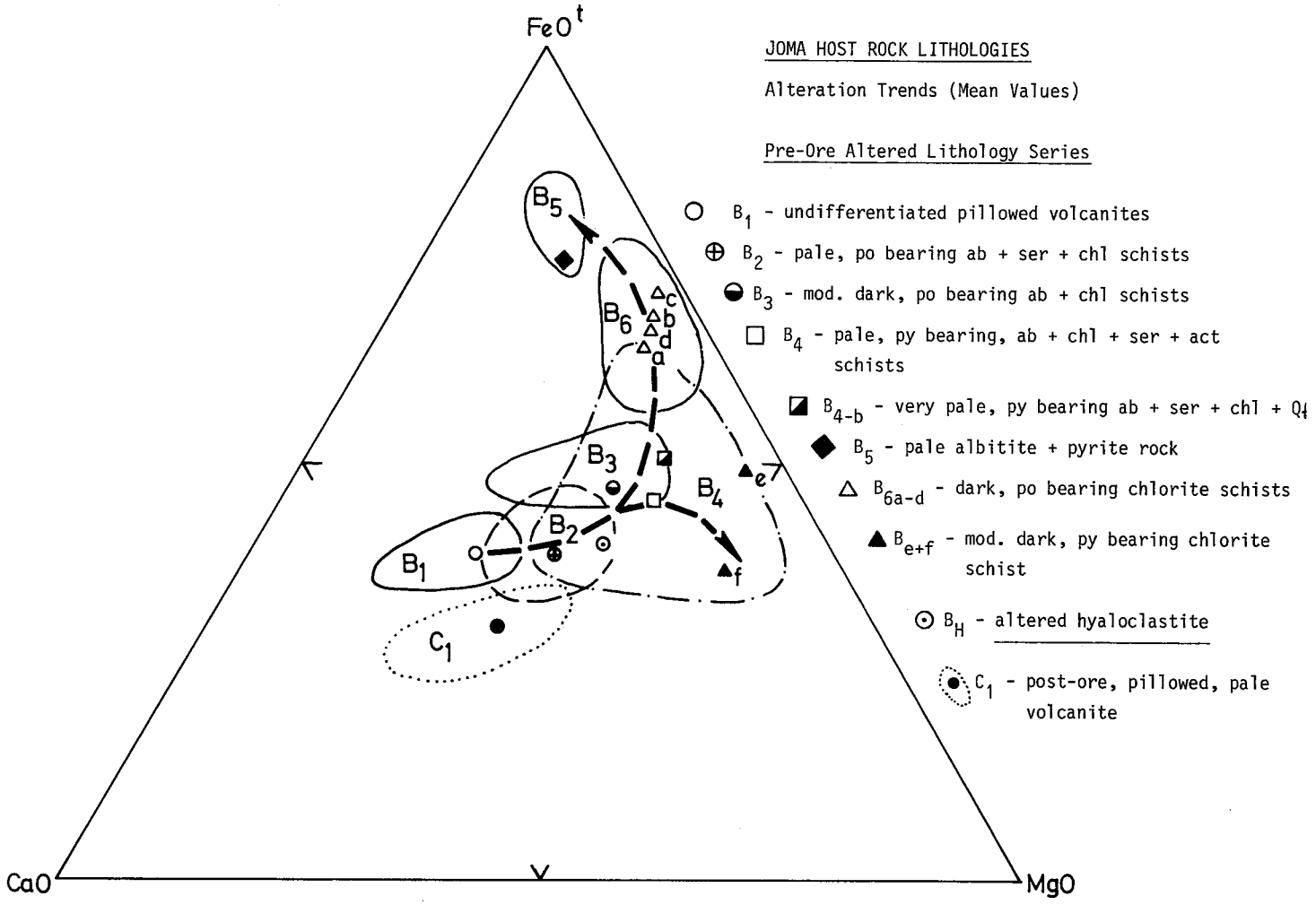

Fig. 4.14. CFM plot of average values for the pre-ore altered host rock series and their group boundaries. The two major alteration trends, Fe and Mg are shown.

FACTOR	VARIANCE EXPLAINED	CUMULATIVE PROPORTION OF TOTAL VARIANCE
1	6.210153	.326850
2	3.793553	.526511
3	2.289555	.647014
4	1.649998	.733856
5	1.039692	.788576 ← 5 faktorer ≈ 80%
6	.827203	.832113
7	.701446	.869032
8	.540840	.897497
9	.459307	.921671
10	.331418	.939114
11	.232961	.951375
12	.212384	.962553
13	.202973	.973236
14	.167335	.982043
15	.133276	.989058
16	.093414	.993974
17	.069399	.997627
18	.026361	.999014
19	.018731	1.000000

THE VARIANCE EXPLAINED BY EACH FACTOR IS THE EIGENVALUE FOR THAT FACTOR.

TOTAL VARIANCE IS DEFINED AS THE SUM OF THE DIAGONAL ELEMENTS OF THE CORRELATION MATRIX.

Fig. 4.15. Print out from Factor Analysis showing the variance (eigenvalue) explained by each factor and the cumulative proportion of the total variance that is explained by each factor.

PAGE 5 BMDP4M NORGE

CORRELATION MATRIX

		SIO2 1	TIO2 2	AL203 3	FE203 4	MNO 5	MGO 6	CAO 7	NA20 8	K20 9	P205 10	S 11	CU 12	ZN 13
SIO2	1	1.000												
TIO2	2	-.020	1.000											
AL203	3	-.138	-.488	1.000										
FE203	4	-.544	.457	-.151	1.000									
MNO	5	.126	.298	-.291	.301	1.000								
MGO	6	-.518	-.352	.264	.075	-.158	1.000							
CAO	7	.074	-.107	-.407	-.466	-.188	-.299	1.000						
NA20	8	.473	.462	-.142	-.057	-.153	-.627	-.069	1.000					
K20	9	.225	-.359	.473	-.273	.098	-.167	-.435	-.297	1.000				
P205	10	.071	.891	-.364	.315	.274	-.425	-.104	.537	-.337	1.000			
S	11	.028	.148	.304	.221	.017	-.045	-.631	.201	.465	.105	1.000		
CU	12	-.160	-.063	.190	.416	-.014	.089	-.449	-.067	.175	-.121	.460	1.000	
ZN	13	-.113	.029	.231	.237	.132	.181	-.505	-.049	.340	-.020	.616	.321	1.000
BA	14	.253	-.201	.210	-.143	.415	.059	-.363	-.270	.762	-.123	.270	.112	.185
V	15	-.050	.941	-.480	.507	.254	-.311	-.140	.428	-.333	.774	.192	-.013	.079
CR	16	-.125	-.674	.526	-.308	-.389	.341	-.005	-.315	.256	-.550	-.028	.082	.043
NI	17	-.141	-.611	.496	-.411	-.363	.414	.071	-.417	.317	-.514	-.094	-.020	-.030
SR	18	.078	.314	-.377	-.180	-.014	-.439	.659	.195	-.481	.368	-.412	-.324	-.391
ZR	19	.072	.894	-.398	.346	.357	-.415	-.067	.472	-.339	.918	.085	-.082	-.023

		BA 14	V 15	CR 16	NI 17	SR 18	ZR 19
BA	14	1.000					
V	15	-.217	1.000				
CR	16	.102	-.665	1.000			
NI	17	.174	-.664	.745	1.000		
SR	18	-.323	.226	-.137	-.014	1.000	
ZR	19	-.124	.762	-.617	-.574	.367	1.000

$TiO_2 \rightarrow P_2O_5$ (V, Zr) $K_2O \rightarrow Ba$ $P_2O_5 \rightarrow V$ (Zr) $S \rightarrow$ wahl Zn $V \rightarrow Zr$ $Cr \rightarrow Ni$

Fig. 4.16. Correlation matrix from Factor Analysis showing which elements and to what degree they are related to each other. Note the strong correlation between Ti, P, V and Zr.

ROTATED FACTOR LOADINGS (PATTERN)

		FACTOR 1	FACTOR 2	FACTOR 3	FACTOR 4	FACTOR 5
SIO2	1	-.085	-.104	-.091	Si → .868	.289
TIO2	2	Ti → .918	.024	-.314	.039	-.078
AL2O3	3	-.259	.411	Al→ .679	-.050	.071
FE2O3	4	.376	.449	-.431	-.517	-.192
MNO	5	.251	-.003	-.530	-.115	Mn→ .646
MGO	6	-.320	.165	.219	÷ Mg→ -.722	.062
CAO	7	-.151	÷ Ca→ -.845	-.063	.126	-.239
NA2O	8	.445	.117	-.027	Na→ .730	-.365
K2O	9	-.277	.414	.315	.128	K→ .702
P2O5	10	P→ .936	-.040	-.136	.145	-.019
S	11	.192	S→ .819	.156	.187	.120
CU	12	-.144	Cu → .680	-.128	-.098	-.145
ZN	13	.080	Zn → .678	.086	-.094	.152
BA	14	-.118	.218	.085	.071	Ba→ .882
V	15	V→ .820	.111	-.387	.021	-.132
CR	16	-.487	.014	Cr→ .683	-.152	-.032
NI	17	-.402	-.144	Ni → .763	-.230	.119
SR	18	.401	÷ Sr → -.705	.083	.129	-.185
ZR	19	Zr → .905	-.052	-.241	.114	.013
	VP	4.527	3.484	2.525	2.309	2.139

THE VP FOR EACH FACTOR IS THE SUM OF THE SQUARES OF THE ELEMENTS OF THE COLUMN OF THE FACTOR PATTERN MATRIX CORRESPONDING TO THAT FACTOR. WHEN THE ROTATION IS ORTHOGONAL, THE VP IS THE VARIANCE EXPLAINED BY THE FACTOR.

Fig. 4.17. The pattern of rotated factor loadings showing which elements have positive or negative affects on each factor.

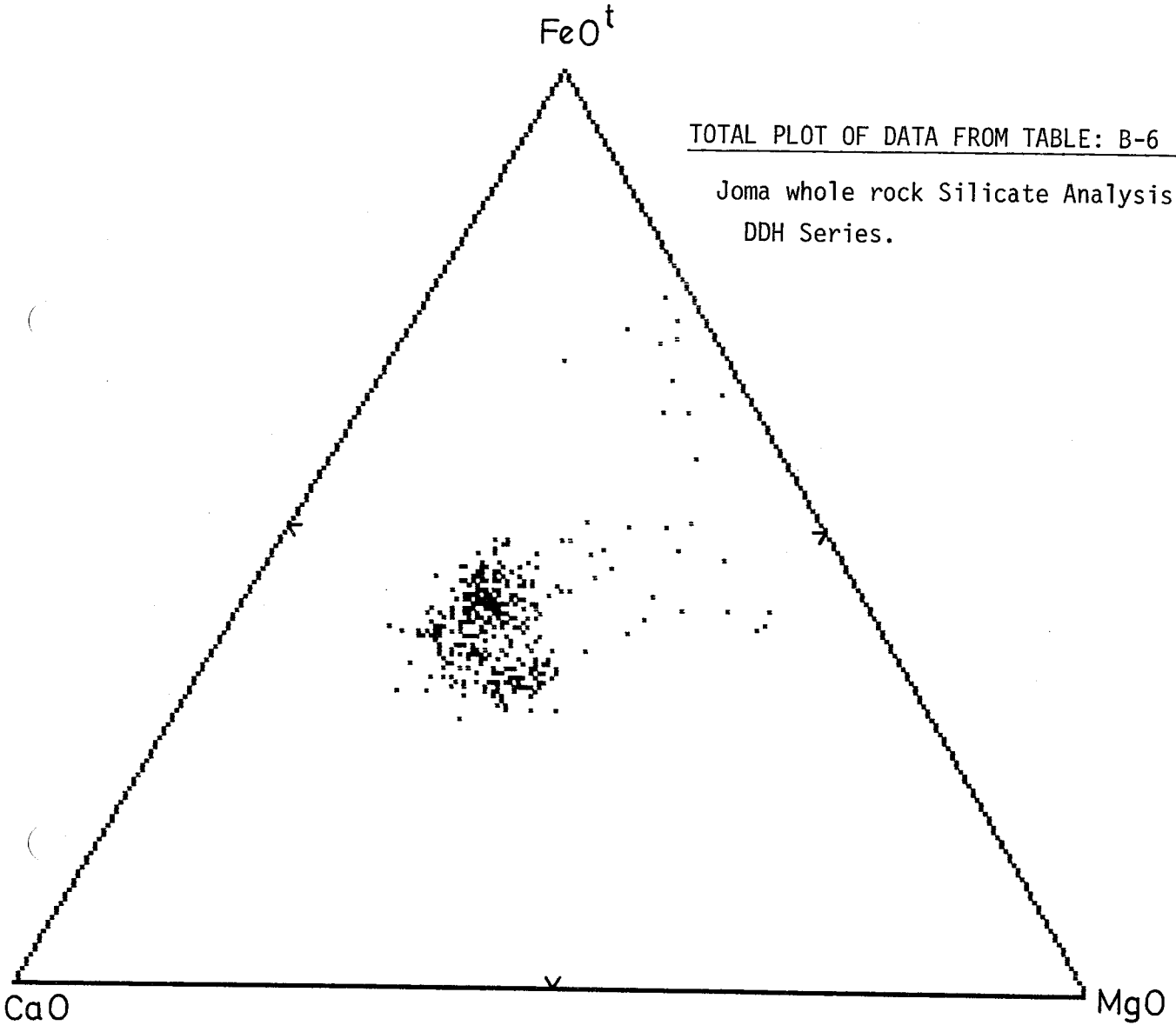

Fig. 4.18. CFM plot of total data (355 samples) from the Joma surface DDH-1986 analytical series (Table B-6). Shows spread of data and clustering of two groups which corresponds to Group B and Group C of the host rock series.

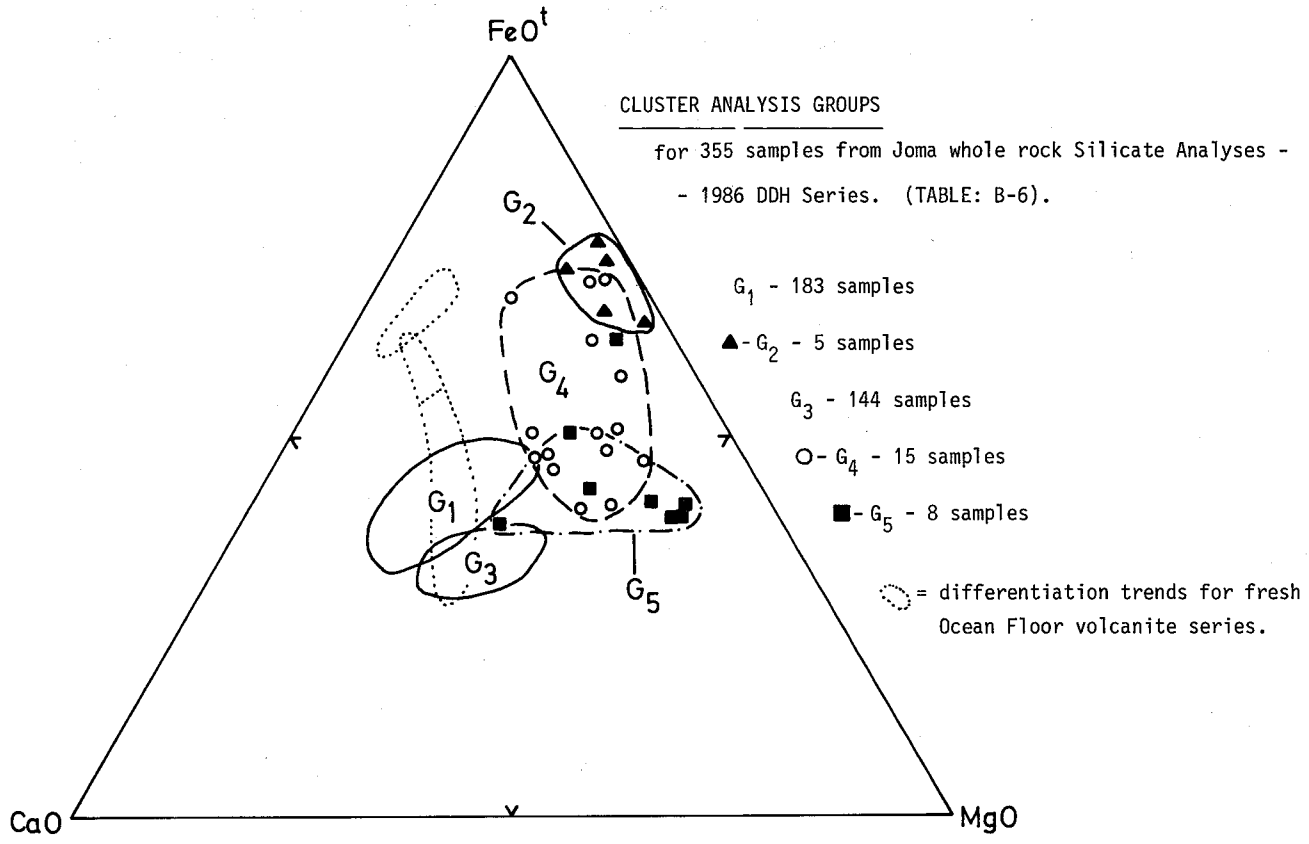

Fig. 4.19. CFM plot of the 5 Cluster Analysis groups for the 355 samples from the Joma surface DDH-1986 analytical program (from Table B-6).

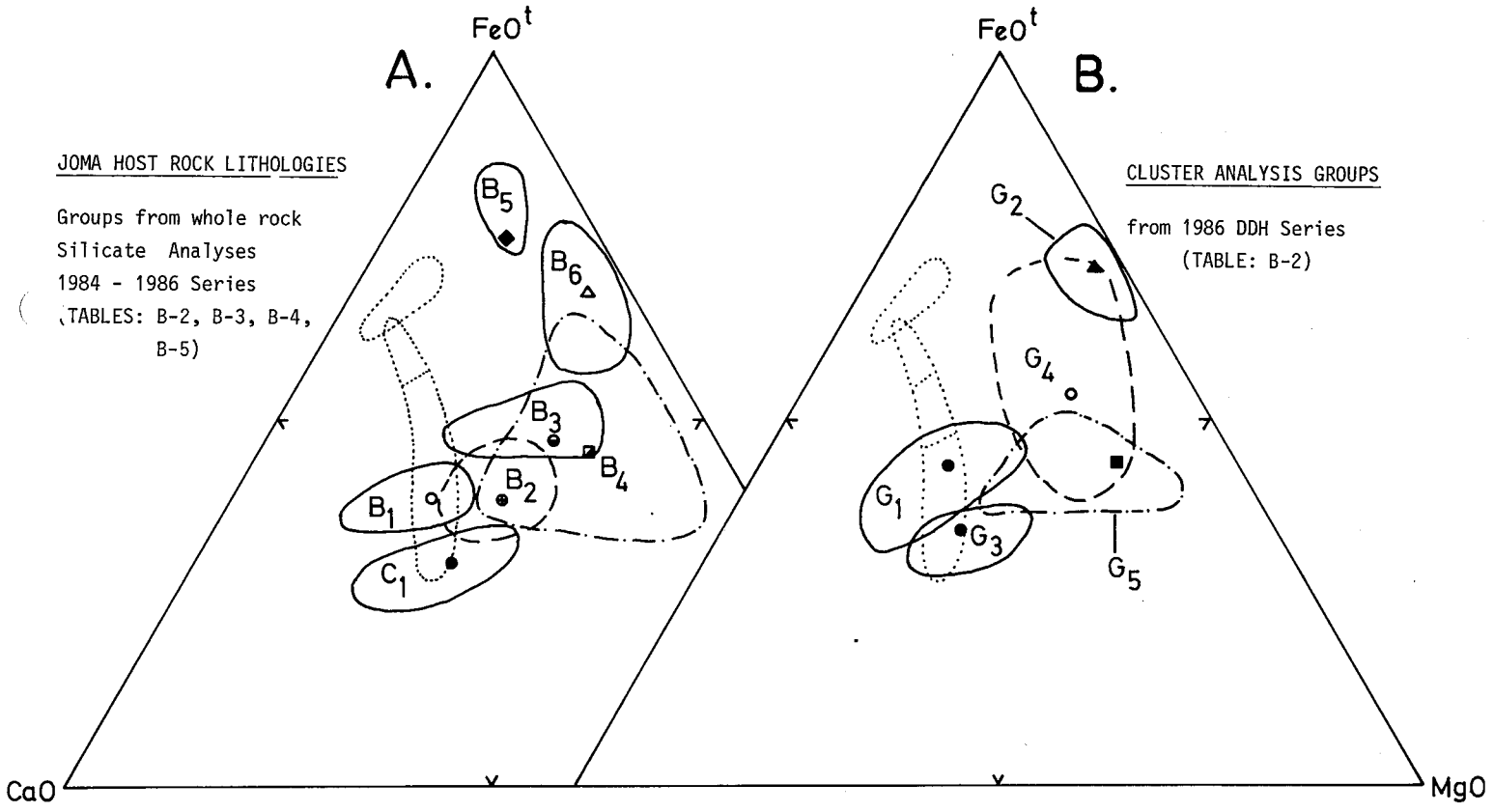

Fig. 4.20. CFM plots to compare the Cluster Analysis Groups (B) from the host rock lithology groups (A) taken from Fig. 4.14. Note the similarities between the lithology groups C_1, B_1, B_4 and B_6 and the Cluster groups G_3, G_1, G_5 and G_2 respectively.

SECTION 5: THE JOMA ORE TYPES

5.1. INTRODUCTION

As discussed earlier (section 1, 2 and 3), the Joma ore horizon lies at the interface between two locally, major pillowed volcanite sequences, the pre-ore, unit B and the post-ore, unit C series. The ore horizon lies in the overturned limb of a major isoclinal fold structure which implies that the whole rock package of silicate and sulphide ore stratigraphy is inverted. There are, however, complications due to isoclinal D_2 folding and thrusting and D_3 overturned folding in which the stratigraphy locally is right-way up.

The Joma ore body at present consists of an en échelon array of massive sulphide lenses that on a surfacial projection forms an arcuate trace that extends over a length of 1200-1500m. The individual lenses vary greatly in thickness and length, the massive ore zone having a maximum thickness of up to 50 m in the open pit area. Much of this thickness may be due to tectonic thickening.

The ore body forms a folded, plate-like body that dips steeply to the W-SW from the surface level (580 m), and flattens out at depth. The ore is presently being mined down to the 350 level, some 230 m below the surface (see Fig. 2.2 and 4.1).

It was early in the project recognized that there are several ore types which can be separated out as distinct sulphide facies on the basis of their textures, mineralogy and major elemental variations (Cu-Zn) and specific gravity. Their geographical distribution within the ore horizon and their relations to the enclosing host rock lithologies and the feeder zone (described in section 4) is also characteristic features.

The ore horizon was studied in detail in conjunction with the investigation of the host rock lithologies, as the spacial relationships between them are fundamental in understanding the original depositional and later deformational history of the Joma ore horizon.

The detailed investigation was carried out at key levels throughout the length of the orebody from the 350 m level at the bottom of the mine up to the surface around the open pit at 580 m above sea level, a depth of some 230 meters. The various levels on which the work was done have been given earlier in section 4.1, pp. 48, and in Fig. 4.1.

The investigation of the ores involved, besides detailed mapping and sampling for thin and polished section (textural) studies and whole rock sulphide analyses, also a study of the Cu-Zn-sp. gravity data available from the large amount of exploration and production diamond drilling done within the mine.

5.2. SEPARATION OF ORE TYPES

The ore types have initially been separated out on the basis of macrotextures, mineral contents, colour, as well as their spatial relationship to each other and the adjacent host rocks and their lateral distribution within the ore horizon.

A detailed study has been carried out on the Cu-Zn specific gravity (sp.gr.) contents of the proposed ore types, using the large amount of analytical data from the exploration and producting drilling program within the mine. The Cu-Zn-sp.gr. variation for the ore types is plotted on a triangular diagram and gives a very practical visual separation of these ore types.

Some 72 samples of the various ore facies were sent to Bondar-Clegg in Canada for a complete major and trace element (36 elements) sulphide analysis using various analytical techniques (AAS, XRF, INAA and wet chemical, see Appendix A.1.5, p. A-4 for details of analytical proceedures and Tables C-1 and C-2, for results. The results from these two sulphide analytical series forms the basis of the chemical variations and trends for the ores noted in this report.

It must be emphasized that the ore types separated out for this report (Table 5.1) is not done on a purely chemical and

statistical basis, but from a combination of textural, mineralogical and major element parameters (Cu-Zn-sp.gravity) as well as their spacial relationship to each other and the enclosing host rocks and their lateral distribution across (within) the ore horizon. The present configuration and distribution of the massive ores is best seen on the vertical geological profiles (Appendix, Table E) and the horizontal geological maps (Appendix, Table F) and geological map of the open pit, Fig. 4.2a.

The ore type investigation carried out for this report consisted of mainly a macrotextural (polished, slabbed hand specimens) and a limited microtextural study on polished and thin sections and from their mineralogy and major element distributions.

A detailed microtextural and mineralogical investigation is not dealt with here as Dr. B. Marshall from Sydney, Australia initiated such a study during his six months involvement at the onset of this project. It was intended that he will report on this aspect of the project in a separate report to Grong Gruber.

At present, an ongoing detailed microtextural, ore mineralogical and trace element investigation is being carried out on the Joma ores by W. Leissmann as a postgraduate (Dr.) study at Clausthal Technical University in W. Germany.

This report will therefore only deal with the textural (grain size) mineralogical and chemical variations (Cu-Zn-sp.gr.) of the ore types that are of a more practical aspect, i.e. that can be used for an ore quality and mineral dressing point of view.

The following ore minerals have been recognized in the Joma deposit (Olsen 1980, Eidsmo et al. 1984, Leissmann, pers. comm. 1985). Major components are pyrite, pyrrhotite, chalcopyrite, sphalerite and magnetite. Minor and trace components include cubanite, tetrahedrite, mackinawite, galena, arsenopyrite, cobaltite, ilmenite, rutile, valleriite, amalgam, electrum, native Ag, argentite and pyrargyrite. A primary FeS phase was suggested by Olsen (1980). Matrix minerals include mainly quartz, calcite and chlorite with trace amounts of amphibole, sericite and stilpnomelane.

Seven major ore types have been recognized at Joma which includes four massive ore facies within the main ore zone (types I, II, III and IV) and two dissemination ore types in the surrounding silicate host rocks. The seventh ore type includes the layered sulphide and silicate horizons which occur both distal to the main Joma ore zone and stratigraphically above and below the Joma ore level.

The numerical order in which the ore types are separated out is purely arbitrary and has no chronological significance. They are, however, given in a roughly stratigraphic order from bottom upwards. The ore types are, from bottom to top, as follows from I to VII:

Type I - fine grained, flinty, massive pyritic facies.
II - Cu-rich, py-po-cp massive ore facies.
III - Cu-rich, cp-po breccia, massive to semimassive ore facies.
IV - Zn-rich, medium to coarse grained, pyritic ore facies, rich in carbonate $\pm$ chlorite.
V - layered, sulphide (po $\pm$ sl) and silicate distal exhalites.

The two disseminated ore types are: 1) Cu-rich, dark chlorite schists containing disseminations and layers of chalcopyrite and pyrrhotite, and 2) pale, albite and white mica rich rocks, rich in pyrite-quartz-calcite veins and disseminations, often rich in Zn and minor Pb. These two ore types will not be discussed here as they have already been described as part of the host rock lithological units to the ore horizon (section 4).

The five main massive to semi-massive ore types, their distinguishing features, their chemical natures and their distributions will be discussed in this section.

The ore types have distinct spatial relationship to each other and the enclosing host rocks and to the feeder zone configuration within the footwall host rocks. This is best seen in the vertical geological profiles and Fig. 5.1. Their spatial relationships, lateral distributions, quantity and their thicknesses within the original basinal deposition has, however, been complicated by

isoclinal folding and thrusting (D_2) and later upright folding (D_3). The thrusting has often transformed the main massive ore horizon into smaller lenses which have an en échelon pattern.

5.3. DESCRIPTION OF THE INDIVIDUAL ORE TYPES

The four main ore facies at Joma (Types I, II, III and IV) and the distal ore facies (type V) are described here. The main ore facies have been further subdivided according to diagnostic features such as mineral variations, structures and textures such as original compositional layering, etc.. that are typical for each specific ore type, besides conforming to the major elemental variations (Cu-Zn-Sp.gr.) for the main ore types.

Some of these subfacies do, however, show gradational features between each other, within the major ore facies and sometimes across the major group boundaries.

The characteristic features of the individual ore types and their subdivisions are shown in Table 5.1. This classification is based on a combined textural, structural mineralogical, and major element variations (Cu-Zn-Sp.gr.).

5.3.1 Type I: Fine grained, massive pyritic ore facies.

Subfacies Ia. This ore type is a typically fine to very fine grained (0.05-0.1 mm grain size), flinty, dense, hard pyritic ore facies, which is almost solely composed of pyrite, with only minor contents of chalcopyrite, pyrrhotite and sphalerite. This is reflected in its low Cu and Zn and high sulphur contents. The almost purely pyritic ores are typically pale yellow to greyish in colour. Only minor quantities of quartz and carbonate (calcite) occurs within the matrix and is most often concentrated as fracture fillings.

The fine grained pyritic ores are usually very homogeneous and seldom show signs of primary layering. Besides being very homogeneous and massive, they are often tectonically brecciated and fractured into larger blocky fragments - which are infilled

with quartz and/or calcite and minor chalcopyrite+pyrrhotite and/or sphalerite. Some zones of more intense brecciation contain smaller angular fragments.

The Type I, pyritic ores generally contain less than 1-2 % combined Cu+Zn and there is a complete gradation between this ore and the Cu-rich facies (type II) with increasing chalcopyrite-pyrrhotite and the fine grained varieties of type IV, with increasing sphalerite and carbonate content.

Thick sections of fine grained pyritic ore (type Ia) occurs in the middle of and at the south end of exploration adit 362 øf and as the major thickness of the south end of the open pit. Cu-rich facies occurs on west side and Zn-rich facies on the east side of the open pit.

Subfacies Ib. In areas of strong D_3 folding and resulting cleaving of the host rock silicates, the fine grained massive pyritic ores show conjugate set of fractures that are infilled with fibrous amphibole and quartz. The more Cu-rich pyritic facies also have chalcopyrite+pyrrhotite concentrated along with amphibole in the fractures. Type Ib pyritic ore is best seen within the 362 øf level, 375 øf synk and along the western wall of 387 vf.s. strosse (see Photo 17).

Subfacies Ic. This ore type is similar to type Ia, with the exception that it contains minor calcite as fracture fillings instead of quartz or pyrrhotite and fibrous amphibole. Subfacies Ic is slightly more sphalerite bearing and has less Cu-rich minerals (cp).

5.3.2. Type II. Cu-rich, massive pyrite-pyrrhotite-chalcopyrite ore facies.

The Type II ores encompass a variety of Cu-rich ores that are fine to medium grained, often layered (primary) and show large variations in their pyrite, pyrrhotite, chalcopyrite, magentite and amphibole contents.

Because of the larger amounts of chalcopyrite and pyrrhotite in these ores, the Type II ores are typically more yellow to brownish-yellow in colour. They often show marked compositional layering between the Cu-rich sulphide layers and the interlayered silicates and oxides. The individual layers which can be quite persistent, are from a few cm's to maximum 10-15 cm thick and are composed of massive magnetite and accompanying dark amphibole, thin bands of fibrous amphibole needles, dark chlorite schists and magnetite+chlorite+stilpnomelane bearing, dark quartzite bands and lenses (recrystallized cherts).

Subfacies IIa. This subfacies comprises only a very minor and local part of the type II ores. It has, however, very diagnostic, irregular zones of coarse grained patches rich in quartz plus chalcopyrite, and calcite plus sphalerite. These patches grade quickly into each other. The coarse grain size, the patchy nature and the qtz+Cu and calcite+Zn zoned nature of this subtype is diagnostic.

These patchy, zoned cp+qtz and sl+calcite rich ore occur as small isolated patches very locally within the mine, within pyritic ores that are both Cu+Zn bearing. So far, it has only been found within the mine drill core, Bh 1640-2 (sample no. 26, Appendix Table C-1) and at the southwest end of the 480 ØH exploration adit.

Discussion.

The patchy zones of qtz+cp and calcite+sl resemble fragments of black smoker chimneys that have been described from the Kuroko deposits of Japan and from the rifting zones of the ocean floor (East Baltic Rise and Juan de Fuca Ridge). These chimneys contain typical quartz+chalcopyrite rich inner walls and carbonate + sphalerite rich out walls. The patches of type IIa ore at Joma probably represents the remnants of an original hydrothermal venting chimney, that has broken up, fallen down and been covered over by, and partially redissolved and digested by through passing hydrothermnal fluids during the continued prosses of massive sulphide build up and deposition.

Subfacies IIb. Within irregular zones, some of the Cu bearing pyritic ore also carry dark, fine to coarse grained disseminations of magnetite and quartz as matrix. This produces a weak salt and pepper texture. Type IIb ores are best seen in the 480 ØH exploration adit (see Appendix F, Horizontal map 480 ØH, sample no. 480 ØH-6).

Subfacies IIc. This is a Cu-rich, massive ore that grades into the type I pyritic ore facies, and consists of a fine to medium grained massive pyrite-chalcopyrite-pyrrhotite ore facies. It often shows compositional layering consisting of pyritic and chalcopyrite-pyrrhotite rich parts, some of which are separated by thin zones of dark amphibole needles. Some of the compositional layering is thought to be primary although much of the compositional layering is now tectonic in nature. The type IIc ores are best seen at the bottom of 375 øf synk (see Photo 20).

Subfacies IId. This Cu-rich ore facies contains conspicuous cm thick layers of dark brown to black amphibole needles interlayered within the sulphides. These layers are quite persistant and are often found in areas that contain magnetite banding and disseminations. The layering is thought to be primary and is often found folded (by both F_2 and F_3) and occurring as fragments within the cp-po breccia ores (type IIIa). The type IId ore facies is well developed at the 387 ØL level, locality 3 (see Fig. 4.3) and at 387 vf.s. strosse, along the western wall (see Photo 18).

Subfacies IIe. This subfacies is very diagnostic, containing numerous interlayered, thin (cm to max. 5-10 cm) persistant bands of magnetite, amphibole and chlorite schist and thicker layers and lenses of dark, magnetite bearing quartzites (recrystallized cherts). Carbonate is also a minor component.

The type IIe ore usually occurs as thin (m thick) layers within the thinned distal parts of the main ore zone. The layering is of a primary sedimentary origin. (see Photo's 29+30)

The type IIe ores are best preserved along the lower limb of the main ore zone (Profile B_2-11) at 385 vf.s. strosse (see Fig. 4.4, locality no. 20).

Subfacies IImt. Thick layers of black magnetite (max. 15-20 cm thick) and associated dark, greyish-brown to green, fibrous, Fe-rich amphibole needles are often found within the Cu-rich py-cp-po massive ores. Chalcopyrite±pyrrhotite occurs along fractures and cleavages within these magnetite bands. The magnetite bands represent primary compositional chemical-sedimentary layering. The thicker magnetite bands are, however, quite inconsistant, often being broken up by post depositional deformation (see Photo 19). Fragments of magnetite and amphibole layers frequently occur within the post-depositional tectonic breccia ores (type III) (see Photo 36).

The thicker magnetite banded ores are best preserved in the massive, Cu-rich ores about midway down the 375 øf synk incline (see Fig. 4.6).

5.3.3. Type III. Cu-rich, chalcopyrite-pyrrhotite breccia ore.

The type III ore is a variety of generally very Cu-rich, chalcopyrite and pyrrhotite bearing ore that carries diagnostic angular to somewhat rounded fragments of dark chlorite schist, magnetite ore, fine grained pyritic ore, white limestone marble and associated amphibolitic greenstone and clear, glassy to white, hydrothermal quartz.

The ore is very irregular in nature, which is reflected in its fragmental content, grain size and amounts of chalcopyrite or pyrrhotite within the ore. The ores vary somewhat in grain size from coarse grained to very coarse grained (2-3 cm sized). They are generally coarser grained in the ores that have large angular country rock fragments. The breccia ores vary greatly in their Cu contents reflecting the varying amounts of host rock fragments and strong variation in the chalcopyrite and pyrrhotite matrix that supports the fragments.

The breccia ores vary greatly in their sulphide mineralogy. Almost all the minerals mentioned earlier (p. 103) occur within these ores.

The breccia ores vary greatly in form. They show strong tectonic control and often occur as distinct layers along minor thrusts (shear zones) that cut through the massive Cu-rich ores (type II) and the adjacent host rocks (see Photo's 34 to 41). Some massive breccia ore horizones have been found up to 2 m thick and carrying up to 20 % Cu. Much of the cp-po breccia ore occurs as thinner (10-50 cm thick) irregular anastomosing zones that surrounds larger lenses of fine grained Cu-rich pyritic ore.

Subfacies IIIa and IIIb.

The type III cp-po breccia ore has been subdivided into two main types. Subfacies IIIa encompasses the majority of this ore facies which is rich in chalcopyrite. Subfacies IIIb consists mainly of pyrrhotite and minor sphalerite as the main sulphides and the fragments are dominated by amphibolites, carbonate and hydrothermal quartz. This facies is typically depleted in Cu and enriched in Zn compared to subfacies IIIa and occurs only locally within the mine, i.e. along the basal thrust zone that separates the main ore from the post-ore, pale, footwall greenstone (see vertical section B_2-11). This Zn-rich subfacies may represent some tectonic brecciation and remobilization of some primary Zn-rich distal mineralization facies.

'Durchbewegt' ore.

The chalcopyrite-pyrrhotite breccia ore is a characteristic and interesting ore type at Joma. It often occurs as distinct layers following minor thrusts (shear zones) that cut the massive Cu-rich ores and adjacent host rocks (see Photo's 6+34+37+42). Numerous angular to subrounded fragments of chlorite schists, white limestone and amphibole schist, magnetite, and fine grained pyritic ores attest to derivation of the breccia ore from the adjacent host rock and ore lithologies (see Photo's 35+36+38+39+40-+41). Isoclinal fold hinges of an early compositional layering within the fragments and rounded hydrothermal glassy quartz frag

ments indicate an early tectonic (D_1-D_2) derivation (cf. Olsen, 1980, who favoured a primary sedimentary-exhalative origin). The fragments become notably smaller and more rounded the further they occur along the thrust away from their source rock. This breccia ore may be classified as a 'durchbewegt' ore type and can be traced several hundred metres along minor thrust surfaces that penetrate out into the enclosing host rock silicates. The chalcopyrite-pyrrhotite breccia ore can locally form distinct layers containing impressive thicknesses (>2m) rich in chalcopyrite, with ore grades up to 20 % Cu.

The competency contrast between the silicate and sulphide layering, and the presence of large quantities of both chalcopyrite and pyrrhotite within the Cu-rich, type II massive ores has probably been the governing factors in the formation of this tectonic breccia ore. Pyrrhotite and chalcopyrite, and for that matter also sphalerite, are minerals which, due to their internal structures (cleavage planes along which gliding can occur), are readily mobilized and redistributed by tectonic shearing movements associated with the 'durchbewegt' phenomena.

Chalcopyrite, pyrrhotite, sphalerite and quartz-calcite are also typically mobilized along D_3 piercement structures and late cross-cutting fracture fillings, adjacent to the Cu-rich massive sulphide ores at Joma.

5.3.4. Type IV: Zn-rich, pyritic ore, massive to semi-massive.

The type IV massive pyritic ores are all Zn bearing to very Zn-rich, generally devoid of Cu and rich in carbonate.

Subfacies IVa. This ore facies grades from fine grained homogeneous and rather massive pyritic ore into medium to coarse grained varieties that are more layered and rich in ubiquitous carbonate, both as matrix and as individual thin to rather thick (max. 2 m) limestone marble bands (see Photo's 32+33 and Microphoto 24). Minor chlorite and amphibolite layers (max. 10-15 cm thick) have been found associated with the limestone bands in the upper stratigraphic levels of the Joma ore zone.

This ore facies forms rather thick sequences in the Joma ore horizon (see Fig. 5.1). The ores are rather homogeneous with an evenly dispersed sphalerite content but can become somewhat layered with the sphalerite being concentrated into irregular elongate (tectonic?) patches and bands, i.e. levels 416 and 429 (see Photo's 21+22+23+31). These Zn-rich zones occur within the more massive homogeneous variety - with the carbonate banded ores containing slightly less Zn.

Subfacies IVb. This ore facies occurs as thinner units of typically darker, grey-brownish coloured, Zn-rich and carbonate bearing pyritic ore (see Photo's 25+26). They show some weak layering or irregular breccia-like structures (tectonic?) in which the darker sphalerite and carbonate rich layers are cleaved (S_2) and filled with a coarser grained paler pyrite. Some well developed breccia structures are found (see Photo 27). Besides the darker, greyish-brown colour, randomly oriented, dark green to black amphibole needles are also a diagnostic feature of this unit. Some small (1 cm sized) dark reddish-brown, rusty-like (oxidixed?) rounded fragments are also seen (i.e. 385 vf.s. strosse, locality 21, Fig. 4.4 + Photo 26). This ore facies may well have been formed by slumping. The amphibole needles probably represent some original detrital material that has recrystallized under metamorphism to form amphibole porphyroblasts.

The Type IVb ore facies is best seen at 385 vf.s. strosse, locality 21, adjacent to the black, magnetiferous quartzites (cherts?) (see Fig. 4.4) and at the western edge of the open pit, locality JD 28/84 (see Fig. 4.2a+b).

Subfacies IVc. This subfacies occurs as thinner sequences of layered (cm scale), semi-massive pyritic ores. The darker compositional layers are rich in chlorite and minor carbonate and pyrite disseminations and the paler semi-massive pyritic layers are rich in sericite, carbonate and actinolite as matrix minerals. This subfacies can be very rich in Zn and contains only minor layers rich in Cu. It occurs only as thinner (1-2 m thich) units and is best seen at the bottom of 375 øf synk - lying between the Cu-rich massive py-cp-po ores and the post-ore, pale greenstones, and along the 362 vf, newer adit (see Photo 28).

Subfacies IVd. Thin units of somewhat irregular laminations (1-2 cm thick) of darker sphalerite and quartz rich versus paler pyritic rich laminae is characteristic for this subfacies (see Photo 24). Some lenses of pale greyish quartzites, rich in pyrite+sphalerite are found within some of these layers and resemble some of the isolated pale, pyrite bearing quartzites (recrystallized cherts!) found within the pale schists adjacent to the main ore zone (i.e. 375 øf locality no.46 and 387 ØL locality no. 4, see Figs. 4.6 and 4.3, respectively).

5.3.5. Type V: Layered sulphide (po+sl) and silicate and carbonate rich, distal exhalites.

There occur numerous lenses and layers of blackish to dark grey, pale grey to whitish, magnetite and sulphide disseminated (po±py) recrystallized cherts, both stratigraphically above and below the Joma ore horizon. The magnetite rich, dark varieties that occur stratigraphically below the ore horizon have been variously bleached and metasomatized, the dark, magnetite rich quartzite occurring as a central core, surrounded by a pyrrhotite disseminated pale quartzite alteration zone. The magnetite has been altered to pyrrhotite (see Photo 42 and Microphoto 23).

Some thin (1 m max. thickness) laminated bands of massive pyrrhotite, chert, carbonate, dark chlorite and pale laminated greenstones and schists rich in dark graphite, occur distal to the main ore zone (within pillowed sequences) (i.e. DDH D63-254.30 m). Some of these units are Zn bearing and devoid of Cu. These may represent distal varieties of the main sulphide horizon at Joma, or more likely, they represent younger minor mineralizations that occur stratigraphically above the main Joma sulphide horizon. Later intense deformation has complicated their stratigraphic relationships greatly.

5.4. CHEMICAL CHARACTER OF THE ORE TYPES

The main ore types at Joma show some diagnostic chemical and physical features when compared with each other. Table 5.2 shows

the average metal and trace element contents of the main ore facies at Joma. The main chemical features for each of the major ore type is as follows:

Type I, fine grained, flinty, pyritic ore. These are characterized by:

High:	specific gravity (Sp.gr.), S, Au, Bi and As.
Moderate:	Pb and Fe
Low:	Cu, Zn, Ag, Hg, Mn, Co, Ni, Mo, V, Cr and Sr.

The high sp. gravity, S and As and the low Hg and Mn contents is typical for the Type I pyritic ore facies.

Type II. The Cu-rich, py-cp-po massive ores are characterized by relatively:

High:	Sp.gr., Cu, Fe. Co, Mo and slight Se.
Moderate:	S, Hg and Mn.
Low:	Zn and As.

Type IIIa. The cp-po breccia ores are characterized by relatively:

High:	Cu, Fe, Ag, Co, Ni (Mo?) and Se.
Low:	Sp.gr., S, Zn, Pb, Au, Cd (Bi?), Sb and As.

The type IIIb ores are typically higher in Zn and lower in Cu.

Type IV a+b+c. The Zn-rich, carbonate bearing pyritic ores are characterized by relatively:

High:	Zn, Pb, Au, Hg, Cd, Mn, Cr, As and Sr.
Moderate:	Ag, Ni.
Low:	Cu, Co and Se.

Type V. The layered distal, po bearing exhalites are characterized by relatively:

High:	Mn, V, Cr, Ni, As and Na (these elements are diagnostic).
Low:	Sp.gr., S, Cu, Zn, Pb, Ag, Au, Hg, Cd, Fe, Bi, Sb and Se.

Variations across the Joma ore zone point to the following individual elemental variations and associations:

Sp.gr. - is highest in the fine grained pyritic ores and magnetite ore.

S - highest in fine grained massive pyritic ore.

Cu and Zn - show an antipathetic relationship.

Pb - is enriched in the Zn-rich pyritic ores and probably follows the increased carbonate content there.

Ag - shows a slight enrichment in the type IIIa. cp-po breccia ores.

Au - shows very little variation within ore zone.

Hg+Cd - follows Zn enrichment and occurs within the sl crystal structure.

Fe - is highest in the po and mt-rich ores.

Mn - appears to follow the Zn enrichment and probably occurs within the sl.

V - follows Mn, is strongly enriched in the distal ores.

Cr - also increases in ore type IV and in the distal ores, type V. These ores carry much chlorite and Cr can occur within the chlorite structure.

Co - is strongly enriched in Cu-rich ores, occurring as cobaltite(?).

Ni - enriched in the po bearing ore types (III) and distal ores (IV). The distal ores are rich in graphite and po as bands and disseminations.

Mo - shows a slight increase in the Cu-rich ores.

Bi - shows slight increase in the fine grained pyritic ore.

Sb - shows no real trend.

As - shows a strong increase in the pyritic and Zn-rich ores and probably occurs within the pyrite crystals.

Se - increases in the cp-po breccia ores.

Na - shows a slight increase in the breccia type ores and the layered silicate + sulphide distal ores. This most likely reflects a strong increase in albite in these ores.

Sr - shows strong enrichment in the carbonate bearing, Zn-rich ores and follows calcite.

The chemical variations within the major ore types at Joma (types I, II, III, IV and V) indicate several elemental correlations and trends. These are:

1) The Cu-rich ores are high in Co, Fe, Mo and Se and low in Zn and As.
2) The Zn-rich pyritic ores are richer in Pb, Hg, Mn, As and Sr and low in Cu, Co, Fe and Se. The Hg, Cd and Mn contents can go into the sphalerite structure.
3) The distal, layered exhalites, with pyrrhotite and graphite, show high values of Mn, V, Cr, Ni, As and Na. The V probably occurs within the graphite, and Ni within the pyrrhotite. The Cr occurs within chlorites, Na within albitite and the As most likely occurs in pyrite.
4) Cu har a positive correlation with Co, Fe and Mo and a negative correlation with As.
5) Zn shows a positive correlation with Pb, Hg, Cd and Sr (+ calcite).
6) Sp. gravity is highest in the pyrite and magnetite rich ores.
7) S is richest in the pyritic ores.
8) Pb follows carbonates + Sr and Zn (?).
9) Sr shows a strong correlation with calcite contents.

5.5. THE USE OF Cu-Zn-SP.GRAVITY DATA TO SEPARATE THE ORE TYPES.

Cu, Zn and specific gravity (sp.gr.) are rutinely analysed on all the exploration drill core that is taken from the Joma ore body. During the process of separating out the Joma ore types on a textural, structural and mineralogical basis, it was noted that the major ore types also show great variations in their Cu, Zn and sp. gravity values. The Cu and Zn values generally show an antipathetic relationship to each other and the sp. gravity increases notably within the fine grained, flinty, pyritic ores and decreases within the silicate- and carbonate bearing ore types (types III, IV and V). In order to study these variations, the analytical results for the various ore types, as described for the drill holes in profile X=95120, were plotted onto a Cu-Zn-Sp.gravity triangular diagram. The individual elemental results (Cu, Zn, Sp.gr.) for each sample was first divided by the mean elemental value for the whole deposit, i.e. the

$$\frac{\text{Cu sample}}{\text{X Cu for whole ore body}}$$

and similarly for Zn and Sp. gravity.

The mean values for x Cu, x Zn and x Sp.gr.were taken from early reserve calculations (1972-1974). This allows for a better spread of the data within the triangular diagram, the average value for the ore body would plot at the middle of the diagram.

The data points for the various ore type samples define distinct groups or clusters on the triangular diagram. Fig.5.2 shows the plot of all the data from profile X=95120, which formed a test case for this study on the Cu-Zn-Sp.gravity variations for the ore types.

The Cu-Zn-Sp.gravity results for 72 samples analyses from the various ores at Joma was also plotted on a triangular diagram to control the clustering of the ore types and to indicate possible trends that occur between these ores when progressing stratigraphically upwards and laterally along the ore horizon. Fig. 5.3 shows the results of the 72 ore sample given in Appendix Table C-1 and C-2. These results show similar ore type groupings or clusters as the profile X=95120 test diagram (Fig. 5.2) and strengthens the group boundaries for the four main ore types. Fig. 5.4 shows the ore type groups and some of the trends visible in the data.

The results from the Cu-Zn-sp.gr. triangular plots have now been incorporated into a computer program at Grong Gruber such that the four main ore types (see Fig.5.5 for boundaries) can now be directly plotted onto the drill holes in the vertical geological profiles, giving an indication of the distributions of the various ore types along and across the massive ore horizon. This will hopefully be used to define minable ore types that can be mined separately and as a possible quality control for the ores going to the mineral dressing plant.

Fig. 5.6 shows a control plot of the various ore types for profile X=95120, taken from the geological descriptions of the drill core. Fig. 5.7 shows a reduction of a computer print out of the ore types for the same profile (X=95120) using a computer program devised for Grong Gruber for this purpose by Jan Myrheim.

5.6. DISTRIBUTION AND ZONATION OF ORE TYPES.

There is a very marked zonation pattern in the Cu-Zn contents and for the ore facies within the Joma ore horizon. The Cu-rich ores (type II and III) are confined to the western and south-western parts of the Joma ore horizon where they are closely associated with the dark Fe-rich chlorite schists. The Cu-rich ores (type II) vary somewhat in thickness but generally occur as thinner horizons than the massive pyritic ores (type I and IV).

The Zn-rich, carbonate bearing, pyritic ores (type IV) forms the thicker parts to the massive ore zone, along the northeastern and southeastern parts of the Joma deposit. These form the major parts of the massive Joma ore horizon.

The fine grained, flinty, pyritic ore facies (type I) separates roughly the Cu-rich (type II) and the Zn-rich (type IV) ores from each other (see Fig. 5.1). There is a gradation between the fine grained pyritic ore (type I) and both the Cu-rich (type II) and the Zn-rich pyritic ore (type IV).

The Cu-rich, cp-po breccia ores (type III) show strong tectonic control, and lie generally along D_2 thrusts that penetrate the Cu-rich massive ore zone. They are also confined to the western side of the ore body where they are associated with the type II, Cu-rich massive ores and the Cu-rich disseminated, Fe-rich chlorite schists from which they are derived.

The Cu-Zn zonation, and the separation of the Cu-rich (type II) and the Zn-rich (type IV) ores between the western and eastern parts of the ore horizon can be demonstrated on a Cu-Zn-sp.gr. triangular plot of the ore types for profile B_2-15, west side of ore body and X=95000, along the eastern parts of the ore body.

The type II and III ores dominate the western side of the ore body (profile B_2-14-16, Fig. 5.8) and the type IV ores dominate the eastern side (profiles X=94980+95000+95020, Fig. 5.9).

TABLE 5.1: JOMA ORE TYPES. A CLASSIFICATION BASED ON TEXTURAL, STRUCTURAL, MINERALOGICAL AND MAJOR ELEMENT VARIATIONS.

Type I:		fine grained, S-rich massive pyritic facies. Grades into both Cu and Zn-rich fine grained pyritic facies.
⊙	Ia	Fine grained, hard, flinty pyritic ore, very pale yellow colour, often tectonic brecciated with fractures infilled with qtz+cc. Minor to moderate Cu+Zn contents, up to several % combined Cu+Zn.
$\odot_A$	Ib	As Ia, with fracture fillings of fibrous amphibole (F_3 assoc.), can have cp+po associated amphibole in Cu-rich facies.
$\odot_C$	Ic	as Ia with minor carbonate as matrix and fracture filling, slightly more Zn bearing.
TYPE II:		Cu-rich massive py-po-cp ore facies. Fine to medium grained, varies greatly in py+po+cp+mt+Amf contents.
◈	IIa	Very irregular zoned Cu+Zn rich ore, Cu+qtz and Zn+cc rich zones.
◪	IIb	Disseminated mt bearing, quartz rich pyritic ore.
□	IIc	Cu-rich, massive po-cp-py ore, often layered (primary and tectonic).
$\boxdot_A$	IId	Massive po-py ore with layering of dark amf. needles.
◪	IIe	Associated mt banding and thin chlorite schist layers, and black mt bearing chert horizons + minor carbonate.
■	IImt	Magnetite ore layer and dark Fe-amphibole + minor cp.
Type III:		chalcopyrite + pyrrhotite breccia ore facies. Very irregular in occurrence and mineral + fragment contents shows very strong tectonic control (F_1-F_2+F_3 associated).
▲	IIIa	cp-po breccia ore, to very Cu-rich. Much fragments of chlorite schist, carbonate and magnetite and fine grained pyritic ore.
$\triangle_{Po}$	IIIb	Massive po rich ore, remobilized ? Part of tectonic breccia, often Zn associated ?
Type IV:		Zn-rich pyritic ore facies, massive to semi-massive.
●	IVa	Medium to coarse grained, Zn-rich massive pyritic ore, grades into fine grained Zn-rich ores, almost devoid of Cu. Carbonate rich matrix and as individual layers.
$+_A$	IVb	Fragmental (slump breccia) to greyish-layered pyritic ore, contains diagnostic dark Amf. needles. Much carbonate matrix and bands (Mn-carbonate ?).
◒	IVc	Semi-massive to massive pyritic ore, Zn-rich. Rich in carbonate and chlorite schists as matrix + layers. Grades into Cu+Zn rich parts near Cu rich massive ores.
⊕	IVd	Quartz rich, semi-massive pyritic ore, much quartz matrix associated Zn rich distal py-qtz veining.
Type V		Sulphide and magnetite rich quartzites (recrystallized cherts) and proximal and distal exhalites and mineralizations both above and below main ore horizon.
	V_{Qmt}	Dark mt bearing quartzites (chert-'Blå kvarts') with minor chl+stilp±po, near and above main ore.
	V_{Qpo}	Same as above, altered to pale quartzite with po disseminations.
	V_{Qpy}	Pale quartzite lenses rich in py ± sl mineralizations, distal level to main ore zone.
	V_{Qd}	Mt-po bearing dark quartzites (Bk) distal ? above or below main ore zone.
	Va	Layered po - pale tuffs - carbonates and minor graphite schists - above main ore zone ?
	Vb	po mineralizations associated cherts+graphitic bearing cherts and phyllites - distal - (Orklumpen).

Disseminated ore types.

▽	D_1	- Cu-rich, cp-po disseminations in dark chlorite schists.
▼	D_2	- Cu+Zn- to Zn-rich pyritic disseminations in moderate to pale greenish chlorite schists.
·	D_3	- Pale albite - pyrite layering.

TABLE 5.1: JOMA ORE TYPES. A CLASSIFICATION BASED ON TEXTURAL, STRUCTURAL, MINERALOGICAL AND MAJOR ELEMENT VARIATIONS.

Type I:		fine grained, S-rich massive pyritic facies. Grades into both Cu and Zn-rich fine grained pyritic facies.
⊙	Ia	Fine grained, hard, flinty pyritic ore, very pale yellow colour, often tectonic brecciated with fractures infilled with qtz+cc. Minor to moderate Cu+Zn contents, up to several % combined Cu+Zn.
$\odot_A$	Ib	As Ia, with fracture fillings of fibrous amphibole (F_3 assoc.), can have cp+po associated amphibole in Cu-rich facies.
$\odot_C$	Ic	as Ia with minor carbonate as matrix and fracture filling, slightly more Zn bearing.
TYPE II:		Cu-rich massive py-po-cp ore facies. Fine to medium grained, varies greatly in py+po+cp+mt+Amf contents.
◇	IIa	Very irregular zoned Cu+Zn rich ore, Cu+qtz and Zn+cc rich zones.
◥	IIb	Disseminated mt bearing, quartz rich pyritic ore.
□	IIc	Cu-rich, massive po-cp-py ore, often layered (primary and tectonic).
$\boxdot_A$	IId	Massive po-py ore with layering of dark amf. needles.
◪	IIe	Associated mt banding and thin chlorite schist layers, and black mt bearing chert horizons + minor carbonate.
■	IImt	Magnetite ore layer and dark Fe-amphibole + minor cp.

Type III: chalcopyrite + pyrrhotite breccia ore facies.

Very irregular in occurrence and mineral + fragment contents, shows very strong tectonic control (F_1-F_2+F_3 associated).

▲ IIIa — cp-po breccia ore, to very Cu-rich.
Much fragments of chlorite schist, carbonate and magnetite and fine grained pyritic ore.

$\triangle_{Po}$ IIIb — Massive po rich ore, remobilized ?
Part of tectonic breccia, often Zn associated ?

Type IV: Zn-rich pyritic ore facies, massive to semi-massive.

● IVa — Medium to coarse grained, Zn-rich massive pyritic ore, grades into fine grained Zn-rich ores, almost devoid of Cu.
Carbonate rich matrix and as individual layers.

$+_A$ IVb — Fragmental (slump breccia) to greyish-layered pyritic ore, contains diagnostic dark Amf. needles. Much carbonate matrix and bands (Mn-carbonate ?).

◒ IVc — Semi-massive to massive pyritic ore, Zn-rich.
Rich in carbonate and chlorite schists as matrix + layers.
Grades into Cu+Zn rich parts near Cu rich massive ores.

⊕ IVd — Quartz rich, semi-massive pyritic ore, much quartz matrix associated Zn rich distal py-qtz veining.

Type V — Sulphide and magnetite rich quartzites (recrystallized cherts) and proximal and distal exhalites and mineralizations both above and below main ore horizon.

V_{Qmt} — Dark mt bearing quartzites (chert-'Blå kvarts')
with minor chl+stilp±po, near and above main ore.

V_{Qpo} Same as above, altered to pale quartzite with po disseminations.

V_{Qpy} Pale quartzite lenses rich in py $\pm$ sl mineralizations, distal level to main ore zone.

V_{Qd} Mt-po bearing dark quartzites (Bk) distal ?
above or below main ore zone.

Va Layered po - pale tuffs - carbonates and minor graphite schists - above main ore zone ?

Vb po mineralizations associated cherts+graphitic bearing cherts and phyllites - distal - (Orklumpen).

Disseminated ore types.

▽ D_1 - Cu-rich, cp-po disseminations in dark chlorite schists.

▽ D_2 - Cu+Zn- to Zn-rich pyritic disseminations in moderate to pale greenish chlorite schists.

• D_3 - Pale albite - pyrite layering.

TABLE 5.2.: AVERAGE METAL CONTENTS OF THE MAJOR MASSIVE ORE TYPES AT JOMA
(Types I, II, III, IV and V.)

Oretypes	IIa-e Cu rich, massive cp-po-py facies, + mt, + amf			IIIa Cp-po breccia ore facies			Ia+b+c fine grained, mass. S rich pyritic facies			IV a+b+c Zn rich, massive pyritic facies, carbonate+chlorite bearing			V qtz+a+b Distal mineral. mass. po bands assoc. chert + graphite		
	(n=19)		x (n=11)	(n=6)		x (n=4)	(n=10)		x (n=7)	(n=21)		x (n=14)	x (n=5)		
	$\bar{x}$		sd	$\bar{x}$		sd	$\bar{x}$		sd	$\bar{x}$		sd	$\bar{x}$		sd
Sp.gr.	4.27	±	0.41	3.93	±	0.35	4.44	±	0.24	4.07	±	0.36	3.21	±	20.49
% S	35.82	±	8.94	29.69	±	6.35	43.78	±	4.11	35.94	±	4.70	12.53	±	12.60
% Cu	3.52	±	2.42	8.19	±	6.38	0.83	±	0.45	0.76	±	0.77	0.13	±	0.24
% Zn	0.93	±	1.13	0.69	±	0.41	0.97	±	1.33	6.36	±	5.62	0.01	±	0.01
Pb	150	±	169	103	±	156	142	±	53	1120	±	1140	15	±	9
Ag	18	±	19	43	±	22	15	±	12	21	±	19	1	±	1
ppb Au	181	±	125	128	±	96	221	±	58	207	±	143	13	±	14
ppb Hg	1937	±	1651	1741	±	1481	869	±	674	3818	±	2329	59	±	66
Cd	50	±	53	31	±	20	66	±	88	335	±	375	0.4	±	0.6
% Fe^x	35.36	±	5.05	37.50	±	5.07	33.00	±	1.63	31.50	±	3.50	12.08	±	8.08
Mn	134	±	111	108	±	95	92	±	57	387	±	319	880	±	805
V	12	±	18	12	±	8	6	±	1	13	±	15	42	±	31
Cr	11	±	27	12	±	16	8	±	7	21	±	39	66	±	73
Co	199	±	142	189	±	90	41	±	49	30	±	49	48	±	24
Ni	11	±	14	25	±	25	5	±	5	14	±	15	101	±	45
Mo	12	±	11	12	±	7	5	±	3	7	±	6	7	±	9
Bi	9	±	5	3	±	4	13	±	7	9	±	5	1.4	±	1
Sb	5	±	4	0.9	±	0.2	7	±	3	8	±	5	0.4	±	0.3
As	290	±	178	79	±	93	615	±	291	602	±	605	465	±	1037
Se	79	±	46	125	±	38	65	±	42	40	±	41	8	±	11
% Na	0.05	±	0.06	0.19	±	0.23	0.01	±	0.01	0.08	±	0.12	1.85	±	2.35
Sr^x	18	±	18	21	±	25	5	±	3	30	±	23	-		

x = no. of samples used in calculations

NB- all elements are in ppm unless otherwise stated.

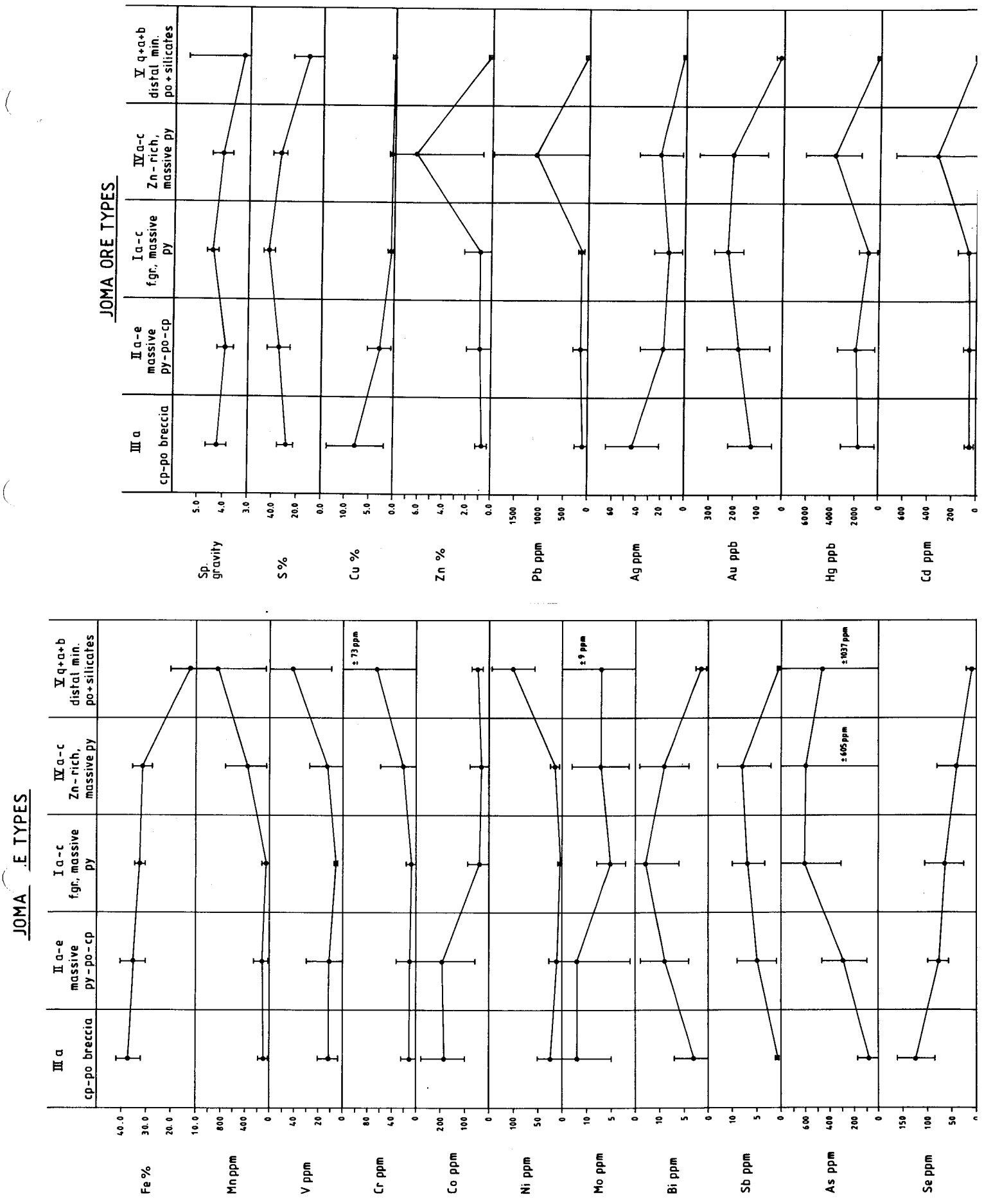

Fig.5.0 Diagram showing major (a) and trace (b) elemental trends of the various massive ore types at Joma (Cu-rich to left and Zn-rich and distal ores to right). The following groups of elements show similar trends:

1) S, Au, Bi, Sb, As; 2) Cu, Ag, Co, Mo(?), Se;
3) Zn, Pb, Hg, Cd; 4) Mn, V, Cr, Ni.

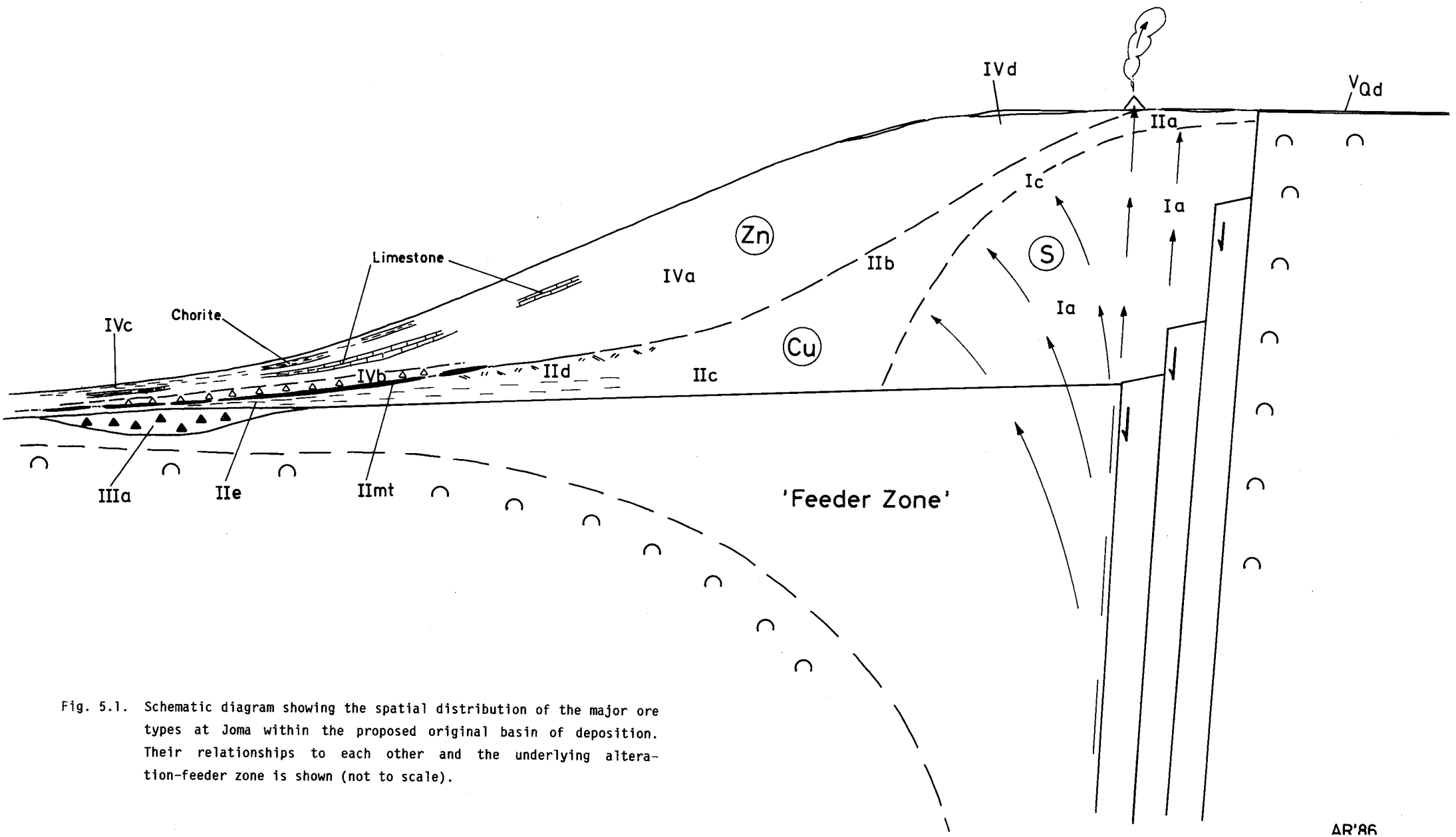

Fig. 5.1. Schematic diagram showing the spatial distribution of the major ore types at Joma within the proposed original basin of deposition. Their relationships to each other and the underlying alteration-feeder zone is shown (not to scale).

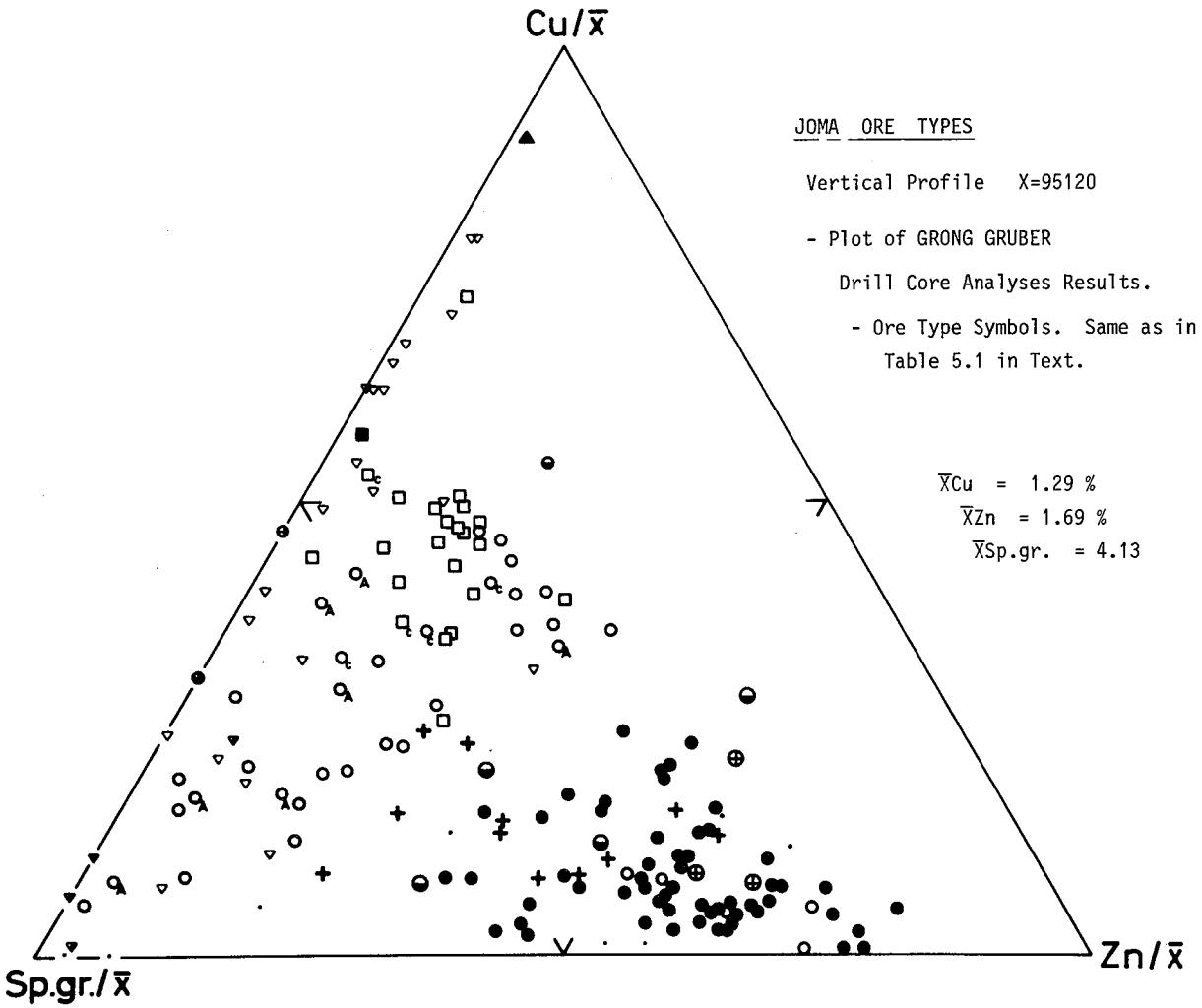

Fig. 5.2. Cu-Zn-Sp.gravity plot of the 4 major ore types for vertical profile X95120 as described in the drill core logs. This is a test case for the separation of ore types on the Cu-Zn-Sp.gr. diagrams. The ore types are as described in Table 5.1 (section 5). The disseminated ore types are also plotted in the diagram.

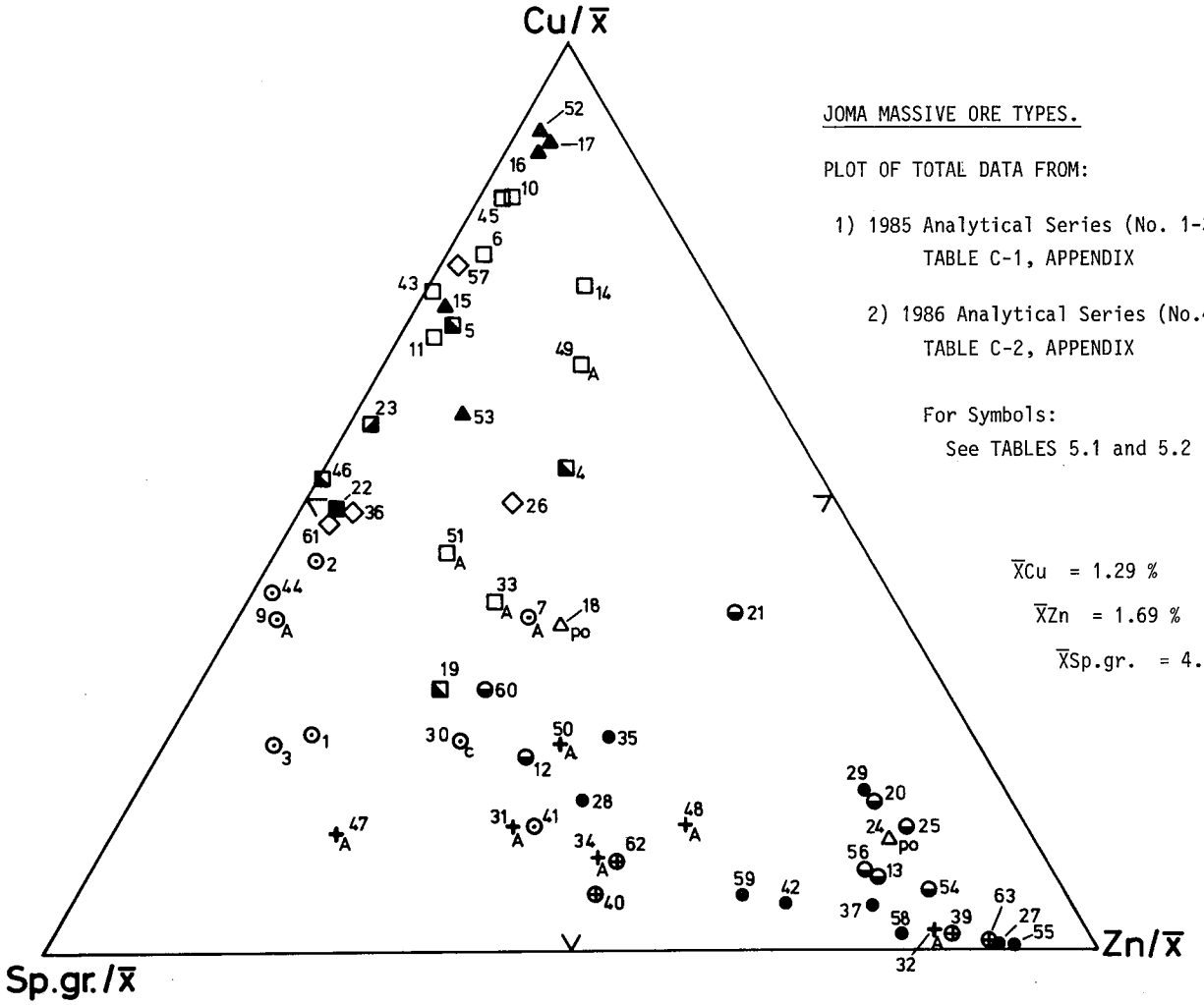

Fig. 5.3. Cu-Zn-Sp.gravity plot of the 72 ore type samples from throughout the Joma ore body (see Appendix, Tables C-1 and C-2). The various sub-types are described in Table 5.1 (section 5).

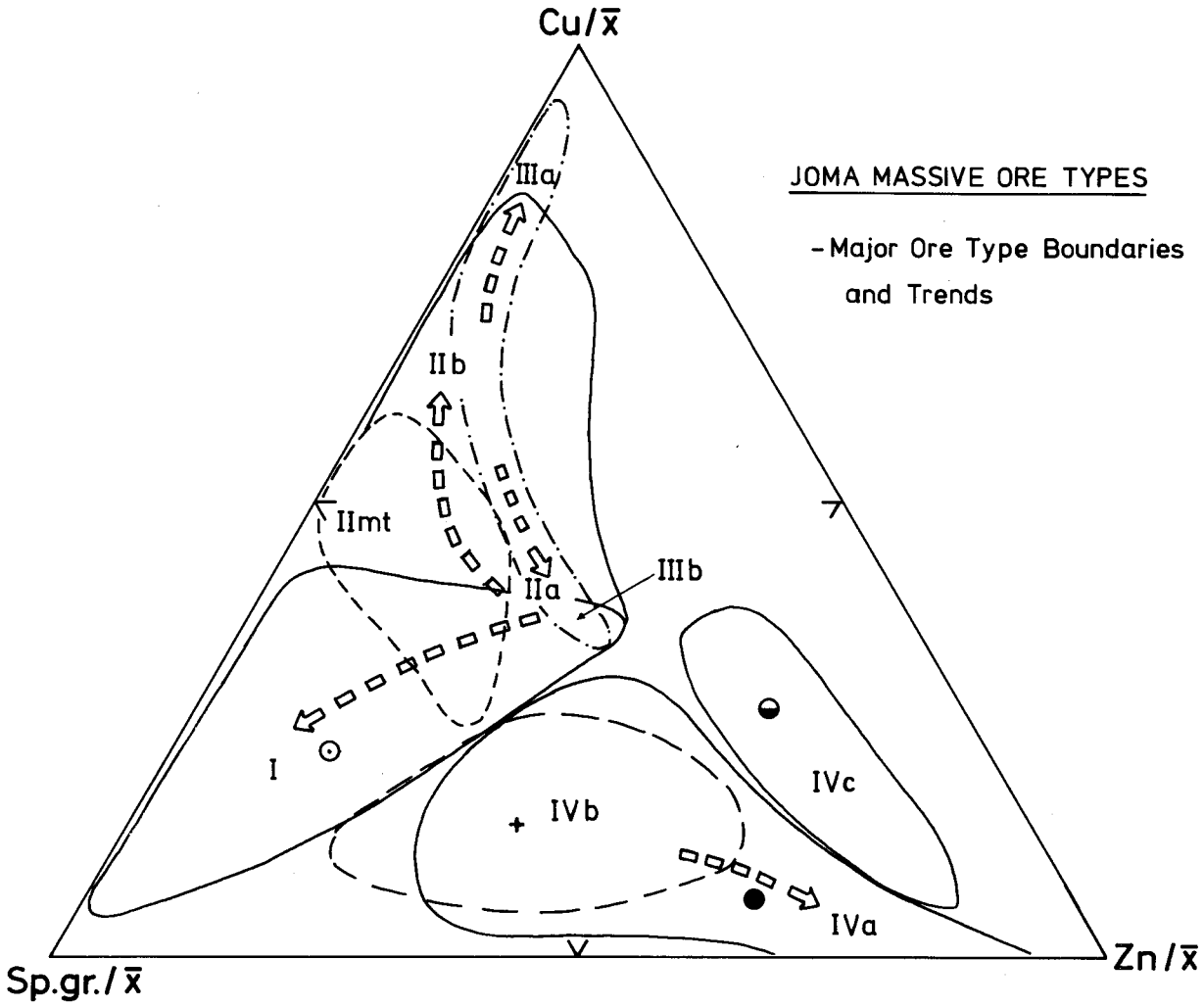

Fig. 5.4. Cu-Zn-Sp.gravity plot showing the boundaries of the major ore types at Joma. Trends between the ore types are shown related to the chronological development of the massive ores as shown in Fig.5.1.

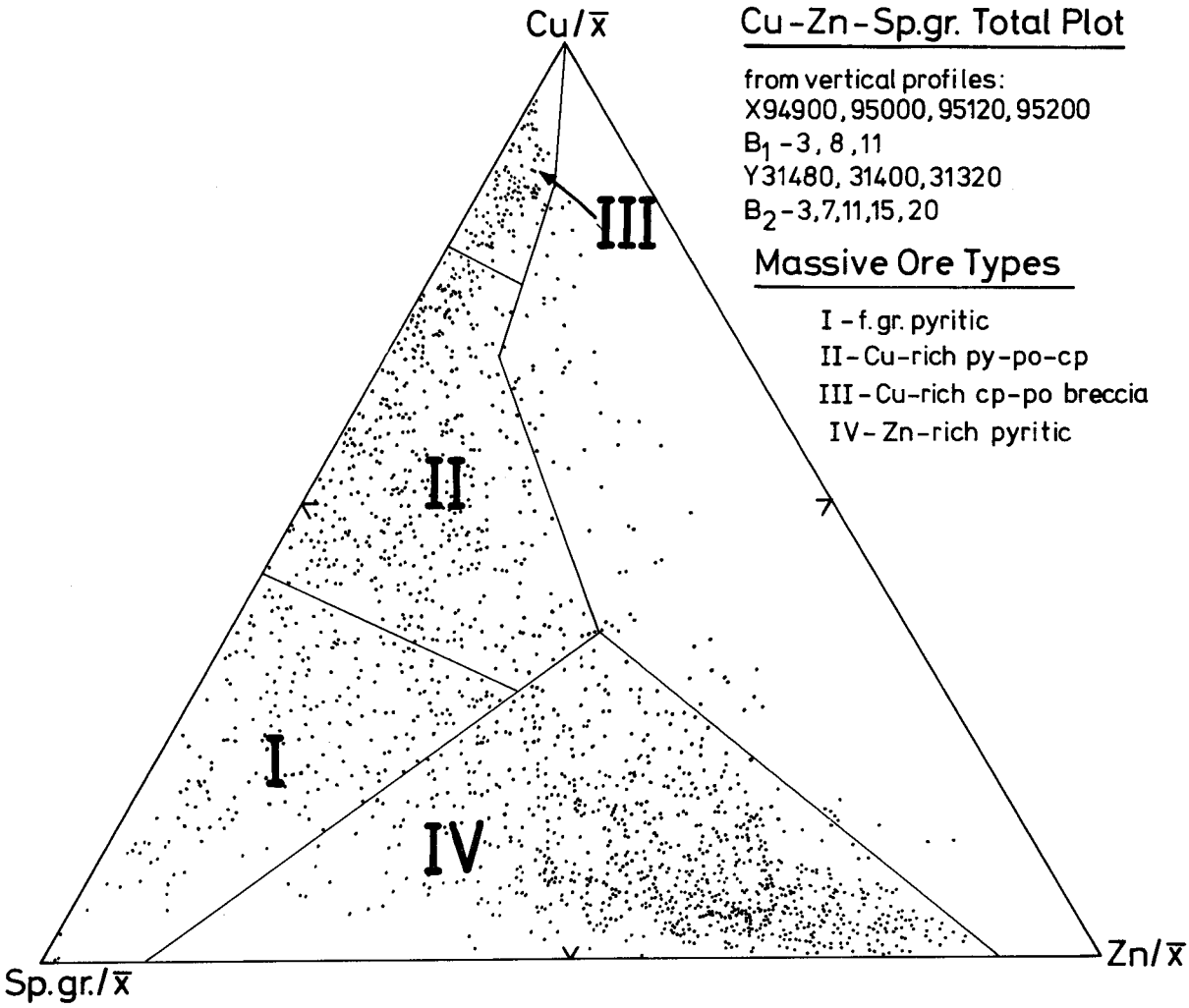

Fig. 5.5. Cu-Zn-Sp.gravity plot showing boundaries of the 4 major ore types that has been used in the computer program to separate the major ore types on the vertical geological profiles.

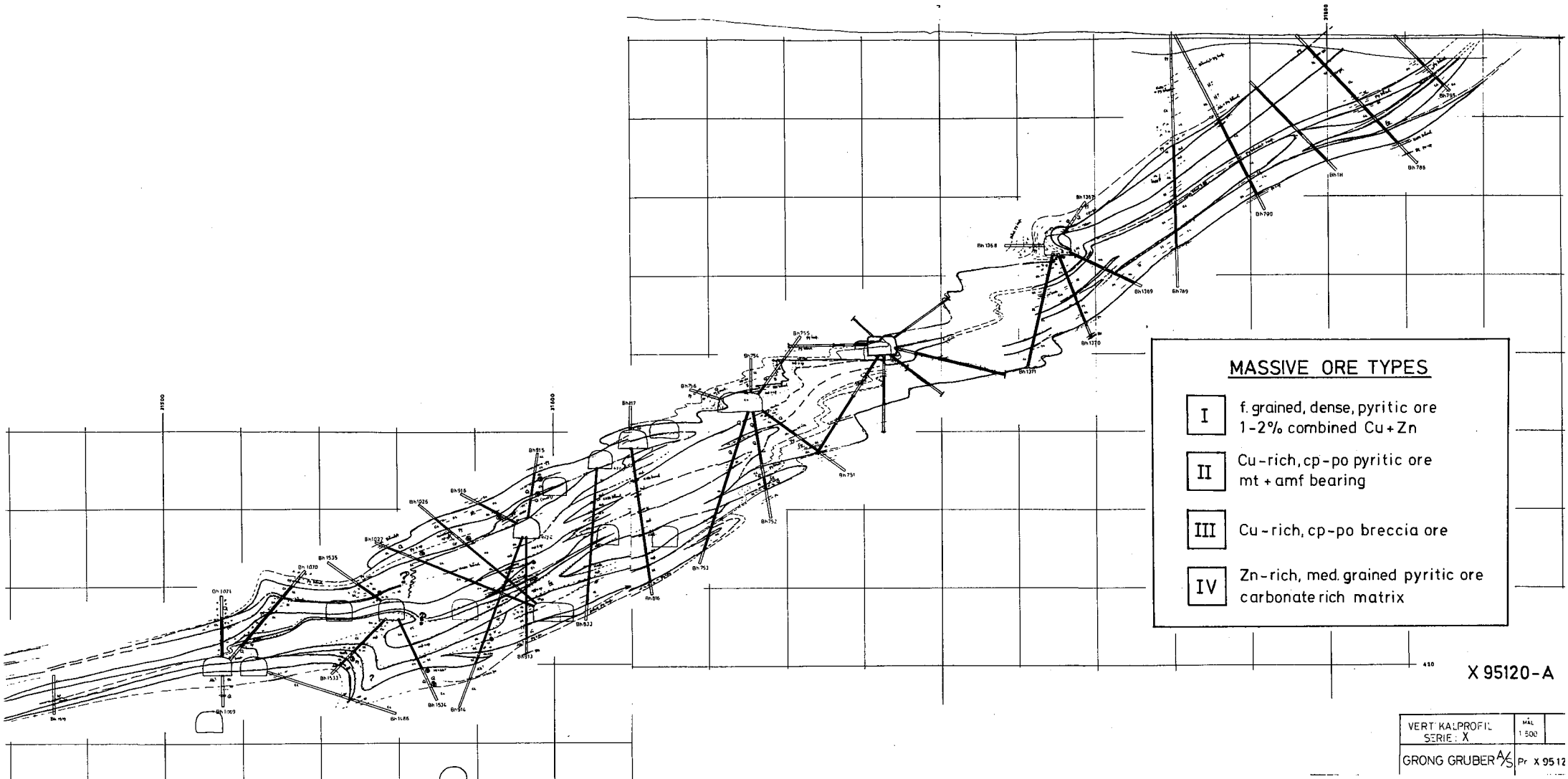

Fig. 5.6. Profile X95120 showing distribution of the 4 major ore types as taken from drill core logs. Profile X95120 has been used as a control case for the development of a computer program to separate the ore types.

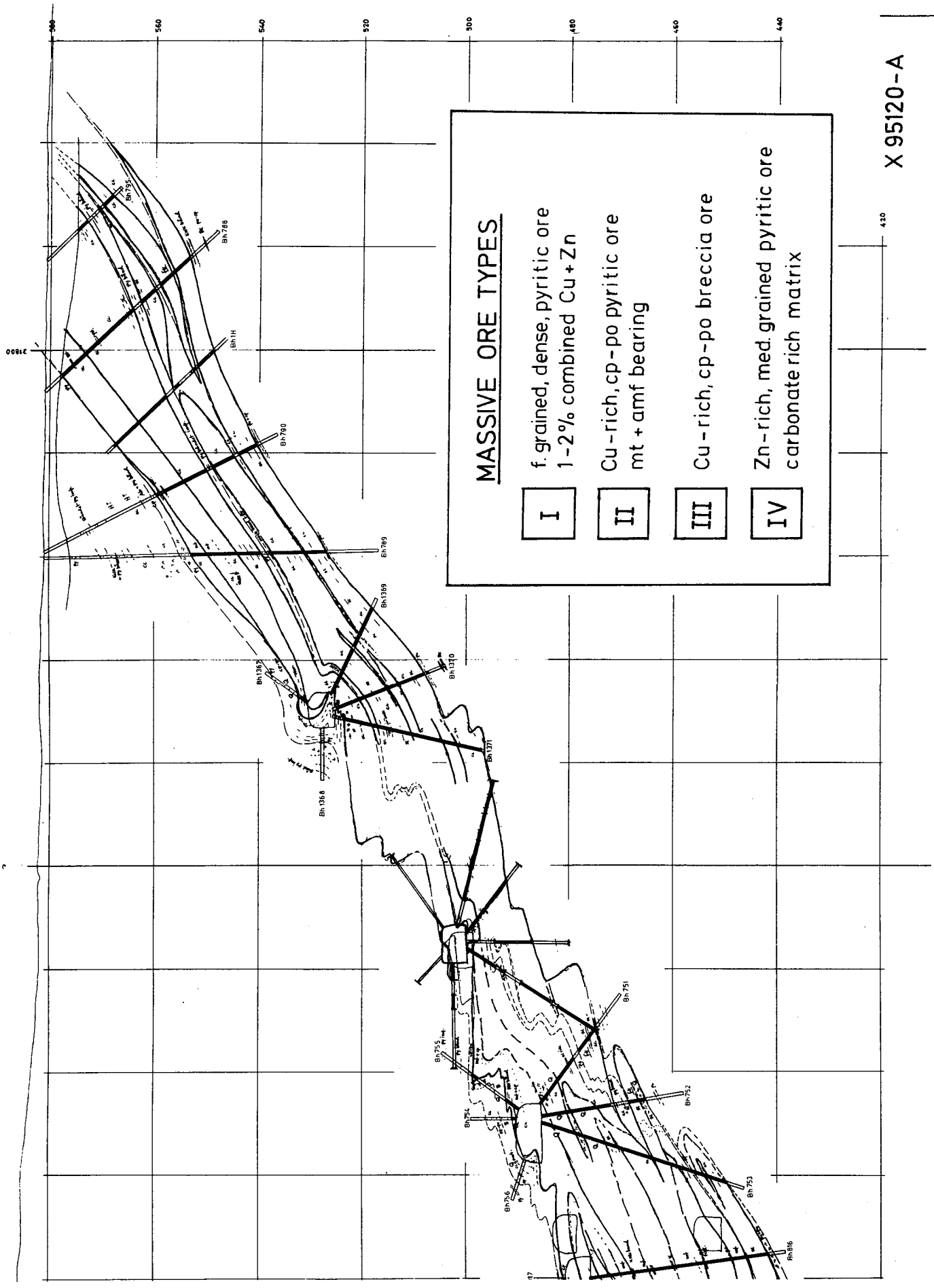

Fig. 5.6. Profile X95120 showing distribution of the 4 major ore types as taken from drill core logs. Profile X95120 has been used as a control case for the development of a computer program to separate the ore types.

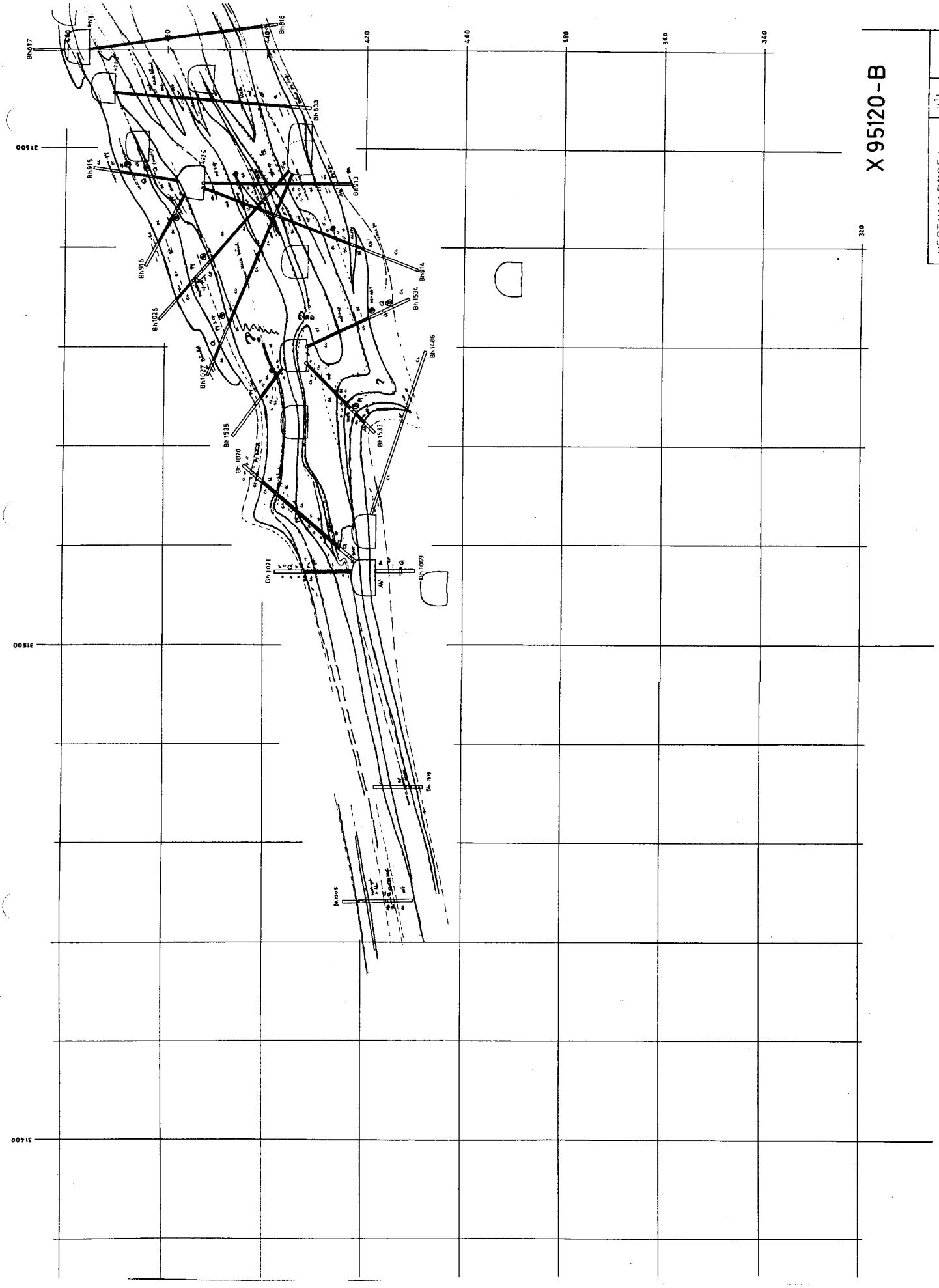

Fig. 5.6. Profile X95120 showing distribution of the 4 major ore types as taken from drill core logs. Profile X95120 has been used as a control case for the development of a computer program to separate the ore types.

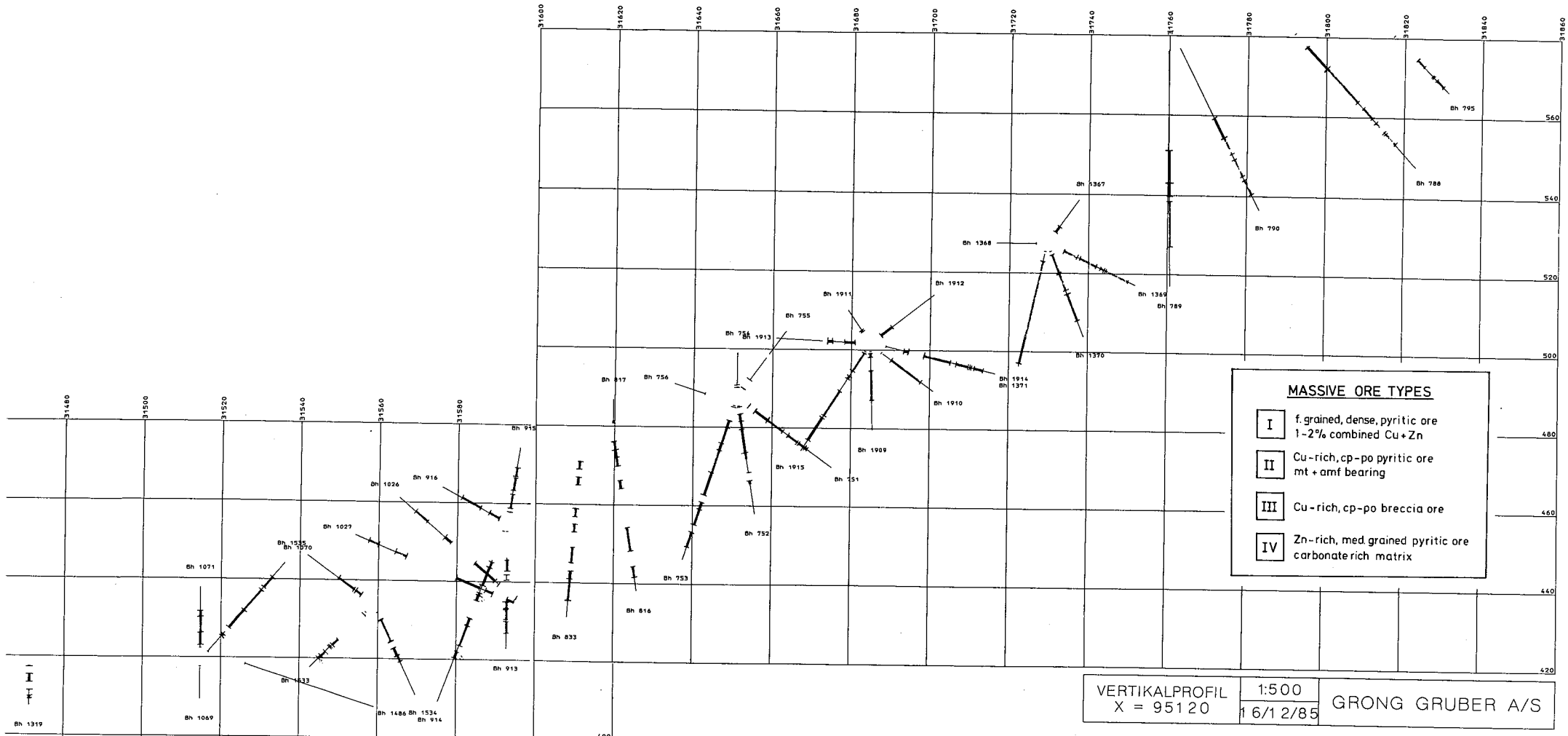

Fig. 5.7. Reduction of vertical profile X95120 showing the major ore types onto the drill holes, as produced by the computer program using the ore boundaries shown in Fig. 5.5.

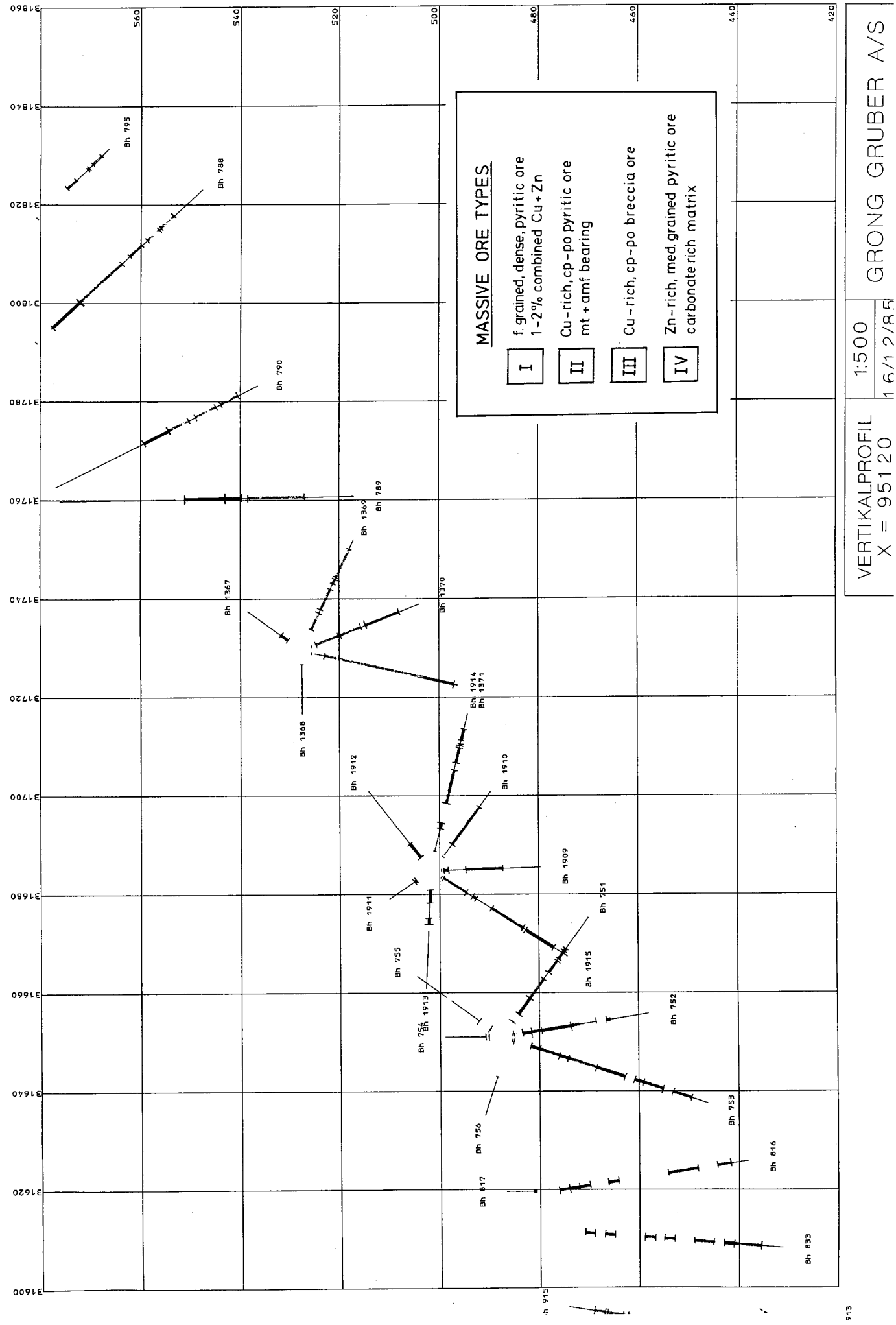

Fig. 5.7. Reduction of vertical profile X95120 showing the major ore types onto the drill holes, as produced by the computer program using the ore boundaries shown in Fig. 5.5.

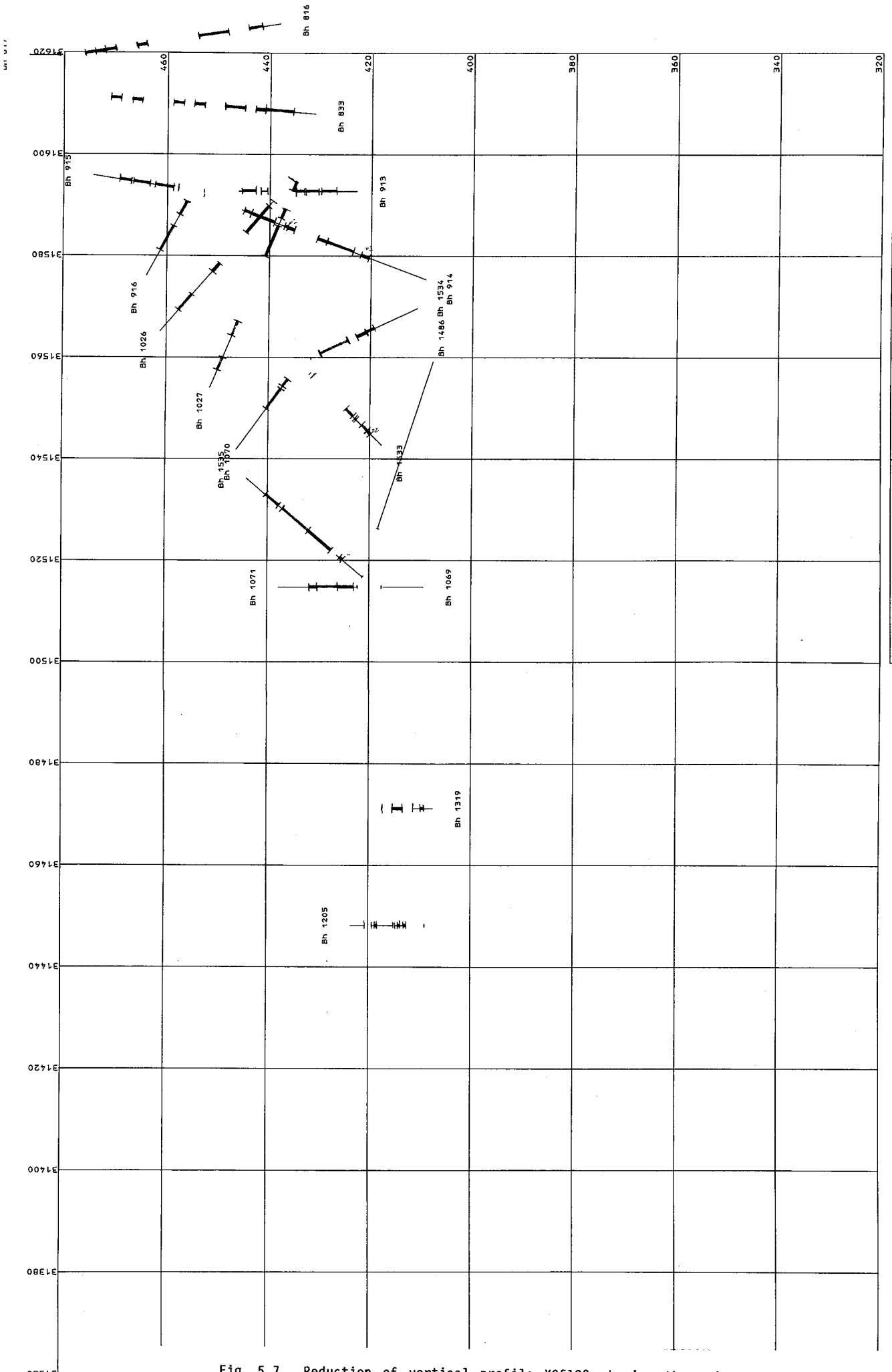

Fig. 5.7. Reduction of vertical profile X95120 showing the major ore types onto the drill holes, as produced by the computer program using the ore boundaries shown in Fig. 5.5.

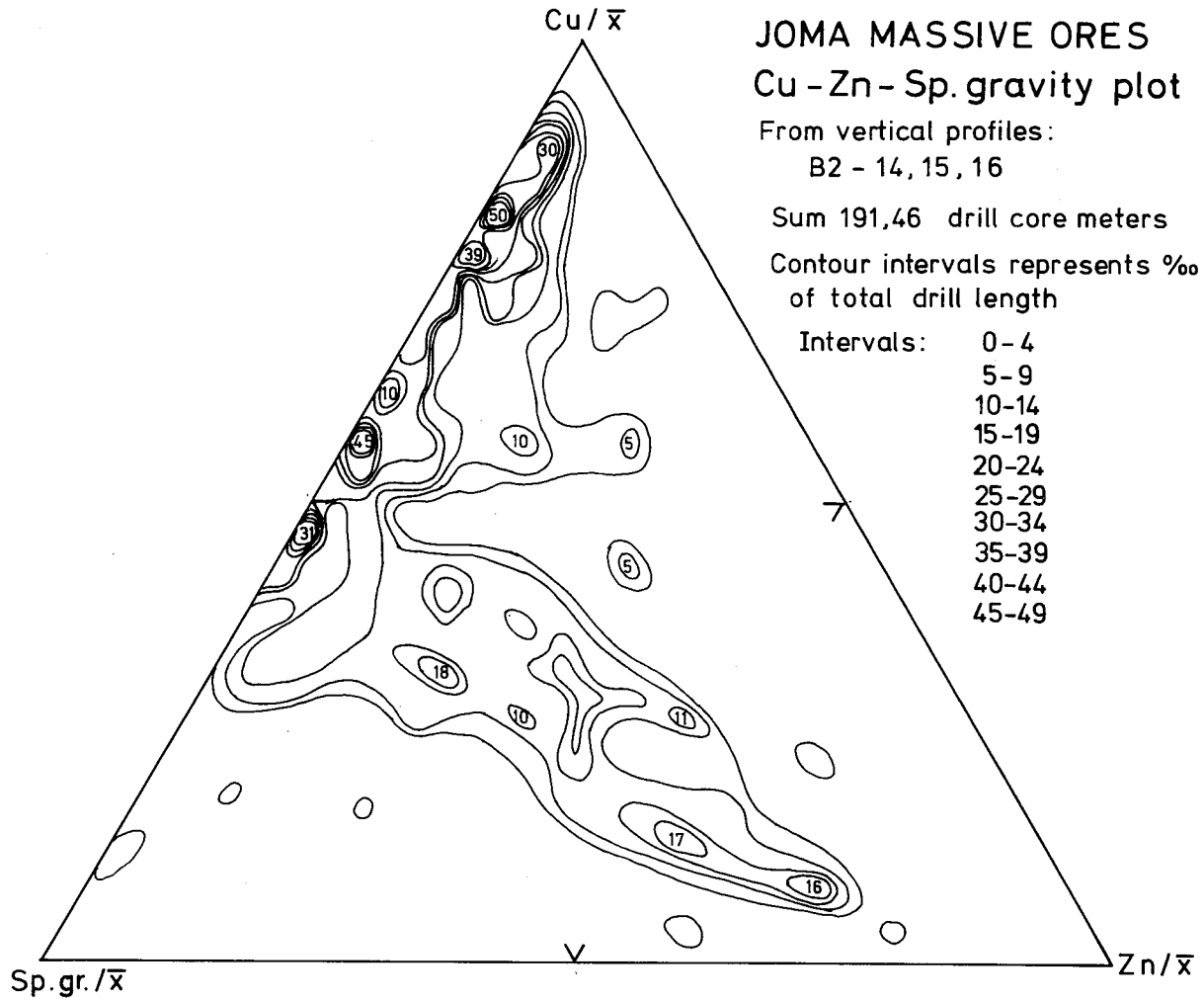

Fig. 5.8. Cu-Zn-Sp.gr. plot of drill hole data from vertical profile B_2-14, 15, 16 giving o/oo of the total sum of 191.46 drill meters of ore within these profiles. Note the dominant Cu-rich ores in these profiles which are from the extreme west side of ore body.

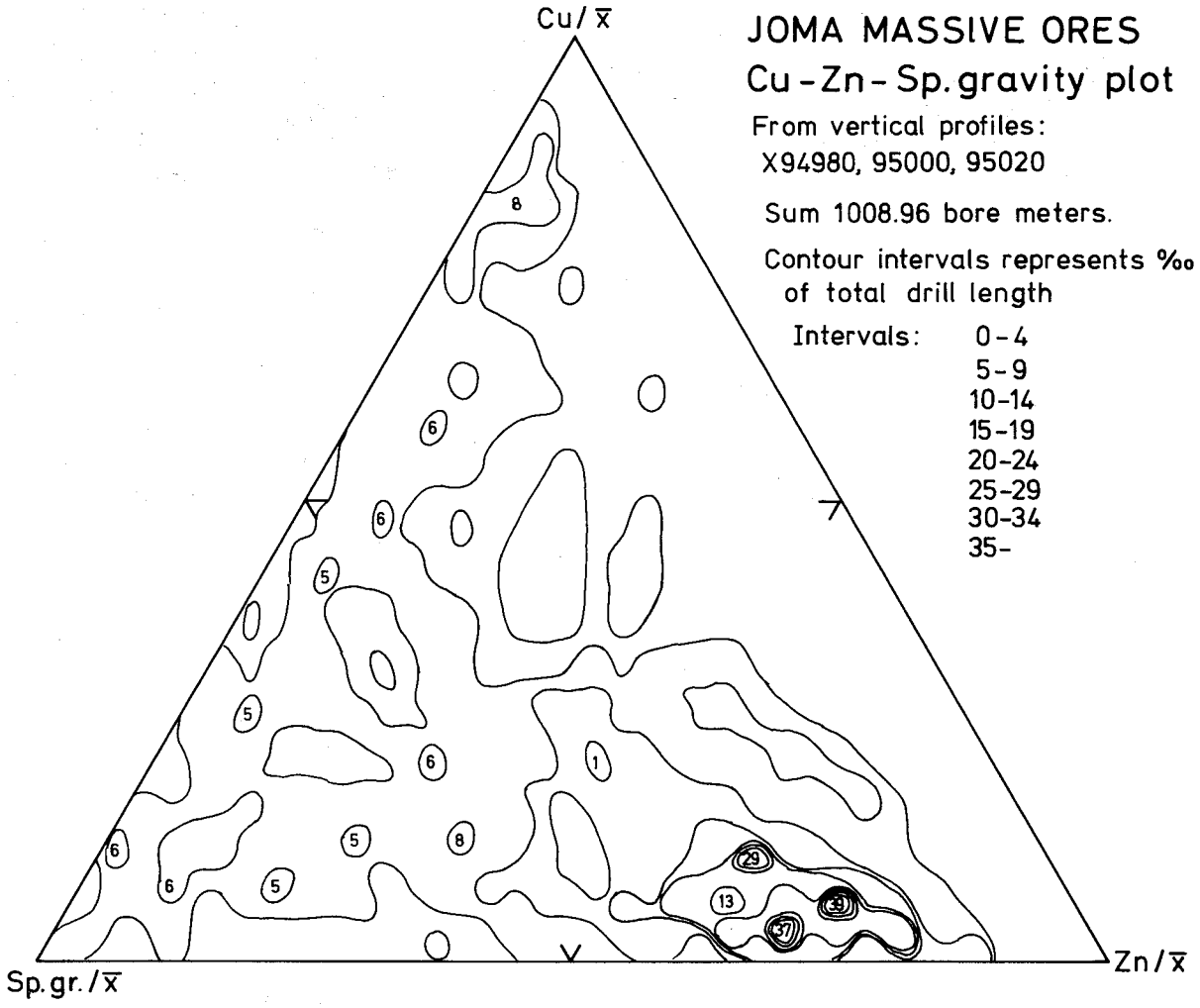

Fig. 5.9. Cu-Zn-Sp.gr. plot of drill hole data for vertical profile X=94980, 95000 and 95020, giving o/oo of a total of 1008.96 meters of ore drilled within these three profiles. Note the dominant Zn-rich and more Sp.gr.-rich ore types in these three profiles which are from the east side of Joma ore body.

SECTION 6: SUMMARY AND CONCLUSIONS

6.1 SUMMARY OF THE JOMA CU-ZN MASSIVE SULPHIDE DEPOSIT

The Joma stratiform massive sulphide deposit lies within the Røyrvik Group (Leipikvattnet Nappe), and outcrops some 2 km south-east of the mine entrance and offices of Grong Gruber A/S at Ornes. From its surface exposure in the river flowing into the eastern end of Huddingsvatnet, the double arc-formed, dish-shaped orebody has a 1200-1500 m horizontal lateral extension and dips steeply to the SW-W, levelling off to nearly horizontal at c. 200 m depth, .

Structure.

The Joma deposit is hosted by the middle of three distinct greenstone units within the Røyrvik Group, contained in the late (D_3) Joma Synform, trending SW-NE from Limingen to Leipikvattnet in Sweden. Structural studies, both on a regional scale and within the mine, have shown that the host rock lithologies to the Joma ore horizon lie in an inverted position. Two major phases of deformation control the geometry. The earlier phase, related to the D_2 structures, is represented by isoclinal folds trending roughly NNW-SSE and plunging gently to the NW. These deform wallrocks as well as ore layers and mesoscale F_2 folds are probably parasitic to much larger isoclinal fold structures, responsible together with associated thrusts for repetitions of the greenstone horizons found within the late D_3 Joma synform (see Photo's 30+31+33). The most spectacular deformation of the orebody occurred during D_3, leading to open, asymmetrical crenulation folds (F_3) found at right angles to F_2 and with fold axes plunging moderately to the SW (see Photo 43). Late D_4 folds, showing opposite vergence to D_3, and having flat-lying axial surfaces are only slightly developed at Joma.

Lithology.

The greenstones show a variety of textures and structures. Although these rocks have undergone a strong pervassive metamorphic recrystallisation and penetrative foliation, remnants of pillows, pillow-breccias and hyaloclastites occur, indicating deposition in a submarine environment. A detailed investigation of the three greenstone belts indicates that the middle and outer greenstones (Joma and Orklumpen, respectively) are similar in their distribution of massive, pillowed lava and volcaniclastic sequences; they are interpreted as belonging to the same volcanite complex, repeated by isoclinal folding and thrusting. Thus, the Joma ore horizon lies in an overturned limb of a major F_2 isoclinal fold structure and is cut out at depth by a major thrust which separates these greenstones.

The Joma deposit itself occurs within the middle greenstone, at the interface between two locally major volcanite units. The older, pre-ore volcanites, in the structural hangingwall, comprise a sequence of massive flows and high level intrusions (?) (Group A), enveloped in and overlain by a pillow lava and pillow breccia sequence (Group B). The pre-ore volcanites (massive and pillows) lie stratigraphically on top of a thick sequence of layered quartz rich and phyllitic rocks ('ribbon cherts') and dark graphitic phyllites. The younger volcanites, in the structural footwall, consist of a thinner pillow lava and pillow breccia unit (Group C_1) which grades, both stratigraphically upwards and laterally into a sequence of well-layered to laminated volcaniclastic rocks (Group C_2). The layered pyroclastic rocks contain minor laminae of grey and dark graphitic phyllites and carbonates, grading upwards into grey phyllites, quartz rich phyllites and dark graphitic phyllites ?

The Røyrvik greenstones show a metabasaltic (spilitic) composition with mixed MORB-WPB affinities. A significent difference between the pre and post-ore lavas is, however, apparent. For example, the post-ore lavas show distinctly lower contents of TiO_2 and Zr at similar Cr contents relative to the pre-ore lavas. Thus, the former shows a N-MORB and the latter an

E-MORB or WPB affinity. The Røyrvik Group metavolcanites appear to have formed in an oceanic, near continent, probably off-axis setting.

Pre ore metavolcanites and their alteration.

The pre-ore metavolcanites in the vicinity of the ore horizon are uniform, moderate to pale green coloured and schistose. They have, however, undergone extensive chemical and mineralogical changes due to the intense, pervasive, hydrothermal alteration, manifested in the feeder zone forming the root to the massive sulphide horizon. Original volcanic textures and structures have been partially or completely destroyed during extensive albitization, chloritization, sericitization and sulphidization. Chemical changes in the feeder-zone involve a dramatic decrease in both Ca, Mg and to a lesser extent K, and a considerable increase in Fe, Na, S and minor Al. Mg decreases considerably in the intensely altered lavas, whereas it increases in the weakly altered lavas adjacent to the 'feeder zone' and is notably enriched in the rocks directly beneath the massive sulphide horizon, lateral to the main fumarolic vent.

A detailed study of the mineralogical and chemical variations in the host rocks at Joma has distinguished six lithologies within the pre-ore volcanites beneath the main ore horizon. They show zonal patterns in both their mineral and elemental distributions which is typical of intense hydrothermal alteration patterns found within 'feeder zones' forming the rootzone to volcanogenic massive sulphide deposits such as Joma. The pre-ore host rock lithologies are, in order of increasing degree of alteration, B_1 to B_6. In addition, the individual units may be divided into sub-units (e.g. B_{6a-e}).

B_1 - moderate-green, undifferentiated pillowed greenstones with chl, act, ab, ep, cc, sp and po disseminations,

B_2 - pale, po bearing, albite+sericite schists

B_3- moderate grey-green, po bearing albite+Fe-chlorite schists,

B_4 - pale, pyrite bearing albite, sericite, chlorite and actinolite schists

B_5 - pale, pyrite bearing, albite rich rock

B_6 - dark chlorite schists.

The altered rocks deepest within the feeder-zone (B_1) show a slight Fe+Na enrichment associated with increases in Fe-chlorite, albite, epidote and pyrrhotite disseminations. These rocks grade upward immediately beneath the main ore zone, into a wider zone, of pale, pyrite veined and disseminated albite+white mica + chlorite+actinolite rich schists (B_4) enriched in Na, K and minor Zn. These grade laterally beneath the orebody into pyrite bearing, Mg-rich chlorite schists (B_{6e}). The stratigraphic upper parts of the stringer zone, above the pyrrhotite bearing pale schists (B_2), and slightly distal to the central parts of the fumarolic vent, terminates in a Cu bearing dark Fe-rich chlorite schist sequence (B_{6a-d}) which forms the lower stratigraphic levels to the Cu-rich massive pyrite-pyrrhotite ores. Thinnly laminated and layered, pyrite bearing albite rich rocks (B_5) form integral parts of the dark chlorite schist in parts of the chlorite schist bottom stratigraphy, slightly distal to the main fumarolic vent.

The layered, pyrite bearing, pale albitites and the chalcopyrite bearing, dark chlorite schists are interpreted as being chemical sediments that formed from fluctuations in dense fumarolic fluids, varying from Fe+Cu rich and S deficient to Na+Fe+S+Zn rich, that vented out onto the seafloor and flowed down slope, becoming deposited as silicate and sulphide concentrations within basinal traps slightly lateral to the main fumarolic vent. Parts of the massive, Fe-rich chlorite schists are in situ, hydrothermally altered original hyaloclastite matrix material associated pillow breccias and pillow lavas. Distal to the main hydrothermal vent and stratigraphically upwards in the sulphide-silicate pile, the chlorite schist becomes more Mg enriched and distinctly pyrite- and carbonate bearing as disseminations and individual layers. The Mg rich chlorite schists are enriched in Zn contrasting to the Cu enriched Fe-chlorite schist stratigraphically below.

The mineral and elemental zonation patterns within the 'feeder zone' at Joma show remarkable similarities to mineral variations described from the sub-seafloor hydrothermal convective cells presently forming within the mid-oceanic spreading ridge sysmtems (Mottl, 1983).

The mineral and elemental zonation patterns within the 'feeder zone' and the Cu-Zn zonations within the massive ore zones at Joma are typical for volcanogenic exhalative-sedimentary massive sulphides deposited on the seafloor at or near fumarolic vents fed by highly reacted, SiO_2, H_2S and metal enriched hydrothermal fluids, products from the upflow part of a sub-seafloor hydrothermal convective cell.

Compared to the host metabasalts, both the albitite and chlorite schists show significant chemical variations. Mg has apparently been depleted from the albitite while the chlorite schist shows a significant enrichment in this element. Na is enriched in the albitite and depleted in the chlorite schists; Ca is depleted and Fe is enriched in both these units. These significant chemical variation can be interpreted as a hydrothermal alteration phenomena for the deposition of the albitite and chlorite schists, in part, as Fe-Mg-Cu-rich syn-depositional layers of tuffaceous bottom mud (?). The Ca leached from the lavas below could have been held in solution and later deposited as extensive, concordant limestone layers within the Zn-rich pyritic ore in the upper parts of the sulphide stratigraphy.

The Joma ores.

The following ore minerals have been recognized in Joma. Major minerals; pyrite, pyrrhotite, chalcopyrite, sphalerite and magnetite. Minor and trace minerals; cubanite, tetrahedrite, mackinawite, vallerite, galena, arsenopyrite, cobaltite, ilmenite, rutile native Au, electrum, amalgam, argentite and pyrargyrite.

The ores at Joma have been subdivided into 4 main massive and 2 disseminated ore types based on their textural and chemical features and their relative positions within the original basin of sulphide deposition.

The four major massive ore facies are (types I to IV)), from top to bottom (4 to 1):

4) Type IV: Medium to coarse grained pyritic facies, with carbonate and chlorite as both matrix and individual layers; rich in Zn and generally devoid of Cu.

3) Type I: Fine grained to flinty pyritic facies; minor to moderate contents of both Cu+Zn.

2) Type II: Fine to medium grained, Cu-rich, pyrite-pyrrhotite-chalcopyrite ore facies; with dissemination layers and thin bands of amphibole needles, chlorite schist and magnetite ore and dark, magnetite- and chlorite rich recrystallized chert layers and lenses.

1) Type III: Cu-rich, chalcopyrite-pyrrhotite breccia ore, containing fragments of chlorite schist, limestone, magnetite ore and fine grained pyrite ore.

The two main disseminated ore-types are 1) dark, Fe-rich chlorite schists containing disseminations and layers rich in chalcopyrite and pyrrhotite, 2) pale, albite-sericite schists, rich in pyrite-quartz-calcite veins and disseminations, often rich in Zn and minor Pb.

A study of the Cu-Zn-sp.gravity analyses using the total data base for the drill core analyses from the massive ore body has been shown to be valuable in distinguishing the above mentioned ore types. When these analyses are plotted in a triangular diagram as $\frac{\text{Cu sample}}{\text{Cu average}}$, $\frac{\text{Zn sample}}{\text{Zn average}}$, and $\frac{\text{sp.gravity sample}}{\text{sp.gravity average}}$, the data points of the different ore types define distinct areas or clusters. The triangular plots show that the ore types form both distinct and gradational facies within the massive ores. The ore types are plotted onto the vertical geological profiles with help of a computer program using the total data base for the Joma ores. This shows that the ore facies distribution, along with the Cu and Zn zonation, conforms to distinct areas within the Joma ore horizon.

The Cu-rich ore facies (ore type II and III) are confined to the western and southern parts of the ore zone and the thicker Zn bearing pyritic ore facies (type IV) to the northeast and eastern parts. The fine grained, flinty, pyritic ore facies (type I) appears to roughly separate the two main ore facies, the Cu- and the Zn-rich ores.

Durchbewegt ore.

The chalcopyrite-pyrrhotite breccia ore is a characteristic and interesting ore type at Joma. It often occurs as distinct layers following minor thrusts (shear zones) that cut the massive Cu-rich ores and adjacent host rocks. Numerous angular to sub rounded fragments of chlorite schist, white limestone and amphibole schist, magnetite, and fine grained pyritic ores attest to their derivation from the adjacent host rock and ore lithologies. Remnants of isoclinal fold hinges of an early compositional layering within the fragments and rounded hydrothermal glassy quartz fragments attest to an early D_1-D_2 tectonic derivation. The fragments become notably smaller and more rounded the farther they occur along the thrust away from their source rock. This breccia ore may be classified as a 'durchbewegung' ore type and these have been found stretched out along the thrust planes for several hundred meters from their source rocks. The chalcopyrite-pyrrhotite breccia ore can locally form distinct layers containing impressive thicknesses (>2 m) rich in chalcopyrite and other minor Cu bearing minerals, with ore grades up to 20 % Cu.

Concerning the genesis of this controversial chalcopyrite-pyrrhotite breccia ore, Olsen (1980) suggested the presence of a primary FeS phase associated with the Cu-rich layered pyrite-pyrrhotite-chalcopyrite ores which originally was or has since recrystallized to pyrrhotite. The compitency contrasts between the silicate- and the sulphide-layering and the presence of large quantities of both chalcopyrite and pyrrhotite in these layers has probably been the governing factor in the formation of these tectonic breccia ores. Pyrrhotite and chalcopyrite, and for that matter also sphalerite, are minerals which, due to their internal structures (cleavage planes along which gliding can

occur), are readily mobilized and redistributed by tectonic shearing movements associated with the 'durchbewegung' phenomena.

Chalcopyrite, pyrrhotite, quartz-calcite and to lesser degrees sphalerite, chlorite, albitite and epidote are also typical mobilized (mobilizates?) along the D_3 'piercement' structures and late cross-cutting fracture fillings, adjacent to the Cu-rich massive sulphide ores at Joma.

A palinspastic reconstruction based on the distribution of ore types and mineralization in relation to host rock lithologies and hydrothermal alteration, including the recognition of a 'feeder zone', has led to the establishment of the following succession surrounding the ore body:

Top 1) Pale, epidote- and calcite bearing post-ore greenstones and minor magnetite bearing, dark recrystallized chert and limestone.

2) Massive, generally pyritic ore with interlayers and lenses of limestone and chlorite schist. The following ore types can be recognized, probably in a vertical sequence:
   a) medium- to coarse grained pyritic ore, with carbonate and chlorite as both matrix and individual layers; rich in Zn and generally devoid of Cu (Type IV),
   b) fine grained to flinty pyritic ore; minor to moderate contents of both Cu and Zn (Type I),
   c) fine to medium grained, Cu-rich pyrite-pyrrhotite chalcopyrite ore; with thin layers and thicker bands of disseminated amphibole needles, chlorite schists, magnetite ore and magnetite, chlorite bearing dark recrystallized cherts (Type II).

3) Cu-rich, pyrrhotite-chalcopyrite breccia ore containing fragments of chlorite schist, white limestone-marble, magnetite ore and fine grained pyritic ore (Type III).

4) Dark, Fe-chlorite schists, rich in disseminations and layers of chalcopyrite-pyrrhotite.

5) Pale, albitites and albite-sericite-chlorite-actinolite schists, rich in pyrite-quartz-calcite veins and disseminations, often rich in Zn and minor contents of Pb; grades laterally beneath massive ore horizon into pale, Mg-rich chlorite schists.

Base 6) Moderate green, chloritic greenstones with epidote knots and pyrrhotite disseminations; minor pyrite veining.

Considerable evidence has accumulated to indicate that all the lithologies described above, except for some of the chalcopyrite-pyrrhotite breccia ores, formed prior to D_1-D_2 deformations and are, therefore, probably syn-depositional in origin. It is concluded that the Joma stratiform massive sulphide deposit formed by a volcanogenic exhalative-sedimentary process, the sequence of events being:

1) Formation of a feeder zone with associated hydrothermal alteration phenomena, including depletion of Mg and Ca and formation of pyrite bearing albitites and pale albite-sericite-chlorite-actinolite schists. The feeder zone forms the roots to the massive ores, the channels through which the metal bearing hydrothermal fluids have ascended on their way to the seafloor.
2) Deposition of a Fe-Mg-Cu- and Fe-Na-K-S-rich chemical sediment (tuffaceous mud?) immediately overlying and adjacent to the top of the feeder zone.
3) Deposition of massive Fe-sulphides at the sea water-pillow lava interface immediately above and adjacent to the fumarolic vent and underlying feeder zone. The sulphide ores grade from an early Cu-rich layer, represented by the present layered Cu-rich sulphide-, silicate- and magnetite rich ore, into a more Zn-rich and Cu-deficient, pyritic top layer. The occurrence of limestone and chlorite schist layers within the upper levels of the massive pyritic ore shows that the deposition of sulphides was not continuous.
4) Relative position and bulk chemistries of these sulphide-silicate layers were maintained during the subsequent deformation and metamorphism except for the tectonic origin of the chalcopyrite-pyrrhotite breccia ores and minor chalcopyrite-pyrrhotite concentrations in later veins and fracture filled mobilizations.

6.2. GENETIC MODEL FOR THE JOMA ORE BODY

Regional geological and structural interpretations have led to the following volcanostratigraphy for the Joma area (see Fig. 2.5, section 2). This is simplified as follows (not to scale):

P	phyllites
C_2	layered volcaniclastics
C_1	post-ore pillowed sequence
———	Joma massive sulphide horizon
B_2 - B_6	hydrothermally altered host rocks
B_1	pre-ore pillowed sequence
A	massive volcanite, ferrobasalts
QP	ribbon cherts
GP	graphitic phyllites

The distribution of the volcanite types; massive, pillow lava, pillow breccias and laminated volcaniclastics , suggests that the middle and outer greenstones (Joma and Orklumpen, respectively) have originally formed as the same volcanic unit that has been disected and the three greenstones separated from each other during later D_2 thrusting. Structural studies show that the individual greenstones lie within a large overturned F_2 structure that is cut off at its base by a major D_2 thrust that separates the two greenstones.

In this structural and stratigraphic model the massive ferrobasalts are confined to the middle greenstone, at depth beneath the Joma ore horizon level and it was deposited onto a phyllite, layered chert-phyllite and graphitic phyllite base. These rocks have been markedly altered at this level and the phyllites have become K_2O-rich, white mica porphyroblastic schists. The layered cherts have lost their graphite content which appears to be remobilized and deposited lateral to the hydrothermal alteration zone that cuts through these rocks at this depth in the stratigraphy.

The hydrothermal alteration zone, at depth, beneath the Joma orebody is typified by pyrrhotite disseminated, Fe-chlorite and albite rich rocks. Similar chlorite and albite rich rocks occur

in the rusty zones along the western margin of the Orklumpen greenstone, near the thick layered chert and phyllites. These are interpreted as forming the upper parts of a hydrothermal alteration system.

The thin mineralized horizons found higher up (to east) in the volcanostratigraphy on Orklumpen are rich in chert, graphite and phyllite and disseminated sulphides (po, py and trace sl). These are interpreted as distal exhalites. The thicker sequences of pillowed volcanites to the east are typical of the distal greenstones (high in both Ti+Cr) and are interpreted as being younger than the layered exhalite mineralizations. The volcanite sequence on Orklumpen is thus, also interpreted as lying in an inverted position as is the case for the middle greenstone complex at Joma.

Figs. 1.2 and 2.1 show that the middle and outer greenstones are thickest within the central parts of the Joma arc (synform). Some of this increase in thickness may be purely a tectonic repetition due to thrusting. Much appears, however, to be primary and related to the build up of a central volcanic complex, giving some validity to what Oftedahl referred to as the Joma volcano. The greatest thicknesses of both the pre-ore massive ferrobasalts (Group A) and the post-ore pillowed sequence (Group C_1) appears to be centred on the Joma deposit. The thicker sequence of massive ferrobasalts underlying the pre-ore pillowed volcanite sequence and the Joma ore horizon is interpreted as forming the core of a large submarine lava dome, rift basin or the build up of an ocean island.

A palinspastic reconstruction of the Joma ore body (Fig. 6.1) has taken into consideration the recognition of the various ore facies and their vertical and lateral distribution within the ore horizon, i.e. Cu-rich bottom, Zn-rich top and distal facies, their relations to the host rocks and the recognition of a hydrothermal alteration feeder zone in the pre-ore volcanites that forms the root zone to the main ore body. The major elemental zonation patterns, Fe, Na, K and Mg conforms to the typical submarine volcanogenic exhalative-sedimentary model of massive

sulphide deposition, being deposited at or immediately beneath the sea water - seafloor interface by the hot fluids of the upwelling parts of a convective hydrothermal system.

This points to the massive sulphide horizon being deposited at the seafloor (basalt) - sea water interface, due to the drastic changes in the physiochemical conditions under abrupt cooling of the upwelling parts of a major sub seafloor convective hydrothermal system. The hot, metal bearing fluids cooled rapidly on mixing with the sideways inflowing cold sea water, causing rapid cooling of the hot highly reacted fluids, decrease in pH and pressure and causing instant precipitation of the unstable metal sulphides, both within the upper parts of the feeder zone and out upon the seafloor, forming the continuous build up of a massive sulphide horizon. Some of the dense, hot metal laden fluids may have flowed down slope from the fumarolic vents, being deposited in seafloor depressions as lateral parts of the main ore horizon or as isolated distal deposits, such as Borvasselv (?). The heating of the sideways influx of cold sea water causes the precipitation of Mg-rich minerals lateral to the main hydrothermal vent and feeder zone below.

The massive ferrobasalts, that occur at depth, may have been the heat source needed to drive the convective hydrothermal system. The ferrobasalts may also have been the source rock for the Fe, Cu and Zn needed to form the Joma deposit, the metals being leached from the ferrobasalt by the upwelling, hot acid, highly evolved hydrothermal fluids.

6.3. CORRELATION TO OUTSIDE AREAS

Throughout the Røyrvik and Joma area, there is an intimate relationship shown between the three rock types, greenstones, layered chert-phyllites (ribbon chert) and graphitic phyllites (see Fig. 1.2). This relationship should help in following the host rocks of the Joma deposit and its tectonic setting within the Røyrvik Group throughout the Leipikvattnet Nappe (see Fig. 1.1). To the south of Joma, the greenstone belt thins and plunges

beneath the overlying Gjersvik Nappe to the east of Ingulsvattnet (see 1:50,000 map Tunnsjøen, NGU). To the northwest of Joma and Røyrvik, the belt is composed of variously thickened and thinned, tectonic slices of greenstone, ribbon chert and graphitic phyllites. Further north, along the west side of the Børgefjell window, the Røyrvik Group greenstones appear to thicken.

The Røyrvik Group has earlier been correlated with the Remdalen Group in Sweden. The Remdalen Group consists of the same rock types, interlayered greenschists, graphitic phyllites and layered quartz rich phyllites. The Remdalen volcanites also show a WPB trace element affinity such as the Røyrvik greenstones. There are some small Cu-Zn bearing massive sulphide mineralizations associated with the Remdalen Greenschists in Sweden, north of Stekenjokk.

It is tantalizing to correlate the Røyrvik Group with the low grade metamorphic (western) part of the Gula Group in the central Trondheims District, which also contain similar rock types in close association; graphitic phyllites, layered quartzite-phyllite, greenstones and minor serpentinites. A serpentinite body does occur with the Joma greenstone. The Gula Group greenstones also show a similar WPB trace element chemistry and several sizable Cu-Zn massive sulphide deposits (Røstvangen-Rødal) occur along this greenstone-amphibole belt associated with noticable thickenings in the greenstone horizons.

The Tverrfjellet Cu-Zn massive sulphide deposit at Hjerkinn also occur with a similar greenstone-amphibolite belt associated graphitic phyllites and minor quartz rich phyllites. Ferrobasalts have also been recognized at Tverrfjellet.

6.4. SUGGESTIONS FOR FURTHER WORK

At the termination of the Joma project, several problems have remainded unsolved or have cropped up during the life of the project. These are listed below but not in any specific order of importance:

1) Completion of surface drill hole sampling for whole rock silicate analyses.

During the description and sampling program for the 15 surface drill holes in 1985, some of the drill core nearest the orebody within the distal parts of the ore horizon was missing, (e.g. D39-230 to 250 m). These represent the massive and disseminated ore zones that were taken out for analyses for Cu+Zn at Grong Gruber and the boxes that remained stored within the drill core shed were unavailable for sampling within the life of this project.

In order to get a true picture of the host rock chemistry and alteration phenomena, especially for areas adjacent to the ores - distal to the main Joma orebody, should these drill cores be sampled and analysed in the same manner as previous. The results should be added to those from this report and subjected to the same statistical analyses etc., to give a more complete picture of the hydrothermal alteration process and the distal and proximal alteration zonation patterns within the host rocks.

2) Study of the host rock relationships to the newly discovered ore horizons to the SW of the main Joma orebody.

Several new, apparently isolated ore horizons have been discovered by recent drilling to the WSW of the main Joma ore horizon, in an area that has previously been pointed out as favourable by recent differential electromagnetic measurements (H. Elvebakk, pers. comm., 1985). A detailed study should be made of the host rock types and their relationships to the ore facies there. Whole rock silicate analyses should be included. These isolated massive ore lenses may represent transposed, énechelon, D_2 thrust remnants of the original Joma sulphide horizon, or, they may well represent some smaller, isolated, subsiduary depositional basin formed adjacent to the main basin of Joma ore deposition.

A study of the immediate host rock types, i.e. chlorite schists, albitites etc., and the host rock hydrothermal alteration patterns may solve this problem. Similarities to the host rock patterns of the Borvasselv deposit should be kept in mind, if indeed Borvasselv is a distal mineralization of the main Joma ore horizon.

3) Statistical analysis of whole rock silicate data.

A Factor and Cluster analysis has been performed on 355 samples from the surface drill core sampling program (see Table B-6). There still remains whole rock silicate data from 128 samples, mostly of host rocks and minor distal greenstones (see Tables B-2, B-3, B-4 and B-5) that have not been included in the Factor and Cluster analysis that was run by M. Martinsen, Geologisk Institutt, NTH. These should be included with the data for the 355 samples and run for both Cluster and Factor analyses. The post ore volcanites, Groups C_1 and C_2, should then be taken out of the data matrix and the statistical analyses performed on only the pre-ore host rocks in order to give a better cluster pattern for the hydrothermal alteration trends for these rocks.

4) Statistical analyses on ore type chemical data.

Seventy-two samples of the various ore types at Joma have been analysed for major and trace elements (36 elements, see tables C-1 and C-2). These have, as yet, not been subjected to any statistical analyses and should therefore be run for both Factor and Cluster analysis.

5) Volcanostratigraphy of the Orklumpen greenstone complex.

From the limited amount of greenstone whole rock geochemical analyses and volcanostratigraphical interpretation that has been done on Orklumpen to date, it has been suggestet in this report (section 6.3) that the Orklumpen greenstone like the Joma greenstone, also lies in an inverted position.

The rusty, sulphide bearing zones found on the west side of the Orklumpen greenstone (see Fig. 2.1), adjacent to the layered chert-phyllites, are sulphide disseminated, Fe-chlorite and albite rich rocks that probably represent the upper parts of a hydrothermally altered feeder zone. These rusty zones are similar to those found to the southwest of the Joma open pit, stratigraphically below the Joma ore horizon.

The rusty sulphide zones within the middle of and towards the eastern side of Orklumpen are thin cherty and phyllitic layers rich in graphite and disseminated Fe sulphide (both po+py). These are interpreted as being distal exhalite horizons derived from the fumarolic activity that produced the alteration zones below, to the west. They may also represent some distal mineralization connected to the main Joma episode of sulphide deposition?

The volcanostratigraphy on Orklumpen should be checked, with detailed whole rock silicate analyses in order to separate the pre-ore volcanites (ferrobasalts) from the post-ore (more primitive) and distal greenstone.

6) Study of Distal Greenstones.

As previously mentioned (section 6.3), the Røyrvik Greenstone belt with its closely associated layered cherts and graphitic phyllites extends to the northwest of Røyrvik around the west side of the Børgefjell window. There the greenstones appear to thicken and should be studied for a possible similar volcanostratigraphy to that surrounding Joma. Whole rock silicate analyses should be considered.

6.5 'GUIDES TO ORE' - REGIONAL AND LOCAL EXPLORATION

There are some features specific to the Joma deposit and its surrounding volcano-tectonic environment that can be used in both regional exploration for deposits similar to Joma and for local exploration that can point to directions for new ore discovery in order to increase local ore reserves.

Regional Exploration Guides.

1) There is an intimate relationship between the Joma greenstone, layered chert-phyllite (ribbon chert) and the dark, partly rusty, graphitic phyllites. This relationships can be used on a regional scale to follow the Røyrvik greenstone belt.

2) It has been established that the Joma deposit lies solely within a basic greenstone complex at a location where the greenstone has its thickest dimension. Much of this thickness is thought to

be primary from the build up of a volcanic centre. Exploration should therefore be concentrated in the thickest parts of the Røyrvik greenstone belt.

3) The Joma ore horizon occurs at the interface between two locally major volcanite sequences, the pre-ore, Fe-Ti-rich pillowed lavas and deeper massive ferrobasalts, and the post-ore, more primitive (high Mg+Cr, low Ti) pillowed lavas and overlying laminated volcaniclastics.

4) The pre-ore massive ferrobasalts and the post-ore, more primitive, pillowed volcanites are local features specific to the Joma deposit area (the middle greenstone). These specific volcanite types have, to date, not been found within the Røyrvik Greenstone belt outside the Joma area. The distal greenstones all show a chemistry that appears to be a mixing of these two volcanite series, being both high in Ti and Cr, a feature typical of WPB volcanites.

Local Exploration Guides.

The distribution of the ore facies, the Cu-Zn zonation patterns, both vertical and horizontal within the Joma ore horizon, the original wedge shaped configuration of the ore body and its relation to the characteristic host rock silicates and feeder zone give clues to local prospecting in the Joma mine area.

1) The Cu+Zn zonation patterns in the ore horizon.
The Cu-rich massive ores are roughly confined to the western side of the orebody and the Zn-rich ore to the eastern parts. The Cu-rich ores form the stratigraphic bottom layered of the ore horizon and has its greatest thickness lateral to and down slope from the main feeder-stringer zone. The Zn-rich massive ores form the stratigraphic top layers where it is associated with thicker limestone beds. The more lateral Zn-rich ore facies are thinner massive to semi-massive pyritic ores that carry thin carbonate and chlorite rich layers.

2) There is an intimate relationship between the po+cp bearing, dark, Fe-rich chlorite schists (and minor associated thin pale albite+pyrite rich rocks) and the massive Cu-rich ores, to which they form the stratigraphic footwall. These are interpreted as having formed slightly lateral and down slope from the main fumarolic vent and feeder zone.

3) Chlorite schists, found more distal to the main feeder zone and beneath the thinned massive sulphide horizons are paler in colour, Fe+Mg-rich and pyrite and carbonate bearing. These chlorite schists are enriched in Zn$\pm$Pb and depleted in Cu. They are associated with more distal, thinned massive to semi-massive pyritic horizons and are rich in carbonate and chlorite as matrix and layers. The sulphide ores are also richer in Zn and depleted in Cu compared to the proximal ores.

4) Pale albitite+pyritic rich rocks occur in three different positions within the stratigraphic footwall of the Joma ore horizon.

   a) massive, dense, hard pale albitite, with interconnected pyrite+quartz veining occurs within the upper central parts of the feeder zone.
   b) albitite breccia material occurs as thicker layers slightly lateral to a)
   c) thin laminations to layers of pale albitite+pyrite, interlayered with dark Fe-rich chlorite schists, occurs distal to the main feeder zone along the stratigraphic footwall to the main ore zone, associated with the Cu-rich massive ores.

5) The main host rock zonation pattern within the feeder zone at Joma is also characteristic and will help in pointing to the deeper, central, upper and the lateral parts of the feeder zone.

   a) the lower parts of the feeder zone are typically darker green, homogeneous, rich in Fe-chlorite, albite, epidote and disseminated po.

b) upper parts of feeder zone are typically pyrite+qtz veined, pale albite+sericite rich rocks.

c) the upper, lateral parts of the feeder zone beneath the main ore body is characterized by pale coloured, Mg-rich, chlorite+albite+sericite+actinolite schists rich in interconnected pyrite+quartz+calcite veins. This host rock facies carries more Zn and less Cu than the central parts of the feeder zone.

6.6. SUGGESTIONS TO CHANGES IN RUTINE AT GRONG GRUBER

There are several changes in the dayly rutine of geological work at Joma that should be strengthened. This is not meant as a personal criticism of any one person but as an introduction to various rutines that would benefit Grong Gruber in documenting the details of the geology encountered at Joma.

1) The drill core descriptions (logs), especially for the deep surface holes that penetrate thick sequences of volcanites, should be more detailed and complete. The volcanite structures; pillows, pillow breccia and hyaloclastites, and the textures and grain size should be described in more detail. The colours of the rocks and their mineral contents are important in differentiating between the various host rock types, i.e. the disappearance of epidote, the presence or absence of pyrite versus pyrrhotite disseminations and veins (differentiates between B_2 and B_4 pale schists) and the disappearance of quartz and calcite as free grains and vein material are all important distinguishing features. Calcite occurs generally more lateral to the hydrothermal alteration feeder zone, and quartz is generally concentrated in the upper parts of the feeder zone.

   The quartz-calcite-epidote and minor chlorite rich veins and fracture fillings associated with the D_3 cleavages are almost totally confined to the post-ore, younger (FW), pale greenstones.

2) The term 'Blåkvarts' should be changed to be more specific. The rocks colour and mineral content is important in placing the quartzite (recrystallized chert) within the stratigraphic pile.
   a) pale grey quartzite with po disseminations (pre-ore, lower stratigraphy)
   b) pale grey quartzite with py disseminations (lateral main ore level)
   c) dark to black quartzite with mt disseminations (post-ore stratigraphic level - within Group C_1, pale greenstones)

3) If at all possible, the core should be washed and cut (sawed) before logging and sampling procedures begin. This allows a much fresher sample and a flat surface in order to see the volcanic structures and textures better. The same applies for the ore textures and minerals.

4) The surface drill core should not be left to overwinter out on the surface, at least not for any length of time. The boxes begin to disintergrate and the core begins to rust and be covered by mosses and lichens.

5) Drill core must not be stored down inside the mine uncovered, where it is damp and dusty. This caused contamination problems for future sampling and chemical analysis programs.

6.7 PRACTICAL APPLICATION OF RESULTS

Some of the results produced during the project can have direct practical application to future regional and local exploration after new ore reserves and to the definition of ore types in order to optimise mine planning and give the best mill results and metal recoveries.

1) It has been recognized that the middle greenstone is underlain by a major thrust which cuts out the Joma ore zone at depth. The middle and outer greenstones are interpreted as being of the same volcanite complex, separated from each other during later thrusting deformation. This has practical consequences for regional exploration.

2) Considerations of the distribution of the greenstone units south and west of the mine area, together with analysis of the direction of nappe movements point to the possibility that the known sulphide occurrences at Borvasselv and the Joma ore body are parts of an original level of continuous sulphide mineralization that have been separated by thrusting at the base of the middle greenstone.

3) The effects of the two major fold phases on the morphology of the ore layers at Joma have been documented, providing a guide to changes in ore thickness and in locating zones of thicker ore.

4) The Ti-Zr-Cr trace element distributions in greenstones have been used to separate the pre-ore from the post-ore volcanite sequences. This is an important step in defining the position of the Joma ore horizon within the volcanostratigraphy. It has also been shown that the thicker layered volcaniclastic units are also confined to the younger (post-ore) volcanite sequence.

5) CaO-FeO^{tot}-MgO major element patterns in the altered pre-ore host rock lithologies have been used to define chemical and mineralogical zonal patterns that reflect the varying intensities of hydrothermal alteration within the central feeder zone beneath the main ore zone. This may prove useful in recognising alteration zones connected to yet undiscovered sulphide bodies.

6) The recognition of volcanic structures and igneous textures such as close-packed pillows, pillow breccias, hyaloclastites, massive flows and coarse grained gabbro dykes has been instrumental in classifying the volcanostratigraphy at Joma. This will help in systemizing future drill core descriptions.

7) Cu-Zn-Sp.gravity data from the total mine drill core data base has been used in separating the four main ore types found at Joma. This is important for future mine planning as several of the ore types carry significantly differing Cu, Zn, Ag and Au contents besides having quite different milling properties.

ACKNOWLEDGEMENTS

The project was carried out as a two year research project at the Geologisk Institutt, NTH. The project was jointly financed by NTNF and Grong Gruber A/S on a 50:50 basis. The author was hired on a two year basis to function as the research geologist and secretary for the steering committee.

Thanks go to the Joma Project steering committee; Professor F.M. Vokes, Professor R. Sinding-Larsen, Research geologist P.M. Ihlen and Expl.manager A. Haugen, for their discussions and advice. I am indebted to Professor F.M. Vokes and N. Odling for critically reading the manuscript. Thanks also go to N. Odling, co-worker, for her discussions throughout the life of the project. L.-I. Skjellum is thanked for crushing most of the whole rock samples that were sent to Finland. A.I. Johannessen draughted most of the figures in the text. R. Skram is especially thanked for her endurance in typing this report.

REFERENCES

Anger, C., Eisbein, P. (1963): Erzmikroskopische Beobachtungen an der Schwefelkies-Kupferkies-Lagerstatte Joma, Grong-Revier (Norwegen). Berg. Wiss., 15, 93-97.

Arnorsson, S., Kononov, V. and Polyak, B. (1974): The geochemical features of Iceland hydrotherms. Geochem. Int., v. 11, 1224-1240.

Aumento, F., Loncarevic, B. and Ross, D.I. (1971): Hudson geotraverse: geology of the Mid-Atlantic Ridge at 45°N. Phil. Trans. Roy. Soc. Lond., A, v. 268, 623-650.

Bischoff, J.L. and Dickson, F.W. (1975): Seawater-basalt interaction at 200°C and 500 bars: Implications for origin of sea-floor heavy-metal deposits and regulation of seawater chemistry. Earth Plan. Sci. Lett., v. 25, 385-397.

Bjørlykke, H. (1959): Rapport over geologisk arbeid i Grongfeltet i tiden 17-29 juli 1959. Internal report, Norsk Bergverk.

Cann, J.R. (1969): Spilites from the Carlsberg Ridge, Indian Ocean. J. Petrol., 10, 1-19.

Coleman, R.G. (1977): Ophiolites: Ancient oceanic lithosphere. New York, Springer, 229 pp.

CYAMEX Scientific Team (1981): First manned submersible dives on the East Pasific Rise at 21°N (Project RITA): General results. Marine Geophysical Researchers, v. 4, 345-379.

Edmond, J.M. and Von Damm, K. (1983): Hot Spring on the Ocean Floor. Sci. American., v. 248, No. 4, 70-85.

Eidsmo, O., Foslie, G., Malvik, T., Vokes, F.M. (1984): The mineralogy and recovery of silver in some Norwegian basemetal sulphide ores. In: Proc. Second International Congress in Applied Mineralogy in the Mineral Industry, Los Angeles, California, 1984. Ed. Park, Hausen and Hagni, 891-910.

Foslie, S. (1924): Rapport i: Årbok for 1923. Nor. geol. Unders. Nr. 122, 59-70.

Foslie, S. (1925): Unpublished 1:50,000 geological map of Huddingsvatnet area. Nor. geol. unders.

Foslie, S. (1926): Norges svovelkisforekomster. Nor. geol. Unders., Nr. 127, 122 pp.

Foslie, S. (1949): Jomafeltet i Grong og dets malm forråd. Tidsskr. f. Kjemi. Bergv. Met., 9, 177-182.

Goodfellow, W.D. (1974): Major and Minor Element Halos in Volcanic Rocks at Brunswick No. 12 Sulphide Deposit, NB., Canada. In: Geochemical Exploration 1974, Spec. Publ. No. 2, Assoc. Expl. Geochemists, Elliot and Fletcher (eds.).

Henley, R.W. and Thornley, P. (1981): Low grade metamorphism and the geothermal environment of massive sulphide ore formation. Buchans, Newfoundland: Geol. Assoc. Canada Spec. Paper 22, 205-228.

Horbach, R., Liessmann, W. (1985): Lagerstattenkunde schichtgebundener Sulfidvererzungen Paragenese, Geochemie und Genese der Vererzungen im Joma-Gebeit (Norwegen). Unpubl. progress report, Univ. Clausthal, Germany, 120 pp.

Humphries, S.E. and Thompson, G. (1978): Hydrothermal alteration of oceanic basalts by seawater. Geochim. et Cosmochim. Acta. v. 107, 107-125.

Juve, G. (1964): Geologisk kart - Joma kisforekomster Ornivået, målestokk 1:500. Grong Gruber A/S. NGU report.

Juve, G. (1964): Skisse over Hovedmalmens skjæring med grunnstollen, horisontal planet, målestokk 1:200. Grong Gruber A/S. NGU report.

Kollung, S. (1979): Stratigraphy and major structure of the Grong District, Nord-Trøndelag. Nor. geol. Unders., 354, 1-51.

Kollung, S. (1979): Unpublished 1:50,000 geological map of Huddingsvatnet area.

Lisler, C.R.B. (1972): On the thermal balance of an oceanic ridge. Geophysical Journal of the Royal Astronomical Soc., v. 26, 515-535.

Logn, O. & Bølviken, B. (1974): Self potentials at the Joma pyrite deposit, Norway. In: Geo-exploration. Elsevier Scient. Publ. Co., Amsterdam, 11-28.

Lutro, O. & Kollung, S. (1983): RØYRVIK, Berggrunnsgeologisk kart 1924 IV 1:50,000. Foreløpig utgave, Nor. Geol. Unders.

Malvik, T., Eidsmo, O & Vokes, F.M. (1984): "Sølv og sølvmineraler i Norske kismalmer og Deres Oppredningsprodukter". BVLI-Teknisk Rapport nr. 64, Trondheim, 71 pp.

Miyashiro, A. (1968): Metamorphism of mafic rocks. In: Basalts: the Poldervaart treatise on rocks of basaltic composition. Hess, H.H. and Poldervaart, A., eds. (New York Interscience) v. 2, 799-834.

Miyashiro, A., Shido, F. and Ewing, M. (1971): Metamorphism on the Mid-Atlantic Ridge near 24 and 30°N. Phil. Trans. Roy. Soc. Lond., A, 268, 589-603.

Mottl, M.J. (1976): Chemical exchange between seawater and basalt during hydrothermal alteration of the oceanic crust. Ph.D. dissertation. Harvard University.

Mottl, M.J. (1983): Metabasalts, arial hot springs, and the structure of hydrothermal systems at mid-ocean ridges. Geol. Soc. Am. Bull., v. 94, 161-180.

Mottl, M.J. and Holland, H.D. (1978): Chemical exchanges during hydrothermal alteration of basalt by seawater. - I. Experimental results for major and minor components of seawater. Geochim. & Cosmochim. Acta., v. 2, 1103-1115.

Mottl, M.J. and Seyfried, W.E. (1980): Sub-sea-floor hydrothermal systems: Rock-vs. seawater-dominated. in Rona, P.A. and Lowell, R.P., eds., Sea-floor spreading centers: Hydrothermal systems. Stroudsburg Pennsylvania. Dowden, Hutchinson and Ross Inc., 424 pp.

Münster, K. (1915): Rapport over Joma Kisforekomst. Pub. Kongsberg, 185 pp.

Oftedahl, C. (1958): Oversikt over Grongfeltets skjerp og malmforekomster. Nor. geol. Unders., Nr. 202, 76 pp.

Olsen, J. (1980): Genesis of the Joma stratiform sulphide deposit, central Norwegian Caledonides. Proc. Fifth. Quadr. IAGOD Symp. E. Schweizerbart'sche Verlagsbachandlung, Stuttgart, Germany, 745-757.

Olsen, J. (1984): Joma - geologisk beskrivelse, sammenstilling av resultater fra kartlegging 1975-1977. Internal report, Grong Gruber A/S, 54 pp.

Padfield, T. and Gray, A. (1971): Major element rock analyses by X-ray fluorescence - A simple fusion method. Philips Bulletins - by analytical equipment dept., N.V. Philips Glocelampen Fabricken, Eindhoven, Nederlands (Aug. 1971).

Reinsbakken, A. (1986): The Joma Cu-Zn Massive Sulphide Deposit Hosted by Mafic Volcanites. In: Stratabound Sulphide Deposits in the Central Scandinavian Caledonides (Stephens, M.B., ed.) Excursion Guide No. 2 to 7th IAGOD Symposium, Luleå, Sweden. Sveriges geol. undersøkn. Nr. 60, Ser. Ca, 42-45.

Reinsbakken, A. and Stephens, M.B. (1986): Lithology and Deformation in the Massive Sulphide-bearing Gelvenåkko and Leipikvattnet Nappes, Upper Allochthon. In: Stratabound Sulphide Deposits in the Central Scandinavian Caledonides (Stephens, M.B., ed.) Excursion Guide No. 2 to 7th IAGOD Symposium, Luleå, Sweden. Sveriges geol. undersøkn. Nr. 60, Ser. Ca, 42-45.

Riverin, G. and Hodgson, C.J. (1980): Wall rock alteration at the Millenbach Cu-Zn mine, Noranda, Quebec: Econ. Geol., v.75, 424-444.

Romaya, J.P. (1982): A field investigation of the geology and structure of the Joma mine area, Norway. Unpublished B.Sc. thesis, Royal School of Mines, Imperial College, London, 61 pp.

Romaya, J.P. (1982): A mineralogical and textural study of the Joma ore body, central Norwegian Caledonides. Unpubl. B.Sc. thesis, Royal School of Mines, Imperial College, London, 35 pp.

Rona, P.A. (1980): TAG hydrothermal field: Mid-Atlantic Ridge crest at lat. 26°N. Geol. Soc. of Lond. Quart. Jour., v. 137, 385-402.

Seyfried, W.E. and others (1978): Seawater-basalt ratio effects on the chemistry and mineralogy of spilites from the ocean floor. Nature, v. 275, 211-213.

Seyfried, W.E. Jr. and Mottl, M.J. (1982): Hydrothermal alteration of basalt by seawater under seawater-dominated conditions. Geochim. & Cosmochim. Acta., v. 46, 985-1002.

Shirozu, H. (1974): Clay minerals in altered wall rocks of the Kuroko-type deposits: Soc. Mining Geologists Japan Spec. Issue 6, 303-310.

Sigmond, E.M.O., Gustavson, M., and Roberts, D. (1984): Berggrunnskart over Norge M 1:1 million. Nor. geol. Unders.

Sjöstrand, T. (1978): Caledonian geology of the Kvärnbergsvattnet area, northern Jämtland, central Sweden. Sver. geol. Unders., C. 735, 107 pp.

Spooner, E.T.C. and Fyfe, W.S. (1973): Sub-sea-floor metamorphism, heat and mass transfer. Contr. to Min. and Petrol., v. 42, 287-304.

Stephens, M.B. & Reinsbakken, A. (1981): Successions related to island arcs in the Köli nappes, Central Scandinavian Caledonides. Guidebook No.14 to Uppsala Caledonide symposium (U.C.S.) 1981, 48 pp.

Trouw, R.A.J. (1973): Structural geology of the Marsfjällen area, Caledonides of Västerbotten, Sweden. Sver. Geol. Unders., Serie C, Nr. 689, 115 pp.

Trøften, P. Fr., (1955): Diplomoppgave over Jomforekomsten. Geol. Inst., NTH, Trondheim.

Vallance, T.G. (1960): Concerning Spilites. Proc. Linn. Soc. N.S.W., v. 85, 8-52.

Vallance, T.G. (1969): Spilites again: some consequences of the deggradation of basalt. Proc. Linn. Soc. N.S.W., v. 94, 8-51.

Wynne, P.J. and Strong, D.F. (1984): The Strickland Prospect of Southwestern Newfoundland: A Lithogeochemical Study of Metamorphosed and Deformed Volcanogenic Massive Sulfides. Econ. Geol., v. 79, 1620-1642.

Zachrisson, E. (1964): The Remdalen syncline, stratigraphy and tectonics. Sver. Geol. Unders., Serie C, Nr. 596, 53 pp.

Zachrisson, E. (1969): Caledonian geology of northern Jämtland - southern Västerbotten. Köli stratigraphy and main tectonic outlines. Sver. Geol. Unders., Serie C, Nr. 644, 33 pp.

Zachrisson, E. (1971): The structural setting of the Stekenjokk ore bodies, central Swedish Caledonides. Econ. Geol., 66, 641-652.

Zachrisson, E. (1973): The westerly extension of Seve rocks within the Seve-Köli nappe complex in the Scandinavian Caledonides. Geol. Foren. Stockh. Förh., 95, 243-251.